INVESTIGATION OF A THERMALLY REGENERATIVE REACTOR SYSTEM

Submitted in fulfilment of the requirements for the degree of
Doctor of Philosophy

at

The University of Leeds

by

C.S. Cockcroft, B.Sc. (Leeds)

under the direction of

P.J. Heggs, Ph.D., C.Eng., M.I.Chem.E.

Department of Chemical Engineering,
Houldsworth School of Applied Science,
The University of Leeds,
Leeds, LS2 9JT.

July 1976

SUMMARY

A novel cyclic reactor system is proposed for heterogeneous, catalytic, gas-phase reactions. This system utilises the inherent characteristics of the thermal regenerator to impose favourable reaction temperature profiles along the catalyst bed without setting up radial temperature gradients. This control of the longitudinal profile enables higher conversions to be obtained than those from steady state reactors. The reactor system is investigated by computer simulation using the endothermic, reversible dehydrogenation of ethylbenzene to styrene in the presence of steam as an example. The higher conversions obtained from the proposed system produce utility cost savings in this process.

Kinetics presented in the literature for this reaction are compared and assessed. None of these is entirely satisfactory and a more representative set is derived. Models for the reacting and regenerating bed are discussed and suitable models are presented. A comparative study of solution methods for these models is carried out in order to determine one which gives an accurate solution and also minimises computing requirements.

The most suitable operating policy for the system, with an endothermic reaction, is the use of constant heat inputs with constant flows during each period of operation. This allows the bed inlet temperatures to vary with time, but it seems likely that the damping effect of the system will be large and the inlet temperatures may be assumed constant. Counter-current, rather than co-current, operation of the system is preferred.

A simple design procedure, which does not require the solution of the cyclic model, is described. This is found to give good predictions of the cyclic steady state performance of the system.

The effect of the various system parameters on the performance is investigated. The major parameters for a given bed size are the period time, reactor and regenerator steam flows and regenerator inlet temperature. It is shown that the system can give higher conversions than a steady state reactor but it may be desirable to operate at lower conversions to reduce the operating cost. Guidelines for optimising the system are discussed.

ACKNOWLEDGMENTS

To Dr. P.J. Heggs for supervising the research and the compiling of this thesis.

To all in the Department of Chemical Engineering who have assisted the author, particularly to Mr. L. Bailey for his readiness to assist with computational problems.

To Miss S. Toon, who typed this thesis, for her patience and for the excellence of the end product.

To Professor G.G. Haselden for the use of the facilities in the Department of Chemical Engineering and to the Science Research Council for providing the Research Studentship.

CONTENTS

Summary i
Acknowledgments iii
Contents iv
List of Figures xi
List of Tables xv

Page

Chapter 1 Introduction and Proposed Research

1.1 Introduction 1

1.2 Proposed Reactor System 5

1.3 Definitions and Terminology 10

1.4 Research Programme 11

Chapter 2 The Reaction System and Process Study

2.1 The Dehydrogenation Reaction 14

2.2 Reactor Types 19

2.2.1 Single Bed Adiabatic Reactors 19

2.2.2 Multibed Adiabatic Reactors 20

2.2.3 Externally Heated Tubular Reactors 21

2.3 Kinetics 21

2.4 Process Study 27

2.4.1 Process Description 28

2.4.2 Process Modelling 30

2.4.3 Studies 32

2.4.4 Results 33

2.4.5 Discussion and Conclusion 35

Chapter 3 Mathematical Models

3.1 Introduction 39

3.2 Packed Bed Models 40

3.2.1 Continuum Model 40

3.2.2 Cell Model 41

3.3 Reactor Models 42

3.3.1 Pellet Model 42

3.3.2 Film Resistance Model 43

3.3.3 Pseudo-homogeneous Model 43

3.3.4 Selection of Model 44

3.3.5 Stability 47

Page

3.4 Regenerator Models 47
3.5 Model Equations 48
3.5.1 Transient Film Resistance Model 48
3.5.2 Transient Pseudo-homogeneous Model 50
3.5.3 Steady State Reactor Models 50
3.5.3.1 Film Resistance Model 50
3.5.3.2 Pseudo-homogeneous Model 51
3.5.4 Diluted Catalyst Models 51

Chapter 4 Solution of Models

4.1 Introduction 54
4.2 Co-ordinate System 57
4.3 Approximation Methods 60
4.3.1 Method of Characteristics 60
4.3.2 Finite Difference Approximations 64
4.3.3 Method of Lines 66
4.3.4 Methods for Steady State Models 67
4.4 Stability 67
4.4.1 Transient Models 67
4.4.2 Steady State Models 69
4.5 Initial Conditions for Transient Reactor Models 71
4.6 Comparison of Transient Solutions 72
4.6.1 Film Resistance Model 73
4.6.2 Pseudo-homogeneous Model 78
4.7 Comparison of Steady State Solutions 84
4.8 Discussion and Conclusions 84

Chapter 5 Cyclic Reactor System

5.1 Development of a Practical System 87
5.2 Operation and Control of the System 94

Page

5.3 Model of the System 98
5.4 Prediction of System Parameters 100
5.4.1 Period Time 101
5.4.2 Regenerator Steam Flow 102
5.4.3 Heat Inputs to the System 104

Chapter 6 Steady State Studies

6.1 Comparison of Kinetics 109
6.1.1 Reactor Size 112
6.1.2 Inlet Temperature 112
6.1.3 Reactor Pressure 112
6.1.4 Dilution Steam Flow 116
6.1.5 Isothermal Temperature Level 119
6.1.6 Discussion 120
6.1.7 Derived Kinetics 121
6.2 Physical Property Variation 124
6.3 Cyclic Reactor Norm 125
6.4 Cyclic Reactor Conversion Limits 128
6.5 Estimation of Cyclic System Parameters 130
6.5.1 Period Time 130
6.5.2 Regenerator Steam Flow 131
6.5.3 Heat Inputs 132
6.5.4 Summary 132

Chapter 7 Transient Single Bed Studies

7.1 Reactor Studies 133
7.1.1 Cyclic Reactor Period Time 138
7.1.2 Effect of Initial Temperature Profile 138
7.1.3 Effect of Feed Temperature 139
7.1.4 Effect of Diluent Steam Flow 139
7.1.5 Effect of Bed Heat Capacity 144

Page

7.2 Regenerator Studies 150
7.2.1 Steam Flow 150
7.2.2 Effect of Bed Heat Capacity 154
7.3 Cyclic Reactor System Heat Inputs 154
7.4 Summary of Predicted Parameters for the Cyclic Reactor System 155

Chapter 8 Cyclic Reactor System Studies

8.1 Introduction 156
8.2 Preliminary Studies 156
8.2.1 Assessment of Predicted Parameters 165
8.2.2 Co-current Operation 166
8.2.3 Efficiency 167
8.2.4 Comparison with Steady State Conversion 167
8.3 Effect of Parameter Variation 167
8.3.1 Variation of Regenerator Steam Flow 167
8.3.2 Variation of Period Time 171
8.3.3 Effect of Bed Heat Capacity 171
8.3.4 Variation of Constant Reactor and Regenerator Inlet Temperatures 175
8.3.5 Variation of Diluent Steam Flow 175
8.4 Varying Reactor and Regenerator Inlet Temperatures 178
8.4.1 Counter-current Operation 179
8.4.2 Co-current Operation 187
8.4.3 Variation of Regenerator Steam Flow 188
8.5 Assessment of the Effect of the System Heat Capacity 188
8.6 Discussion 196

Chapter 9 Guidelines for Optimisation

9.1 Introduction 199
9.2 Optimisation Parameters 199

Page

9.2.1 Fixed Parameters 201

9.2.2 Variable Parameters 202

9.3 The Objective Function 203

9.4 Optimisation Procedure 204

9.5 Conclusions 205

Chapter 10 Summary of Conclusions 207

10.1 Suggestions for Further Work 211

Appendix 1 Summary of Kinetic Models for the Dehydrogenation of Ethylbenzene 213

Appendix 2 Method of Characteristics for the Transient Film Resistance Reactor Model 218

Appendix 3 Fourier Series Method for the Stability of the Regenerator Equations 221

A3.1 Pseudo-homogeneous Model 221

A3.2 Film Resistance Model 222

A3.2.1 Lagrangian Equations 223

A3.2.2 Eulerian Equations 224

Appendix 4 Solution of the Transient Film Resistance Model 226

A4.1 Reactor Equations 226

A4.2 Regenerator Equations 229

A4.3 Subroutine TM1SC 229

Appendix 5 Effect of Wall Heat Capacity in a Pilot Scale Reactor 230

A5.1 Wall Effect in a Transient Regenerator 232

A5.2 Wall Effect in a Transient Reactor 235

A5.3 Wall Effect in a Cyclic Reactor System 235

A5.4 Conclusions 236

Page

Appendix 6 Description of the Cyclic Reactor Model Program - CH3SC 237

A6.1 Data Input 240

A6.2 Output 241

A6.3 Use of the Program 242

A6.4 Details of Ancillary Calculations 246

A6.4.1 Average Temperatures and Conversions 246

A6.4.2 Heat Balance Equations 246

A6.4.3 Estimation of HT_{IN} 246

A6.5 Flags used in CH3SC 247

Appendix 7 Listing of the Program CH3SC 248

A7.1 CH3SC 248

A7.2 Subroutine TM3SC 257

A7.3 Subroutine TM4SC 258

A7.4 Subroutine TM5SC 260

Nomenclature 262

References 266

LIST OF FIGURES

Figure		Page
1.1	Conversion Profiles in a Single Bed Adiabatic Reactor	4
1.2	Conversion Profiles in a Two-bed Adiabatic Reactor	4
1.3	Conversion Profiles in a Multitubular Reactor	4
1.4	Counter-current Operation of a Thermal Regenerator	6
1.5	Temperature Variation During a Cycle in a Thermal Regenerator	6
1.6	Solid Temperature Profiles at the end of (a) the heating period and (b) the cooling period in a thermal regenerator	8
2.1	Effect of Temperature and Steam/ethylbenzene Ratio on Equilibrium Conversion	17
2.2	Effect of Pressure on Equilibrium Conversion	18
2.3	Dow Process Flowsheet for the Dehydrogenation of Ethylbenzene	29
2.4	Monsanto Distillation Train	31
4.1	Characteristic Directions for the Transient Film Resistance Reactor Model	61
4.2	Effect of the Transformation to Lagrangian Co-ordinates on the Transient Film Resistance Model Characteristics	61
4.3	Characteristic Directions for the Transient Pseudo-homogeneous Reactor Model	63
4.4	Section of Finite Difference Grid	63
4.5	Breakthrough Curves for Film Resistance Model Central Difference Solution	74
4.6	Breakthrough Curves for Film Resistance Model Backward Difference Solution	75
4.7	Film Resistance Model - Exothermic Reaction Temperature Profiles	76
4.8	Film Resistance Model - Endothermic Reaction Temperature Profiles	77
4.9	Pseudo-homogeneous Regenerator Model - Temperature Profiles after a Step Change	79
4.10	Pseudo-homogeneous Model - Endothermic Reaction Temperature Profiles	81

Figure		Page
4.11	Pseudo-homogeneous Model - Exothermic Reaction Temperature Profiles	82
5.1	Simple Cyclic Reactor System	88
5.2	Cyclic Reactor System with Superheater	91
5.3	Cyclic Reactor System with Recycle	93
5.4	Regeneratively Cooled Reactor of Gavalas[11,12]	95
5.5	Flows in the Cyclic Reactor System during a Single Counter-current Period	105
6.1	Effect of Reactor Size on Conversion and Efficiency	113
6.2	Effect of Inlet Temperature on Conversion and Efficiency	114
6.3	Effect of Reactor Pressure on Conversion and Efficiency	115
6.4	Effect of Steam Flow on Conversion and Efficiency	117
6.5	Effect of Isothermal Temperature Level on Conversion and Efficiency	118
6.6	Rate Constants for Side-reactions	123
7.1	Temperature Profiles in a Transient Reactor	134
7.2	Conversion Profiles in a Transient Reactor	135
7.3	Variation of Reactor Outlet Temperature and Conversion with Time	136
7.4	Variation of Efficiency with Time from a Transient Reactor	137
7.5	Effect of Diluent Steam Flow on the Observed Conversion of a Transient Reactor	141
7.6	Effect of Diluent Steam Flow on the Average Conversion of a Transient Reactor	142
7.7	Effect of Diluent Steam Flow on the Efficiency of the Average Conversion of a Transient Reactor	143
7.8	Reactor with a Region of Inert Material within the Catalyst Bed	147
7.9	Temperature Profiles in a Transient Reactor with Region of Inert	148
7.10	Outlet Temperature and Conversion with Time for a Uniformly Diluted Bed and one Containing a Region of Inert	149

Figure		Page
7.11	Comparison of the Pseudo-homogeneous Analytical Solution with the Film Resistance Model Breakthrough Curves	152
7.12	Comparison of Breakthrough Curves for an Initially Isothermal Bed and one with a Steady State Reactor Profile	153
8.1	Standard Conditions for Cyclic Reactor Studies in Chapter 8	158
8.2	Temperature and Conversion Profiles at the Ends of Successive Cycles	159
8.3	Reactor Temperature Profiles During Period at Cyclic Steady State	160
8.4	Reactor Conversion Profiles During Period at Cyclic Steady State	161
8.5	Reactor Outlet Temperature and Conversion During a Period at Cyclic Steady State	162
8.6	Regenerator Temperature Profiles During a Period at Cyclic Steady State	163
8.7	Regenerator Outlet Temperature During a Period at Cyclic Steady State	164
8.8	Co-current Regenerator Temperature Profiles During a Period at Cyclic Steady State	168
8.9	Effect of Regenerator Steam Flow on Average Conversion and Final Regenerator Outlet Temperature	169
8.10	Effect of Period Time on Average Conversion with the Norm Bed Size	172
8.11	Effect of Period Time on Average Conversion with the 0.726 m Bed	172
8.12	Comparison of Reactor Temperature Profiles for the 0.726 m Bed	173
8.13	Effect of Different Constant Reactor and Regenerator Inlet Temperatures on the Average Conversion	176
8.14	Effect of Reactor Steam Flow on Average Conversion, Efficiency and Steam Consumption	177
8.15	Counter-current Regenerator Temperature Profiles during a Period with Varying Inlet Temperatures	181
8.16	Reactor Temperature Profiles during a Period with Varying Inlet Temperatures	182

Figure		Page
8.17	Reactor Conversion Profiles during a Period with Varying Inlet Temperatures	183
8.18	Reactor Outlet Temperature and Conversion during a Period with Varying Inlet Temperatures	184
8.19	Counter-current Bed Inlet and Regenerator Outlet Temperatures during a Period	185
8.20	Co-current Bed Inlet and Regenerator Outlet Temperatures during a Period	185
8.21	Co-current Regenerator Temperature Profiles during a Period with Varying Inlet Temperatures	186
8.22	Effect of Regenerator Steam Flow with Varying Inlet Temperatures	189
8.23	Counter-current Final Regenerator Temperature Profiles with Varying Inlet Temperatures	190
8.24	Co-current Final Regenerator Temperature Profiles with Varying Inlet Temperatures	190
8.25	Counter-current Regenerator Temperature Profiles with Varying Inlet Temperatures and Inert Material at the Reactor Entrance	192
8.26	Counter-current Reactor Temperature Profiles with Varying Inlet Temperatures and Inert Material at Reactor Entrance	193
8.27	Co-current Regenerator Temperature Profiles with Varying Inlet Temperatures and Inert Material at Reactor Entrance	194
8.28	Co-current Reactor Temperature Profiles with Varying Inlet Temperatures and Inert Material at Reactor Entrance	195
9.1	Reactor System for Use in an Optimisation	200
A5.1	Section of Reactor Wall Showing External and Internal Insulation	231
A5.2	Effect of Wall Heat Capacity on Regenerator Breakthrough Curve	233
A5.3	Effect of the Reactor Wall on a Transient Reactor	234
A6.1	Flowsheet for the Program CH3SC	238
A6.2	Flowsheet for Reactor Period of Program CH3SC	239

LIST OF TABLES

Table		Page
2.1	Typical Product Compositions for the Dehydrogenation of Ethylbenzene	22
2.2	Temperatures and Heat Loads for Reactor Section	34
2.3	Feeds to the Distillation Train (kmol h^{-1})	34
2.4	Flows Down Columns and Condenser and Reboiler Heat Loads for Dow Distillation Train	36
2.5	Flows Down Columns and Condenser and Reboiler Heat Loads for Monsanto Distillation Train	37
3.1	Data Used in Estimation of Diffusion Effects	45
4.1	Data for the Dehydrogenation Reaction Used in Chapters 4 and 6	56
4.2	Data for the Oxidation Reaction Used in Chapter 4	56
4.3	Summary of Stability of Linear Finite Difference Schemes	68
4.4	Effect of Step Size Variation on the Steady State Conversion (%) of Ethylbenzene to Styrene for Various Solution Methods	70
6.1	Rate Constants for Reactions 2.1 - 2.3 at 630°C	109
6.2	Reactor Product Composition Given by Bogdanova et al[29]	122
6.3	Effect of Variation of Physical Properties on Steady State Results	126
6.4	Data for Norm Conditions in Chapters 6, 7 and 8	127
6.5	Steady State Conversion and Rate of Temperature Fall at Various Isothermal Temperatures	130
6.6	Parameters for the Cyclic Reactor System Predicted from Steady State Studies	132
7.1	Average Conversion (%) at Various Initial Isothermal Bed Temperatures with the Inlet Temperature at 650°C	140
7.2	Average Conversion (%) at Various Reactor Inlet Temperatures with the Initial Isothermal Bed Temperature at 650°C	140
7.3	Effect of Uniformly Mixed Inert Material on the Response of a Transient Reactor	145
7.4	Regenerator Data for the Norm Conditions	151
7.5	Parameters for Cyclic Reactor System Predicted from Transient Studies	155

Table		Page
A1.1	Reactions Proposed in the Dehydrogenation of Ethylbenzene	214
A1.2	Rate Expressions for Reactions in the Dehydrogenation of Ethylbenzene	215
A1.3	Rate Constants for the Reactions in Table A1.1 and the Rate Expressions in Table A1.2	216
A5.1	Parameters Used in Study of Wall Effect	231
A6.1	Sample Output from CH3SC Using Standard Data in Figure 8.1	243
A6.2	Effect of Console Switches on the Program CH3SC	245

CHAPTER 1

INTRODUCTION AND PROPOSED RESEARCH

1.1 Introduction

The provision of heating or cooling in heterogeneous gas-phase chemical reactors can pose considerable problems for the reactor designer, especially if the reaction is highly exothermic or endothermic. These problems are considered in detail in the reaction engineering textbooks such as those of Levenspiel[1], Smith[2], Aris[3], Thomas and Thomas[4] and Petersen[5]. The reactor designer aims to minimise the reactor size required to produce a specified conversion by manipulation of the operating conditions. The reactor temperature is an important parameter as the reaction rate increases exponentially with absolute temperature. Thus, for an irreversible reaction, the maximum rate, and minimum size, is given by isothermal operation at the highest allowable temperature. This temperature is determined by the materials of construction and the sintering temperature of the catalyst. It may also be limited by the temperature dependence of parallel or consecutive side-reactions. However, to obtain isothermal operation, a varying heat flux into or out of the reaction zone is required along the reactor to balance the changing heat of reaction. This is clearly not possible in practice and the designer tries to approximate this optimum temperature profile as inexpensively as possible.

Adiabatic reactors[3] are often used because of their relatively simple design and construction[4] but they do not approximate isothermal conditions closely unless the heat of reaction is small. The temperature rises along the length if the reaction is exothermic and falls if it is endothermic and the only means of control is by manipulation of the inlet conditions. A common means of reducing the temperature change is by the addition of a diluent gas to the feed mixture. This reduces the reactant concentration and provides additional heat capacity. Multibed adiabatic reactors with interstage heating or cooling are used to obtain a closer approximation to isothermal conditions. The interstage heat transfer may be indirect, by means of a heat exchanger, or by the direct injection into the reaction mixture of a diluent or reactant gas at a suitable temperature. A one-dimensional mathematical model is sufficient for design and, unless the conditions within the pellet or axial diffusion are considered, the only transport properties required are the interphase heat and mass transfer coefficients. In many cases, a pseudo-homogeneous model is used, which requires no transport properties at all.

Non-adiabatic, non-isothermal, multitubular reactors, in which heat is transferred through the reactor tube walls, are used when the heat of reaction is very large[2]. However, the lack of control of heat flux along the tubes causes a temperature peak or trough in the region of the greatest reaction rate. This is somewhat self-correcting with endothermic reactions as the rate is reduced by the lower temperature. However, with exothermic reactions, the temperature peak must be controlled to prevent damage to the catalyst or the reactor tubes. Radial temperature gradients are also set up, causing large variations in rate across the tube[4]. These adversely affect the conversion and also the selectivity if side-reactions occur. Multitubular reactors are much more complex to construct than adiabatic reactors and they require more sophisticated mathematical models for their design. A two-dimensional model must often be used and this requires the evaluation of radial transport properties. Methods presently available for evaluating these, especially correlations for the wall heat transfer coefficient, are subject to some uncertainty[5,6].

The problems of design are further complicated if the reaction is reversible and the thermodynamic equilibrium needs to be considered, as is the case in this research. From Le Chatelier's principle, a high equilibrium conversion is favoured by a high temperature for an endothermic reaction and by a low temperature for an exothermic one. Thus, the effect of the heat of reaction opposes the desirable equilibrium conditions. The minimum reactor size for a reversible endothermic reaction is again given by isothermal operation at the maximum allowable temperature. However, the optimum profile for a reversible exothermic reaction is one which falls along the length from the maximum allowable temperature[1]. This profile imposes a high initial reaction rate and also gives favourable equilibrium conditions at the exit. The exit temperature is important with all equilibrium controlled reactions as it determines the highest attainable equilibrium conversion irrespective of the reactor configuration.

Adiabatic reactors do not produce favourable equilibrium conditions due to the temperature change along their length. A typical conversion profile, with its corresponding equilibrium profile, is shown in Figure 1.1 which represents either an exothermic or an endothermic reaction. The driving force of the reaction, i.e. the net forward rate, depends on the difference between the two curves and this is reduced by the falling equilibrium. The equilibrium conversion can never be achieved and so it sets an upper limit on the possible reactor conversion. Multibed adiabatic reactors produce more favourable equilibrium conditions due to the interstage heat transfer. This is shown in Figure 1.2 for a two-bed reactor. Nevertheless, even multibed adiabatic reactors cannot closely approach the optimum temperature profiles unless a large number of beds is used and this is not a practical proposition. Multitubular reactors may produce favourable equilibrium conditions at the reactor exit as there is some control of

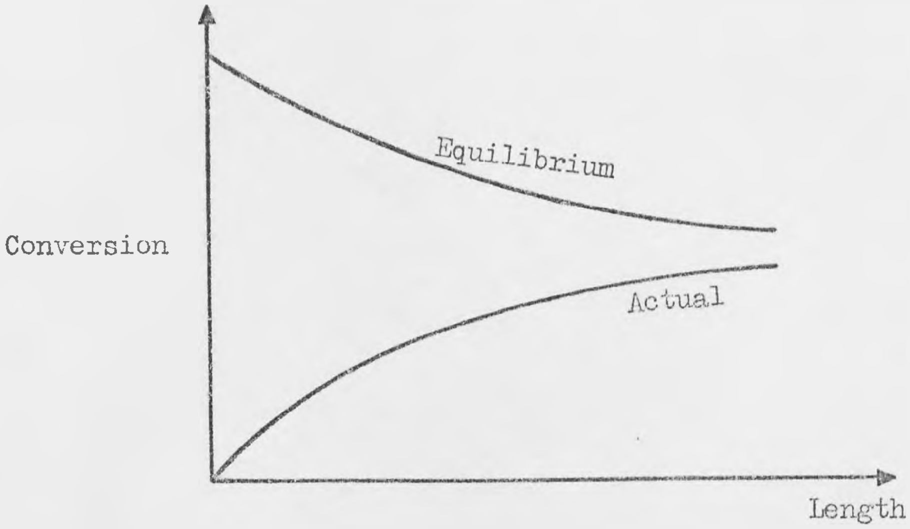

Figure 1.1: Conversion Profiles in a Single Bed Adiabatic Reactor

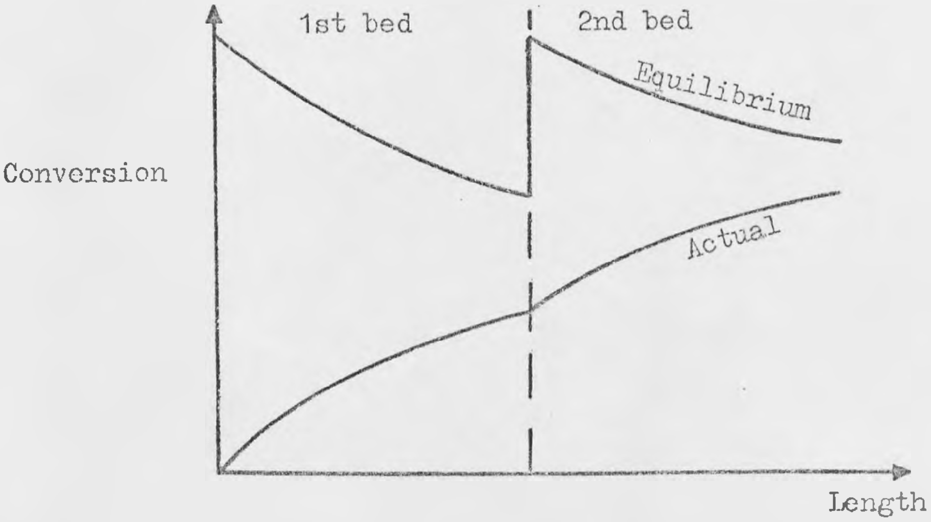

Figure 1.2: Conversion Profiles in a Two-Bed Adiabatic Reactor

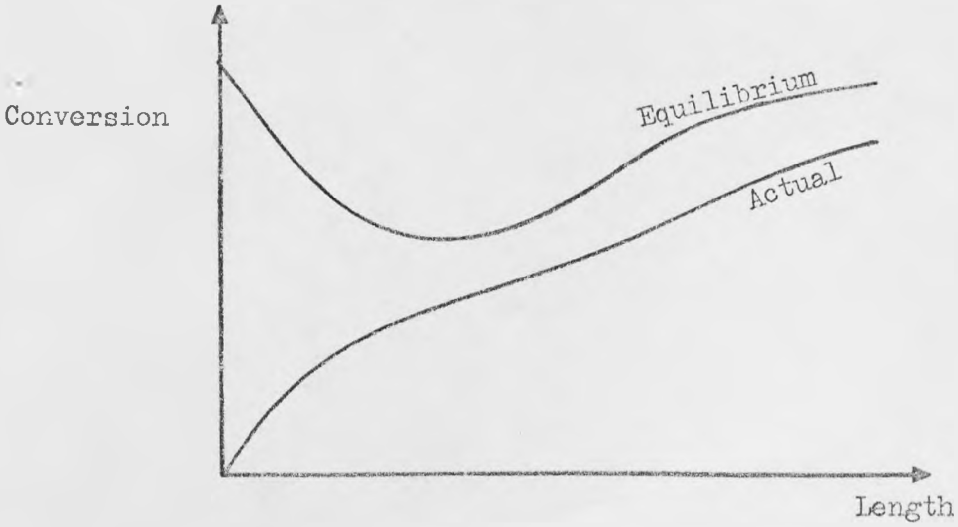

Figure 1.3: Conversion Profiles in a Multitubular Reactor

temperature other than by manipulation of the inlet conditions. Typical conversion profiles are shown in Figure 1.3.

However, adiabatic reactors are often used for reversible reactions despite their lower conversions[3,4]. A larger recycle of reactants within the process is then required, which increases capital and operating costs[7]. This seems to be accepted as the price of a low initial reactor cost and greater ease and confidence in design and operation.

1.2 Proposed Reactor System

This work reports on a novel reactor system for heterogeneous reactions which utilises the inherent characteristics of the counter-current thermal regenerator. The principles and operation of the regenerator are fully discussed by Jakob[8] and only an outline is presented here. The regenerator transfers heat from a hot to a cold gas stream by the alternate passage of the gases over the same heat storage medium and simply consists of an adiabatic packed bed. During the heating period (Figure 1.4a), the hot gas passes through the bed and heats up the packing. When sufficient heat has been transferred, the flow is reversed and the cold gas passes through the bed in the opposite direction (Figure 1.4b). The packing now gives up its stored heat to the gas during the cooling period until the next flow reversal. This cycle of operation is repeated and a cyclic steady state is eventually achieved. This is defined as when temperatures at a given time during a cycle are the same in successive cycles. The operation is necessarily intermittent and two (or more) beds are required for continuous operation. The following discussion will consider a two-bed system with equal heating and cooling periods.

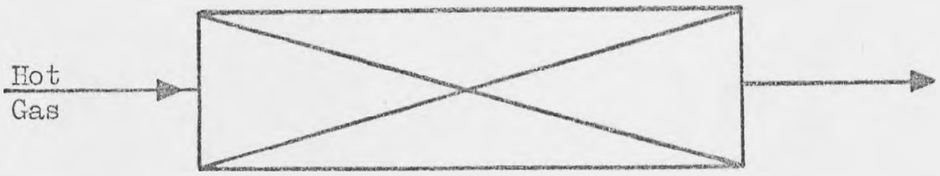

(a) Heating Period

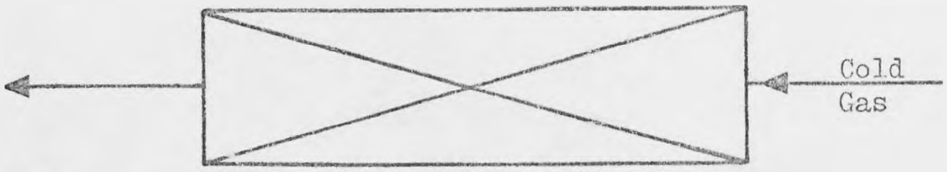

(b) Cooling Period

Figure 1.4: Counter-current Operation of a Thermal Regenerator.

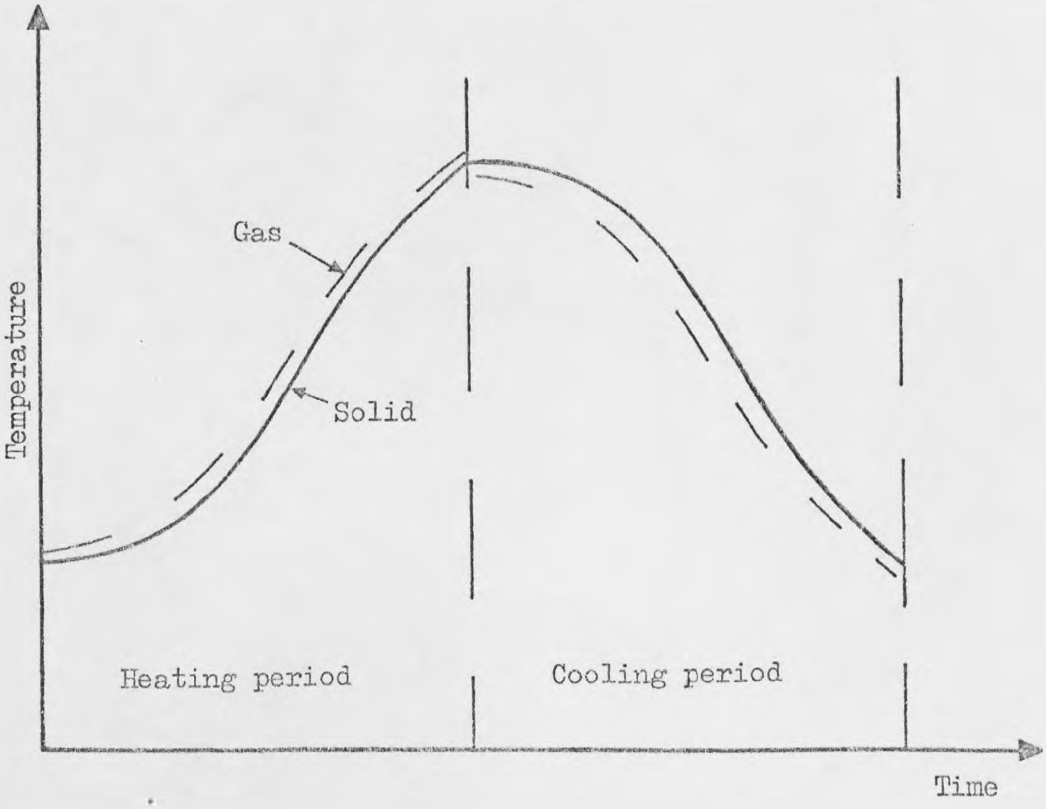

Figure 1.5: Temperature Variation During a Cycle in a Thermal Regenerator.

The main disadvantages of the regenerator are the time varying outlet temperatures and the mixing of the two gas streams at flow reversals. This mixing may be avoided if the system is purged with an inert gas. However, large amounts of heat can be transferred in a relatively small construction due to the high heat transfer coefficients and the large available surface area.

Figure 1.5 shows typical temperature variation at a point within a bed during a complete cycle. The temperature difference between the phases is small because of the high rate of heat transfer. If the bed is short, or the periods long, the temperature approaches the inlet temperature and the bed tends to saturation (isothermal conditions). Under these conditions, the rate of heat transfer towards the end of each period is low and heat is lost in the exit gas during the heating period. Hence, to obtain efficient overall heat transfer, the flows are reversed before saturation is closely approached.

Typical bed temperature profiles at the end of each period are shown in Figure 1.6. The profile at the end of the cooling period is that which favours a reversible exothermic reaction if the flow of the reaction mixture is in the opposite direction to that of the coolant gas. The profile at the end of the heating period is not the optimum (isothermal) one for a reversible endothermic reaction. However, if the flow is in the opposite direction to that of the heating gas, the outlet temperature is high, which is favourable for the equilibrium. A closer approach to an isothermal profile can be obtained, at the expense of heat transfer efficiency, by operating closer to saturation. This also approximates the optimum conditions for an irreversible reaction. It is therefore proposed to use a catalyst packing as the heat storage medium and to replace one of the

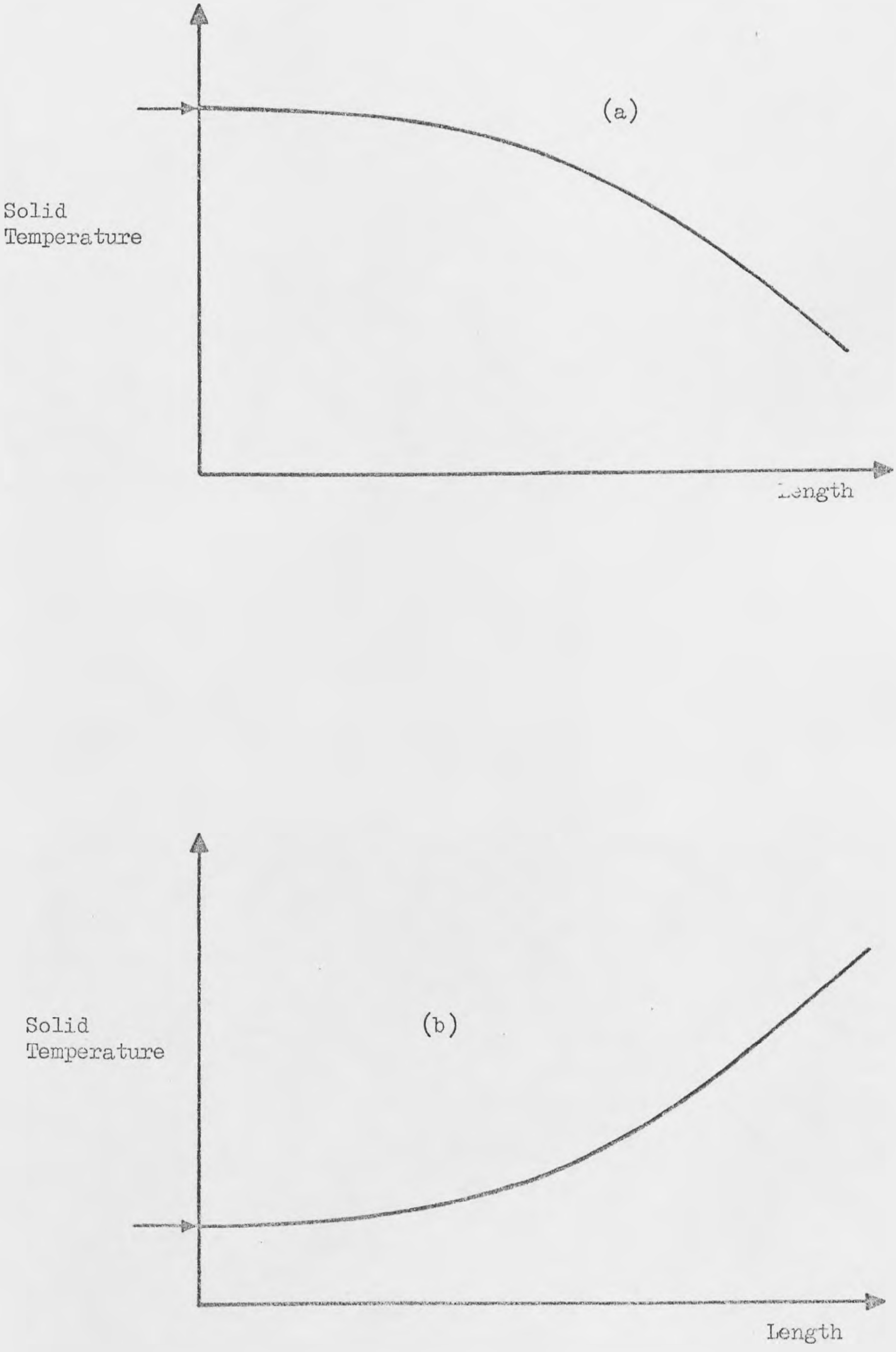

Figure 1.6: Solid Temperature Profiles at the end of (a) the heating period and (b) the cooling period in a thermal regenerator.

thermal periods by a chemical reaction. The temperature profile becomes less favourable as the reaction period proceeds due to the heat of reaction and the finite heat capacity of the catalyst support, but the flow reversal causes the favourable profile to be regenerated during the next thermal period. Hence the duration of each period should be as short as possible and is determined by the acceptable fall in conversion during the reacting period.

Co-current operation of the thermal regenerator is unlikely to produce favourable temperature profiles for the proposed reactor system. Jakob[8] shows that oscillating bed profiles are obtained at the end of each period unless saturation is closely approached. Even then, the outlet temperature is not the most favourable for the equilibrium and so lower conversions would be obtained. This work is therefore mainly concerned with counter-current operation although co-current operation will also be examined.

Two beds are again required for continuous operation, only one of which is reacting at a given time. The amount of catalyst required may be more than that in a single bed steady state reactor, but the inherent temperature control should give higher conversions. The product composition will vary over the reactor period and damping must therefore be provided downstream of the reactor or else other process units (e.g. distillation columns) may be adversely affected.

It is desirable to use one of the gases present in the reaction mixture as the heat transfer fluid in order to eliminate contamination problems at the flow reversals. This is also advantageous for endothermic reactions where a close approach to saturation of the bed during the thermal period is required. The heat lost from the thermal period is then not lost from the system but heats up the reactor feed.

The main advantage of this system is that it employs simple adiabatic beds and uses the inherent characteristics of the thermal regenerator to obtain favourable temperature conditions along the bed without setting up radial temperature gradients. It is suitable for equilibrium or kinetically controlled reactions and should give higher conversions than steady state reactors. The extra pipework and switching gear make the system more complex than the simple adiabatic reactor, but not more so than many non-adiabatic ones. The operation and control of the system will be affected by the parameters associated with its cyclic nature (e.g. duration of period). However these are operational parameters and can be determined by the use of a mathematical model of the system. None of the extra transport properties required in non-adiabatic reactor design are necessary.

There is a considerable amount of literature available to guide the design of adiabatic and non-adiabatic reactors[1-6,9,10]. However, there is no guidance on the design of the system proposed above. Gavalas[11,12] used a simple model to optimise such a system but does not describe how the system was designed in the first place. There is therefore a need for a comprehensive study of the system and for a design procedure to be laid down.

1.3 Definitions and Terminology

It is desirable at this stage to define terms relating to the proposed system which will be used in this work. The two-bed system described above, employing thermal regeneration of the favourable temperature conditions, is called the 'cyclic reactor system'. The term 'reactor' or 'cyclic reactor', when applied to this system, refers to the bed in which the reaction is occurring. The 'regenerator' is the bed in which the favourable temperature profile is being regenerated and, to avoid confusion with the thermally regenerative heat exchanger, the latter is called the 'thermal regenerator'. The 'period' or 'period time' is the time interval between flow reversals. The 'cycle time' is twice this as each cycle consists of a 'reactor period' and a 'regenerator period' for each bed.

1.4 Research Programme

The aim of this research is to investigate the cyclic reactor system by means of computer simulation. It is intended to establish the feasibility of the system and to propose a suitable procedure for determining the design parameters. The system will be studied using the endothermic reversible dehydrogenation of ethylbenzene to styrene as an example. This process is industrially important as styrene monomer is widely used in the manufacture of plastics and artificial rubbers[13,14]. The reaction takes place in the presence of a large excess of steam which, of course, is a suitable heat transfer fluid. It is also advantageous that the reaction is endothermic as this is more suitable for experimental work which is proposed to complement this work.

The dehydrogenation reaction and associated side-reactions will be examined. Reactor types used for this reaction will be reviewed and the process as a whole will be studied to determine the effect of improved reactor performance on the rest of the process.

The validity of the simulation of the system will depend largely on that of the mathematical model chosen to represent the reactor and the regenerator. A simple model is desirable, but it must give an adequate representation of the physical situation. Analytical solutions can be discounted due to the non-linearities in the reactor model and in its coupling to the regenerator model. Hence approximate numerical techniques are employed to solve the differential equations which describe the system. A quick solution is also important as the transient nature of the system requires comparatively large time intervals to be followed. Possible models will be discussed with respect to these criteria and a suitable model will be selected.

There is little guidance in the literature on which to base the selection of an approximation method which provides a quick and convergent solution of the original differential equations. A comparative study of available methods will therefore be carried out to determine the 'best' for the chosen model.

A steady state reactor model will first be used to compare the various kinetics presented in the literature for the dehydrogenation of ethylbenzene and a suitable set will be chosen for investigation of the proposed cyclic reactor system. The performance of adiabatic reactors in the steady state and operating transiently will be investigated in order to establish the effect of various parameters on the conversion. These results, together with an investigation of the regenerator, will be used to predict operational parameters of the cyclic system.

The cyclic reactor system will then be studied. The usefulness of the predicted parameters from the previous studies will be evaluated and the effect of varying the system parameters will be investigated. The parameters which can be expected to affect the performance of the system are

(a) Reactor parameters - pressure, temperature and concentration.

(b) Period time.

(c) Heat input to the regenerator - inlet temperature and steam flowrate.

(d) Heat capacity of the beds.

(e) Mode of operation - co-current or counter-current.

The parameters which have the major effect on the system will be determined and strategies for design and operation will be deduced. Guidelines for optimisation of the system will also be presented.

CHAPTER 2

THE REACTION SYSTEM AND PROCESS STUDY

The reaction chosen in the previous chapter to illustrate the cyclic reactor system is the catalytic dehydrogenation of ethylbenzene to styrene in the presence of steam. The reaction is industrially important[13,14] and the steam is a suitable heat transfer fluid for use in the regenerator.

2.1 The Dehydrogenation Reaction

The catalytic dehydrogenation of ethylbenzene[13,14,15]

$$C_6H_5CH_2\text{-}CH_3 \rightleftharpoons C_6H_5CH{=}CH_2 + H_2 \tag{2.1}$$

is the only commercial process used for the production of styrene[14] although the catalytic oxidation of ethylbenzene has also been proposed[16]. The reaction is reversible, endothermic and accompanied by an increase in volume. Hence a high equilibrium conversion is favoured by a high reaction temperature and a low ethylbenzene partial pressure. A large number of possible side-reactions have been proposed[17,18] but the most important ethylbenzene consuming side-reactions are those producing benzene and toluene.

$$C_6H_5C_2H_5 \longrightarrow C_6H_6 + C_2H_4 \tag{2.2}$$

$$C_6H_5C_2H_5 + H_2 \longrightarrow C_6H_5CH_3 + CH_4 \tag{2.3}$$

At normal operating conditions these reactions can be considered to be irreversible[19]. Due to the side-reactions, not all the ethylbenzene which disappears in the reactor is converted to styrene and so a term to define the quality of the conversion is required. In the literature, the terms 'yield', 'selectivity', 'efficiency' or even 'conversion' are used and this can lead to some confusion. The following terms are therefore defined.

$$\text{Conversion to component A} = \frac{\text{mol A produced}}{\text{mol ethylbenzene passed}} \qquad (2.4)$$

$$\text{Efficiency} = \frac{\text{mol styrene produced}}{\text{mol ethylbenzene consumed}} \qquad (2.5)$$

If the term 'conversion' is not referred to any particular component it will always refer to the conversion to styrene. The ethylbenzene consuming side-reactions reduce the styrene production. Reaction 2.2 is the reverse of the process used to manufacture ethylbenzene[15,20] and so the benzene production is a loss to the system. As the raw materials comprise about 65% of the final styrene cost[13], it is desirable to operate at a high efficiency.

Pyrolysis of ethylbenzene occurs at temperatures above 540-560°C but, in the presence of steam, it is not significant below 610-615°C[21]. Pyrolysis has been studied by several workers[22-25] and, although styrene is produced, the efficiency is not greater than 74% and may be considerably less[24]. A wide range of by-products is formed[24]. Reaction temperatures in the catalytic dehydrogenation reaction may be as high as 660°C[15] and so, to reduce pyrolysis, the residence times of the reaction mixture in zones without catalyst must be minimised.

The use of a mixed metal oxide catalyst in the presence of steam gives an efficiency of up to 94%[14]. The catalyst[26-28] consists largely of Fe_2O_3 with 2-3% chromia and small amounts of other metal oxides may also be present. An alkali salt is included in the catalyst formulation to promote the reaction

$$C + 2H_2O \longrightarrow CO_2 + 2H_2 \qquad (2.6)$$

Hence regular regeneration of the catalyst to remove deposited carbon is not required.

The main purpose of the steam is to dilute the ethylbenzene and so obtain a low partial pressure without the expensive use of vacuum operation[14,15]. The reaction is then carried out under just sufficient pressure to overcome the pressure losses of the system and the steam/ethylbenzene molar ratio is typically 12-20 for an adiabatic reactor, but may be as low as 6 for a tubular reactor[14]. The maximum operating temperature (650-660°C) is determined by the degree of pyrolysis which can be tolerated and by the catalyst sintering temperature. Operating temperatures are normally in the range 580-650°C[13,14,17].

The equilibrium conversion, x_e, of the dehydrogenation reaction can be calculated from

$$x_e = \frac{-SR + \sqrt{SR^2 + 4(1 + P/Kp)(1 + SR)}}{2(1 + P/Kp)} \qquad (2.7)$$

where SR is the steam/ethylbenzene molar ratio; P the system pressure; and Kp, the equilibrium constant which is given by[29]

$$Kp = \exp(16.12 - 15350/T) \qquad (2.8)$$

where T is the absolute temperature. Figure 2.1 shows clearly the effect of the dilution steam flow. At 600°C the equilibrium conversion increases from 43% to 80% as SR increases from 0 to 12 and it varies almost linearly with temperature over the range. The effect of the system pressure, shown in Figure 2.2, is more pronounced at the lower pressures. It would appear from the figures that conversions of 70-90% could be expected under normal operating conditions, but the reactor size required, and the efficiency, must also be considered. As the equilibrium is approached, the driving force of the reaction, and hence the rate, falls off. Thus, as the conversion increases, the gain from a given increase in reactor size becomes less and, to achieve the equilibrium conversion, an infinitely large reactor would be required.

The rates of reactions 2.1 - 2.3 all depend on the absolute temperature and the quantity of ethylbenzene present but the side-reactions are not subject to the equilibrium effects. Thus, as the

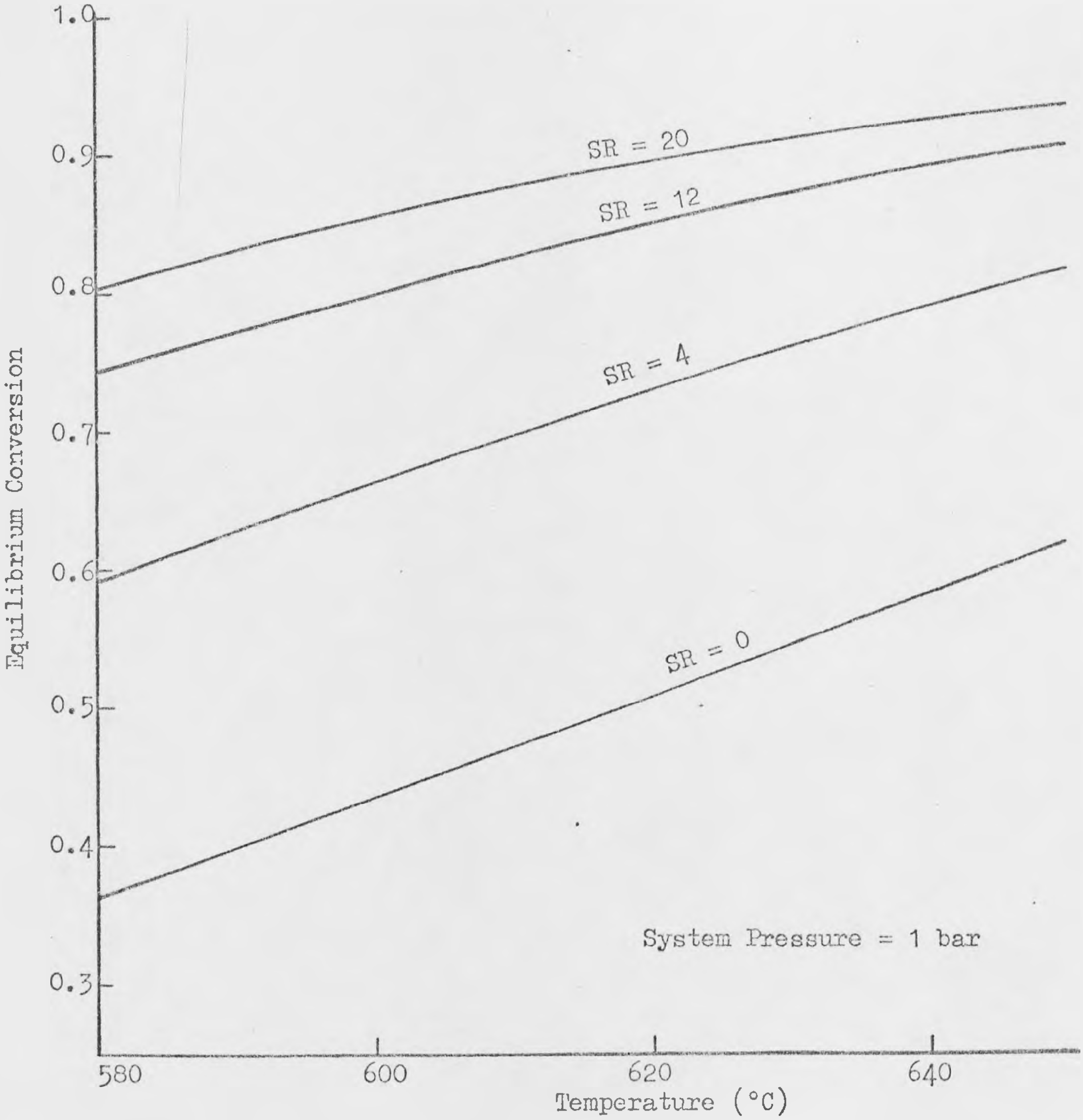

Figure 2.1: Effect of Temperature and Steam/Ethylbenzene Ratio on Equilibrium Conversion.

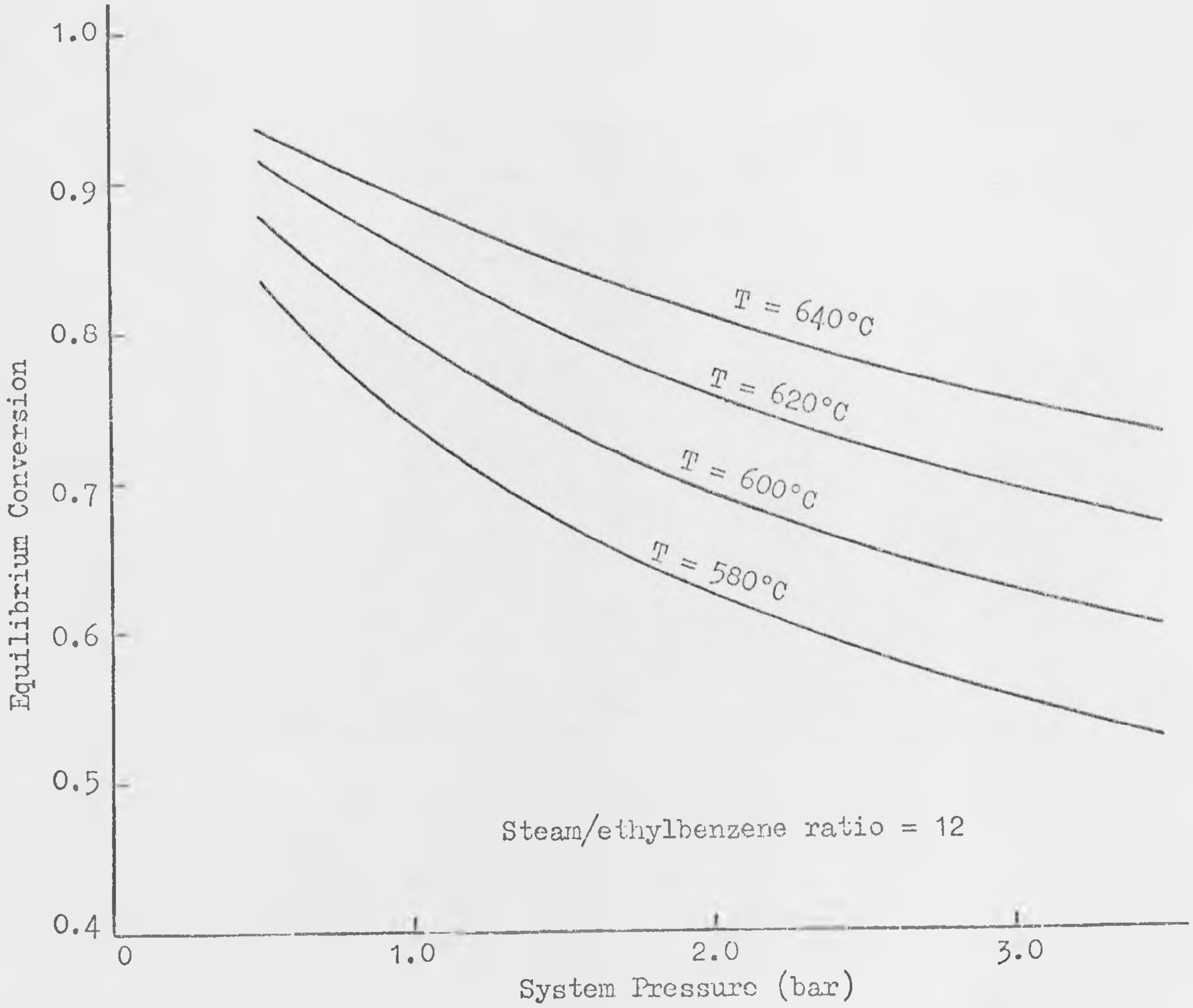

Figure 2.2: Effect of Pressure on Equilibrium Conversion.

conversion increases, the rates of the side-reactions decrease more slowly than that of the dehydrogenation reaction and the efficiency falls[30]. An increase in the system pressure or a decrease in the steam/ethylbenzene ratio reduces the equilibrium conversion. The driving force of the reaction, and hence the efficiency, are therefore lowered[14]. The effect of temperature on efficiency is difficult to assess as, in the literature, an increase in temperature is always accompanied by an increase in conversion. The effect depends on the relative activation energies of the reactions and the values in the literature[17,19,31-33] vary too much for an assessment to be made. However, pyrolysis at higher temperatures reduces the efficiency.

The reactor operation must therefore be a compromise between the various desirable features. A high conversion is desired to reduce the quantity of ethylbenzene which must be recycled as a larger recycle gives higher operating costs[7]. A high temperature gives high reaction rates and therefore minimises the required reactor size. However the high conversion and temperature cause a lower efficiency and so the choice of parameters must be based on economic criteria. The 'best' operating conditions are those which minimise the final product cost.

2.2 Reactor Types

The performance of the proposed cyclic reactor system will be compared with that of reactors currently in use. At present, the dehydrogenation of ethylbenzene is carried out in the following types of reactor:

2.2.1 Single bed adiabatic reactors[14,17,34] have been used for many years[15] and are still the basis of many processes. Steam and ethylbenzene, in a molar ratio of about 15:1, are fed to the reactor at a temperature of 630-650°C and a pressure of 1.2 - 1.8 bars. The feed temperature is gradually raised to 660°C through the life of the catalyst to counteract the effect of falling activity[15]. The steam provides the heat of reaction and the temperature falls along the bed, giving an outlet temperature of about 580°C. The conversion is 35 - 40% with an efficiency of 88 - 92%. The low conversion leads to a large ethylbenzene recycle but the reactor is cheap, reliable and simple to design.

2.2.2 Multibed adiabatic reactors[26,27,35-37] with interbed heating have been introduced more recently to increase the conversion to 50 - 60%. The heating may be accomplished by passage through a heat exchanger or by the direct injection of superheated steam into the reaction mixture. In the latter case, the reaction mixture will enter the first bed with a low steam/ethylbenzene ratio and, if many beds are used, the steam requirement is high. The inlet temperature to each bed is approximately the same at about 630°C. The pressure drop through the system is greater than for a single bed and the initial pressure may be above 3 bars[36]. The efficiency is less than that of a single bed reactor due to the higher pressure and conversion and also because of pyrolysis at the interbed heating. A large number of beds have a large heat requirement and give a low efficiency. In practice it is not worthwhile to use more than two or, at most, three beds[26,35].

The injection of air with the feed and between beds has been proposed[28] in order to produce more nearly isothermal conditions. The combustion with the oxygen provides heat for the reaction and so less steam is required. Conversions in excess of 70% at an efficiency of 85-90% are claimed. However, the report is based on laboratory scale reactor results and it is not used commercially.

2.2.3 Externally heated tubular reactors[14,38] are employed by BASF in Germany. The steam does not supply the reaction heat and so only 6 mols/mol ethylbenzene are used. The temperature rises from 580°C at the reactor inlet to 610°C at the exit and the conversion is 40% with an efficiency of about 90%. The comparatively low temperatures cause minimal pyrolysis. but the efficiency is adversely affected by the small amount of steam used. The cost of the reactor and associated heat transfer equipment is high and so adiabatic reactors are still more commom.

It would seem that the performance of the cyclic reactor system should be compared with that of a multibed adiabatic steady state reactor as this type is becoming more common and gives the highest conversions.

2.3 Kinetics

Typical reactor product compositions given by experimental workers[19,29,39] together with some quoted for industrial reactors[14,15,17,38] are summarised in Table 2.1. All studies show that styrene, benzene and toluene are virtually the only liquid organic products. Heavier hydrocarbons are observed in very small quantities or not at all. The amounts of benzene and toluene vary considerably but most reports show a larger amount of toluene than benzene with the total amount in the region of 7-10% of the ethylbenzene consumed. The off-gas consists mainly of hydrogen (83-92%) and carbon dioxide (6-10%) with small amounts of methane and ethylene. Traces of carbon monoxide and ethane may also be present.

Source	Bogdanova et al[29]	Carra and Forni[39]	Wenner and Dybdal[19]	Sheel and Crowe[17]	Ohlinger and Stadelmann[38]	Kirk-Othmer[14]	Mitchell[15]
Reactor	Isothermal	Isothermal	Isothermal	Adiabatic	Tubular	Adiabatic	Adiabatic
Inlet temperature (°C)	580	630	633	650	580	650	650
Pressure (bar)	-	1.0	1.4	2.37	-	1.3 - 2.0	-
SR	11.8	17.7	22.4	12.3	6.0	11.8-17.7	15.3
Liquid Product (%)							
Ethylbenzene	64.69	64.12	57.6	50.83	c.60	57.05	61.1
Styrene	44.5	33.25	39.3	41.39	38 - 40	38.5	37.0
Benzene	0.14	1.5	0.74	3.00	0.8	1.56	0.6
Toluene	0.67	1.13	2.28	4.78	1.38	2.64	1.1
Others	-	-	0.08	-	0.25	0.25	0.2
Off-Gas Composition (%)							
H_2	92.4	88.29	88.7	83.54	85-88		
CO_2	5.8	6.19	7.2	9.28	6.10		
CH_4	1.5	2.56	1.6	2.80	c.2.0		
C_2H_4	0.4	1.83	0.6	3.18	c.0.4		
CO	-	0.19	0.2	0.04	-		
C_2H_6	-	0.24	1.7	-	-		
Others	-	0.70	-	1.16	-		

Table 2.1: Typical Product Compositions for the Dehydrogenation of Ethylbenzene.

Wenner and Dybdal[19] carried out an experimental investigation and give rate expressions for reactions 2.1 - 2.3 as follows.

$$r_1 = k_1(p_{EB} - p_H p_{ST}/K_p) \qquad (2.9)$$

$$r_2 = k_2\, p_{EB} \qquad (2.10)$$

$$r_3 = k_3\, p_{EB} p_H \qquad (2.11)$$

They evaluated the three rate constants for a catalyst operating without steam but only k_1 for a commercial catalyst operating in the presence of steam. The experimental errors were considered to be too large to permit calculation of k_2 and k_3. In particular, heat losses caused large radial gradients across the catalyst bed. The dehydrogenation reaction rate constant is given by

$$\log_{10} k_1 = \frac{-4770}{T} + 4.10 \qquad (2.12)$$

which corresponds to an apparent activation energy of 91,000 kJ kmol^{-1}.

Bogdanova et al[29] give product analyses of experimental runs at varying temperatures and conversions. The quantities of benzene and toluene produced are low, which may be due to their experimental procedure. The reaction gases are not preheated to the reaction temperature, but enter a heated catalyst bed at about 300°C. Thus the contact time at the reaction temperature is reduced, and the side-reactions are minimised. However the results show clearly the decrease in efficiency with increasing conversion and the equilibrium constant (equation 2.8) is evaluated.

Carra and Forni[39] investigated the reaction in order to obtain a kinetic model. They suggest that the reaction rate depends on the competitive adsorption of ethylbenzene and styrene on the catalyst surface. They show that the forward reaction rate is independent of ethylbenzene partial pressure and steam/ethylbenzene ratio at atmospheric pressure. Above atmospheric pressure the effect on the rate is small. The effect of the reverse reaction is eliminated by operating with a conversion of less than 3%. Increasing the amount of styrene in the feed significantly reduced the forward reaction rate and these observations support the assumption that a Langmuir-Hinshelwood[40] model is the best representation of the system. These observations have been confirmed by Bohm and Wenske[41]. The rate is given by the expression

$$r_1 = k_1 \frac{b_{EB}(p_{EB} - p_{ST}p_H/K_p)}{1 + \Sigma b_i p_i} \tag{2.13}$$

This assumes that the reaction is unimolecular and that the adsorption and desorption processes are in equilibrium. The rate is then controlled by the surface reaction. The adsorption coefficients of the permanent gases and the steam are lower than those of hydrocarbons and so can be ignored. Carra and Forni simplified the rate equation to

$$r_1 = \frac{k_1 b_{EB}(p_{EB} - p_{ST}p_H/K_p)}{1 + b_{EB}p_{EB} + b_{ST}p_{ST}} = \frac{k_1(p_{EB} - p_{ST}p_H/K_p)}{\alpha + p_{EB} + \beta p_{ST}} \tag{2.14}$$

Rase and Kirk[42] had previously shown this to be a suitable expression. The benzene and toluene producing reactions are represented by the single equation

$$r_2 = \frac{k_2\, p_{EB}}{\alpha + p_{EB} + \beta p_{ST}} \tag{2.15}$$

and these two equations were found to agree well with their experimental results. They give tabulated values of k_1 and calculated the activation energy at 191,000 kJ kmol^{-1}. The rate constant can be expressed as[32]

$$k_1 = 3.032 \times 10^6 \exp(-23050/T) \tag{2.16}$$

However, only a single value of k_2 at 630°C is given with no indication of its temperature dependence.

Sheel and Crowe[17] modelled an existing single bed adiabatic reactor and considered reactions 2.1 - 2.3 together with

$$\tfrac{1}{2}C_2H_4 + H_2O \rightarrow CO + 2H_2 \qquad (2.17)$$

$$CH_4 + H_2O \rightarrow CO + 3H_2 \qquad (2.18)$$

$$CO + H_2O \rightarrow CO_2 + H_2 \qquad (2.19)$$

The rate constants were fitted to equations 2.9 - 2.11 and

$$r_4 = k_4 p_{STM} (p_{C_2H_4})^{\frac{1}{2}} \qquad (2.20)$$

$$r_5 = k_5 p_{STM} p_{CH_4} \qquad (2.21)$$

$$r_6 = k_6 \frac{P}{T^3} p_{STM} p_{CO} \qquad (2.22)$$

using a simple plug flow model. The activation energy of reaction 2.1 is given as 91,000 kJ kmol^{-1}. However, the reactor modelled was operating at sub-optimal conditions; in particular a high pressure and low steam/ethylbenzene ratio were employed. The efficiency was therefore low at 85%. The rate constants appear to have been fitted to data obtained at a single set of operating conditions and so it is uncertain how well the proposed kinetics will represent a reactor operating at different conditions.

Abet et al[31] present a simple model and consider reactions 2.1 - 2.3 with the cracking reaction

$$CH_4 \longrightarrow C + 2H_2 \qquad (2.23)$$

The rate constants are presented as functions of temperature and steam/ethylbenzene ratio and the proposed rate equations are similar to those of Sheel and Crowe[17] above. The authors are, however, concerned with economic aspects of the process and no reaction data are presented. Eckert et al[33] present a similar model for the same purpose. Instead of reaction 2.23, they consider the reaction

$$C_6H_5C_2H_5 + 16H_2O \longrightarrow 8CO_2 + 21H_2 \qquad (2.24)$$

and again no reaction data are presented. Abet et al and Eckert et al give the activation energy of the dehydrogenation reaction as 78,000 and 126,000 kJ $kmol^{-1}$ respectively.

Heynen and Van der Baan[43] have recently investigated the dehydrogenation reaction over an alumina-supported uranium dioxide catalyst. This showed high activity and they obtained conversions of 50% at temperatures below 500°C. They confirmed that the rate expression (equation 2.14) given by Carra and Forni[39] gives the best representation of the system. The efficiency was greater than 95% and so side-reactions were ignored. However, this is a novel catalyst formulation and so it is not considered in this research.

Davidson and Shah[18] simulated the process with reactions 2.1 - 2.4, 2.18, 2.19 and

$$C_2H_4 \longrightarrow C_2H_2 + H_2 \qquad (2.25)$$

$$C_2H_2 \longrightarrow 2C + H_2 \qquad (2.26)$$

The rate expressions are similar to those given by Sheel and Crowe[17] above and the rate constants are taken from various sources in the literature. Only the first three reactions were found to give significant conversions. However, although the simulated reactor operates in the presence of steam, the rate constants used for these three reactions are those given by Wenner and Dybdal[19] for a catalyst operating without steam. As the values for k_1 given for operation with and without steam are considerably different, the value of this model is dubious. The model also predicts unreasonably high efficiencies in the range 95-98%[44].

Modell[32] performed an optimisation of reactor temperature profiles using a model comprising only reactions 2.1 - 2.3. The rate expression used for the dehydrogenation reaction was equation 2.14 as given by Carra and Forni[39] and both side-reactions were modelled by expressions of the form of equation 2.15. The individual rate constants for the side-reactions were obtained by assuming that the contribution of each to the value of Carra and Forni is proportional to the relative amounts of benzene and toluene formed. The temperature dependance of Wenner and Dybdal's[19] data was then incorporated into each constant. Unfortunately, equation 2.15 represents a first order reaction and is therefore not suitable for the second order reaction 2.3. Modell showed that the optimum temperature profile to minimize by-product formation is either uniform or slightly rising along the bed. However, all the optimum profiles predicted lie far outside the normal operating range (580-650°C) for this process.

None of the kinetics reviewed can be considered, at this stage, to be entirely satisfactory. The rate expression given by Carra and Forni[39] for the dehydrogenation reaction seems most likely to give a good representation of the system. There is, however, considerable uncertainty in the possible kinetics for the side-reactions. The various kinetics and reaction schemes are summarised in Appendix 1 and will be compared at a later stage when the necessary reactor models have been developed.

2.4 Process Study

Most industrial processes for the dehydrogenation of ethylbenzene operate with a conversion of about 40%. The process as a whole is studied to assess the effect of improved reactor performance on the rest of the process.

2.4.1 Process description

The process has been described by a number of authors[13-15,45-47] and a typical process flowsheet for the Dow[13] process is shown in Figure 2.3. The feed of fresh and recycled ethylbenzene is vapourised and then heated to about 530°C by indirect exchange with the reactor effluent. A small amount (c. 10%) of the dilution steam is added to the ethylbenzene before heating to suppress pyrolysis. The remaining steam is preheated to about 350°C by the reactor products before passing to an externally fired superheater in which it is heated to 720-750°C. The steam and ethylbenzene are mixed as close as possible to the catalyst bed in order to minimise pyrolysis. The feed mixture is at a temperature of 630-650°C. After passing through the heat exchangers, the reactor effluent is cooled by a water spray and then condensed. The aqueous and organic products are decanted and the residual gases, mainly hydrogen, are used as a fuel.

Polymerisation of the styrene in the distillation train must be avoided and sulphur (0.3%) is added as an inhibitor. However polymerisation will still be significant if the styrene is held for a significant period of time above 90-100°C. Thus the columns through which the styrene passes are designed for minimum hold-up and operate under vacuum to keep the temperature below 100°C.

The toluene and benzene are separated from the mixture in the first column and the small amount of ethylbenzene carried over is removed and added to the recycle. The separation of styrene and ethylbenzene is difficult due to their similar boiling points (145°C and 136°C respectively at atmospheric pressure). 80 trays are required and, due to pressure drop considerations, two columns are employed. Recently, however, new tray designs[48] have allowed this separation to be carried out in a single column[45]. The overhead

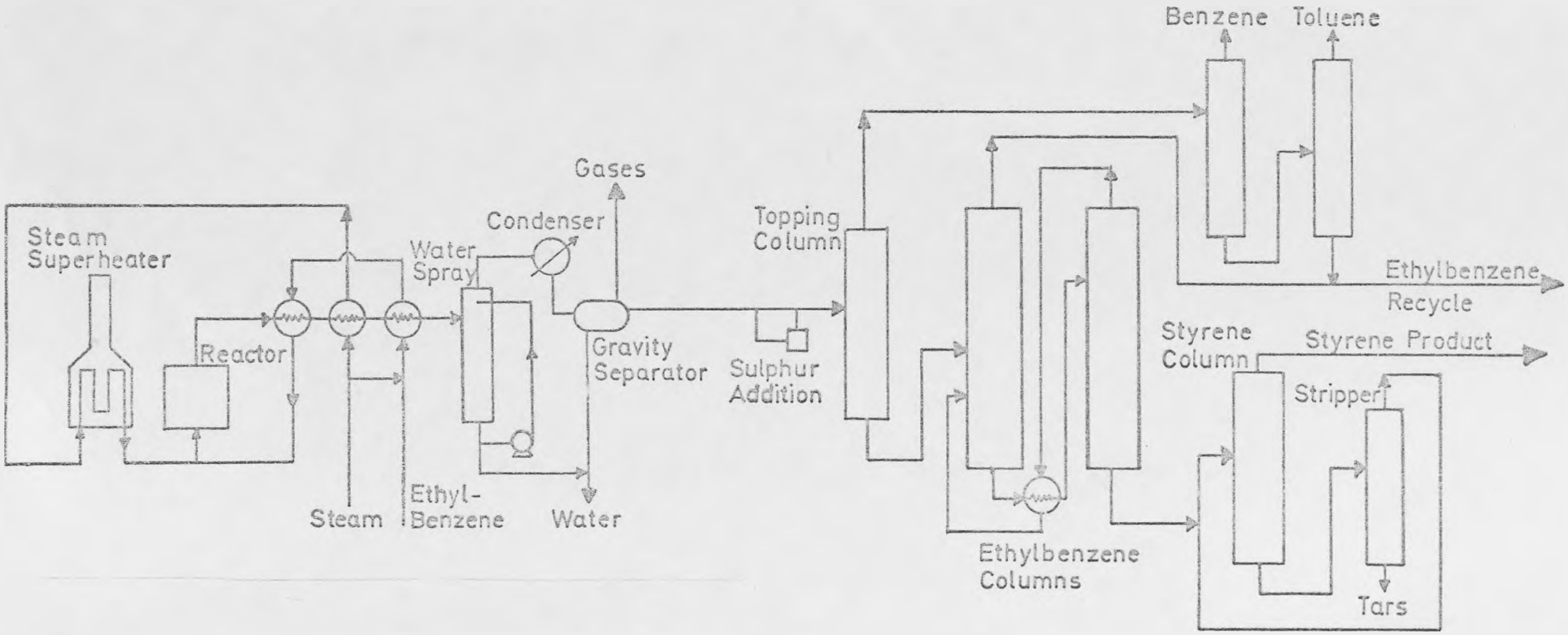
Benzene
Toluene
Gases
Condenser
Topping Column
Steam Superheater
Water Spray
Ethylbenzene Recycle
Reactor
Gravity Separator
Sulphur Addition
Styrene Column
Styrene Product
Stripper
Steam
Ethyl-Benzene
Water
Ethylbenzene Columns
Tars

Figure 2.3: Dow Process Flowsheet for the Dehydrogenation of Ethylbenzene.

product from this separation contains 98% ethylbenzene and is recycled to the reactor. The bottom product passes to the styrene column where a 99.6% styrene product is recovered overhead. The bottoms are stripped of styrene and the stripper bottom product contains the tars and sulphur. 5-15 ppm of p-tert-butylcatechol are added to the styrene product to inhibit polymerisation during storage and transportation.

The flowsheet for the more recent Monsanto distillation train[20,47] is shown in Figure 2.4 and this operates with a reactor section similar to that of the Dow process. The separation of the ethylbenzene and styrene is carried out in the first column and the ethylbenzene recycle is taken from the bottom of the ethylbenzene column. This uses two fewer columns than the above Dow train.

2.4.2 Process Modelling

The process was modelled using the process simulation computer program Flowpack[49]. The process is considered as a network of modules, each of which represents an actual process unit. A more detailed description of the unit models used and the modular flowsheet is given by Heggs and Cockcroft[7].

The reactor model uses specified conversions for each reaction and operates adiabatically, isothermally or with a fixed outlet temperature. The reactor was modelled on the plant data given by Sheel and Crowe[17]. The reactions considered are

$$C_6H_5C_2H_5 \rightleftharpoons C_6H_5C_2H_3 + H_2 \qquad (2.1)$$

$$C_6H_5C_2H_5 \longrightarrow C_6H_6 + C_2H_4 \qquad (2.2)$$

$$C_6H_5C_2H_5 + H_2 \longrightarrow C_6H_5CH_3 + CH_4 \qquad (2.3)$$

$$\tfrac{1}{2}C_2H_4 + H_2O \longrightarrow CO + 2H_2 \qquad (2.17)$$

$$CH_4 + H_2O \longrightarrow CO + 3H_2 \qquad (2.18)$$

$$CO + H_2O \longrightarrow CO_2 + H_2 \qquad (2.19)$$

$$C_6H_5C_2H_5 + C_2H_4 \longrightarrow C_6H_4(C_2H_5)_2 \qquad (2.27)$$

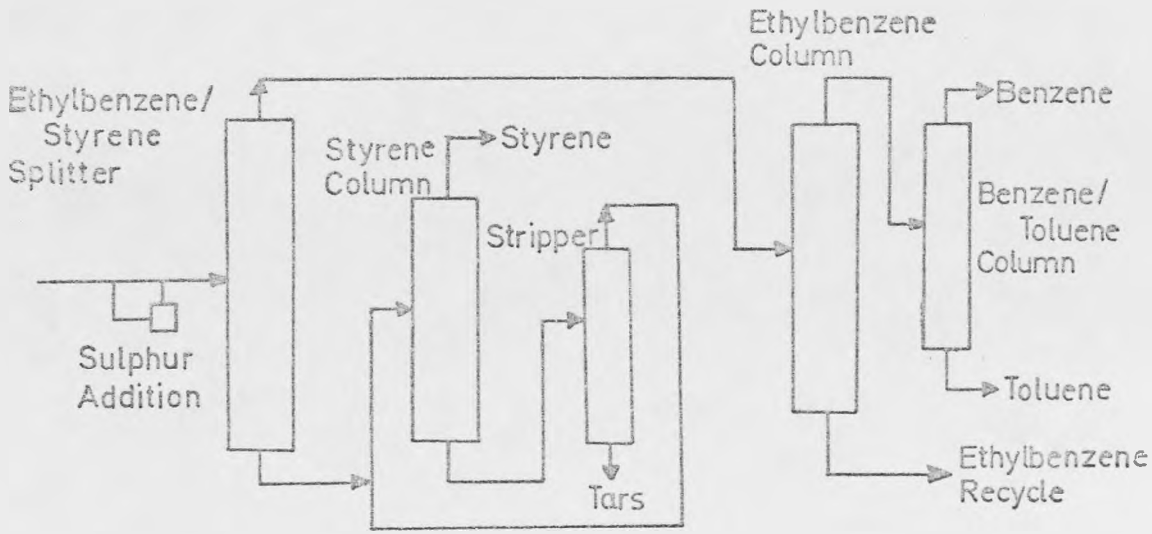
Ethylbenzene/
Styrene
Splitter
Sulphur
Addition
Styrene
Column
Styrene
Stripper
Tars
Ethylbenzene
Column
Benzene
Benzene/
Toluene
Column
Toluene
Ethylbenzene
Recycle

Figure 2.4: Monsanto Distillation Train.

The first six reactions are those given by Sheel and Crowe[17] and the last is introduced to produce the tar required in modelling the distillation train. The effect of this on the reactor will be negligible as the conversion to the tar is only 0.5% and the tar makes up 0.04% of the reactor effluent.

The model for the distillation columns uses the Fenske[50], Gilliland[51] and Underwood[52] correlations and operates in the design mode. The top and bottom recoveries are specified for the key components and the column size, reflux ratio and condenser and reboiler heat loads are calculated. The Dow distillation train was modelled on the data of Mitchell[15] and the specified recoveries were varied to obtain the closest possible agreement. Exact agreement cannot be expected due to the assumption of ideality in the model. The styrene and tar columns of the Monsanto train were also modelled on Mitchell's data and, due to lack of information on the other columns, reasonable values were assumed in order to give the same product recoveries as the Dow train.

2.4.3 Studies

The following reactor types were considered in order to investigate the effect of higher conversion on the process.

(a) A single bed adiabatic reactor: Sheel and Crowe's[17] data is used to represent an existing reactor giving a conversion of 40%. This is the reactor with which the others are compared.

(b) An isothermal reactor operating at 600°C and at 630°C with a conversion of 60%. This could be considered to be a tubular reactor operating at a higher conversion than described previously[38]. This would be achieved by higher temperature or steam/ethylbenzene ratio.

(c) A multi-bed adiabatic reactor, again with a conversion of 60%, is modelled using a fixed reactor outlet temperature. The final exit gas temperature will depend on the number of beds used and so values of 580°C and 600°C are considered. The interbed heating is assumed to be provided by exchange with the dilution steam and so the extra heat is supplied by the steam superheater.

The efficiency will fall if the conversion is increased from 40% to 60%. It is therefore reduced by a further 2% giving equal additional amounts of benzene and toluene. The distillation train will not handle a 50% increase in styrene production without a severe deterioration in product quality. The same styrene production is therefore considered in each case. The ethylbenzene fed to the process is the same but the recycle, and hence the reactor feed, is reduced. Thus, the amount of steam required to maintain the same steam/ethylbenzene ratio is less. The flows through the steam and ethylbenzene preheat heat exchangers are reduced by about 30% and hence the overall heat transfer coefficients are reduced by 25% as the coefficient is proportional to the 0.8 power of the mass velocity[53].

2.4.4 Results

The temperatures and heat loads for the reactor section of the process are shown in Table 2.2. The higher reactor outlet temperatures at the increased conversion cause higher preheat temperatures, but this is paid for in the heat required for the reactor. The superheater load for the isothermal reactor is reduced by 54% at 600°C and 51% at 630°C compared with the single bed adiabatic reactor. The overall heat requirement (reactor and superheater) is reduced by 21% and 17.5% at the same temperatures. The multibed adiabatic reactor shows a reduction of 21% in superheater load with an outlet temperature of 600°C and 22% with an outlet temperature of 580°C.

	Single Bed Adiabatic	Isothermal		Multibed Adiabatic	
		600°C	630°C	Outlet Temp. 580°C	Outlet Temp. 600°C
Ethylbenzene Vapouriser					
Outlet 1 (°C)	160	160	160	160	160
Outlet 2 (°C)	237	238	251	230	238
Heat Load (MJ h^{-1})	2056	1411	1411	1411	1411
Ethylbenzene Preheater					
Outlet 1 (°C)	534	560	586	542	560
Outlet 2 (°C)	433	442	462	429	442
Heat Load (MJ h^{-1})	4111	3035	3274	2885	3035
Steam Preheater					
Outlet 1 (°C)	350	366	381	357	366
Outlet 2 (°C)	319	321	334	313	321
Heat Load (MJ h^{-1})	1746	2186	2332	2089	2186
Steam Superheater					
Heat Load (MJ h^{-1})	6167	2780	2998	4802	4873
Reactor					
Heat Load (MJ h^{-1})	-	2093	2093	-	-

Table 2.2: Temperatures and Heat Loads for Reactor Section.

	40% Conversion	60% Conversion
Ethylbenzene	19.29	6.79
Styrene	15.59	15.59
Benzene	1.50	1.71
Toluene	2.03	2.25
Tar	0.19	1.19
Sulphur	0.36	0.36
Total	38.96	27.89

Table 2.3: Feeds to the Distillation Train (kmol h^{-1})

The change in reactor performance will affect the composition of the feed to the distillation train, and this is shown in Table 2.3. The ethylbenzene flow is reduced by the increased conversion and so the reboiler and condenser heat loads of the columns through which it passes are less. These are shown in Tables 2.4 and 2.5 for the Dow and Monsanto trains respectively. The heat loads on the styrene and tar columns are unchanged as the amount of styrene is the same in each case. The reduced efficiency causes an increase of about 10% in the flows and heat loads in the toluene-benzene separation. This increase should be within the design safety factor of the columns although the quality of the separation may be adversely affected. The overall reboiler and condenser heat requirements for the Dow train are each reduced by over 22% and for the Monsanto train by 35%.

2.4.5 Discussion and Conclusions

There are considerable utility savings to be made by increasing the conversion in the ethylbenzene dehydrogenation reactor. The savings in the reactor heat requirements of about 20% are due to the reduced steam flow. The increase in conversion from 40% to 60% results in a reduction in steam consumption from 5.0 to 4.0 kg/kg styrene produced. The savings are enhanced by operation with the reactor outlet temperature as low as possible because less heat is lost in the condensation of the products. The savings in the distillation train are in the reboiler heat loads, usually supplied by low pressure steam, and the condenser cooling requirements. The monetary value of the savings cannot be determined due to the variation in utility costs from plant to plant. However, the cost of steam is a major operating cost and may comprise 22% of the final styrene cost.[13] The reduced flows in the distillation columns will allow smaller diameter columns

	40% Conversion	60% Conversion	Percentage Change
Topping Column			
Flow (kmol h^{-1})	25.4	15.2	-40.2
Condenser (MJ h^{-1})	1038	682	-34.3
Reboiler (MJ h^{-1})	1369	904	-33.9
1° Ethylbenzene Column			
Flow (kmol h^{-1})	107.7	67.0	-37.8
Condenser (MJ h^{-1})	5225	3048	-41.7
Reboiler (MJ h^{-1})	5397	3195	-40.8
2° Ethylbenzene Column			
Flow (kmol h^{-1})	141.1	127.9	-9.4
Condenser (MJ h^{-1})	6159	5539	-10.1
Reboiler (MJ h^{-1})	5527	4919	-11.0
Benzene Column			
Flow (kmol h^{-1})	4.7	5.3	12.8
Condenser (MJ h^{-1})	193	218	13.0
Reboiler (MJ h^{-1})	222	247	11.3
Toluene Column			
Flow (kmol h^{-1})	2.7	2.8	3.7
Condenser (MJ h^{-1})	151	163	8.3
Reboiler (MJ h^{-1})	151	163	8.3
Overall Heat Loads			
Condenser (MJ h^{-1})	13850	10735	-22.5
Reboiler (MJ h^{-1})	13699	10467	-23.6

Table 2.4: Flows Down Columns and Condenser and Reboiler Heat Loads for Dow Distillation Train.

	40% Conversion	60% Conversion	Percentage Change
Ethylbenzene/styrene splitter			
Flow (kmol h^{-1})	346.0	214.9	-37.9
Condenser (MJ h^{-1})	14926	9157	-38.7
Reboiler (MJ h^{-1})	15093	9282	-38.5
Ethylbenzene column			
Flow (kmol h^{-1})	15.3	7.6	-50.3
Condenser (MJ h^{-1})	545	389	-39.6
Reboiler (MJ h^{-1})	988	553	-44.1
Benzene/toluene column			
Flow (kmol h^{-1})	4.6	5.1	10.9
Condenser (MJ h^{-1})	188	209	11.1
Reboiler (MJ h^{-1})	193	218	13.0
Overall heat loads			
Condenser (MJ h^{-1})	16810	10806	-35.7
Reboiler (MJ h^{-1})	17296	11066	-36.0

Table 2.5: Flows Down Columns and Condenser and Reboiler Heat Loads for Monsanto Distillation Train.

to be used in new plants and the capital cost will therefore be reduced.

These savings can be made with presently available reactors and it is hoped that the proposed reactor system will equal or exceed them. The process has the necessary capacitance to damp out the time varying product composition before it affects the distillation train. All that is required is a sufficiently large holding vessel for the condensed organic product. The effect of the time-varying reactor outlet temperature will be assessed at a later stage when the magnitude of the variation is known.

Thus, this process could be enhanced by the use of the proposed reactor system. Utility savings of at least 20% can be expected in the reactor section and even more in the distillation train. The time varying product of the proposed system should not create any serious problems.

CHAPTER 3

MATHEMATICAL MODELS

3.1 Introduction

The purpose of mathematical modelling is to represent a physical system by mathematical expressions which can then be used to predict the system behaviour. Valstar[54] classifies possible models as mechanistic, empirical or stochastic.

(a) Mechanistic models attempt to describe the actual processes within a system using mass, momentum and energy balances. Experimental data are not essential for their formulation but are useful to verify their predictions. These models can be used for design purposes and the range of their applicability depends on the assumptions made in their formulation. They can also give an insight into the interactions of the processes within the system.

(b) An empirical model correlates observed inputs and outputs of an existing system and is treated as a "black box". The model can simulate the system from which it was derived, but cannot be used with confidence for design at different operating conditions.

(c) Stochastic models, based on statistical considerations, are used where various conditions have a statistical chance of occurring. Residence time distribution problems are an example of this type of model.

The aim of this research is to determine the design parameters of the proposed reactor system and to investigate their interactions. Thus, only mechanistic models will be considered.

The model of the cyclic reactor system as a whole will be discussed in Chapter 5 but individual models for the reactor and the regenerator must first be derived. The performance of the model of the system will be largely determined by that of the reactor model. The regenerator is modelled as a simplified reactor, in which no reaction occurs and only the heat transfer need be considered. Possible reactor and regenerator models will therefore be discussed to determine the simplest which adequately represents the physical situation.

3.2 Packed Bed Models

The flow of a gas through a packed bed is very complex, with considerable local fluctuations due to the random nature of the packing. Simplifying assumptions must therefore be made about the nature of the bed and it is necessary to distinguish between the important mechanisms and those which can be neglected. The bed can be described by a continuum model or by a cell model[54].

3.2.1 Continuum Model

Continuum models are the more common, as shown in the review papers of Froment[9] and Ray[10]. Packed beds are made up of discrete particles, but these are generally small compared with the reactor volume. The continuum model therefore considers the bed to be statistically homogeneous in each phase and the variables are assumed to vary smoothly along the length. This concept is discussed more fully by Beek[55] and allows the bed to be described by a set of differential mass, momentum and energy balances. These form partial differential equations for transient operation and ordinary differential equations in the steady state. Analytical solutions are generally not possible for the reactor equations due to their non-linearity and so approximation methods must be employed.

3.2.2 Cell Model

In this model, the bed is represented by a series of stirred tanks or cells. Each cell contains the volume of a single particle and its associated void space. The model was proposed by Deans and Lapidus[56] and has since been used by several authors[57-60]. The cell model equations are simpler than those of the continuum model as only algebraic equations are required for the steady state and ordinary differential equations for transient operation. However, Valstar[54] has shown that a large number of cells are required to obtain a good representation and the computing time becomes excessive. Roemer and Durban[57] found that the solution of the cell model tends towards that of the continuum model as the number of cells increases and Levenspiel and Bischoff[61] and Feick[62] have shown that the cell model is, in fact, a particular case of the continuum model. Thus the cell model will only be considered insofar as it is used by Gavalas[11,12] in his simulation of a regeneratively cooled reactor system.

This work is concerned only with adiabatic beds and so a one-dimensional model can be used. Plug flow will be assumed. In tubular reactors, which have radial temperature gradients and relatively few particles across the diameter, there may be significant deviations from plug flow[4,63]. Adiabatic reactors, however, normally have a large number of particles across the diameter and so the radial variation of velocity is small. The plug flow model also assumes that axial dispersion is negligible. This has been shown to be the case unless the bed length is small[64,65] and Jefferson[66], in experimental work, found that the effect was too small to measure. The axial diffusion of heat has also been shown to be negligible compared with the transfer due to the bulk flow[64,67,68].

3.3 Reactor Models

The reaction occurs on the catalyst surface, most of which is inside the porous pellets. Hence diffusion of mass and heat between the two phases and within the pellets may be important. Three possible models can be formulated, depending on which diffusional processes are considered.

3.3.1 Pellet Model

This model includes the effects of both interphase and intraparticle diffusion of mass and heat and is discussed in the review papers of Froment[9] and Ray[10]. Individual catalyst pellets are considered in a fluid continuum and the temperature and concentration profiles within a pellet are calculated at each integration step. Separate heat and mass balances are required for each phase and these are coupled by the pellet surface boundary condition. Large computing times are required to solve the model[69,70] as the pellet equations must be iterated at each step to satisfy the boundary conditions. Hence much work has been done to simplify the model. McGreavy and Cresswell[70] have shown that the main resistance to heat transfer is between the pellet and the bulk gas, rather than within the pellet. Thus the temperature profile within the pellet can often be assumed isothermal. The reaction rate, and hence the concentration, within the pellet may be related to that at the surface, or the fluid conditions, by means of an effectiveness factor. Relatively simple correlations for effectiveness factors have been obtained for isothermal pellets. However, for non-isothermal pellets, the evaluation of the effectiveness factor may involve as much effort as solving the original equations[70].

The solution of the pellet model requires effective transport properties within the pellet to be evaluated. Satterfield[71] reviews experimental work in this field and proposes correlations. However, there is some uncertainty in the predicted values even with detailed information on the catalyst structure. This information is not available for the catalyst used in the dehydrogenation of ethylbenzene and hence accurate values cannot be predicted.

3.3.2 Film-resistance Model

The film-resistance model assumes that intraparticle diffusion can be neglected, i.e. the effectiveness factor is unity, but it includes the effect of interphase processes. It has been considered by Liu and Amundson[72,73] and Feick and Quon[69]. Separate heat and mass balances for each phase are again required, but the solution is much quicker than the pellet model as iteration across the pellet is not required. The only transport properties required are the interphase heat and mass transfer coefficients and correlations for these are well established[9].

3.3.3 Pseudo-homogeneous Model

All resistances to heat and mass transfer between the phases and within the catalyst are assumed to be negligible. The temperature or concentration at a given point can then be described by a single value and separate mass and heat balances are not required. As the diffusion processes are neglected, no transport properties are required. Several authors[9,69,74,75] have shown that this model can give different results from a heterogeneous model with an exothermic reaction. In particular, it shows high parametric sensitivity as it cannot account for diffusion control. Nevertheless, it is widely used[76-79], especially in transient studies, because of its simplicity and ease of solution.

3.3.4 Selection of Model

Feick and Quon[69] compared all three models and observed significant differences in results when diffusion processes were important. Under these conditions, a pellet model is required. A simpler model can only be used when some or all of the diffusion processes can be ignored. The effect of the various processes must be determined for the particular reaction being studied; in this work, the dehydrogenation of ethylbenzene.

The intraparticle temperature effects can be assessed from the simple analysis of Prater[80]. The temperature, T_p, at any point within a particle is

$$T_p = T_s - \frac{\Delta H\, D_e}{k_e}(c_s - c_p) \tag{3.1}$$

where c_p is the concentration at the same point. The maximum temperature difference within the pellet can then be obtained by setting c_p to zero.

$$\Delta T\text{max} = T_p - T_s = -\frac{\Delta H\, D_e c_s}{k_e} \tag{3.2}$$

Typical values for these parameters are given in Table 3.1. The effective diffusivity is calculated by the procedure given by Satterfield using quoted catalyst properties for a water-gas reaction catalyst[81] and a gas phase diffusivity given by Perry[82]. The effective thermal conductivity is a typical refractory metal oxide value[83]. The maximum inlet concentration is used and gives a temperature difference of -0.38°C. Feick and Quon[69] suggest that the intraparticle temperature gradient is negligible if

$$\left| \frac{\Delta T\text{max}}{T_s} \right| < 0.001 \tag{3.3}$$

D_e - $0.3451 \times 10^{-5}\ m^2 s^{-1}$

ΔH - $124,900\ kJ\ kmol^{-1}$

k_e - $1.7307\ W\ m^{-1}\,°K^{-1}$

c_s - $1.531 \times 10^{-3}\ kmol\ m^{-3}$

T_s - $903°K$

e - 0.4

ρ_s - $1750\ kg\ m^{-3}$

S_v - $1234\ m^2 m^{-3}$

h - $252.2\ W\ m^{-2}\,°K^{-1}$

k_g - $0.1155\ m\ s^{-1}$

Table 3.1: Data used in estimation of diffusion effects

At 630°C, the above value gives

$$\left| \frac{\Delta T_{max}}{T_s} \right| = 0.0004 \qquad (3.4)$$

and hence the pellet can be assumed to be isothermal.

The effect of intraparticle mass diffusion can be determined from the criterion of Weisz[84]. This states that the diffusion effects can be neglected if

$$\Phi = \frac{\rho_s\ r}{S_v^2 D_e c_s} < 1 \qquad (3.5)$$

where r is the reaction rate ($kmol\ s^{-1} kg\ cat^{-1}$). This depends on the kinetics used, which are summarised in Appendix 1. With the parameter values in Table 3.1, the reaction rates at 630°C of Carra and Forni[39], Wenner and Dybdal[19], Sheel and Crowe[17] and Eckert et al[33] give Φ as 3.5, 0.37, 0.12 and 0.084 respectively. Thus intraparticle diffusion is unlikely to be significant although it may affect results using Carra and Forni's[39] kinetics. However, even then, it is doubtful whether the large computing times required for the solution of a pellet model are justified. There is some uncertainty in the value of the effective diffusivity, and hence in Φ, and this would have to be used in the solution of a pellet model or the evaluation of an effectiveness factor. The results of such a model would therefore also be uncertain and the use of a pellet model will not be considered. Any error introduced by ignoring intraparticle effects will reduce the bed size required for a specified conversion, and this will be shown later to represent the 'worst case' for the cyclic reactor system.

To assess the effect of the film resistance, Feick and Quon[69] suggest that if

$$\left| \frac{T - T_s}{T_s} \right| < 0.001 \tag{3.6}$$

and

$$\left| \frac{c - c_s}{c_s} \right| < 0.001 \tag{3.7}$$

then the film resistance is negligible. These criteria can be solved at the inlet conditions without solving the film resistance model. The heat absorbed by the reaction per unit time, per unit volume is

$$H = (1 - e)\, \rho_s\, \Delta H\, r \tag{3.8}$$

This must also be the amount of heat transferred from the fluid to the catalyst, and hence

$$H = S_v\, h (T - T_s) \tag{3.9}$$

Equating 3.8 and 3.9 gives

$$\frac{T - T_s}{T_s} = \frac{(1 - e)\, \rho_s\, \Delta H\, r}{S_v\, h\, T_s} \tag{3.10}$$

Similar consideration of the mass transfer leads to

$$\frac{c - c_s}{c_s} = \frac{(1 - e)\, \rho_s\, r}{S_v\, k_g\, c_s} \tag{3.11}$$

Equations 3.10 and 3.11 must be solved simultaneously by an iterative technique as the reaction rate is a non-linear function of both temperature and concentration. At 630°C, the reaction rate of Carra and Forni[39] gives

$$\frac{T - T_s}{T_s} = 0.0052 \qquad (3.12)$$

and

$$\frac{c - c_s}{c_s} = 0.056 \qquad (3.13)$$

using the data in Table 3.1. The heat and mass transfer coefficients are evaluated using j-factor correlations[85,86]. The criteria of equations 3.6 and 3.7 are still not satisfied if any of the other reaction rates discussed in Chapter 2 are used. A film resistance model therefore appears to be required. However, this will be compared with a pseudo-homogeneous model because the latter is simpler and is often used.

3.3.5 Stability

The stability of chemical reactors and the problems of multiple steady states and parametric sensitivity have been extensively studied[9,10]. However, these phenomena are only observed with exothermic reactions and stability is not a problem with an endothermic reaction[87,88] such as that considered in this research.

3.4 Regenerator Models

The temperature effects within the catalyst were shown to be insignificant in the reactor. Intraparticle temperature gradients will be reduced if no reaction occurs, and thus the pellets can also be assumed isothermal in the regenerator. It is desirable to use the same type of model for both the reactor and the regenerator. Hence a film resistance, and a pseudo-homogeneous, regenerator model will be compared.

3.5 Model Equations

The model equations are derived with the following assumptions:

(a) Ideal gas behaviour:- This should be satisfactory as the system operates at high temperature and low pressure.

(b) Perfect mixing at the reactor entrance:- The mixing zone will be highly turbulent and so good mixing can be expected. However, if good mixing is not obtained it would not be feasible to allow for this in the model.

(c) No entrance effects:- It is assumed that fully developed flow is established immediately at the entrance to the bed. It would again be difficult to include these effects in the model.

(d) Constant physical properties:- The equations will be written with constant properties. This is a common assumption as it greatly reduces the computing time and should be valid if temperature variations are not large. However, the validity of this assumption will be assessed.

If the pressure drop is included, it is calculated for all models from the Ergun[89] equation

$$\frac{dP}{dz} = - \frac{10^{-5} u(1 - e)}{D_p e^3} \left[\frac{150 \mu (1 - e)}{D_p} + 1.75 \, u \, \rho_g \right] \qquad (3.14)$$

where P is in bars.

3.5.1 Transient Film Resistance Model

The reactor mass and heat balances for the fluid phase are

$$\frac{dc_i}{dt} = - \frac{u}{e} \frac{dc_i}{dz} - \frac{S_v k_g}{e} (c_i - c_{si}) \qquad (3.15)$$

$$\frac{dT}{dt} = - \frac{u}{e} \frac{dT}{dz} - \frac{S_v \, h}{e \rho_g C_{pg}} (T - T_s) \qquad (3.16)$$

and for the solid phase are

$$\frac{\partial c_{si}}{\partial t} = \frac{S_v k_g}{(1-e)e_p}(c_i - c_{si}) + \frac{\rho_s}{e_p} \sum_j a_{i,j} r_j \qquad (3.17)$$

$$\frac{\partial T_s}{\partial t} = \frac{S_v h}{(1-e)\,\rho_s C_{ps}}(T - T_s) - \frac{1}{C_{ps}} \sum_j \Delta H_j r_j \qquad (3.18)$$

where r_j is the rate of the j^{th} reaction (kmol s^{-1}kg cat^{-1}) and $a_{i,j}$ is the stoichiometric coefficient of the i^{th} component in the j^{th} reaction (negative for reactants and positive for products).

Initial Conditions:

$$\left.\begin{aligned} c_i &= c_{si} = 0 \\ T &= f_1(z) \\ T_s &= f_2(z) \end{aligned}\right\} \quad \text{at } z \geq 0 \text{ and } t = 0 \qquad (3.19)$$

Boundary Conditions:

$$\left.\begin{aligned} c_i &= c_{io} \\ T &= T_o \end{aligned}\right\} \quad \text{at } z = 0 \text{ and } t > 0 \qquad (3.20)$$

The regenerator heat balances are

$$\frac{\partial \bar{T}}{\partial t} = -\frac{\bar{u}}{e}\frac{\partial \bar{T}}{\partial z} - \frac{S_v \bar{h}}{e\,\bar{\rho}_g C_{pg}}(\bar{T} - \bar{T}_s) \qquad (3.21)$$

$$\frac{\partial \bar{T}_s}{\partial t} = \frac{S_v \bar{h}}{(1-e)\,\rho_s C_{ps}}(\bar{T} - \bar{T}_s) \qquad (3.22)$$

Initial Conditions:

$$\left.\begin{aligned} \bar{T} &= f_3(z) \\ \bar{T}_s &= f_4(z) \end{aligned}\right\} \quad \text{at } z \geq 0 \text{ and } t = 0 \qquad (3.23)$$

Boundary Condition:

$$\bar{T} = \bar{T}_o \qquad \text{at } z = 0 \text{ and } t > 0 \qquad (3.24)$$

The parameters with a bar are particular to the regenerator and need not have the same value as the corresponding reactor parameters.

3.5.2 Transient Pseudo-Homogeneous Model

Ignoring the effect of the interstitial fluid, the pseudo-homogeneous reactor is described by

$$\frac{\partial c_i}{\partial t} = - \frac{u}{e} \frac{\partial c_i}{\partial z} + \frac{(1-e)}{e} \rho_s \Sigma_j a_{i,j} r_j \qquad (3.25)$$

$$\frac{\partial T}{\partial t} = - \frac{u \rho_g C_{pg}}{(1-e)\rho_s C_{ps}} \frac{\partial T}{\partial z} - \frac{1}{C_{ps}} \Sigma_j \Delta H_j r_j \qquad (3.26)$$

Initial conditions:

$$\left.\begin{array}{l} c_i = 0 \\ T = f_1(z) \end{array}\right\} \quad \text{at } z \geq 0 \text{ and } t = 0 \qquad (3.27)$$

Boundary Conditions:

$$\left.\begin{array}{l} c_i = c_{io} \\ T = T_o \end{array}\right\} \quad \text{at } z = 0 \text{ and } t > 0 \qquad (3.28)$$

The regenerator heat balance is

$$\frac{\partial \bar{T}}{\partial t} = \frac{- \bar{u} \bar{\rho}_g \bar{C}_{pg}}{(1-e)\rho_s C_{ps}} \frac{\partial \bar{T}}{\partial z} \qquad (3.29)$$

Initial Condition:

$$\bar{T} = f_2(z) \quad \text{at } z \geq 0 \text{ and } t = 0 \qquad (3.30)$$

Boundary Condition:

$$\bar{T} = \bar{T}_o \quad \text{at } z = 0 \text{ and } t > 0 \qquad (3.24)$$

3.5.3 Steady State Reactor Models

The steady state reactor models are obtained by omitting the time derivatives from the transient models in the previous sections.

3.5.3.1 Film Resistance Model

The heat and mass balances for the fluid phase are

$$\frac{dc_i}{dz} = - \frac{S_v k_i}{u} (c_i - c_{si}) \qquad (3.31)$$

$$\frac{dT}{dz} = - \frac{S_v h}{u \rho_g C_{pg}} (T - T_s) \qquad (3.32)$$

and for the solid phase are

$$c_{si} = c_i + \frac{(1-e)\ \rho_s}{S_v k_g} \quad \sum_j a_{i,j}\ r_j \qquad (3.33)$$

$$T_s = T - \frac{(1-e)\ \rho_s}{S_v h} \quad \sum_j \Delta H_j\ r_j \qquad (3.34)$$

Boundary Conditions:

$$\left.\begin{array}{l} c_i = c_{io} \\ T = T_o \end{array}\right. \quad \text{at } z = 0 \qquad (3.35)$$

3.5.3.2 Pseudo-homogeneous Model

This is described by

$$\frac{dc_i}{dz} = \frac{(1-e)\ \rho_s}{u} \quad \sum_j a_{i,j}\ r_j \qquad (3.36)$$

$$\frac{dT}{dz} = -\frac{(1-e)\ \rho_s}{u\ \rho_g\ C_{pg}} \quad \sum_j \Delta H_j\ r_j \qquad (3.37)$$

with the boundary conditions 3.35.

3.5.4 Diluted Catalyst Models

It may be desirable to dilute the catalyst by the addition of inert material in order to increase the heat capacity of the bed and allow longer periods in the cyclic reactor system. This inert material is assumed to be particles of catalyst support with the same physical properties as the catalyst. Dilution of the catalyst does not affect steady state reactors and hence it can be ignored in the steady state models. There need be no distinction between catalyst and inert material in the transient regenerator and so the effect of dilution is accounted for, in the models previously described, by the increased bed size.

A distinction must, however, be made in the transient reactor models between the catalyst and the inert material. Assuming that the catalyst and inert material are uniformly mixed, the heat balance on the inert material is

$$\frac{\partial T_I}{\partial t} = \frac{S_v\ h}{(1-e)\rho_s C_{ps}} (T - T_I) \qquad (3.38)$$

with the initial condition

$$T_I = f_2(z) \text{ at } z \geqslant 0 \text{ and } t = 0 \qquad (3.39)$$

The fluid phase heat balance is

$$\frac{\partial T}{\partial t} = -\frac{u}{e}\ \frac{\partial T}{\partial z} - \frac{(1-\gamma)\ S_v\ h}{e\rho_g\ C_{pg}} (T - T_s) - \frac{\gamma S_v\ h}{e\rho_g C_{pg}} (T - T_I) \qquad (3.40)$$

and that on the catalyst is equation 3.18.

The concentration changes much more rapidly than the temperature and the mass transfer between the fluid and the inert material can be assumed to be in equilibrium. The mass balance on the fluid phase (equation 3.15) then becomes

$$\frac{\partial c_i}{\partial t} = -\frac{u}{e}\ \frac{\partial c_i}{\partial z} - \frac{(1-\gamma)\ S_v\ k_g}{e} (c_i - c_{si}) \qquad (3.41)$$

and that on the solid phase (equation 3.17) becomes

$$\frac{\partial c_{si}}{\partial t} = \frac{(1-\gamma)\ S_v\ k_g}{(1-e)e_p} (c_i - c_{si}) + \frac{(1-\gamma)\ \rho_s}{e_p}\ \sum_j a_{i,j}\ r_j \qquad (3.42)$$

The use of a separate heat balance for the inert material may be avoided if its temperature is assumed to be the same as that of the fluid. The fluid phase heat balance is then

$$\frac{\partial T}{\partial t} = -\frac{u}{e}\ \frac{\partial T}{\partial z} - \frac{(1-\gamma)\ S_v\ h}{e\rho_g\ C_{pg}} (T - T_s) \qquad (3.43)$$

and that on the solid is

$$\frac{\partial T_s}{\partial t} = \frac{(1-\gamma)\ S_v\ h}{(1-e)\rho_s\ C_{ps}} (T - T_s) - \frac{(1-\gamma)}{C_{ps}}\ \sum_j \Delta H_j\ r_j \qquad (3.44)$$

The mass balances are again equation 3.41 and 3.42.

A uniform mixture of catalyst and inert material is allowed for in the transient pseudo-homogeneous reactor model simply by reducing the rate constants by a factor which corresponds to the inert fraction of the bed. This represents the use of a greater amount of lower activity catalyst. A separate heat balance for the inert material cannot be used as this would negate the pseudo-homogeneous nature of the model. Hence only the kinetic data, and not the model, need be altered. This approach could be used to represent lower activity catalyst in the film resistance model but it would not correspond to the addition of inert material as the interphase transfer occurs over a larger catalyst volume.

It will be difficult in practice to obtain a uniform mixture of catalyst and inert material. The effect of introducing the inert as a single plug within the bed will be investigated. This requires no modification of the transient reactor equations as the rate constants are simply set to zero in the inert plug.

CHAPTER 4

SOLUTION OF MODELS

4.1 Introduction

The reactor and regenerator models described in the previous chapter consist of partial or ordinary differential equations. Analytical solutions are not possible for the reactor models due to the non-linear reaction term and approximate numerical solutions must be used. Analytical solutions may be obtained for the linear regenerator equations[90], but different solutions are required for different initial bed temperature profiles. Hence, numerical solutions are used throughout. This also allows relatively simple coupling of the transient reactor and regenerator models in the model of the cyclic reactor system.

Reviews of approximation methods in the literature[6,54,91] consider only second order differential equations and there is little guidance on methods suitable for the first order equations used in this work. A number of methods will, therefore, be studied, and their results compared, in order to determine the most suitable one for these equations. The criteria used in this investigation are the following.

(a) Accuracy and stability

(b) Computation time

(c) Computer storage

and (d) Ease of implementation.

An accurate solution, which closely approximates the true solution of the differential equations, is clearly required. A quick solution is also desirable, especially for the transient models, and a compromise may be required if there is a conflict between these criteria. The computer used in this work is an IBM 1130 with a hardware floating-point unit and 16K of core storage. An ICL 1906A was also available. The IBM 1130 is a relatively slow machine by today's standards and so the computing time must be minimised. The computer storage required should not be a problem with the models considered, as a marching technique through time will be used and, thus, previous time levels may be overwritten. Ease of implementation is the least important criterion and this will only be applied to methods of similar accuracy and solution time.

The lack of analytical solutions makes it difficult to assess the accuracy of the approximate solutions of the reactor equations. These are affected by the integration step size and some assessment may be made by observing how step size variation affects the solutions[91]. This approach will be used with the steady state models. However, approximation methods used to solve the transient regenerator models may be assessed by comparison with the analytical solutions. Methods which accurately represent the regenerator need not necessarily give accurate solutions of the transient reactor equations, but it seems likely that they will. Certainly, methods which do not accurately represent the linear regenerator equations will not do so for the non-linear reactor ones. Suitable approximation methods can then be compared on the basis of computing time and the other criteria given above.

Two reactions are considered in the investigation; the dehydrogenation of ethylbenzene (equation 2.1) and also the first order, exothermic oxidation of carbon monoxide in an excess of air:

$$CO + \tfrac{1}{2}\,O_2 \longrightarrow CO_2 \qquad (4.1)$$

This is the reaction considered by Gavalas[11] in his study of a regeneratively cooled reactor. The data used for the dehydrogenation reaction is given in Table 4.1 in which the catalyst properties are

C_{pg} – 2.399 kJ $kg^{-1}°C^{-1}$

ρ_g – 5.475×10^{-4} kg l^{-1}

C_{ps} – 1.047 kJ $kg^{-1}°C^{-1}$

ρ_s – 1.750 kg l^{-1}

e, e_p – 0.4

S_v – 1240 m^2m^{-3}

k_g – 0.1182 ms^{-1}

h – 252.3 $Wm^{-2}°C^{-1}$

u – 0.6197 m s^{-1}

A – 0.00811 m^2

P – 1.7 bar

SR – 14.0

T_{IN} – 630°C

ΔH_1 – 124881 kJ $kmol^{-1}$

ΔH_2 – 101640 kJ $kmol^{-1}$

ΔH_3 – -65090 kJ $kmol^{-1}$

c_{EB_o} – 1.532×10^{-3} kmol m^{-3}

k_1 – $3.032 \times 10^{6} \exp(-23050/T)$ kmol s^{-1}kg catalyst^{-1}

$$r_1 = \frac{k_1(p_{EB} - p_{ST}p_H/K_p)}{\alpha + P_{EB} + \beta P_{ST}}$$

α – 0.06 bar

β – 8.03

Table 4.1: Data for the Dehydrogenation Reaction used in Chapters 4 and 6.

C_{pg} – 1.080 kJ $kg^{-1}°C^{-1}$

ρ_g – 0.4906×10^{-3} kg l^{-1}

C_{ps} – 0.837 kJ $kg^{-1}°C^{-1}$

ρ_s – 1.0 kg l^{-1}

e, e_p – 0.4

S_v – 1000 m^2m^{-3}

k_g – 0.0436 ms^{-1}

h – 50.24 $Wm^{-2}°C^{-1}$

Ze/u – 2.5 s

T_{IN} – 450°C

ΔH – -280515 kJ $kmol^{-1}$

c_o – 1.692×10^{-3} kmol m^{-3}

k_1 – $7.8 \times 10^{7} \exp(-\frac{30000}{1.987}/T)$ kmol $s^{-1}l^{-1}$

$r_1 = k_1c_1$

Table 4.2: Data for the Oxidation Reaction used in Chapter 4

those quoted by manufacturers[30,92] and the surface/volume ratio by Satterfield[71]; the heat and mass transfer coefficients are calculated from j-factor correlation[85,86]; and the heat of reaction and gas specific heat from Sheel and Crowe[17] and Kobe[93] respectively. The remaining data are either typical values, or calculated from the other data. The feed to the reactor contains only ethylbenzene and steam. Table 4.2 shows the data for the oxidation reaction. The values of Gavalas[11] are given together with heat and mass transfer coefficients quoted by Thornton[74] and a typical surface/volume ratio.

In order to simplify the solutions and reduce the computing time, the change in volume during the reaction is ignored and the physical properties and pressure are assumed constant.

4.2 Coordinate System

The transient models described in the previous chapter are presented in Eulerian coordinates, in which the fluid passing a fixed point in the bed is considered. The equations can also be presented in Lagrangian coordinates, in which an element of fluid is followed through the bed. The two forms of equations are discussed by Ames[94] and Fox[95]. The equations are transformed from Eulerian to Lagrangian coordinates by the substitution

$$\theta = t - \frac{ze}{u} \tag{4.2}$$

where ${}^{ze}/_{u}$ is the time taken by the fluid to travel the length z.

The film resistance reactor model (equations 3.15 - 3.20) then becomes:

$$\frac{\partial c_i}{\partial z} = -\frac{S_v k_g}{u}(c_i - c_{si}) \tag{4.3}$$

$$\frac{\partial T}{\partial z} = -\frac{S_v\ h}{u\rho_g\ C_{pg}}(T - T_s) \tag{4.4}$$

$$\frac{\partial c_{si}}{\partial \theta} = \frac{S_v k_g}{(1-e)e_p}(c_i - c_{si}) + \frac{\rho_s}{e_p} \sum_j a_{i,j} r_j \tag{4.5}$$

$$\frac{\partial T_s}{\partial \theta} = \frac{S_v h}{(1-e)\rho_s C_{ps}}(T - T_s) - \frac{1}{C_{ps}} \sum_j \Delta H_j r_j \tag{4.6}$$

Initial Conditions:

$$\left.\begin{aligned} c_i &= f_1(z) \\ c_{si} &= f_2(z) \\ T &= f_3(z) \\ T_s &= f_4(z) \end{aligned}\right\} \quad \text{at } z \geqslant 0 \text{ and } \theta = 0 \tag{4.7}$$

Boundary Conditions:

$$\left.\begin{aligned} c_i &= c_{io} \\ T &= T_o \end{aligned}\right. \quad \text{at } z = 0 \text{ and } \theta > 0 \tag{4.8}$$

The film resistance regenerator model (equations 3.21 - 3.24) becomes

$$\frac{\partial \bar{T}}{\partial z} = - \frac{S_v \bar{h}}{\bar{u}\bar{\rho}_g \bar{C}_{pg}}(\bar{T} - \bar{T}_s) \tag{4.9}$$

$$\frac{\partial \bar{T}_s}{\partial \theta} = \frac{S_v \bar{h}}{(1-e)\rho_s C_{ps}}(\bar{T} - \bar{T}_s) \tag{4.10}$$

Initial Conditions:

$$\left.\begin{aligned} \bar{T} &= f_5(z) \\ \bar{T}_s &= f_6(z) \end{aligned}\right. \quad \text{at } z \geqslant 0 \text{ and } \theta = 0 \tag{4.11}$$

Boundary Condition:

$$\bar{T} = \bar{T}_o \quad \text{at } z = 0 \text{ and } \theta > 0 \tag{4.12}$$

The pseudo-homogeneous reactor model (equations 3.25 - 3.28) in Lagrangian coordinates is

$$\frac{\partial c_i}{\partial z} = \frac{(1-e)\rho_s}{u} \sum_j a_{i,j} r_j \tag{4.13}$$

$$\frac{\partial T}{\partial \theta} = -\frac{u\rho_g C_{pg}}{(1-e)\rho_s C_{ps}}\frac{\partial T}{\partial z} - \frac{1}{C_{ps}}\sum_j \Delta H_j r_j \qquad (4.14)$$

Initial Conditions:

$$\left.\begin{array}{l} c_i = f_7(z) \\ T = f_8(z) \end{array}\right\} \quad \text{at } z \geqslant 0 \quad \text{and} \quad \theta = 0 \qquad (4.15)$$

Boundary Conditions:

$$\left.\begin{array}{l} c_i = c_{io} \\ T = T_o \end{array}\right\} \quad \text{at } z = 0 \quad \text{and} \quad \theta > 0 \qquad (4.8)$$

and the regenerator (equations 3.29, 3.30 and 3.24) is

$$\frac{\partial \overline{T}}{\partial \theta} = -\frac{\overline{u}\overline{\rho}_g \overline{C}_{pg}}{(1-e)\rho_s C_{ps}}\frac{\partial \overline{T}}{\partial z} \qquad (4.16)$$

Initial Condition:

$$\overline{T} = f_9(z) \quad \text{at } z \geqslant 0 \quad \text{and} \quad \theta = 0 \qquad (4.17)$$

Boundary Condition:

$$\overline{T} = \overline{T}_o \quad \text{at } z = 0 \quad \text{and} \quad \theta > 0 \qquad (4.12)$$

The Lagrangian forms of the equations are simpler than the Eulerian forms as certain time derivatives have been eliminated. However, the initial conditions for the reactor models are more complex as $\theta = 0$ is not the same as $t = 0$. For example, if the concentration of reactant, say, is zero at $t = 0$, the concentration at the outlet at $\theta = 0$ is the value after the first residence time. Fox[95] states that "The two forms of differential equation are formally equivalent, but this may not be true for the truncated finite-difference equivalents of these equations." Thus, when comparing finite difference solutions, both forms of the equations will be considered.

4.3 Approximation Methods

4.3.1 Method of characteristics

The method of characteristics[94,96] is generally the most accurate method for hyperbolic partial differential equations[97] such as the Eulerian forms of the transient models. The characteristic directions $(\frac{dz}{dt})$ of the system are first evaluated, along which the partial differential equations become ordinary differential ones. These equations are then solved along the characteristic directions at the intersections of pairs of characteristics. Approximate solutions are normally required to solve these ordinary differential equations although they are an exact representation of the partial differential ones.

The evaluation of the characteristic directions and the equations to be solved along them is shown in Appendix 2 for the film resistance reactor model. The fluid equations (3.15 and 3.16) reduce to equations 4.3 and 4.4 along the characteristic

$$\left.\frac{dz}{dt}\right|_{I} = \frac{u}{e} \tag{4.18}$$

and the solid is represented by equations 3.17 and 3.18 along the characteristic

$$\left.\frac{dz}{dt}\right|_{II} = 0 \tag{4.19}$$

with the initial and boundary conditions 3.19 and 3.20.

These characteristics are shown in Figure 4.1 on a t vs z domain. The fluid characteristic represents the flow through the bed and covers the time interval $\frac{Ze}{u}$, i.e. the residence time. Thus, these equations are the same as the Lagrangian form of the model, in which an element of fluid is followed along the bed. The effect of the transformation (equation 4.2) is to make the fluid characteristic

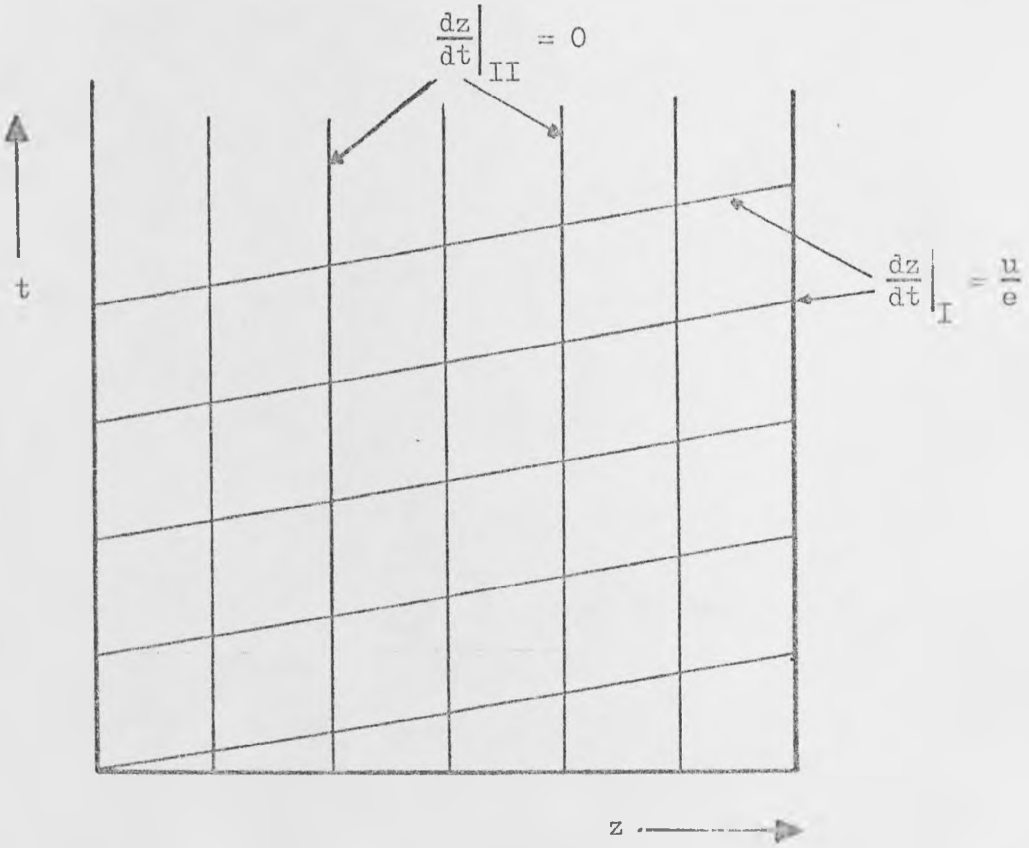
$\frac{dz}{dt}\Big|_{II} = 0$
t
$\frac{dz}{dt}\Big|_{I} = \frac{u}{e}$
z

Figure 4.1: Characteristic Directions for the Transient Film Resistance Reactor Model.

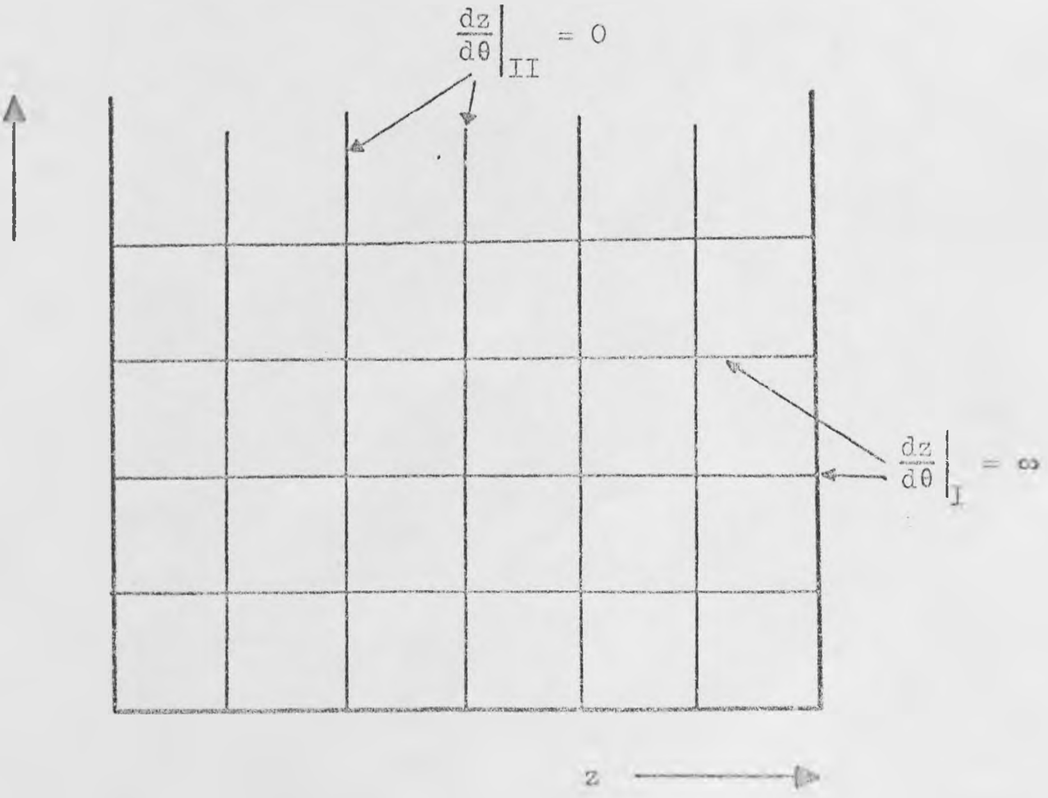
$\frac{dz}{d\theta}\Big|_{II} = 0$
$\frac{dz}{d\theta}\Big|_{I} = \infty$
z

Figure 4.2: Effect of the Transformation to Lagrangian Co-ordinates on the Transient Film Resistance Model Characteristics.

horizontal on a θ vs z domain and thereby give a rectangular grid (Figure 4.2). This is also true for the regenerator equations (3.21 and 3.22) and hence the method of characteristics for the transient film resistance model will not be considered separately from the Lagrangian form of the model.

The transient pseudo-homogeneous reactor model gives separate characteristics for the heat and mass balances. The mass balance (equation 3.25) reduces to equation 4.13 along the characteristic 4.19 and the heat balance (equation 3.26) is

$$\frac{dT}{dz} = - \frac{(1-e)\rho_s}{u\rho_g C_{pg}} \sum_j \Delta H_j r_j \qquad (4.20)$$

along the characteristic

$$\left.\frac{dz}{dt}\right|_{II} = \frac{u\rho_g C_{pg}}{(1-e)\rho_s C_{ps}} \qquad (4.21)$$

The initial and boundary conditions are equations 3.27 and 3.28. The characteristic $\left.\frac{dz}{dt}\right|_{II}$ represents the passage of a 'thermal wave' through the bed, with a residence time of

$$t = \frac{(1-e)\rho_s C_{ps} Z}{u\rho_g C_{pg}} \qquad (4.22)$$

The characteristics are shown in Figure 4.3 at the entrance of the bed. The slope of the characteristic representing the heat balance is more than 2000 times that representing the mass balance using the data in either Table 4.1 or 4.2. This therefore requires the use of a large time step or a small length step for the method used to solve the ordinary differential equations along the characteristics. A large time step causes a large truncation error and a small length step requires excessive computing times. Thus, this method will not be considered for the transient pseudo-homogeneous reactor model.

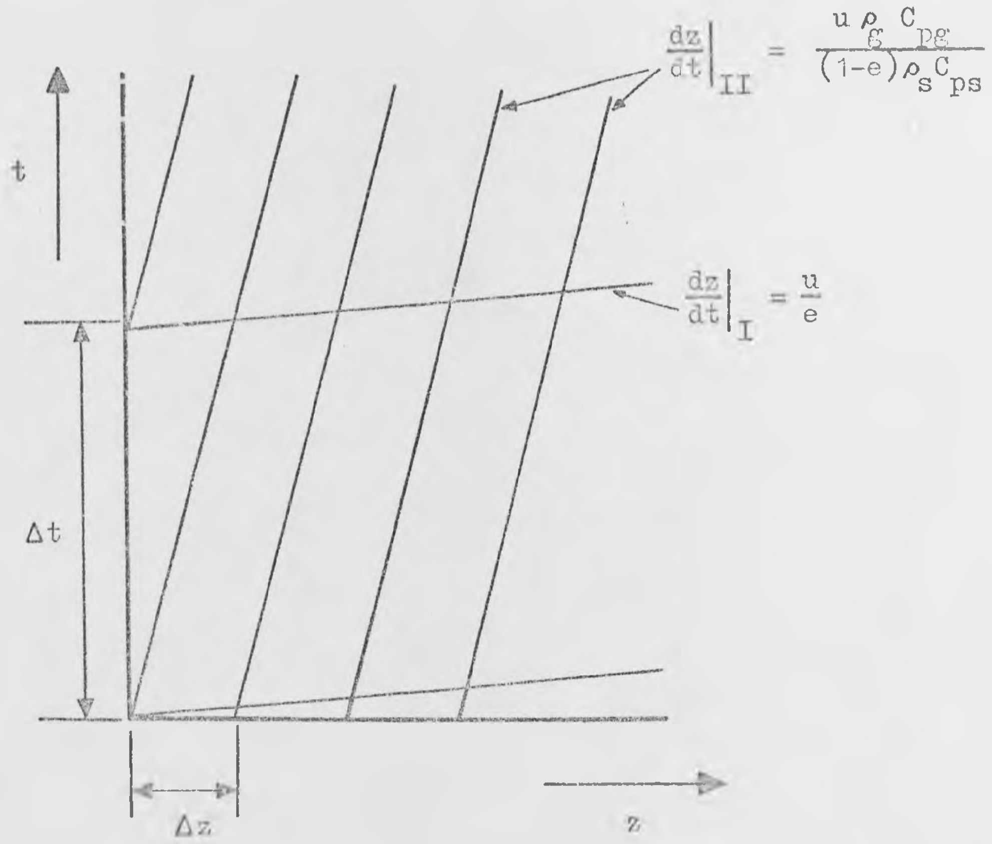
$\left.\frac{dz}{dt}\right|_{II} = \frac{u \rho_g C_{pg}}{(1-e)\rho_s C_{ps}}$
t
$\left.\frac{dz}{dt}\right|_{I} = \frac{u}{e}$
Δt
Δz
z

Figure 4.3: Characteristic Directions for the Transient Pseudo-Homogeneous Reactor Model.

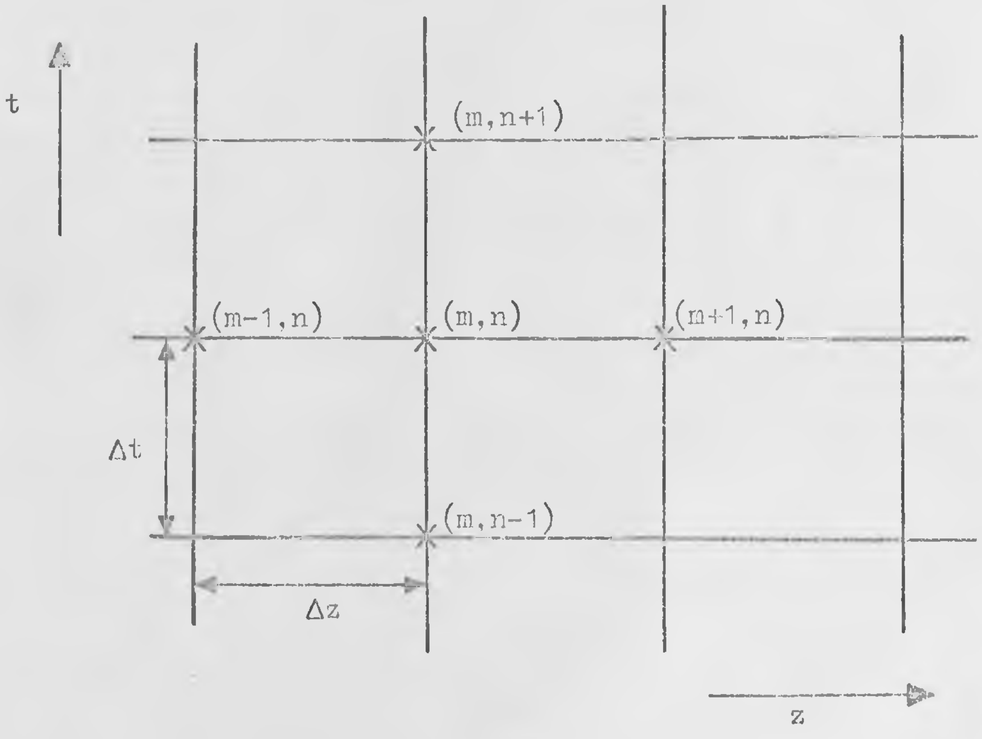
t
(m,n+1)
(m-1,n)
(m,n)
(m+1,n)
Δt
(m,n-1)
Δz
z

Figure 4.4: Section of Finite Difference Grid.

The method of characteristics for the pseudo-homogeneous regenerator (equation 3.29) gives the analytical solution

$$d\bar{T} = 0 \qquad (4.23)$$

i.e. the temperature is constant, along the single characteristic

$$\frac{dz}{dt} = \frac{\bar{u}\,\bar{\rho}_g\,\bar{C}_{pg}}{(1-e)\rho_s\,C_{ps}} \qquad (4.24)$$

with the initial and boundary conditions 3.30 and 3.24.

4.3.2 Finite Difference Approximations

Finite difference approximations[97] are used to reduce differential equations to algebraic ones. For ordinary differential equations, the differences are replaced by finite differences along a line. For partial differential equations, the domain is covered by a rectangular grid and the differentials are replaced by finite differences between the grid intersections. The method for ordinary differential equations is therefore a simple case of that for partial differential ones and will not be discussed separately. A section of grid is shown in Figure 4.4 where m refers to the length direction and n refers to the time direction.

The forward difference approximation is

$$\frac{dT(m,n)}{dt} = \frac{T(m,n+1) - T(m,n)}{\Delta t} \qquad (4.25)$$

and

$$\frac{dT(m,n)}{dz} = \frac{T(m+1,n) - T(m,n)}{\Delta z} \qquad (4.26)$$

This leads to explicit schemes in which no iteration is required, even for non-linear equations. The backward difference approximation is

$$\frac{dT(m,n)}{dt} = \frac{T(m,n) - T(m,n-1)}{\Delta t} \qquad (4.27)$$

and

$$\frac{dT(m,n)}{dz} = \frac{T(m,n) - T(m-1,n)}{\Delta z} \tag{4.28}$$

Both the forward and backward difference approximations are single step formulae, that is, only a single grid increment is considered. The usual central difference approximation is

$$\frac{dT(m,n)}{dt} = \frac{T(m,n+1) - T(m,n-1)}{2\Delta t} \tag{4.29}$$

which is a two-step formula and gives problems at the boundaries. To overcome this, a trapezoidal formula is used. This is

$$\frac{dT(m,n-\frac{1}{2})}{dt} = \frac{1}{2}\left[\frac{dT(m,n)}{dt} + \frac{dT(m,n-1)}{dt}\right] = \frac{T(m,n) - T(m,n-1)}{\Delta t} \tag{4.30}$$

and

$$\frac{dT(m-\frac{1}{2},n)}{dz} = \frac{T(m,n) - T(m-1,n)}{\Delta z} \tag{4.31}$$

These are single step formulae and have been shown[98] to have the same truncation error as the two-step formula.

The use of this central difference approximation for partial differential equations allows the possibility of each derivative being approximated about a different point. The time and length derivatives in equations 4.30 and 4.31 are taken about the points $(m,n-\frac{1}{2})$ and $(m-\frac{1}{2},n)$ respectively. If both derivatives are represented by central difference approximations, it might be better to take them both about the point $(m-\frac{1}{2}, n-\frac{1}{2})$. This would apply regardless of whether or not both derivatives appear in the same equation. A similar situation arises if a backward or a forward difference approximation is used in combination with a central difference one. If the same point is used, the equations become more complex and equations 4.30 and 4.31 become

$$\frac{dT(m-\frac{1}{2},n-\frac{1}{2})}{dt} = \frac{T(m,n) - T(m,n-1) + T(m-1,n) - T(m-1,n-1)}{2\Delta t} \tag{4.32}$$

and

$$\frac{dT(m-\frac{1}{2},n-\frac{1}{2})}{dz} = \frac{T(m,n) - T(m-1,n) + T(m,n-1) - T(m-1,n-1)}{2\Delta z} \tag{4.33}$$

The results obtained using these forms of approximation will be compared with those from the simpler forms previously described.

The use of backward and/or central difference approximations for the reactor equations gives a set of non-linear algebraic equations and iterative solutions are required. Three iterative techniques were compared for this purpose and these are

(a) Simple repeated substitution[109]

(b) Modified secant method[99]

(c) A combination of the Newton and steepest descent methods given by Powell[100].

All these techniques gave identical results with appropriate tolerances on the residual errors. However, to obtain the same accuracy, the repeated substitution method was considerably faster than the other, more sophisticated, techniques. For a typical calculation in which it required 12 minutes computing time, the modified secant method required 32 minutes and Powell's[100] method required 77 minutes. Convergence is always obtained in very few substitutions because the initial guess (the value from the previous step) is close to the required value. The repeated substitution method is therefore used in these iterative solutions.

4.3.3 Method of Lines

The method of lines[94] replaces partial differential equations by differential-difference ones by means of a backward or trapezoidal central difference approximation for the length derivative. These equations are then solved by the 4th order Runge-Kutta-Gill[101] technique or by an Euler (equation 4.25)-Trapezoidal (equation 4.30) predictor-corrector method. Neither a forward nor a two-step central difference approximation can be used, as they require the value at (m+1,n) to evaluate that at (m,n).

Using a backward difference approximation, these differential-difference equations are the same as the equations for the cell model described in Chapter 3. The cell model used by Gavalas[11,12] is a differential-difference representation of the transient pseudo-homogeneous model, equations 3.24 - 3.30.

4.3.4 Methods for Steady State Models

The steady state reactor models (equations 3.31 - 3.37) are solved by the use of finite difference approximations or the 4th order Runge-Kutta-Gill[101] technique.

4.4 Stability

Instability of approximation methods arises when the errors involved in the approximations, or rounding errors, accumulate in successive integration steps. In this case, the solution obtained will not represent that of the differential equations, and it is desirable to eliminate methods which may be unstable.

4.4.1 Transient Models

There are no analytical methods of determining the stability of approximation methods when applied to non-linear equations[102]. The stability depends on the integration step sizes[103] and the simplest method of investigating this is to observe the effect of step size variation on the approximate solutions.

The stability of linear finite difference schemes can be established by the Fourier series method[95,97]. The method is illustrated in Appendix 3 and the stability of the various linear schemes is summarised in Table 4.3. A finite difference scheme is called 'stable' only if it is so for all step sizes. A 'conditionally stable' scheme may be stable or unstable depending on the values of the

Finite Difference Approximation		Pseudo-homogeneous model	Film Resistance Model	
Time derivative	Length derivative		Eulerian	Lagrangian
Forward	Forward	Conditionally stable	Conditionally stable	Conditionally stable
Forward	Backward	Stable	Conditionally stable	Conditionally stable
Forward	Central	Stable	Conditionally stable	Conditionally stable
Backward	Forward	Stable	Conditionally stable	Stable
Backward	Backward	Stable	Conditionally stable	Stable
Backward	Central	Stable	Conditionally stable	Stable
Central	Forward	Stable	Conditionally stable	Stable
Central	Backward	Stable	Conditionally stable	Stable
Central	Central	Stable	Conditionally stable	Stable

Table 4.3: Summary of Stability of Linear Finite Difference Schemes.

coefficients and step sizes. All the explicit forward difference schemes are at least conditionally stable for the regenerator equations but, when the reaction term was included, they were all found to be unstable. All the linear schemes involving only backward and/or central difference approximations were also shown to be stable. These schemes were also found to be stable when the reaction term was included and, with the conditionally stable schemes, no unstable conditions were observed with different step sizes.

Using the method of lines for the Eulerian reactor models, very small step sizes were found necessary to ensure stability and large computing times were required. No instability was observed for the Lagrangian forms with the Runge-Kutta-Gill technique even with large step sizes. However, small step sizes were again required for stability using the predictor-corrector method.

The comparison of approximation methods for transient models will, therefore, only consider backward and/or central difference approximations and the method of lines for the Lagrangian models using the Runge-Kutta-Gill technique.

4.4.2 Steady State Models

The stability of the steady state reactor model solutions was investigated by observing the effect of step size variation, and this is shown in Table 4.4. No instability was observed for any of the methods used. The Runge-Kutta-Gill technique applied to the pseudo-homogeneous model was found to be the most stable to changing step size. The conversion, to five significant figures, was constant if more than 50 length steps were used. This technique is not suitable for the film resistance model as the solid phase equations must be iterated at each Runge-Kutta evaluation. Only finite

No. of steps	Film Resistance Model			Pseudo-homogeneous Model			
	Central Difference	Backward Difference	Forward Difference	Central Difference	Backward Difference	Forward Difference	Runge-Kutta-Gill
25	44.20	43.70	44.80	44.93	44.08	45.56	44.81
50	44.28	44.02	44.56	44.83	44.43	45.39	44.80
100	44.33	44.20	44.46	44.81	44.61	45.32	44.80
200	44.35	44.29	44.42	44.81	44.71	45.22	44.80
400	44.36	44.34	44.40	44.81	44.76	44.99	44.80
600	44.36	44.35	44.39	44.81	44.77	44.76	44.80

Table 4.4: Effect of Step Size Variation on the Steady State Conversion (%) of Ethylbenzene to Styrene for Various Solution Methods.

difference approximations were used for this model, of which the central difference approximation was the least sensitive to changing step size.

4.5 Initial Conditions for Transient Reactor Models

The initial concentrations of reactants and products in the Eulerian reactor models are zero. Hence the reactor can be considered to initially contain only inert fluid, to which the reactant is added at $t = 0$. To allow for the flow of reactant during the first residence time, it would appear that the time step should not initially exceed the residence time, regardless of its subsequent value. This was tested by the use of time steps less than, equal to, and greater than the reactor residence time. However, the difference between the results obtained in each case was negligible unless the time step was several times greater than the residence time, when the truncation errors became significant.

For the Lagrangian models, the initial concentrations along the reactor are those set up as the reactant moves through the bed. To obtain this, the number of time steps during the first residence time must be equal to the number of length steps and it would, therefore, be more convenient if the concentrations could be assumed initially zero. This possibility was tested by comparing two extreme cases; the first, in which the concentrations were zero, and the second, in which the concentrations were the maximum isothermal steady state values. Differences between results obtained for these cases were negligible after only a few time steps as was the effect of initial step sizes less than, equal to, or greater than the residence time.

The initial reactor concentration will, therefore, be assumed zero for all models and the initial conditions will not be considered in determining the time step size.

4.6 Comparison of Transient Solutions

The results obtained using the various approximation methods were compared for both the regenerator and the reactor models. The following observations were made for both the film resistance and the pseudo-homogeneous models.

(a) The results were not significantly affected by the choice of coordinate system.

(b) The results obtained using a backward or central difference approximation, or the Runge-Kutta-Gill technique, for the time derivative were not significantly different provided the approximation used for the length derivative was the same in each case. Thus, the terms 'backward difference solution' and 'central difference solution' will refer to the approximation used for the length derivative.

(c) The results were insensitive to time step size provided it was not too large. A time step of up to 1 second was found to be satisfactory.

(d) When a central difference approximation was used, no significant differences were observed between the results using the equations taken about the same point (e.g. equations 4.32 and 4.33) and those taken about different points within the step (equations 4.30 and 4.31).

(e) The computing time required was found to depend largely on the number of grid points used at each step.

The solution time required for the pseudo-homogeneous model was about 1.25 times that required for the film resistance model if the same solution method was used for each.

4.6.1 Film Resistance Model

Analytical solutions of the Lagrangian regenerator equations have been compared by Price[104] and breakthrough curves tabulated. He gives the solution of Schumann[105] as

$$F = \exp(-Y-X) \sum_{k=0}^{\infty} \left[\left(\frac{X}{Y}\right)^{\frac{1}{2}} I_k \left(2X^{\frac{1}{2}}Y^{\frac{1}{2}}\right) \right] \qquad (4.34)$$

where $$F = \frac{\overline{T}outlet - \overline{T}s,initial}{\overline{T}inlet - \overline{T}s,initial} \qquad (4.35)$$

$$Y = \frac{S_v \, \overline{h} \, \overline{u} \, Z}{\overline{\rho}_g \, \overline{C}_{pg}} \qquad (4.36)$$

$$X = \frac{S_v \, \overline{h} \, \theta}{\rho_s \, C_{ps}} \qquad (4.37)$$

and I_k is a modified Bessel function of the first kind. Price[104] also compared these solutions with a central difference approximate solution and obtained good agreement. Heggs[106] showed that these approximate results agreed well with experimental observations, when experimental conditions corresponded to the assumptions of the model.

Significant differences were observed between the approximate results obtained using a backward or central difference approximation for the length derivative. The length step size also had a significant effect. Breakthrough curves obtained from these solutions are shown, with the analytical solution, in Figures 4.5 and 4.6. The central difference solutions give a good representation of the analytical solution if not less than 100 length steps are used. The backward difference solutions all cross the analytical solution and, even if 1000 length steps are used, these are not as good as the central difference solutions using 100 steps.

The central difference solution of the reactor equations were also insensitive to step size if at least 100 steps were used. This

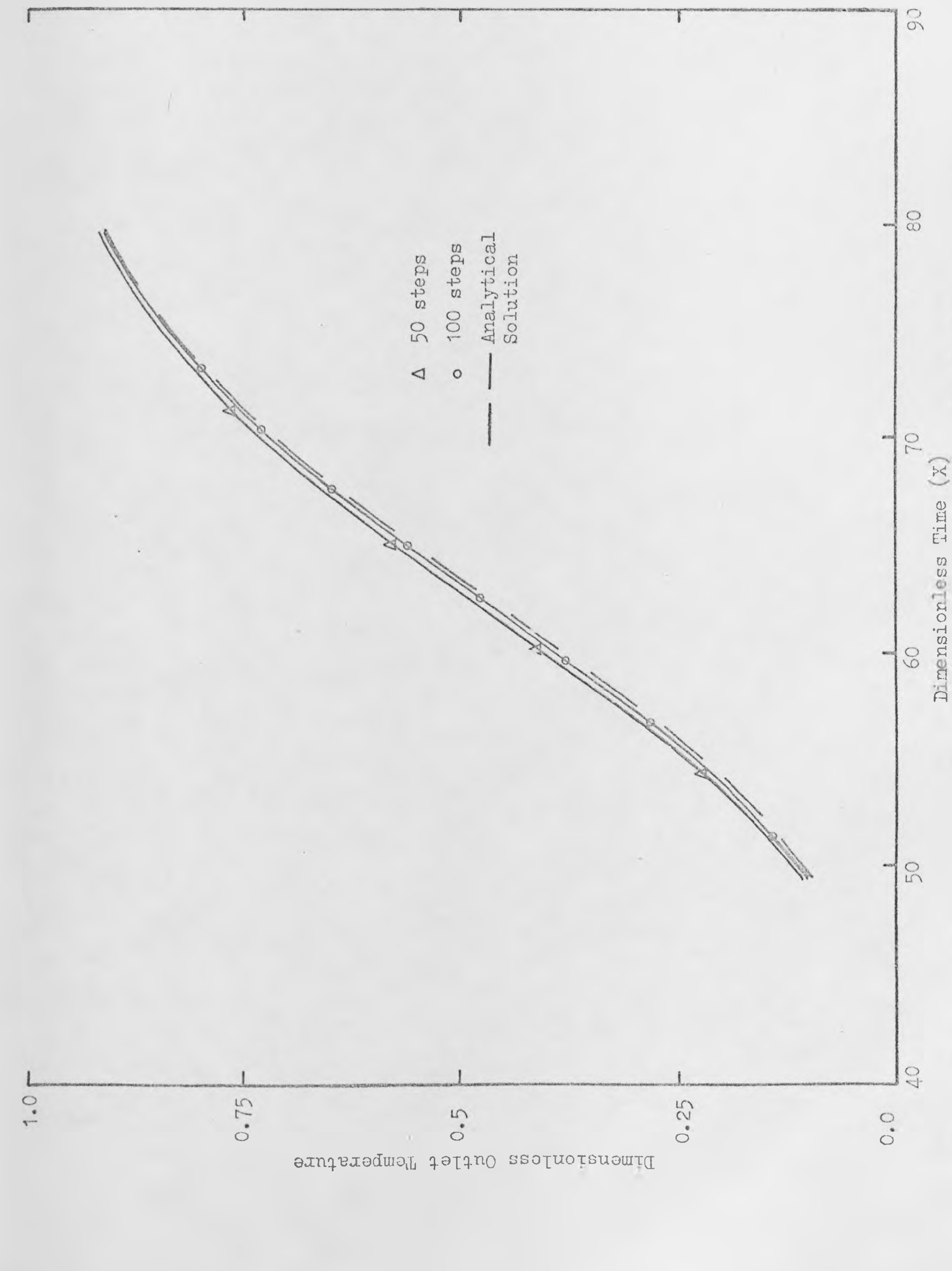

Figure 4.5: Breakthrough Curves for Film Resistance Model Central Difference Solution.

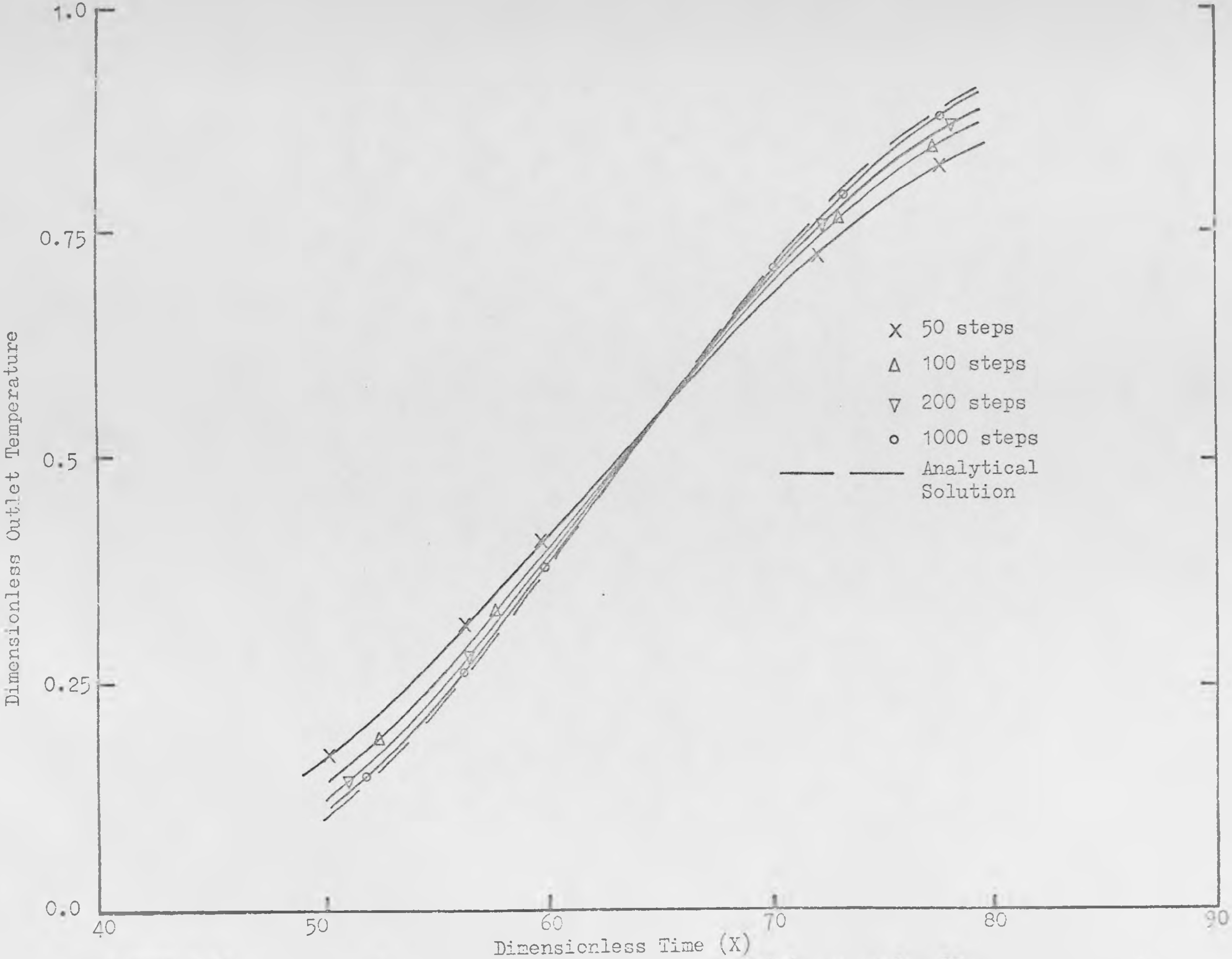

Figure 4.6: Breakthrough Curves for Film Resistance Model Backward Difference Solution.

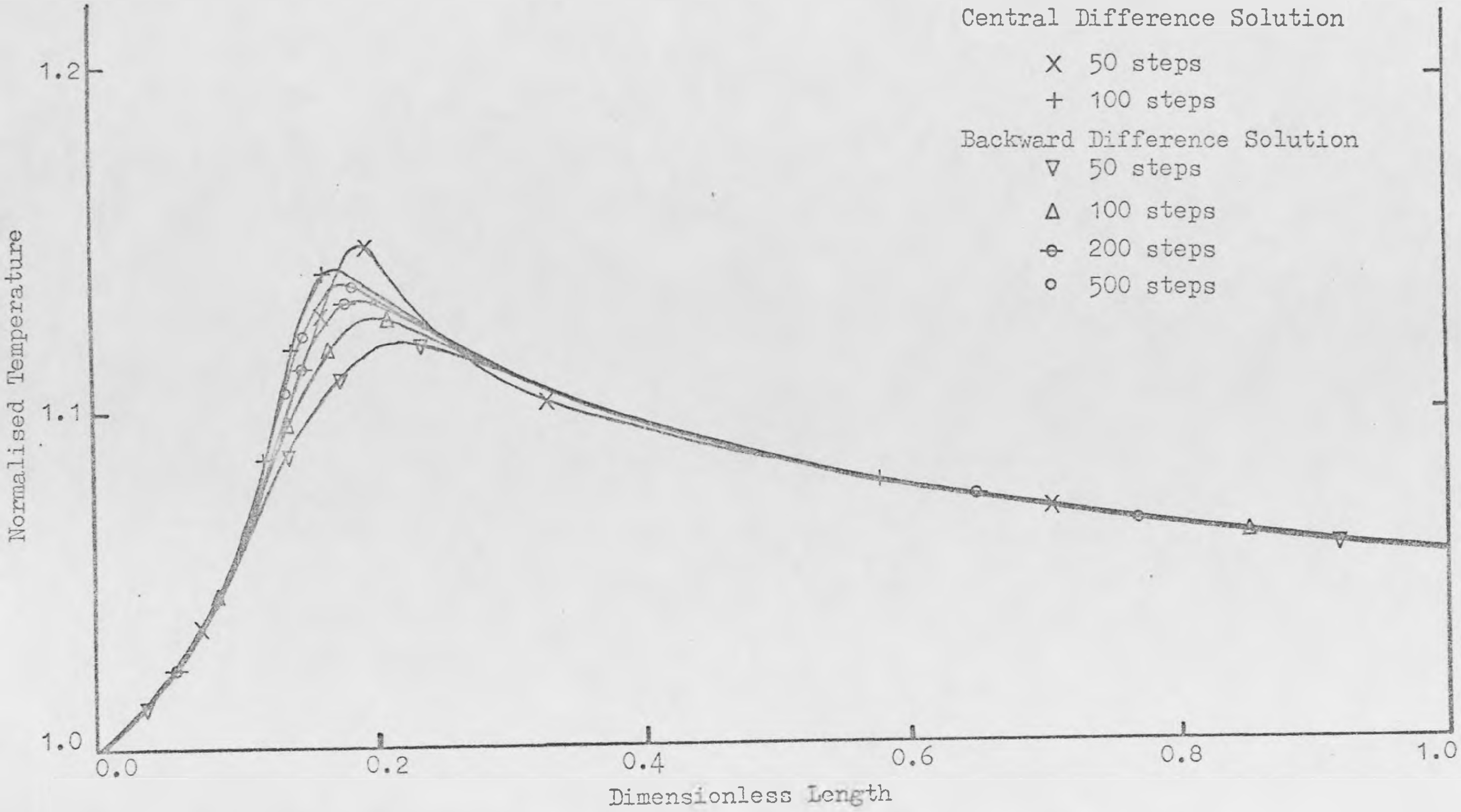

Figure 4.7: Film Resistance Model - Exothermic Reaction Temperature Profiles.

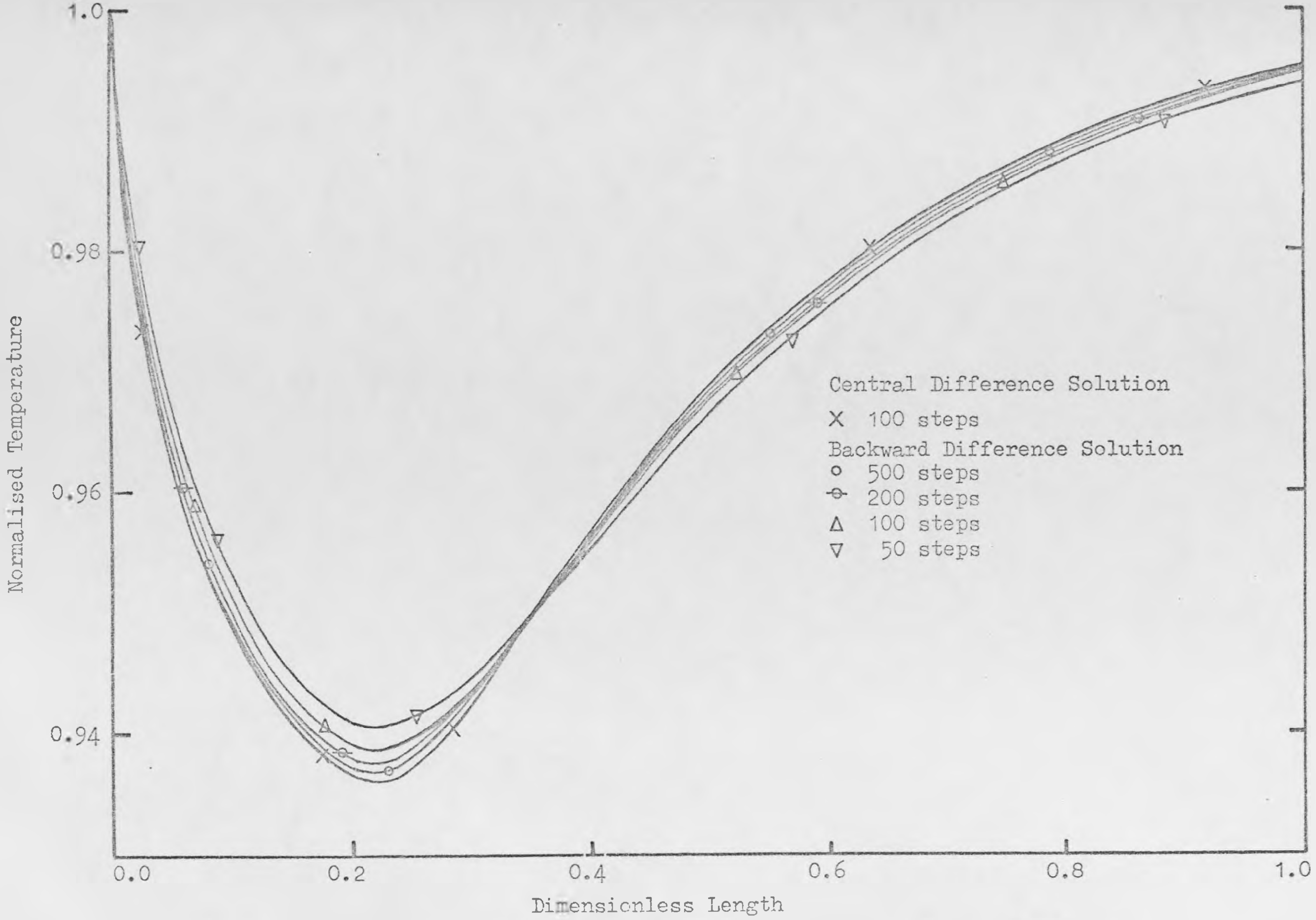

Figure 4.8: Film Resistance Model - Endothermic Reaction Temperature Profiles.

solution is compared with backward difference solutions for the exothermic and endothermic reactions in Figures 4.7 and 4.8 respectively. The temperature profile in each case was initially uniform at unity and the profiles shown are those observed after a given time interval. They are not steady state profiles. The figures show that the backward difference solution approaches, but does not reach, the central difference one as the number of length steps increases. The maximum number of steps was limited to 500 by the computer storage available.

4.6.2 Pseudo-homogeneous Model

The analytical solution of the regenerator equation is obtained by the method of characteristics or by a Laplace transform[90]. The response to a step change of the inlet temperature from $\bar{T}_1$ to $\bar{T}_0$ is given by

$$\begin{aligned} \bar{T} &= \bar{T}_1 \quad \text{for } 0 < t < z/a \\ \bar{T} &= \bar{T}_0 \quad \text{for } \quad t > z/a \end{aligned} \qquad (4.38)$$

$$\text{where } a = \frac{\bar{u}\,\bar{\rho}_g\,\bar{C}_{pg}}{(1-e)\rho_s C_{ps}} \qquad (4.39)$$

Thus the step change passes unaltered through the bed and the outlet temperature also shows a step change. This would be expected in a homogeneous plug flow system but in a heterogeneous system, which this model represents, an S-shaped breakthrough curve is observed[106].

The profiles obtained at a given time after a step change, using a backward and a central difference approximation for the length derivative, are compared with the analytical solution in Figure 4.9. The approximate solutions all show S-shaped profiles which become steeper as the number of length steps increases. The central difference solution is insensitive to length step size if

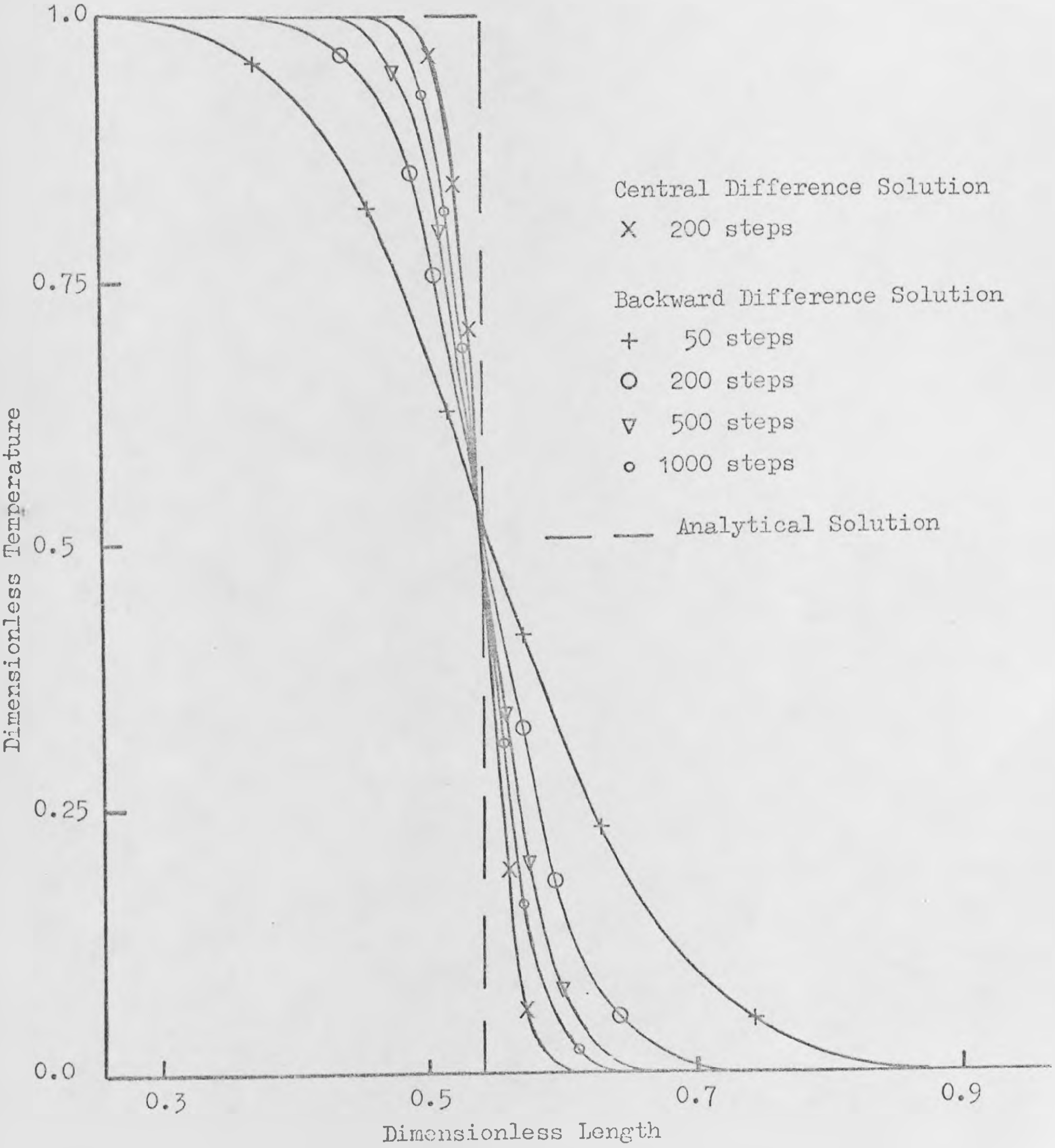

Figure 4.9: Pseudo-Homogeneous Regenerator Model - Temperature Profiles after a Step Change.

at least 200 steps are used, and this is a better representation than the backward difference solution using 1000 steps. When these very large numbers of length steps are used, the solution becomes more sensitive to the time step size. However, a large reduction in time step size is necessary to obtain a significantly closer approach to the analytical solution and the computing time becomes prohibitive.

It is of interest to compare the above analytical solution with that of the cell model given by Gavalas[11]. The cell model regenerator equation at the mth cell is given by

$$\frac{d\overline{T}_m}{dt} = -\frac{a}{\Delta z}\left(\overline{T}_m - \overline{T}_{m-1}\right) \qquad (4.40)$$

and for the same step change, the solution is

$$\overline{T}_m = \overline{T}_o + e^{-\left(\frac{at}{\Delta z}\right)} \sum_{k=0}^{m-1} \frac{\left(\frac{at}{\Delta z}\right)^k}{k!} \left(\overline{T}_1 - \overline{T}_o\right) \qquad (4.41)$$

It can be shown that this gives an S-shaped profile occurring over the same number of cells regardless of the size of Δz. Thus it will only tend to the true solution (equation 4.38) as the number of cells over which the change occurs becomes negligible compared with the total number used. This confirms the observations of Roemer and Durbin[57], who found that the solution of the cell model tends towards that of the continuum model as the number of cells increases and of Valstar[54], who found that a large number of cells were required to give a good representation. The solutions of equation 4.40 obtained using approximation methods were identical to the analytical solution (equation 4.41), again showing that the choice of approximation used for the time derivative has no significant effect.

The film resistance regenerator model has been shown to predict the expected S-shaped breakthrough curves if a realistic interphase heat transfer coefficient is used. If the heat transfer coefficient is allowed to become very large, the solutions tend towards the

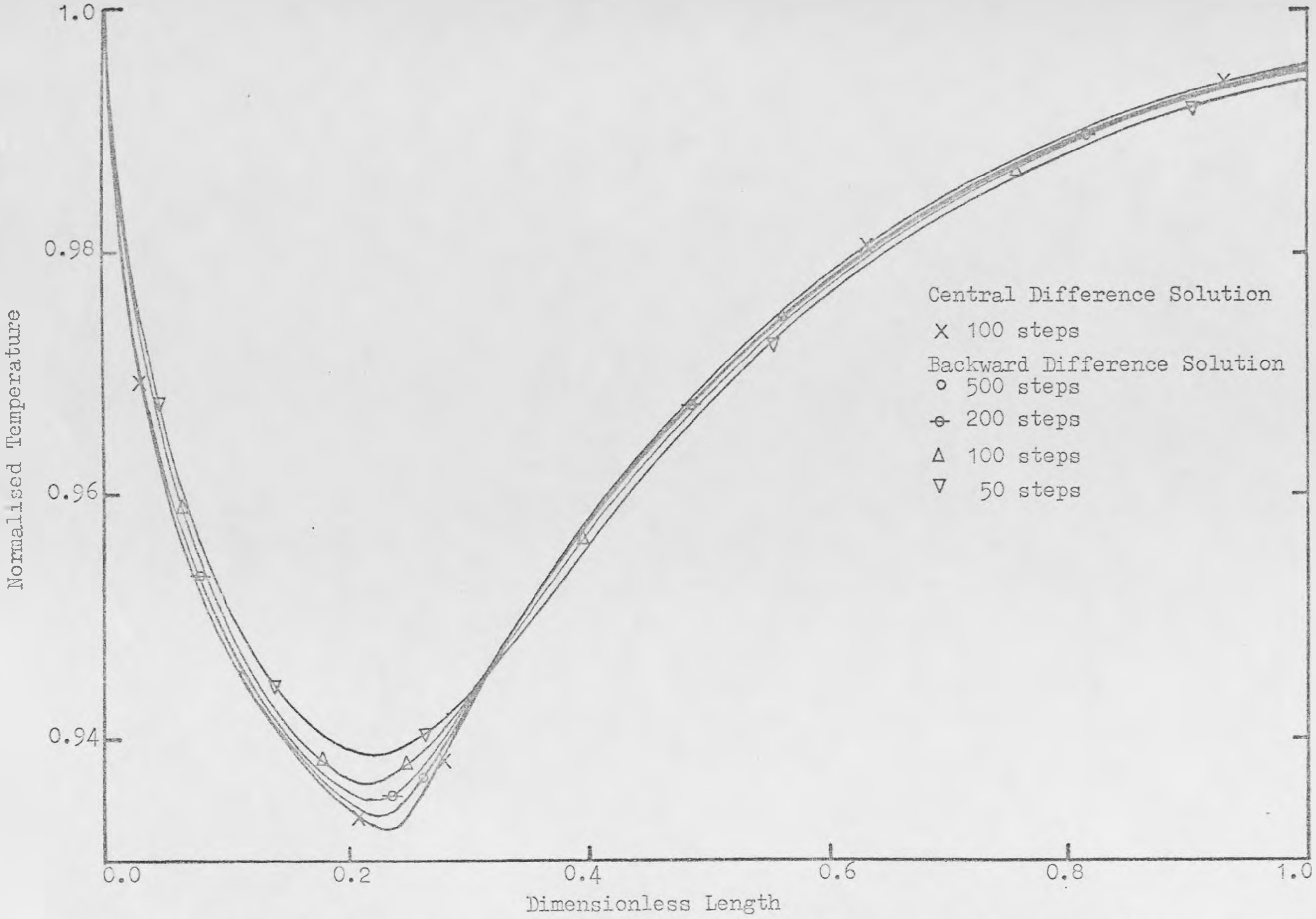

Figure 4.10: Pseudo-Homogeneous Model - Endothermic Reaction Temperature Profiles.

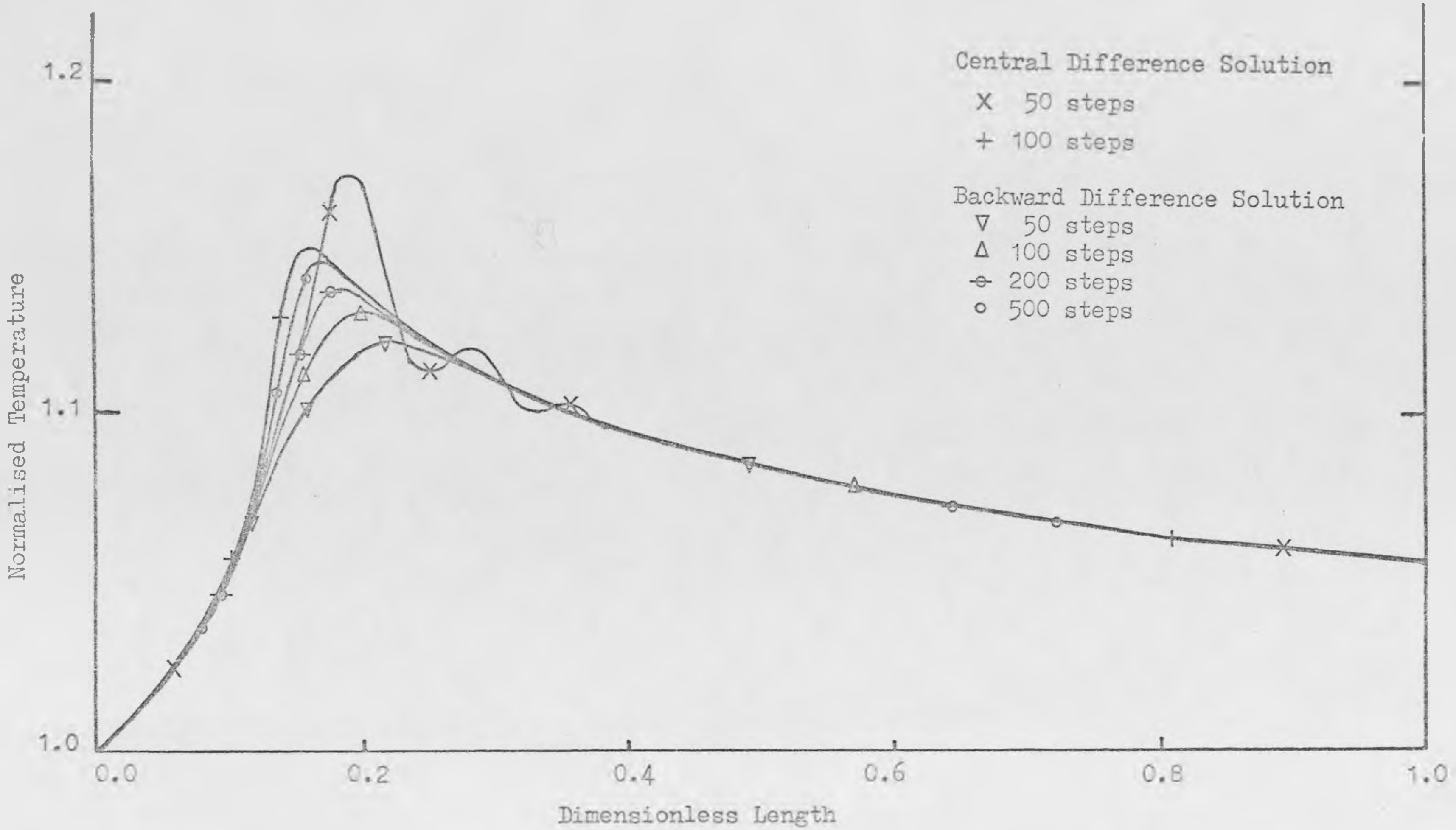

Figure 4.11: Pseudo-Homogeneous Model - Exothermic Reaction Temperature Profiles.

approximate pseudo-homogeneous solutions. However, very small step sizes are again required to approximate the analytical solution. Thus the unrealistic pseudo-homogeneous solution is due to the assumption of an infinite interphase heat transfer coefficient. As the pseudo-homogeneous model is based on this assumption this must throw doubt on its validity.

When the endothermic reaction was included, the central difference solution was again insensitive to length step size above 100 steps. This is compared with the backward difference solution in Figure 4.10 which again approaches it as the number of length steps increases. Both solutions show greater sensitivity to length step size with the exothermic reaction (Figure 4.11). At the temperature peak, the central difference solution shows a decrease in temperature with increasing number of steps whilst the backward difference solution shows an increase. However, the former is the less sensitive to step size variation.

The film resistance reactor model solutions also tended towards the pseudo-homogeneous solutions if the interphase transfer coefficients were allowed to become very large.

It is clear from Figure 4.11 that the use of a backward difference solution with few length steps may hide temperature runaway when it should be predicted by the model. This was found to be the case in the situation considered by Gavalas[11]. He used only 50 length steps on such a model and obtained stable reactor operation. However, if the number of length steps is increased or a central difference solution is used, temperature runaway is observed. Under similar conditions the film resistance model does not predict runaway. Thus a seemingly correct solution is obtained because the numerical inaccuracy does not give the true solution.

4.7 Comparison of Steady State Solutions

Typical steady state reactor results obtained using the various approximation methods are shown in Table 4.4. These are for the dehydrogenation reaction using the data in Table 4.1. The central difference and Runge-Kutta-Gill solutions of the pseudo-homogeneous model are almost identical and, from the consideration of stability to step size variation, these would seem to be the most correct. The other two finite difference solutions are on either side of this. The central difference solution of the film resistance model is also between the other two and so would seem to be the best solution although it requires the greatest computing time.

The two models give slightly different results but the solution of the film resistance model tends towards that of the pseudo-homogeneous model as the heat and mass transfer coefficients increase, i.e. as the solid phase temperature and concentration tend towards those of the gas phase.

4.8 Discussion and Conclusions

The analytical solution of the transient pseudo-homogeneous regenerator model does not represent the physical situation, due to the assumption of no resistance to interphase heat transfer. It is therefore unlikely that the transient reactor model is valid. Approximate results may appear to give a good representation, but this is likely to be due to differences between these and the true analytical solution. The transient film resistance model can represent the regenerator adequately depending on the solution method employed. This model is therefore more likely to represent the transient reactor. As the computing time required for the pseudo-homogeneous model is greater, there is no advantage in its use for transient situations, except in that it is easier to program. Hence, the film resistance model will be used in all transient studies.

The difference between the two steady state reactor models is due only to the effect of the interphase resistance. The assumption of no interphase resistance was shown to be invalid in transient situations, but it seems acceptable in the steady state reactor models, as the conversions given by the two models differ by only about 1%. It therefore appears that either model may be used in the steady state.

The transient results are not affected by the choice of approximation used for the time derivative. In order to minimize computing time, a backward difference approximation is desirable. The approximation used for the length derivative has a significant effect on the results. The central difference solution is always better than the backward difference one and 100 length steps are sufficient. The method of lines, which uses a backward difference approximation, is therefore not satisfactory. The solutions are insensitive to time step size providing it does not become too large. A time step of 1 second is used as the maximum satisfactory value. The choice of coordinate system does not affect the transient results but the Lagrangian equations are simpler and quicker to solve. Similarly, it is not worthwhile to take the finite difference approximations about the same point.

Gavalas[11,12], in his study of a regeneratively cooled reactor, used a pseudo-homogeneous cell model. Both the pseudo-homogeneous model and the cell model have been shown to be unsatisfactory. It has also been shown that the operating conditions in his report[11] predict temperature runaway, but this is hidden by inaccuracies in his numerical solution.

The model used in this work for transient studies is, therefore, the film resistance model. This will be solved by the use of backward and central difference approximations for the time and length derivatives respectively. This finite difference representation is shown in Appendix 4. Both steady state models are considered. The pseudo-homogeneous model will be solved by the Runge-Kutta-Gill technique, and the film resistance model by means of a central difference approximation.

CHAPTER 5

THE CYCLIC REACTOR SYSTEM

The principle of the cyclic reactor system was outlined in Chapter 1 but, in order to design a practical system, the constraints of the given process must be considered. The system is therefore discussed with reference to the dehydrogenation of ethylbenzene to styrene. This is an endothermic reaction and hence, to approximate the optimum temperature profile, a close approach to saturation is desired in the regenerator.

5.1 Development of a Practical System

A simple reactor system based on the principles discussed in Chapter 1 is shown in Figure 5.1, where the two beds are identical and the inlet ethylbenzene and steam temperatures to the system are fixed. Bed A operates as the reactor and bed B as the regenerator. The temperature level in the reactor falls during the period because the reaction is endothermic. Bed B, which was the reactor in the previous period, is heated by the steam entering the system through the 4-way valve. After leaving bed B, the steam mixes with the ethylbenzene feed and passes to the reactor. The reactor products leave the system by the 4-way valve. At the end of the period, the valve is rotated through 90° which reverses the flows through the beds. The flows into and out of the system do not change. The steam now heats bed A and bed B is the reactor. Cyclic steady state operation of the system is achieved when conditions at a given time during the cycle are the same in successive cycles.

The temperature variation of the steam leaving the regenerator causes a corresponding variation of the reactor feed temperature. However, the regenerator outlet temperature rises during the period

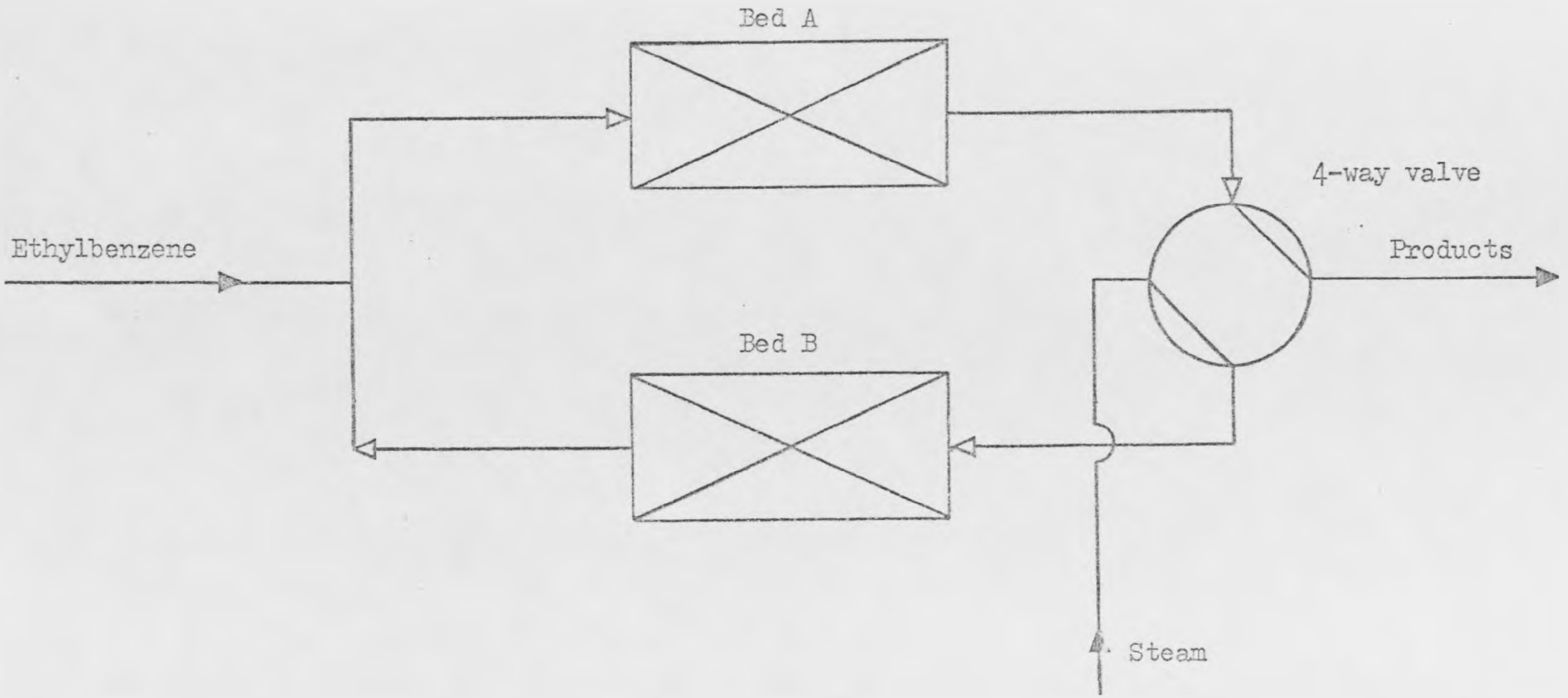
Bed A
4-way valve
Ethylbenzene
Products
Bed B
Steam

Figure 5.1: Simple Cyclic Reactor System.

as the bed heats up and the effect on the reactor feed temperature may partially offset the fall in temperature caused by the reaction. The conversion from the reactor falls during the period due to the falling temperature and the overall conversion of the system is therefore taken as the average over a period.

This simple system usefully illustrates the cyclic operation but it does not take into account the constraints on temperature levels which were discussed in Chapter 2. Temperatures of up to 660°C are used[15] towards the end of the catalyst life to counteract reduced activity, but 650°C is quoted by catalyst manufacturers[30] as a more acceptable maximum temperature. This gives the maximum catalyst performance with an acceptable level of by-product formation. In a steady state reactor, the minimum feed temperature is determined by the acceptable level of conversion. The reaction heat for the cyclic reactor is supplied by the heat stored in the bed and so the effect of the feed temperature on conversion is less significant. However, it is undesirable to have a large temperature difference between the reactor feed and the catalyst at the bed entrance as thermal shock may damage the catalyst. Hence, if the bed approaches saturation, the feed temperature should be close to that of the regenerating steam. This cannot be the case throughout the period, because the feed temperature changes, and a layer of inert material at the front of the bed could be used to lessen the temperature fluctuation of the catalyst.

The temperature of the catalyst in the regenerator approaches the steam temperature because of the high interphase heat transfer. Similarly, the temperature of the reaction mixture tends towards that of the catalyst in the reactor. Thus, the regenerating steam temperature cannot exceed 650°C and consequently the temperature of the steam mixing with the ethylbenzene is below this value. The ethylbenzene feed temperature cannot be greater than 540°C without pyrolysis occurring[21] and it was shown in Chapter 2 that this requires a diluent steam temperature of about 740°C to produce a reactor feed temperature of 630°C. A superheater is therefore required between the regenerator and the entrance of the ethylbenzene feed to raise the temperature of the steam. This now allows the above temperature constraints to be satisfied.

Figure 5.2 shows the revised system, including the superheater. Bed A is again the reactor, and the valve directing the steam feed and the reactor products operates as before. The additional 4-way valve directs the steam leaving the regenerator to the superheater, and the ethylbenzene/steam mixture to the reactor. The flow through the superheater is always in the same direction and both valves are switched simultaneously at the end of each period.

The reactor system described above considers the same steam flow through both the reactor and the regenerator. However, heat balances over the two beds show that the diluent steam flow is not sufficient for the regenerator. Considering only the dehydrogenation reaction and using the nomenclature in Figure 5.2, where the temperatures shown are average values over the period of t_f seconds, the enthalpy change of the catalyst in the reactor for an average conversion, x, is

$$H = F_{EB}\, x\, \Delta H t_f - (F_{EB} MW_{EB} + F_{STM} MW_{STM}) C_{pg} (T_{IN} - T_{OUT}) t_f \qquad (5.1)$$

where F_{STM} is the diluent steam flow and the change in volume with the reaction is ignored. The specific heats of steam and ethylbenzene are very close and are assumed equal. The variation with temperature is neglected. This must also be the enthalpy change of the bed during the regenerator period and hence

$$H = \overline{F}_{STM} MW_{STM}\, C_{pg}\, (\overline{T}_{IN} - \overline{T}_{OUT}) t_f \qquad (5.2)$$

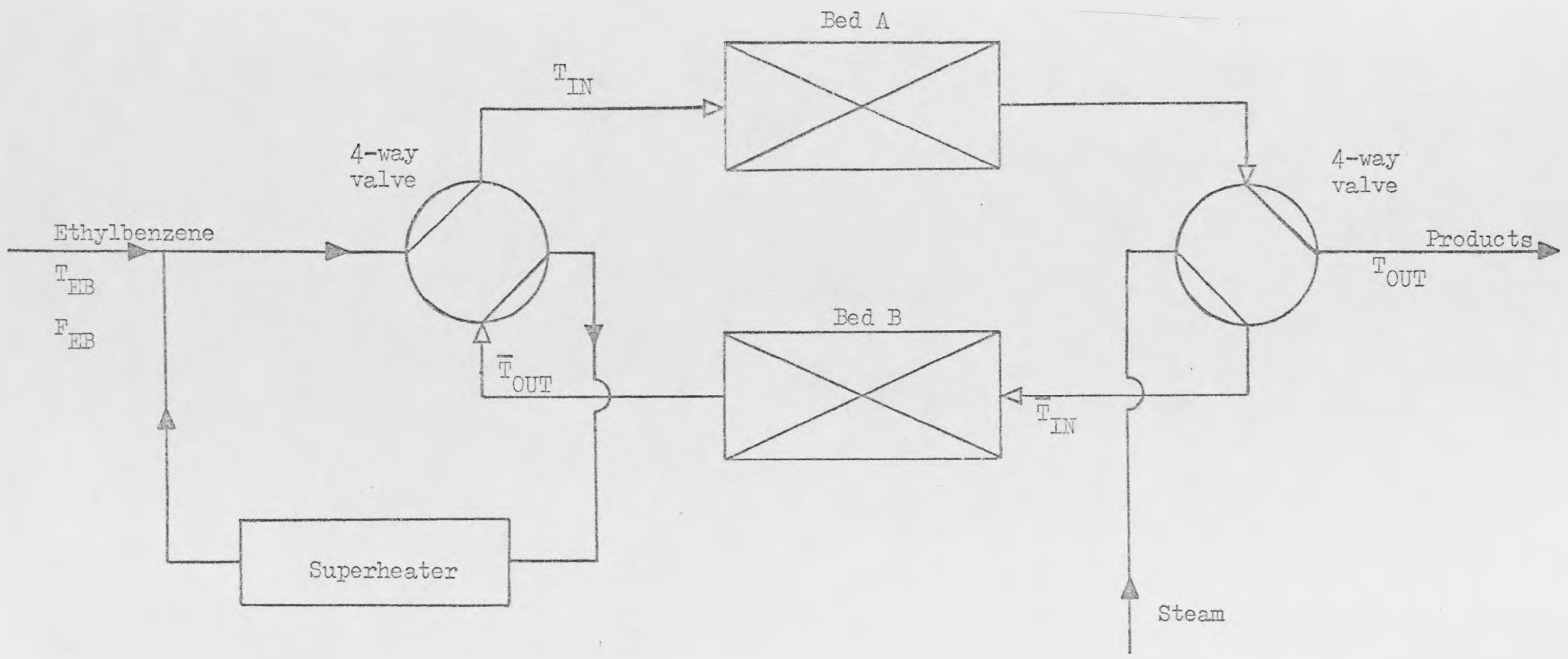
Bed A
T_{IN}
4-way valve
Ethylbenzene
T_{EB}
F_{EB}
$\overline{T}_{OUT}$
Superheater
Bed B
4-way valve
Products
T_{OUT}
$\overline{T}_{IN}$
Steam

Figure 5.2: Cyclic Reactor System with Superheater.

where $\overline{F}_{STM}$ is the regenerating steam flow. Equating 5.1 and 5.2 gives

$$(\overline{T}_{IN} - \overline{T}_{OUT}) = \frac{F_{EB} \times \Delta H}{\overline{F}_{STM} MW_{STM} \, C_{pg}} - \frac{(F_{EB} MW_{EB} + F_{STM} MW_{STM})}{\overline{F}_{STM} MW_{STM}} (T_{IN} - T_{OUT}) \qquad (5.3)$$

A typical temperature drop across a single bed steady state reactor is 50°C[13]. The cyclic reactor will not approach steady state and a drop of 25°C in average temperature is assumed. Then, with a steam/ethylbenzene ratio of 15 and a conversion of 60%, equal regenerating and diluent steam flows give a drop in average temperature of 90°C across the regenerator. If the reactor temperature drop is 50°C, that across the regenerator is still 55°C. To obtain the optimum isothermal reactor profile, saturation must be approached in the regenerator and hence the fluctuation in regenerator outlet temperature will be approximately twice the drop in average temperature because the inlet temperature is constant. This fluctuation will adversely affect the reactor conversion and will infringe the reactor feed constraints. Thus the temperature drop across the regenerator must be reduced and equation 5.3 shows that this can only be done by increasing $\overline{F}_{STM}$ as the reaction heat term is greater than that involving the reactor temperature difference. An increase in diluent steam would have a smaller effect but, as this is lost from the system with the products, it is more economic to use the same diluent steam flow and recycle the excess steam around the regenerator as shown in Figure 5.3.

The operation of this system is similar to that described in Figure 5.2, when operating counter-currently with valve 2 open and valve 3 closed. Valve 1 controls the split of the recycle steam. The diluent steam is superheated and mixed with the ethylbenzene feed, whilst the recycle fraction is mixed with make-up steam at a suitable temperature. For co-current operation, valve [illegible] is closed and valve 3

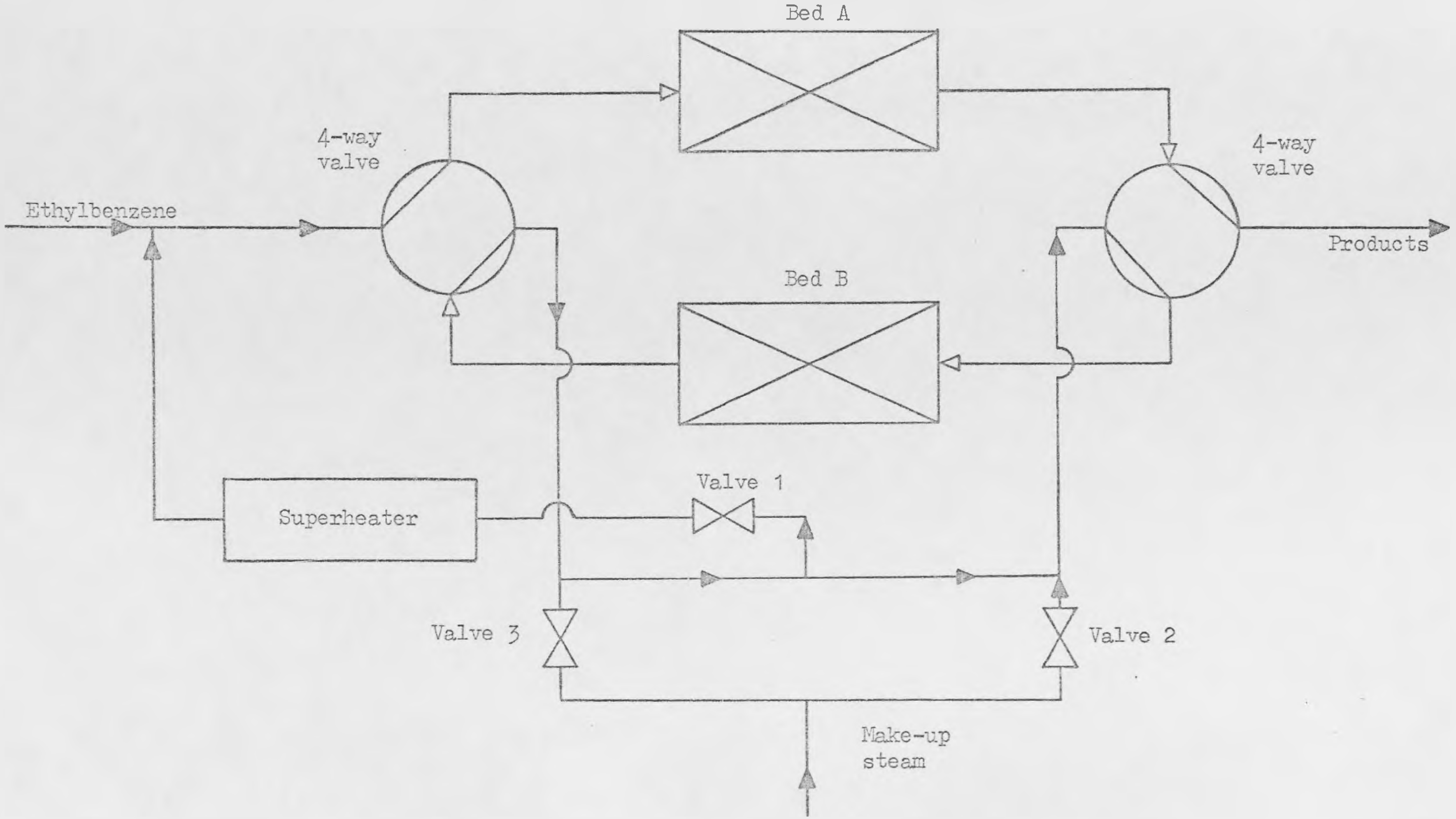
Bed A
4-way
valve
4-way
valve
Ethylbenzene
Products
Bed B
Valve 1
Superheater
Valve 3
Valve 2
Make-up
steam

Figure 5.3: Cyclic Reactor System with Recycle.

open and the direction of the regenerating steam flow is thereby reversed. The temperature of the steam entering the regenerator is no longer constant as it is affected by the varying outlet temperature. An isothermal profile along the regenerator at the end of the period is now impossible and temperatures above the maximum may be produced with a constant make-up steam temperature. However, the temperature variation will be damped to some extent by the pipework and the addition of make-up steam and the magnitude of this variation is difficult to predict at this stage.

The system shown in Figure 5.3 is a practical one for the dehydrogenation of ethylbenzene as it allows the temperature constraints to be met. This is the system which will be referred to in the remainder of this work.

5.2 Operation and Control of the System

Cyclic reactor systems have been proposed for homogeneous reactions[107,108] where the regenerative operation is used to provide the high reaction temperatures required. The only published work on the use of such a system for a heterogeneous reaction is that of Gavalas[11,12] who considers an exothermic oxidation reaction with air as the regenerative cooling medium as well as the oxidising agent. Shortcomings in his model and numerical analysis were shown in Chapter 4, but it is worthwhile to consider how he proposes to operate the system which is shown in Figure 5.4.

Gavalas[11,12] controls the regenerator inlet temperature, by varying the amount of recycled air, in order to impose an optimum temperature profile within the bed at the end of the regenerator period. He also proposes controlling the reactor inlet temperature, by venting heated air and/or the addition of cold air, to optimise

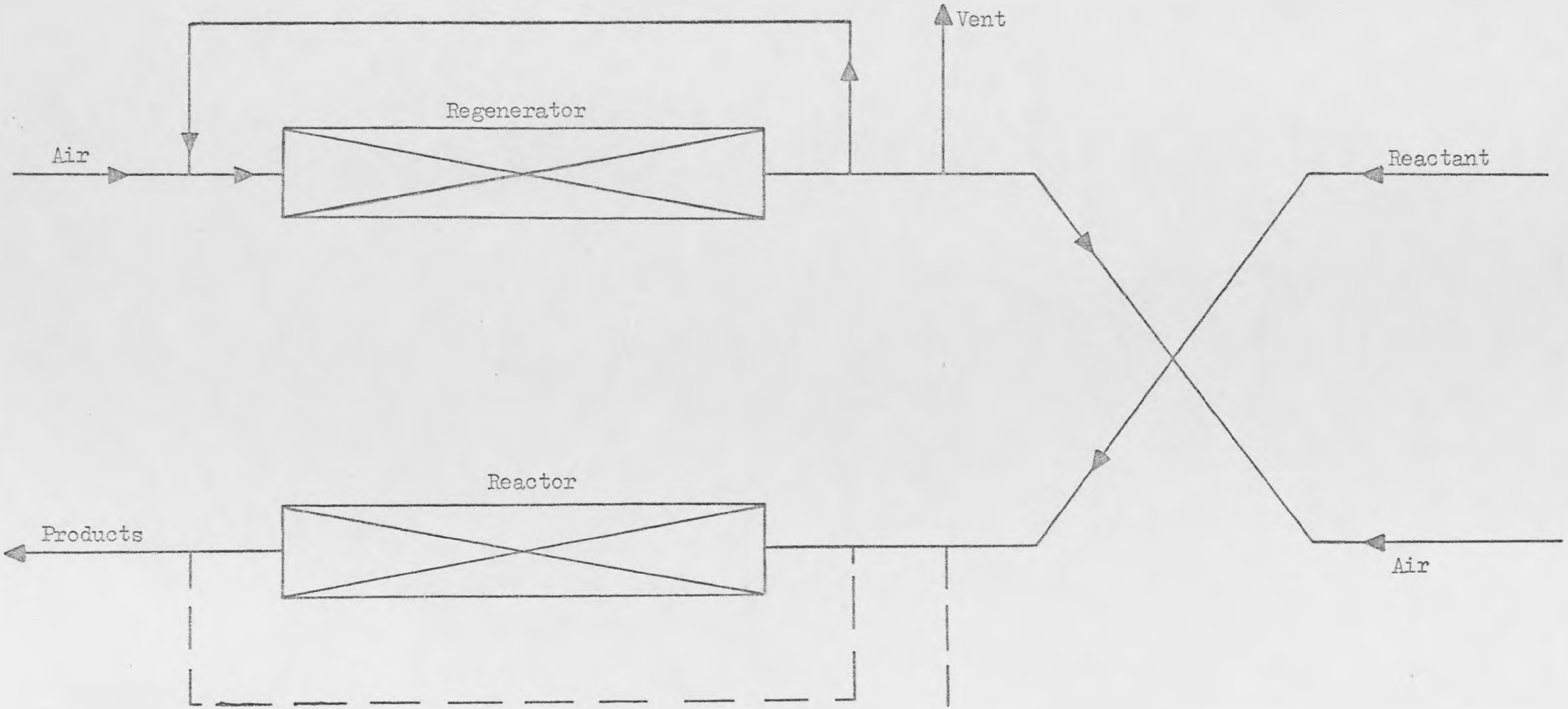
Vent
Regenerator
Air
Reactant
Reactor
Products
Air

Figure 5.4: Regeneratively Cooled Reactor of Gavalas[11,12].

the reactor performance. Hence the flows in the system vary with time to produce the desired temperatures. This may be acceptable in a system with a low cost regenerating fluid but, in the dehydrogenation of ethylbenzene, the steam cost is a major operating cost[13] and so it must be used efficiently. The diluent steam flow should be constant at the most economic value because any excess is lost from the system in the reactor products. A time-varying recycle flow is then not possible without venting some steam from the recycle and it therefore seems more practical to use constant flows throughout each period.

With constant flows, control of the inlet temperatures must be achieved by manipulation of the heat inputs to the system. However, the response of superheaters is slow and it is unlikely that satisfactory control could be achieved over periods which are expected to be, at most, a few minutes. Gavalas[11,12] only proposes controlling valves and these give an almost instantaneous response. Another difficulty is that the exact control procedure, including the effects of the response lag, must be known in advance. If the heat input to the system is changed from one period to the next, cyclic steady state will not be achieved. Thus the system must be allowed to reach cyclic steady state before the effect of a change can be observed and further control action applied. The time required to achieve satisfactory performance could then be large due to the thermal inertia of the system.

Hence, direct control of the inlet temperatures is not practical with this system. A more suitable operating policy seems to be constant heat inputs to the system and allowing the temperatures to vary. Large temperature fluctuations were shown previously to be undesirable but their magnitude can be reduced by a suitable recycle steam flow. A compromise must be reached as the flow must be minimised to reduce operating costs. The heat capacity of the system also helps to reduce these fluctuations and their effect on the inlet temperaturesmay not be excessive.

When the flow is reversed between periods, the reactor contents flow back into the recycle but the reactor steam take-off acts as a purge and prevents a build up of reaction gases. Some of the hydrocarbons removed from the recycle with the reactor steam decompose in the superheater but the steam prevents appreciable carbon deposits being formed. The remaining hydrocarbons again enter the reactor. However, this decomposition represents a loss of ethylbenzene from the system. To minimise this loss it will be ensured that the period time is not less than 100 reactor residence times. For mechanical reasons also, the period should be as long as possible and a reasonable minimum value of one minute will be assumed.

The optimum cycle time depends on the transient response of the reactor. The temperature, and hence conversion, fall during the period and the flows are reversed when the conversion reaches the minimum acceptable value. The determination of what constitutes an acceptable conversion is one of the objects of this research and will be established later. If the required cycle time is too short, it may be lengthened by increasing the heat capacity of the bed by the addition of inert material. This allows more heat to be stored in the bed during the regenerator period and slows the rate of temperature fall in the reactor. Additional heat capacity also occurs in the walls of the reactor. The effect of this may be small in a commercial reactor but, in a pilot scale reactor, the wall heat capacity may be of the same order of magnitude as that of the bed. This effect is considered in detail in Appendix 5.

In the discussion of the dehydrogenation reaction in Chapter 2, it was concluded that the reactor pressure should be as low as possible. The higher initial pressure required by multibed steady state reactors causes a reduction in the efficiency. The cyclic reactor system uses only a single reacting bed at any time and so the pressure need be no higher than in a single bed steady state reactor. The pressure of the steam entering the regenerator must be at a higher pressure to allow for the additional pressure drop. This has the advantage that any leakage at the valves will be of steam into the reaction gases rather than the reverse. The use of a mechanical compressor in the recycle may be avoided by introducing the make-up steam at a higher pressure through a thermal compressor (an ejector).

The diluent steam/ethylbenzene ratio required by an externally heated tubular steady state reactor may be as low as 6 whilst that required by an adiabatic one is 12-20[14]. This is because the feed does not supply the heat of reaction. The reaction heat in the cyclic reactor system is largely supplied by the heat stored in the bed during the regenerator period. Thus it may also be possible to operate this system at a low steam/ethylbenzene ratio.

5.3 Model of the System

The cyclic reactor system is modelled by the computer program CH3SC. A description of the program and a discussion of the computational aspects is given in Appendix 6. The present discussion is concerned with the assumptions and limitations of the model as these determine how closely it will predict the behaviour of a physical system.

The program combines the Lagrangian form of the transient reactor and regenerator models presented in Chapter 4, with constant heat inputs to the system. The film resistance model (equations 4.3 - 4.12) is used throughout and the method of solution is described in Appendix 4. The cyclic steady state performance will be studied and this is obtained when the conversion and the normalised outlet temperatures from both beds at the end of successive cycles vary by less than $5x10^{-5}$. This represents a difference of approximately 0.05°C in the actual outlet temperatures. The model will start from isothermal conditions in each bed and run until cyclic steady state is achieved. The number of cycles required to reach this will be less than in a physical system because the thermal inertia of the pipework and superheaters cannot be considered. Nevertheless, the relative number of cycles required for different conditions and assumptions will reflect the relationships in a physical system.

At cyclic steady state, the operation of one bed is the same as that of the other in the previous, and the following, period provided that the two beds are identical. Thus, only a single bed need be considered, operating alternately as a reactor and as a regenerator in successive periods. This halves the required computing time, but the regenerator outlet temperature at each time step must now be stored in order to calculate the reactor inlet temperature during the next period. There will be some delay before a temperature change at the regenerator outlet is seen by the inlet temperatures due to the residence time of the pipework. Some allowance is made for this by introducing a delay of one time step (1 second).

The conversion from the reactor varies over the period and, therefore, this is integrated by Simpson's Rule to obtain an average value. The varying inlet and outlet temperatures are similarly averaged. The loss of reaction gases at flow reversals is ignored as the period is always greater than 100 reactor residence times.

The most serious limitation of the model lies in its inability to allow for the heat capacity of the system, other than the two beds, and its effect on the transient response. However, the two possible extremes of operation are modelled. In the first case, the additional heat capacity of the system is neglected and the inlet temperatures vary directly with the regenerator outlet temperature. The other extreme is to assume that the system completely damps out the temperature variation and hence the inlet temperatures are constant during each period. The only interaction between the beds is then the temperature profiles within them at the end of each period. This reduced interaction will allow the cyclic steady state to be achieved more quickly than if the inlet temperatures vary.

In the previous section it was concluded that it is not practical to control the inlet temperatures during operation of the system. However, the range over which they vary must be limited to ensure that the temperature constraints are not infringed. This will be achieved by the selection of suitable values for the diluent steam superheater heat load and the temperature of the make-up steam. These are interdependent and some means of ensuring that a change made in order to satisfy the constraints in one bed does not cause an infringement in the other. Such a procedure will be described in the following section.

5.4 Prediction of System Parameters

A suitable norm bed size and operating conditions must be chosen for use in predicting the parameters of the cyclic reactor system. It is desirable that this norm is related to the performance of an existing steady state reactor as direct comparisons can then be made. It was concluded in Chapter 2 that the cyclic system should be compared with a multibed adiabatic steady state reactor, as this gives the highest conversion of existing reactor types. A convenient choice for the norm is therefore the use of the same volume of catalyst as in a typical two-bed steady state reactor. Each bed in the cyclic system is then the same size as a single adiabatic bed. The norm operating conditions are therefore taken as those which give a 40% steady state conversion from a single bed.

The overall conversion from a two-bed steady state reactor which gives 40% from the first bed is typically 50-60%[26,27]. This will be considered as the minimum conversion required from the cyclic reactor system. The maximum attainable conversion is the isothermal steady state value at the highest allowable temperature. These conversion limits will be determined from steady state reactor studies and the cyclic system parameters will be evaluated to give average conversions in this range. The reactor conditions are fixed by the choice of the norm and the parameters to be determined are

(a) period time

(b) regenerator steam flow

and (c) heat inputs to the system.

5.4.1 Period Time

The initial temperature profile in the cyclic reactor will be almost isothermal if the regenerator approaches saturation. An estimate of the allowable period time to give a specified conversion can clearly be obtained from the transient reactor model assuming an initially isothermal profile. This is given by the time elapsed when the average conversion falls to the specified value. However, it is possible to obtain an approximate value from steady state results, which are easier and quicker to obtain. The heat removed by the reaction per second is:

$$H = F_{EB} \; \Sigma_j \, (x_j \, \Delta H_j) \qquad (5.4)$$

where x_j is the isothermal steady state conversion of the j^{th} reaction. The fall in bed temperature produced by this heat removal is given by the bed heat capacity and the rate of temperature fall, in °C s^{-1}, is therefore

$$\text{Tfall} = \frac{F_{EB} \; \Sigma_j \, (x_j \, \Delta H_j)}{AZ(1-e) \, \rho_s \, C_{ps}} \qquad (5.5)$$

Inspection of steady state conversions at various isothermal temperatures will show* the fall in temperature (ΔT) which can be allowed to give a desired average conversion. The period time, t_f, is then

$$t_f = \frac{\Delta T}{\text{Tfall}} \qquad (5.6)$$

The temperature fall in a transient reactor will not be uniform along the bed, but the isothermal temperatures used in the calculation can be considered to be averaged along the length. The allowable period time in the cyclic reactor will be reduced if the bed is not initially isothermal, but the exact temperature profile cannot be determined until the cyclic system is studied. Nevertheless, the above procedure is simple and should give a useful first approximation.

5.4.2 Regenerator Steam Flow

The heat required for the reaction is stored in the bed during the regenerator period. The period time is fixed by the reactor requirements and the regenerating steam temperature is limited by the constraints described earlier. Thus only the flow of the regenerating steam can be independently varied to control the heat input to the regenerator. It was shown in Chapter 1 that it is desirable to approach saturation of the regenerator as this gives the optimum initial reactor temperature profile. However, for

*See section 6.5.1

economic reasons, it is also necessary to keep the steam flow to a minimum. An approximate value for the time required to saturate the bed for a given steam flow is obtained from the analytical solution (equation 4.38) of the pseudo-homogeneous regenerator model (equation 3.29). The saturation time (t_{sat}) is the time required for a step change in inlet temperature to move through the bed and is

$$t_{sat} = \frac{(1-e)\, \rho_s\, C_{ps}}{\bar{u}\, \bar{\rho}_g\, \bar{C}_{pg}} Z \qquad (5.7)$$

where Z is the overall bed length. The velocity, $\bar{u}$, is given by

$$\bar{u} = \frac{\bar{F}_{STM}\, MW_{STM}}{\bar{\rho}_g\, A} \qquad (5.8)$$

and the steam flow required to just saturate the bed in a period of t_f seconds is therefore

$$\bar{F}_{STM} = \frac{(1-e)\, \rho_s\, C_{ps}\, AZ}{t_f\, \bar{C}_{pg}\, MW_{STM}} \qquad (5.9)$$

It was shown in Chapter 4 that the pseudo-homogeneous model does not predict the S-shaped breakthrough curves obtained in practice. The true saturation time is therefore greater than that given by equation 5.7. In addition, equation 5.7 does not include the effect of the initial bed temperature profile, which affects the approach to saturation. The calculated saturation time will therefore be compared with the breakthrough curves obtained from the more representative film resistance model (equations 3.21 and 3.22). If the calculated value is not adequate, it is still desirable to make use of equation 5.9, by the inclusion of an appropriate factor, as it gives a simple means of determining the steam flow.

5.4.3 Heat Inputs to the System

The heat inputs must be determined in order to calculate the inlet temperatures to the reactor and the regenerator. Hence, they are not required if the inlet temperatures are assumed constant, and the following discussion is only concerned with varying inlet temperatures. The nomenclature used is given in Figure 5.5 which shows the flows during a single period for counter-current operation. The following discussion would not, however, be affected if co-current operation was considered. The superheater heat load and the make-up steam temperature must be evaluated, but this is complicated by the interactions of the system. The superheater heat load can be determined explicitly if the regenerator outlet temperature is known, but this is affected by the make-up steam temperature. Conversely, the superheater affects the initial regenerator temperature profile, which in turn affects the required values of both the make-up steam temperature and the superheater heat load.

However, the amount of heat which must be put into the regenerator can be estimated from the steady state reactor studies. It was shown in Section 5.4.1 that the fall in averaged temperature (ΔT) and the period time (t_f) can be found for a specified conversion. Thus the heat input to the regenerator to restore the initial reactor temperature level is

$$H = AZ(1-e)\,\rho_s C_{ps}\,\Delta T \tag{5.10}$$

A heat balance on the regenerator over the period then gives

$$\overline{T}_{OUT} = \overline{T}_{IN} - \frac{AZ(1-e)\,\rho_s C_{ps}\,\Delta T}{\overline{F}_{STM}\,C_{pg}\,MW_{STM}\,t_f} \tag{5.11}$$

where $\overline{T}_{OUT}$ and $\overline{T}_{IN}$ are time averaged over the period. The superheater heat load per second is given by a heat balance over the superheater and the entrance of the ethylbenzene feed.

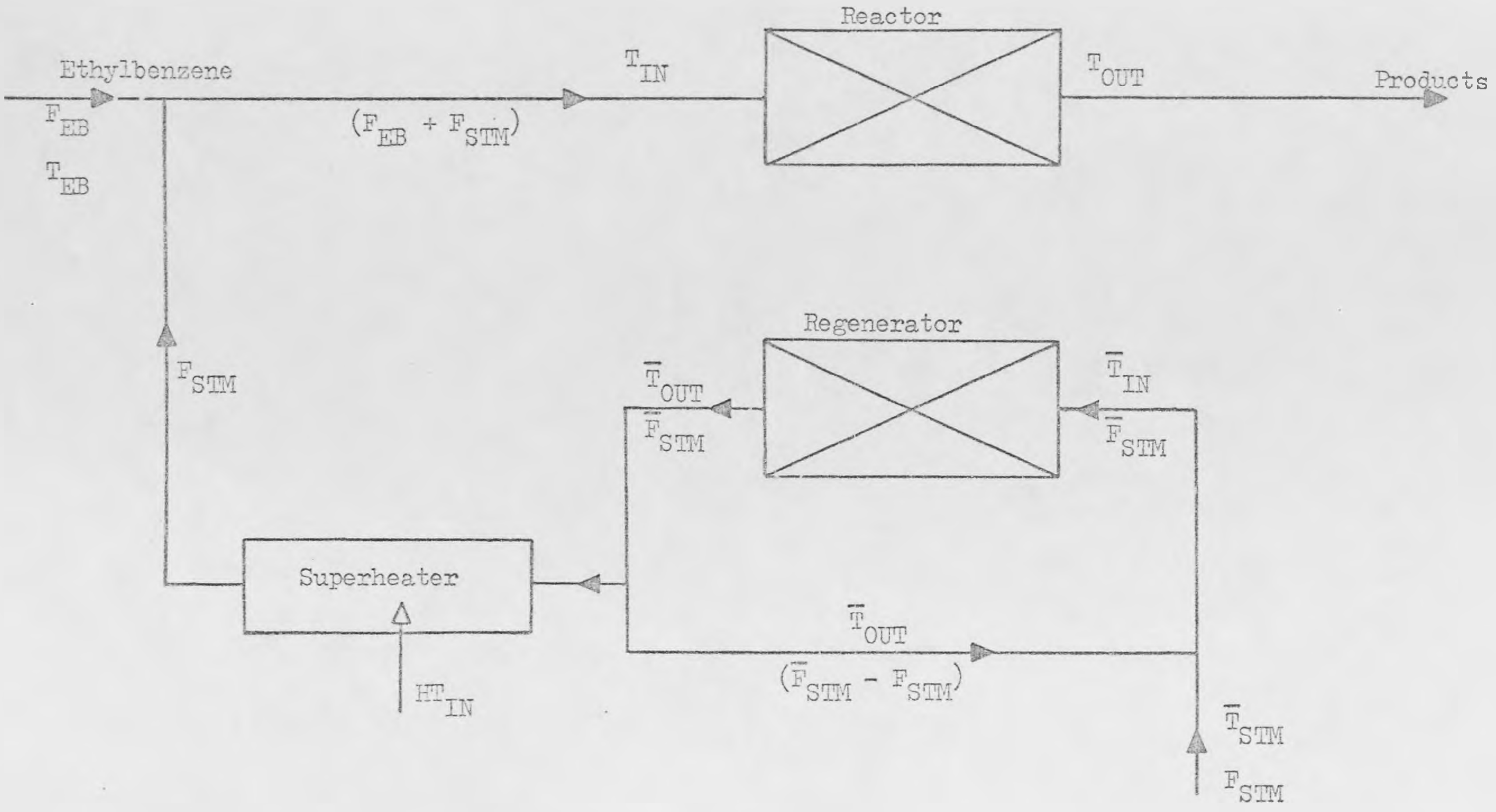
Ethylbenzene
F_{EB}
T_{EB}
$(F_{EB} + F_{STM})$
T_{IN}
Reactor
T_{OUT}
Products
F_{STM}
Regenerator
$\overline{T}_{OUT}$
$\overline{F}_{STM}$
$\overline{T}_{IN}$
$\overline{F}_{STM}$
Superheater
HT_{IN}
$\overline{T}_{OUT}$
$(\overline{F}_{STM} - F_{STM})$
$\overline{T}_{STM}$
F_{STM}

Figure 5.5: Flows in the Cyclic Reactor System during a Single Counter-current Period.

$$HT_{IN} = (F_{EB}\,MW_{EB} + F_{STM}\,MW_{STM})C_{pg}\,T_{IN} - F_{EB}\,MW_{EB}\,C_{pg}\,T_{EB} - F_{STM}\,MW_{STM}\,C_{pg}\,\bar{T}_{OUT} \qquad (5.12)$$

where again all temperatures are average values and the variation of specific heat with composition and temperature is neglected. Eliminating $\bar{T}_{OUT}$ from equations 5.11 and 5.12 and setting $\bar{T}_{IN}$ equal to T_{IN} gives

$$HT_{IN} = F_{EB}\,MW_{EB}C_{pg}(T_{IN} - T_{EB}) + \frac{F_{STM}\,AZ(1-e)\rho_s C_{ps}\,\Delta T}{\bar{F}_{STM}\,t_f} \qquad (5.13)$$

If the value of $\bar{F}_{STM}$ calculated from equation 5.9 is used, equation 5.13 can be further simplified to

$$HT_{IN} = F_{EB}\,MW_{EB}\,C_{pg}(T_{IN} - T_{EB}) + F_{STM}\,MW_{STM}\,C_{pg}\,\Delta T \qquad (5.14)$$

T_{EB} is a known constant value but some estimate for T_{IN} must be chosen. A suitable estimate might be the maximum allowable bed temperature less half the averaged bed temperature difference, ΔT. This gives a means of estimating the superheater heat load without knowledge of the make-up steam temperature. The reactor conversion is not directly included, but it is incorporated in the value of ΔT.

Clearly a similar procedure could be used to evaluate the make-up steam temperature. However, both variables would then be expressed in terms of average inlet temperatures, with no check on whether the actual temperatures infringe the constraints. It is more suitable, therefore, to estimate the make-up steam temperature using actual temperatures. The value of $\bar{T}_{STM}$ at a given time is

$$\bar{T}_{STM} = \frac{\bar{F}_{STM}}{F_{STM}}\bar{T}_{IN} - \frac{(\bar{F}_{STM} - F_{STM})}{F_{STM}}\bar{T}_{OUT} \qquad (5.15)$$

where $\bar{T}_{IN}$ and $\bar{T}_{OUT}$ are the values at the same time. Equation 5.12 is also valid if the temperatures are the values at a set time, rather than averaged. Equating this to 5.15 to eliminate $\bar{T}_{OUT}$ gives

$$\bar{T}_{STM} = \frac{\bar{F}_{STM}}{F_{STM}} \bar{T}_{IN} - \frac{\bar{F}_{STM} - F_{STM}}{(F_{STM})^2 MW_{STM}} \left[\begin{array}{l} (F_{EB} MW_{EB} + F_{STM} MW_{STM}) T_{IN} \\ - F_{EB} MW_{EB} T_{EB} - \dfrac{HT_{IN}}{C_{pg}} \end{array} \right] \qquad (5.16)$$

This is the value of $\bar{T}_{STM}$ which will produce $\bar{T}_{IN}$ at the regenerator inlet if, and only if, HT_{IN} is the correct value to produce T_{IN} at the reactor inlet. Thus, if both T_{IN} and $\bar{T}_{IN}$ are specified as the maximum value, the constraint on the maximum temperature must be satisfied at the regenerator inlet if it is satisfied at the reactor inlet.

However, an iterative procedure is required to evaluate the correct value of HT_{IN} to give T_{IN} at the reactor inlet, and equation 5.13 or 5.14 can be used to obtain an initial estimate. An iterative procedure would also be required if equations 5.11 and 5.15 were used to estimate $\bar{T}_{STM}$ as equations 5.11, 5.13 and 5.14 are only approximate relationships whilst equation 5.16 is exact. Once the cyclic steady state performance has been calculated using estimates from equation 5.13 or 5.14 and equation 5.16, a better estimate of HT_{IN} can be evaluated from equation 5.12. A value for $\bar{T}_{OUT}$ can be obtained by altering the calculated value by the difference between the maximum observed, and the maximum allowed, inlet temperature. Subsequent estimates of HT_{IN}, if required, may be obtained by interpolation and $\bar{T}_{STM}$ is obtained in each case from equation 5.16.

Unless a constant check is kept on the inlet temperatures, the time at which the maximum values occur must be known in advance. The regenerator outlet temperature rises during the period and so the maximum inlet temperatures seem likely to occur at the end of the period. These values will therefore be used to check that the maximum temperature constraint is not infringed.

The inlet temperatures to the reactor and regenerator at each time step are calculated from equations 5.12 and 5.15 respectively, using the regenerator outlet temperature from the previous time step.

CHAPTER 6

STEADY STATE STUDIES

The steady state models were first used to compare the various sets of kinetics for the dehydrogenation of ethylbenzene which were described in Chapter 2. The aim of the study is to determine which set gives the best representation of a steady state reactor and which will, therefore, be the most suitable for use in the cyclic reactor system. The models were also used to establish the norm conditions for the cyclic system described in the previous chapter and to evaluate parameters for the system.

6.1 Comparison of Kinetics

The kinetic models presented in the literature are summarised in Appendix 1 and the values of the rate constants at 630°C for reactions 2.1 - 2.3 are given in Table 6.1.

Source	Reaction 2.1	2.2	2.3
*Modell[32]	2.489×10^{-5}	1.256×10^{-6}	9.615×10^{-7}
+Wenner and Dybdal[19]	1.541×10^{-5}	-	-
+Sheel and Crowe[17]	5.112×10^{-6}	5.322×10^{-7}	6.889×10^{-6}
+Davidson and Shah[18]	3.768×10^{-6}	1.765×10^{-7}	8.470×10^{-7}
+Abet et al[31]	1604	160.8	1655
+Eckert et al[33]	3.418×10^{-6}	7.212×10^{-8}	1.632×10^{-6}

*Units are kmol s^{-1} kg cat^{-1}

+Units are kmol s^{-1} kg cat^{-1} bar^{-1}

Table 6.1: Rate constants for reactions 2.1-2.3 at 630°C

The values of Abet et al[31] are several orders of magnitude greater than all the others and are quite unrealistic. The data used in deriving their rate constants are not presented and so these cannot be checked. Wenner and Dybdal[19] give only the single rate constant for the dehydrogenation reaction in the presence of steam. Since the efficiency is an important consideration, this single rate expression is not sufficient. Hence, neither of these kinetics will be considered further and the kinetics to be studied are those of Modell[32], Sheel and Crowe[17], Davidson and Shah[18] and Eckert et al[33]. These will be abbreviated to M, SC, DS and E respectively.

In the discussion of Chapter 2 it was concluded that M, SC and DS have weaknesses in their derivations. DS give very high efficiencies, typically greater than 95%, and are based on the rate constants of Wenner and Dybdal[19] for reactions 2.1-2.3, which were derived for a catalyst which operates without steam. SC give low efficiencies of about 85% and appear to have been derived from data obtained at a single set of operating conditions, from a reactor operating with sub-optimal performance. M gives efficiencies of about 92% which are in the expected range and use the dehydrogenation reaction rate expression of Carra and Forni[39] which seems the most reliable. However, the rate constants for reactions 2.2 and 2.3 are based to some extent on Wenner and Dybdal's[19] values for catalyst operating without steam, and the second order toluene producing reaction is represented by a first order rate expression. Eckert et al[33] do not present any of the data or techniques used in deriving their kinetics and so no conclusions about their reliability can be drawn.

All the sets of kinetics are presented with pseudo-homogeneous models and so this type of model is used in their comparison. The model includes the variation of velocity and physical properties along the reactor length. The results of Davidson and Shah[44] are reproduced exactly by the model, as are the conversions and temperatures given by Sheel and Crowe[17]. However, unless the bulk density of the catalyst is high (c. 4500 kg m^{-3}), the reactor size quoted by the latter is significantly less than that predicted by the model. Neither Modell[32] nor Eckert et al[33] present sufficient data to permit reproduction of their results. Indeed, the latter present no quantitative results which can be checked.

Each set of kinetics required a different reactor size to achieve a given conversion. Using the data in Table 4.1 with a constant reactor diameter, the lengths required to give 40% conversion in a single adiabatic bed are 0.20 m (M), 1.53 m (DS), 1.65 m (SC) and 3.05 m (E). To allow direct comparison between these sets of kinetics, the above values are used as the norm and, as the pressure drop would be different in each case, constant pressure is assumed.

It was concluded in Chapter 2 that the benzene and toluene producing reactions are the main side-reactions. These are the only ones considered by Modell[32] and Davidson and Shah[18] found that, out of the seven side-reactions considered, only these two give significant conversions. The effect of ignoring the other side-reactions in SC and E is a change of approximately 3% and 5% respectively in the conversion to styrene. However, in the following comparison, all the reactions in each are included.

In order to compare the sets of kinetics, the effect of varying the following parameters on a single bed reactor is investigated.

(a) Reactor size

(b) Inlet temperature

(c) Reactor pressure

(d) Dilution steam flow,

for adiabatic operation, and also

(e) Temperature level for isothermal operation.

The variation of conversion and efficiency with these parameters is shown in Figures 6.1 - 6.5.

6.1.1 Reactor Size (Figure 6.1)

To vary the reactor size, the diameter is kept constant and the length altered. The normalised lengths of unity represent the lengths given above for 40% conversion. M, SC and E give similar conversions except at short lengths but DS shows considerably greater variation. It was concluded in Chapter 2 that the efficiency should fall as the conversion increases and this is shown by all except DS, which increases slightly. The efficiencies given by DS and E are higher than would be expected.

6.1.2 Inlet Temperature (Figure 6.2)

In each case, the expected increase of conversion with inlet temperature is observed and the change is found to be linear over the range studied. DS and E again give high efficiencies which fall as the temperature increases. In Chapter 2, it was concluded that this fall was to be expected and it is also shown by SC. However, M shows an increase in efficiency with temperature.

6.1.3 Reactor Pressure (Figure 6.3)

Significant differences are observed in the effect of pressure on conversion for the various kinetics. A maximum conversion is observed in each case although the pressure at which it occurs varies. This is to be expected as the forward reaction rate of reaction 2.1 is proportional to pressure, whereas the reverse reaction rate is proportional to the square of the pressure. Thus there must be a pressure at which the net forward rate, and hence the conversion, will be a maximum. The literature gives no guidance as to where this

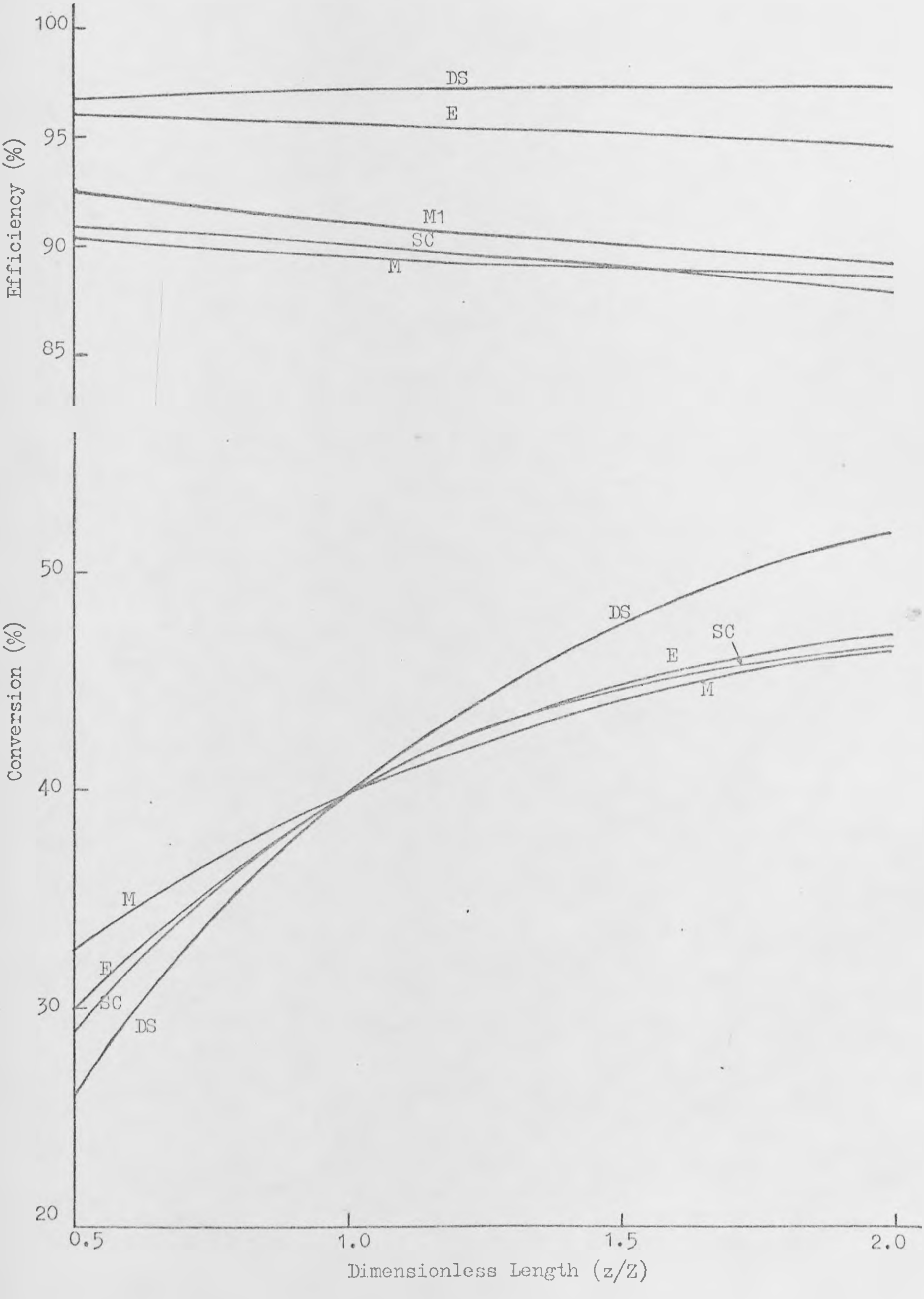

Figure 6.1: Effect of Reactor Size on Conversion and Efficiency

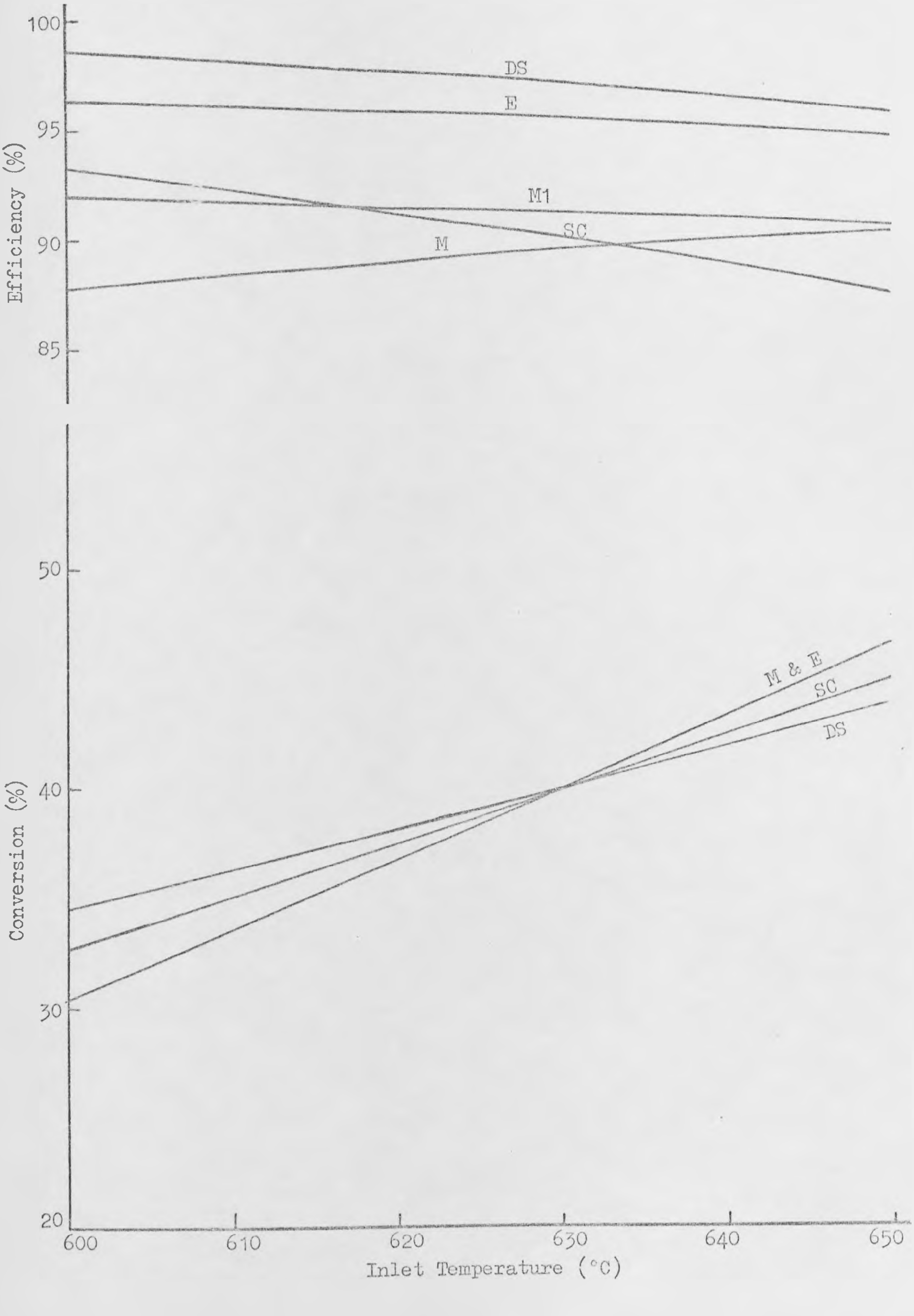

Figure 6.2: Effect of Inlet Temperature on Conversion and Efficiency

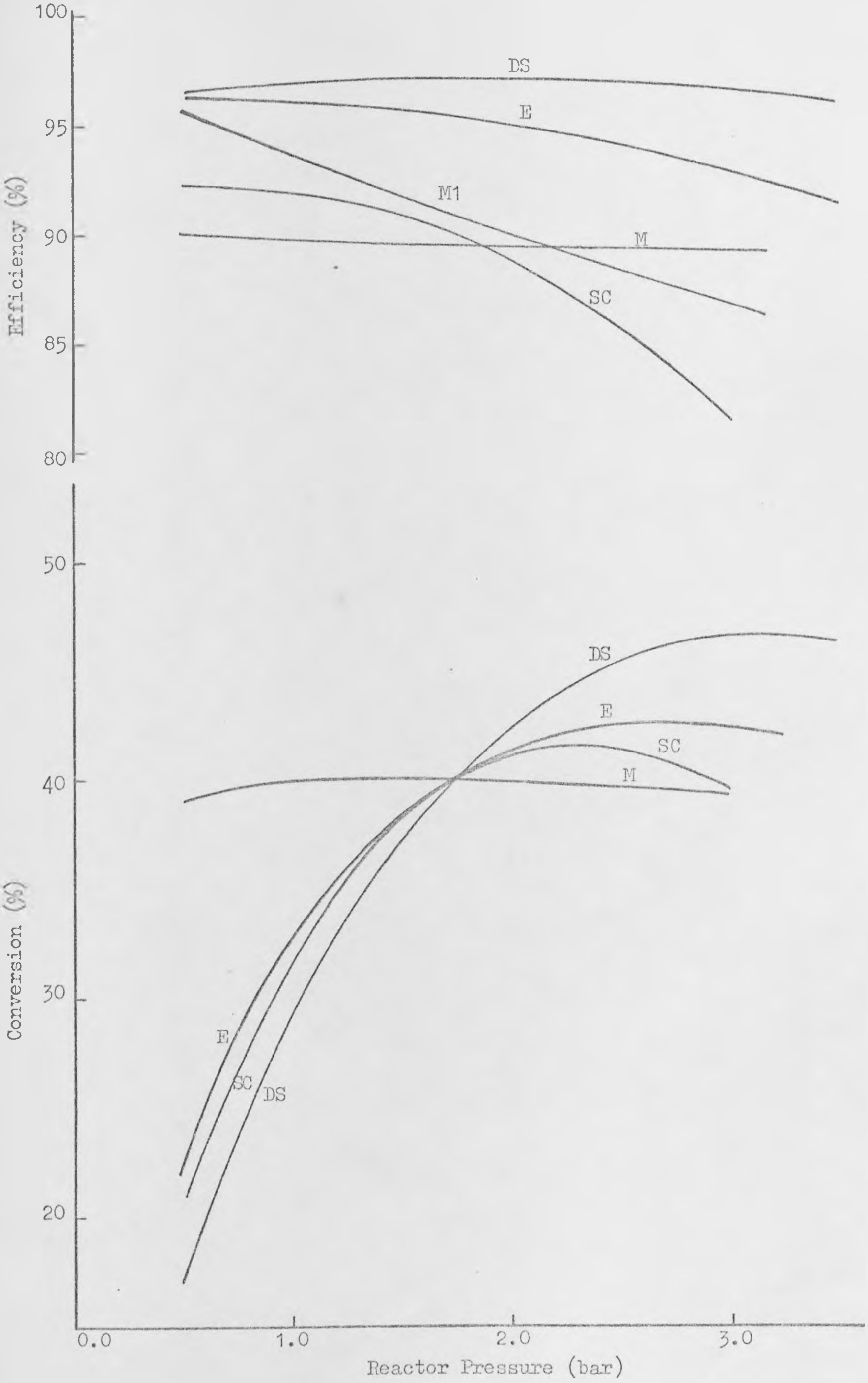

Figure 6.3: Effect of Reactor Pressure on Conversion and Efficiency

maximum should occur but if it occurred at about 3 bars, as shown by E and DS, then one might expect industrial reactors to operate in this range. In practice, reactors operate at as low a pressure as possible, normally 1.2 - 1.8 bars[13], and M shows the maximum conversion within this range. Sheel and Crowe[17] state that the reactor which they modelled would give higher conversions at a pressure of 1.4 bars rather than the value of 2.37 bars which was used. It may be significant that they predict the maximum conversion near this latter value, at which they fitted their rate constants.

SC, DS and E all show a rapid fall in conversion at low pressures. It is suggested in the literature[27] that the reaction may be carried out under vacuum but this would seem unlikely if the low conversions predicted by these kinetics were obtained. It therefore appears that M gives a more likely representation of the variation of conversion with pressure than do the others. This is supported by the fact that the rate expression used by M for the dehydrogenation reaction was derived from results obtained over a large pressure range[39].

It was concluded in Chapter 2 that the efficiency should fall as the pressure increases and this is observed in each case except for the initial increase shown by DS. High efficiencies are again shown by DS and E. The efficiency of SC falls rapidly with increasing pressure and is only 82% at 3 bars. Operation of two bed reactors is reported[36] to require an initial pressure in excess of 3 bars and to give an efficiency in the region of 90%. Thus the efficiency of SC is too low, and so M also appears to give the most likely representation of the efficiency.

6.1.4 Dilution Steam Flow (Figure 6.4)

Increasing the steam flow increases the steam/ethylbenzene ratio which should result in increased conversions and efficiencies[30].

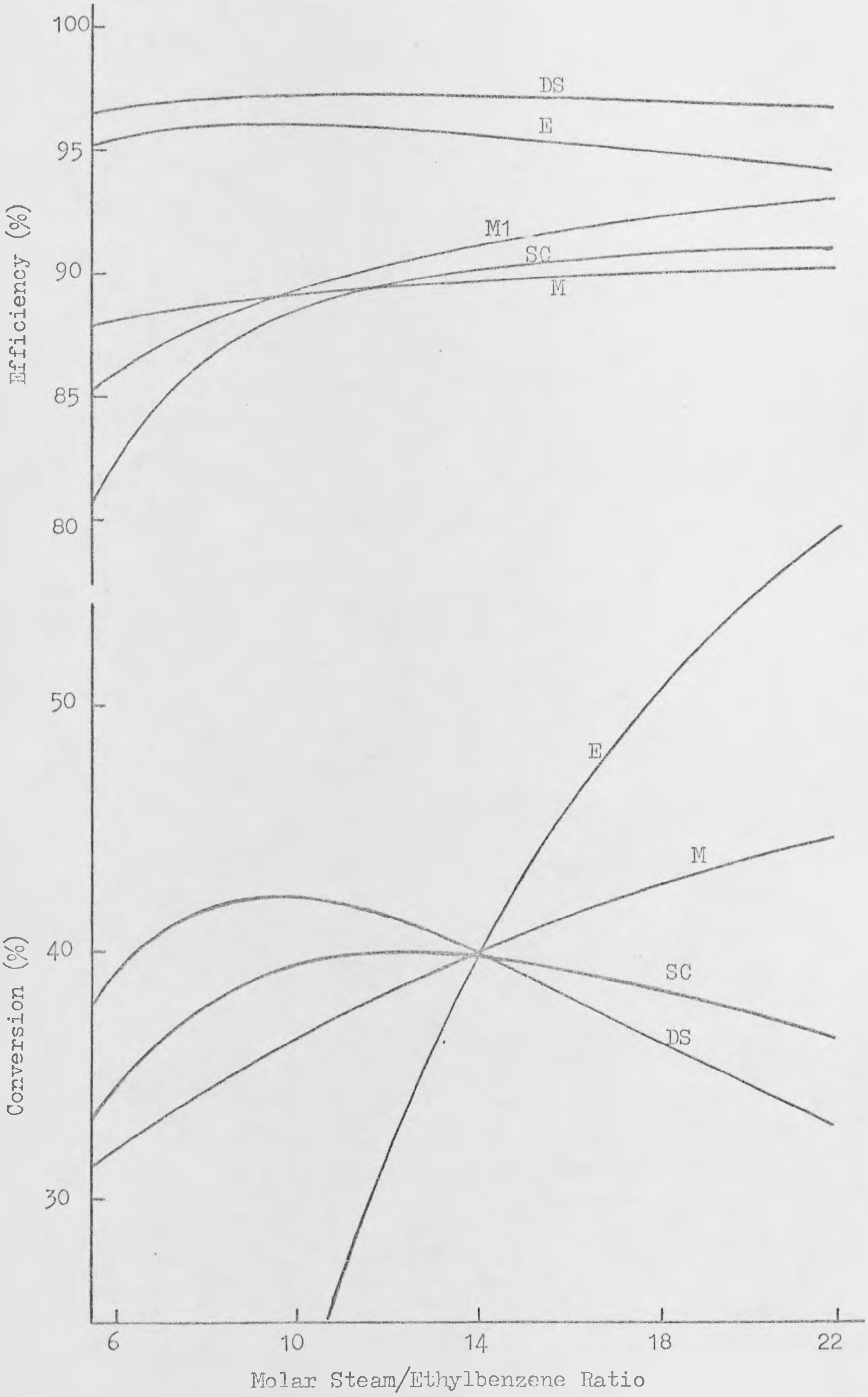

Figure 6.4: Effect of Steam Flow on Conversion and Efficiency

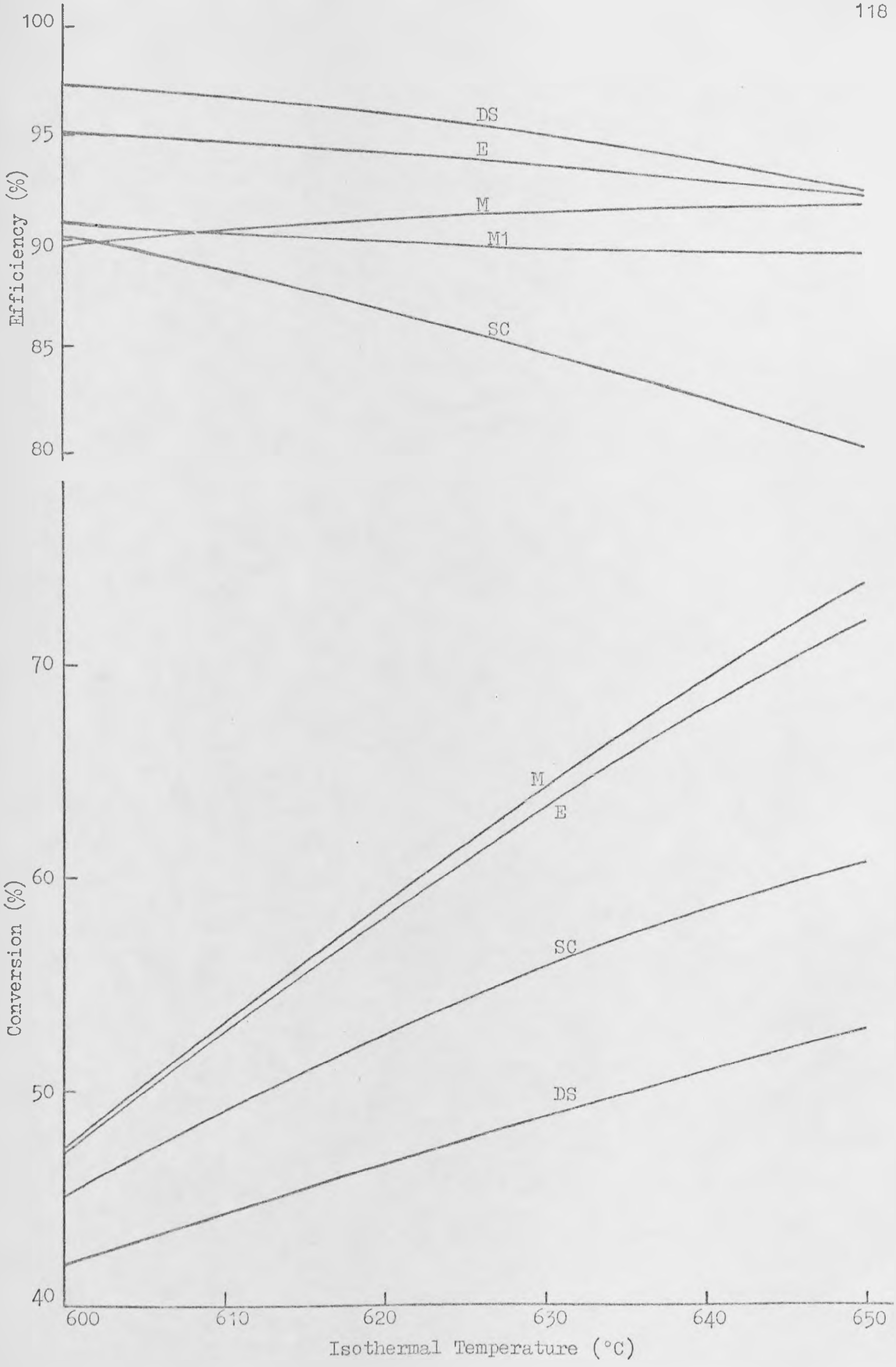

Figure 6.5: Effect of Isothermal Temperature Level on Conversion and Efficiency.

The drastic variation of conversion shown by E is due to the inclusion of terms containing the steam/ethylbenzene ratio in the rate constants. This causes a much greater variation of reaction rate than is observed with the other kinetics, none of which include this ratio. M also shows the expected increase in conversion but both SC and DS show maximum conversions at relatively low steam flows. The partial pressure of the ethylbenzene is reduced as the steam flow increases and, as shown in Figure 6.3, this causes a fall in conversion. If the terms including the steam/ethylbenzene ratio are omitted from the rate constants of E, the conversions predicted show the same trend as SC and DS. This confirms that the fall in conversion is due to the falling ethylbenzene partial pressure.

The high efficiencies of DS and E fall off after the expected initial rise. SC shows the expected increase in efficiency but, at low steam flows, it is less than 82%. The BASF tubular reactor operates with a steam/ethylbenzene molar ratio of 6 and gives an efficiency of over 90%[38]. Thus, even allowing for the higher temperature, the values of SC are very low. The conversion and efficiency given by M again, therefore, appear to be 'best'.

6.1.5 Isothermal Temperature Level (Figure 6.5)

As is to be expected, isothermal operation produces higher conversions which cover a wider range than those given with adiabatic operation. The conversions of SC and DS are much less sensitive to temperature than those of M and E. If the reactor size is increased, it is found that the conversion of SC shows a maximum of about 63% and then falls if the size is further increased. This is due to the falling efficiency which is only 74% at 650°C with a reactor size of twice the norm. Thus SC can never predict the high (>70%) conversions reported in the literature[28,29] for some isothermal conditions. DS gives 52.5% conversion at 650°C which increases to 71% if the reactor size is doubled. This again seems low compared with reported values in the literature.

The efficiencies of DS and E are again high but, with SC, show the expected fall with increasing temperature. M again shows an increase in efficiency with temperature. The conversion of reaction 2.2 increases with temperature whilst that of reaction 2.3 decreases and it is this decrease which causes the higher efficiencies. The reason for this is that the activation energy for reaction 2.3 is considerably lower than those of the other reactions and so the actual change with temperature is less. The increase in the rate constant with temperature is clearly outweighed by the fall in the ethylbenzene partial pressure and, as the increasing hydrogen partial pressure is not included in the rate expression, the rate falls with increasing temperature.

6.1.6 Discussion

The above comparison shows that M seems to give the best representation of the dehydrogenation reaction although the side-reactions, and hence the efficiency, show anomalous behaviour with varying temperature. The variation of the conversions given by SC and DS with pressure, steam flow and isothermal temperature level seem less likely to represent an actual reactor. DS always predict excessively high efficiencies and these do not show the expected response to variation of reactor size, pressure or steam flow. The efficiency given by SC falls rapidly as the conversion increases and hence high conversions cannot be predicted. As there are also weaknesses in their derivations, neither SC nor DS will be considered further.

The response of the conversion given by E to variation in pressure and steam flow does not seem satisfactory and the efficiency is always high. The efficiency shows an unexpected fall with increasing steam flow but this may be due to the rapidly increasing conversion. Thus these kinetics do not seem to be suitable for further use.

The variation of conversion shown by M is, in each case, what is to be expected from the discussion of Chapter 2. This is given by the rate expression of Carra and Forni[39] which was shown to be likely to give a good representation. The efficiencies given by M are in the expected range but show an anomalous increase with increasing temperature. This is a serious defect as the cyclic reactor system is expected to operate at higher temperatures and any comparison of efficiencies would be invalid if these kinetics were used. Thus some improvement in the rate expressions for the side-reactions is required. Only the benzene and toluene producing side-reactions will be considered as these have been shown to be the only important ethylbenzene consuming ones. It would seem desirable to base these on experimental results, and Bogdanova et al[29] present suitable tabulated data.

6.1.7 Derived Kinetics

The rate expressions for the side-reactions are assumed to be of the same type as that of the dehydrogenation reaction and are

$$r_2 = k_2 \frac{p_{EB}}{\alpha + p_{EB} + \beta p_{ST}} \qquad (6.1)$$

$$r_3 = k_3 \frac{p_{EB} p_H}{\alpha + p_{EB} + \beta p_{ST}} \qquad (6.2)$$

Assuming that

$$\frac{r_2}{r_1} = \frac{x_{Bz}}{x_{ST}} \qquad (6.3)$$

and using equation 2.14 for r_1,

then $$\frac{k_2 \, p_{EB}}{\alpha + p_{EB} + \beta p_{ST}} = \frac{x_{Bz}}{x_{ST}} \cdot k_1 \cdot \frac{p_{EB} - p_{ST} p_H / K_p}{\alpha + p_{EB} + \beta p_{ST}} \qquad (6.4)$$

and $$k_2 = \frac{x_{Bz}}{x_{ST}} k_1 \left(1 - \frac{p_H \, p_{ST}}{p_{EB} \, K_p}\right) \qquad (6.5)$$

Similarly

$$k_3 = \frac{x_{TOL}}{x_{ST}} k_1 \left[\frac{1}{p_H} - \frac{p_{ST}}{p_{EB} \, K_p}\right] \qquad (6.6)$$

Table 6.2 shows the composition of reactor products obtained at various temperatures by Bogdanova et al[29] and from these x_{EB}, x_{Bz} and x_{TOL} can be obtained. (The values must first be converted to mol fractions.)

Temperature (°C)	Reactor Products (weight %)		
	Styrene	Benzene	Toluene
630	75.0	0.34	2.27
623	72.0	0.24	2.25
621	68.5	0.34	2.13
613	66.5	0.36	1.64
599	58.5	0.26	1.20
589	50.5	0.17	1.05
580	44.5	0.14	0.67

Table 6.2: Reactor product compositions given by Bogdanova et al[29]

The steam/ethylbenzene weight ratio was 2.6 and assuming a typical reactor pressure of 1.4 bars, the partial pressures can be obtained. k_1 is calculated from equation 2.16 and hence k_2 and k_3 can be found from equations 6.5 and 6.6.

k_2 and k_3 were calculated at each temperature and are shown plotted against inverse temperature in Figure 6.6. The lines shown in the figure were obtained by a least squares method and the rate constants are given by:

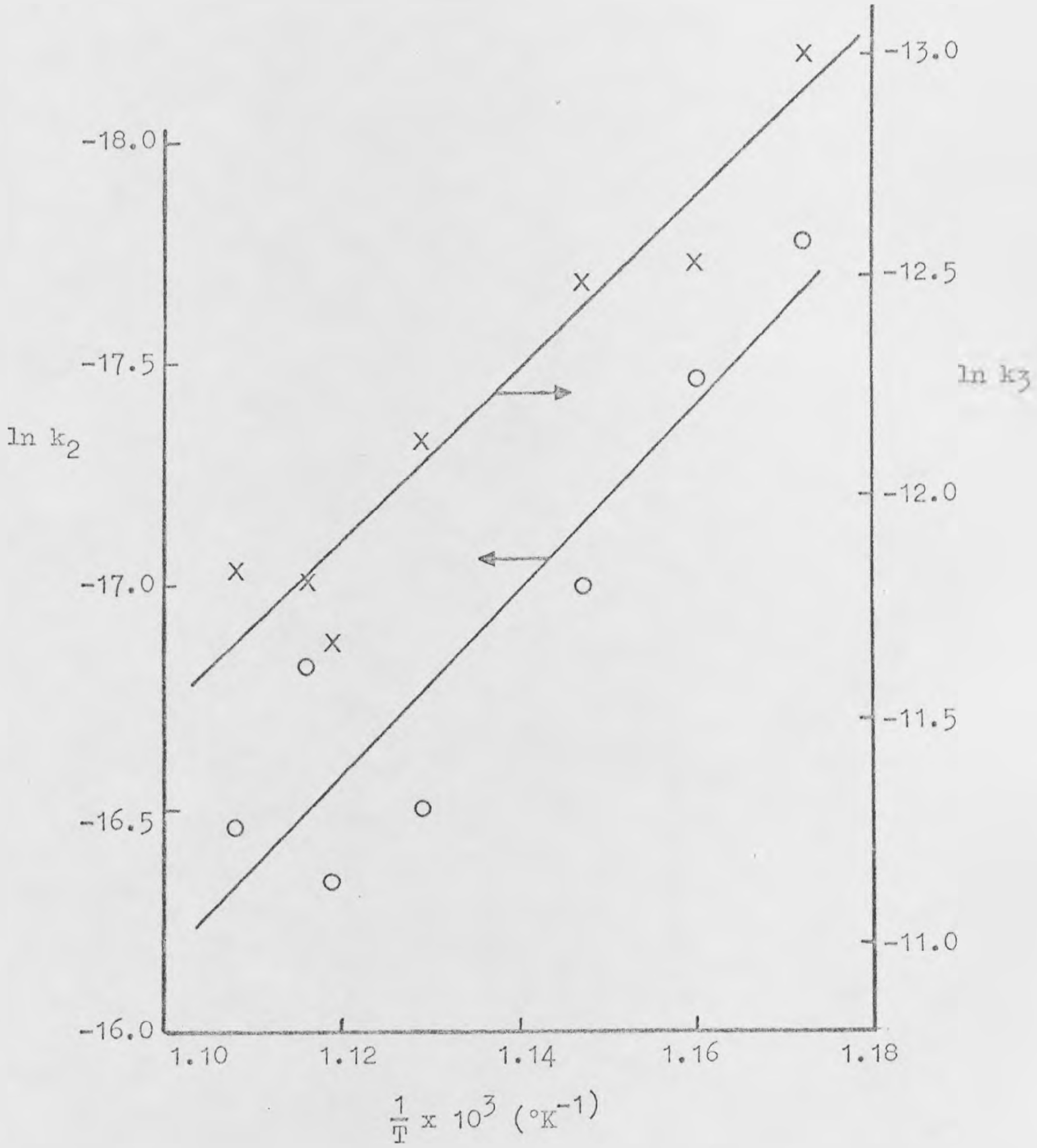

Figure 6.6: Rate Constants for Side-Reactions

$$k_2 = \exp(6.1860 - 20336/T) \quad (6.7)$$

$$k_3 = \exp(9.1634 - 18820/T) \quad (6.8)$$

When used with the dehydrogenation rate constant of Carra and Forni[39] (equation 2.16), these values give high (c. 98%) efficiencies and so they were increased sevenfold to obtain values in the expected range of 89-92%. The values are then

$$k_2 = \exp(8.1319 - 20,336/T) \quad (6.9)$$

$$k_3 = \exp(11.1093 - 18,820/T) \quad (6.10)$$

The conversions obtained from these kinetics were not greatly different from those given by M. The efficiencies are shown in Figures 6.1-6.5 as the curves M1 and behave as expected in each case. In Figures 6.3 and 6.4 the efficiency goes beyond the expected range but is within it over the range of normal operating conditions. The bed length required for a 40% conversion is 0.19 m compared with 0.20 m for M.

Thus these derived kinetics seem to give the 'best' representation of reactor performance and will be used in all the following work.

6.2 Physical Property Variation

In the comparison of kinetics the physical properties were allowed to vary along the length of the bed although the pressure was kept constant. The variation of physical properties is due to the varying temperature along the bed and the increase in volume due to the reaction. These will affect the velocity, density and specific heat of the gas. The pressure, heat of reaction and the interphase heat and mass transfer coefficients will also vary.

In the literature, the variation of parameters is usually ignored as this simplifies the computation and reduces the computation time. Although it is often stated that the variation could be included if desired, the effect of doing so is rarely considered. Results obtained with variable and constant properties are therefore compared, and the effect of temperature, pressure and volume change with reaction on the physical properties are considered separately and in the various combinations.

The differences in results obtained with variable and constant properties are the same for both the film resistance and the pseudo-homogeneous model. Thus results are only presented for the film resistance model. These are shown in Table 6.3 in which the base case is 40% conversion when all property variations are included.

The effect of ignoring the pressure drop is negligible as it is only 0.004 bar and the conversion at constant pressure is 40.02%.

The conversion obtained when the volume change is ignored is 40.35%, an increase of approximately 1%. The effect of evaluating the physical properties at a constant (inlet) temperature is greater, reducing the conversion by approximately 2%. However, these have opposite effects and, if constant physical properties are used, the conversion only changes by 1%.

The use of constant values reduces the computing time for one calculation along the bed from 10.7 seconds to 5.3 seconds. This saving in computing time may not be important for the steady state models but, in the transient models, a 1% difference is acceptable to achieve a halving of the computing time, because the results will be used for comparison purposes only.

6.3 Cyclic Reactor Norm

It was concluded in Chapter 5 that the norm bed size for each bed in the cyclic reactor system should be that of a typical single bed adiabatic reactor. The model used in determining the norm is the

Initial Parameter Values:

T - 630°C

P - 1.7 bar

u - 0.6197 ms^{-1}

C_{pg} - 2.399 kJ kg^{-1}°C^{-1}

ρ_g - 5.475 x 10^{-4} kg l^{-1}

h - 252.3 Wm^{-2}°C^{-1}

k_g - 0.1155 ms^{-1}

Key	x (%)	Efficiency (%)	T_{OUT} (°C)	P (bar)	h (Wm^{-2}°C^{-1})	kg (ms^{-1})	u (ms^{-1})	C_{pg} (kJ kg^{-1}°C^{-1})	ρ_g x 10^4 (kg l^{-1})
0	39.58	90.78	846.37	1.700	252.3	0.1155	0.6197	2.399	5.475
1	39.22	90.85	846.13	1.696	252.3	0.1198	0.6379	2.399	5.318
2	39.56	90.78	846.36	1.696	252.3	0.1156	0.6212	2.399	5.461
3	39.24	90.84	846.14	1.700	252.3	0.1197	0.6363	2.400	5.331
4	40.37	90.92	846.46	1.700	218.7	0.1081	0.5809	2.346	5.841
5	40.02	90.98	846.24	1.700	218.7	0.1120	0.5966	2.348	5.687
6	40.35	90.92	846.45	1.696	218.7	0.1082	0.5822	2.346	5.828
7	40.00	90.98	846.23	1.696	218.7	0.1121	0.5980	2.348	5.674

Key	Variation due to:
0	No variation
1	Pressure drop, volume change
2	Pressure drop
3	Volume change
4	Temperature change
5	Temperature and volume change
6	Temperature change and pressure drop
7	Temperature and volume change and pressure drop.

Table 6.3: Effect of Variation of Physical Properties on Steady State Results.

C_{pg} - $2.417\ \mathrm{kJ\ kg^{-1}\,{}^{\circ}C^{-1}}$

ρ_g - $5.359 \times 10^{-4}\ \mathrm{kg\ l^{-1}}$

C_{ps} - $1.047\ \mathrm{kJ\ kg^{-1}\,{}^{\circ}C^{-1}}$

ρ_s - $1.750\ \mathrm{kg\ l^{-1}}$

e, e_p - 0.4

S_v - $1240\ \mathrm{m^2 m^{-3}}$

k_g - $0.1182\ \mathrm{ms^{-1}}$

h - $265.4\ \mathrm{Wm^{-2}\,{}^{\circ}C^{-1}}$

u - $0.6331\ \mathrm{ms^{-1}}$

EBfeed - $2.935\ \mathrm{kg\ h^{-1}}$

STM feed - $6.967\ \mathrm{kg\ h^{-1}}$

A - $0.00811\ \mathrm{m^2}$

P - 1.7 bar

SR - 14.0

ΔH_1 - $124972\ \mathrm{kJ\ kmol^{-1}}$

ΔH_2 - $101481\ \mathrm{kJ\ kmol^{-1}}$

ΔH_3 - $-65354\ \mathrm{kJ\ kmol^{-1}}$

$c_{EB,o}$ - $0.0015\ \mathrm{kmol\ m^{-3}}$

α - 0.093 bar

β - 8.03

Table 6.4: Data for Norm Conditions in Chapters 6, 7 and 8.

film resistance model (equations 3.31-3.35) with constant physical properties because this is the one used in the cyclic system. The typical steady state performance is assumed as 40% conversion with an inlet temperature of 630°C. The other data for the model are given in Table 6.4 and the kinetics derived in Section 6.3 are employed. The bed size required for 40% conversion is found to be 0.204 m and this norm, together with the data in Table 6.4, will be used in all subsequent studies unless otherwise stated.

6.4 Cyclic Reactor Conversion Limits

It is hoped that the cyclic reactor will give higher conversions than existing steady state reactors because of the inherent temperature control. The minimum desired conversion is that given by a two-bed steady state reactor using the same total volume of catalyst as the cyclic reactor system. This steady state reactor is therefore modelled using the norm size for each bed and the data in Table 6.4. A suitable value for the inlet pressure to the first bed must be selected as this is higher than for a single bed reactor. A typical report in the literature[36] gives this as 3.1 bar with an outlet pressure of 2.3 bar for a first bed conversion of 40%. There is a pressure drop of 0.7 bar in the interstage heater and the inlet pressure to the second bed is therefore 1.6 bar. The outlet pressure from the second bed is not given and is assumed to be 1 bar. Sheel and Crowe[17] reported that the commercial reactor which they studied had a negligible pressure drop and this is supported by the model results. The significant pressure drops quoted above must therefore be due to the reactor configuration or the use of a small particle size or a high mass velocity. Whatever their cause, it is assumed that they occur across the beds and that the pressure varies linearly with length.

A two-bed model, using these pressures and the quoted inlet temperatures (630°C), gives an overall conversion of 60.8% with an efficiency of 86.7%. The maximum conversion of the system is obtained when the inlet temperatures are at the maximum permitted value (650°C). If both inlet temperatures are increased to 650°C, the conversion becomes 68.6% but the efficiency falls to 85.8%. However, it is unlikely that the inlet temperature to the second bed would be as high as 650°C as this would cause excessive pyrolysis in the interstage heater, reducing both the conversion and the efficiency. In the literature, the maximum conversion quoted for a two-bed reactor is 63% and in no case is the inlet temperature to the second bed given as greater than 630°C. With inlet temperatures of 650°C and 630°C for the first and second beds respectively, the overall conversion is 63.9% with an efficiency of 85.7%. This would seem to be more realistic as the maximum conversion obtainable from such a reactor.

The cyclic reactor system does not include any interstage heating as only a single bed is reacting at any time. An inlet temperature of 650°C can therefore be used and the inlet pressure need be no higher than for a single steady state bed. The low efficiency of the two-bed steady state reactor is largely due to the high pressure in the first bed and hence the cyclic reactor system should give an improved efficiency.

The maximum conversion of the cyclic system is the isothermal steady state value. At a temperature of 650°C, this is 72.0% with an efficiency of 88.5%. Thus the desired conversion from the cyclic reactor system is in the range 64 - 72%.

6.5 Estimation of Cyclic System Parameters

6.5.1 Period Time

The rate of temperature fall in the reactor is given by

$$T_{fall} = \frac{F_{EB} \Sigma_j (x_j \Delta H_j)}{AZ(1-e)\rho_s C_{ps}} \tag{5.5}$$

and, as shown in Chapter 5, this can be used to determine an initial estimate for the period time of the cyclic reactor system. The conversions and rate of temperature fall are given in Table 6.5 for various isothermal reaction temperatures.

Isothermal Temperature (°C)	Conversion (%)	T_{fall} (°C s^{-1})
650	72.0	0.368
640	67.8	0.348
630	63.1	0.324
620	57.9	0.298

Table 6.5: Steady state conversion and rate of temperature fall at various isothermal temperatures

If the cyclic reactor is initially at 650°C and only a slight improvement over the two-bed steady state reactor conversion of 64% is sought, a 30°C temperature drop can be allowed. The actual conversion will fall from 72% to 57.9% giving an arithmetic mean of approximately 65%. The mean rate of temperature fall over this range is 0.333°C s^{-1} and, from equation 5.6, the allowable period time (t_f) is therefore

$$t_f = \frac{30}{.333} = 90 \text{ seconds} \tag{6.11}$$

A higher conversion can be obtained by allowing only a 20°C temperature fall. The mean conversion and rate of fall are then approximately 68% and 0.346°C.s^{-1} respectively and the allowable period is about 58 seconds. The minimum period time was chosen in Chapter 5 as 60 seconds and thus 68% would appear to be the maximum attainable conversion. However, it must be remembered that the kinetics used predict a much smaller bed size than the others considered. Equation 5.5 shows that the rate of temperature fall is inversely proportional to the bed size and so the predicted period time is directly proportional to it. The rate of temperature fall predicted by the kinetics of Sheel and Crowe[17] or Davidson and Shah[18] would be approximately 8 times less and, if the kinetics of Eckert et al[33] were used, the rate of fall would be reduced by a factor of 15. These rates of temperature fall would allow a longer period or, if the period was the same, a reduced temperature drop and higher conversion.

Sheel and Crowe[17] specify the dimensions of the commercial reactor, and the reactant flowrate, used in their simulation. The rate constants of the kinetics derived in Section 6.3 must be reduced by a factor of 0.28 to reproduce the quoted styrene production with this reactor size and flowrate. Application of this factor to the data in Table 6.4 predicts a bed size approximately 3.6 times the norm to give a 40% conversion. Thus, in considering the allowable period time and attainable conversion, the norm bed size will always give predictions on the pessimistic side.

6.5.2 Regenerator Steam Flow

It was shown in Chapter 5 that an approximation to the regenerator steam flow required to saturate the bed is given by

$$\bar{F}_{STM} = \frac{(1-e)\,\rho_s\,C_{ps}\,AZ}{t_f\,\bar{C}_{pg}\,MW_{STM}} \qquad (5.9)$$

which is obtained from the analytical solution of the pseudo-homogeneous regenerator model. Using the norm bed size and data in Table 6.4, this gives steam flows of 46.73 kg h^{-1} and 30.11 kg h^{-1} for the periods of 58 and 90 s predicted in the previous section.

6.5.3 Heat Inputs

An estimate for the superheater heat load can be obtained from

$$HT_{IN} = F_{EB} MW_{EB} C_{pg} (T_{IN} - T_{EB}) + F_{STM} MW_{STM} C_{pg} \, \Delta T \qquad (5.14)$$

where the regenerator steam flow is that given by equation 5.9 and ΔT is the fall in average bed temperature determined in Section 6.5.1. The observed values of ΔT for periods of 58 and 90 s were 20°C and 30°C respectively. If T_{IN} is 650°C, the corresponding superheater heat loads are 0.3103 kW and 0.3571 kW.

The make-up steam temperature is given by

$$\overline{T}_{STM} = \frac{\overline{F}_{STM}}{F_{STM}} \overline{T}_{IN} - \frac{\overline{F}_{STM} - F_{STM}}{(F_{STM})^2 \, MW_{STM}} \left[(F_{EB} \, MW_{EB} + F_{STM} \, MW_{STM}) \, T_{IN} - F_{EB} \, MW_{EB} \, T_{EB} - \frac{HT_{IN}}{C_{pg}} \right] \qquad (5.16)$$

This cannot be estimated accurately at this stage as only approximate values of HT_{IN} have been evaluated. However, using these values, with T_{IN} and $\overline{T}_{IN}$ at 650°C, gives $\overline{T}_{STM}$ as 764°C and 750°C for periods of 58 and 90 s respectively.

6.5.4 Summary

The predicted values of period time, regenerator steam flow, superheater heat load and make-up steam temperature for the cyclic reactor system are summarised in Table 6.6 below.

Average Conversion	t_f (s)	$\overline{F}_{STM}$ (kg h^{-1})	HT_{IN} (kW)	$\overline{T}_{STM}$ (°C)
68%	58	46.73	0.3103	764
65%	90	30.11	0.3571	750

Table 6.6: Parameters for the cyclic reactor system predicted from steady state studies

CHAPTER 7

TRANSIENT SINGLE BED STUDIES

Transient reactor and regenerator models were developed in Chapter 3 for use in the model of the cyclic reactor system. However, it is desirable to investigate the performance of each separately before considering the system as a whole. This will help to understand their behaviour in the cyclic system and guides the evaluation of the operational parameters.

7.1 Reactor Studies

Figure 7.1 shows the variation of the reactor temperature profile with time, for the norm bed size and data in Table 6.4. The feed and initial bed temperatures are 650°C and the reactor proceeds to the steady state. As would be expected, the temperature near the entrance rapidly approaches steady state as most of the reaction occurs in this region. The temperature minimum moves along the bed, but the rate of temperature fall near the exit is considerably slower. This causes a rising temperature profile near the exit, which enhances the equilibrium and will be beneficial in the cyclic reactor system as long as the steady state is not closely approached. Figure 7.2 shows that the conversion also quickly approaches steady state near the entrance but the fall near the exit is again much slower.

The variation of outlet temperature and conversion with time is shown in Figure 7.3. This shows both the observed values at a given time, and the average values which are integrated over the elapsed time interval. The conversion approaches the steady state sooner than the outlet temperature and thus the temperature gives a better indication of when steady state is achieved. The slower fall of the average values is expected but it is noteworthy as the cyclic system

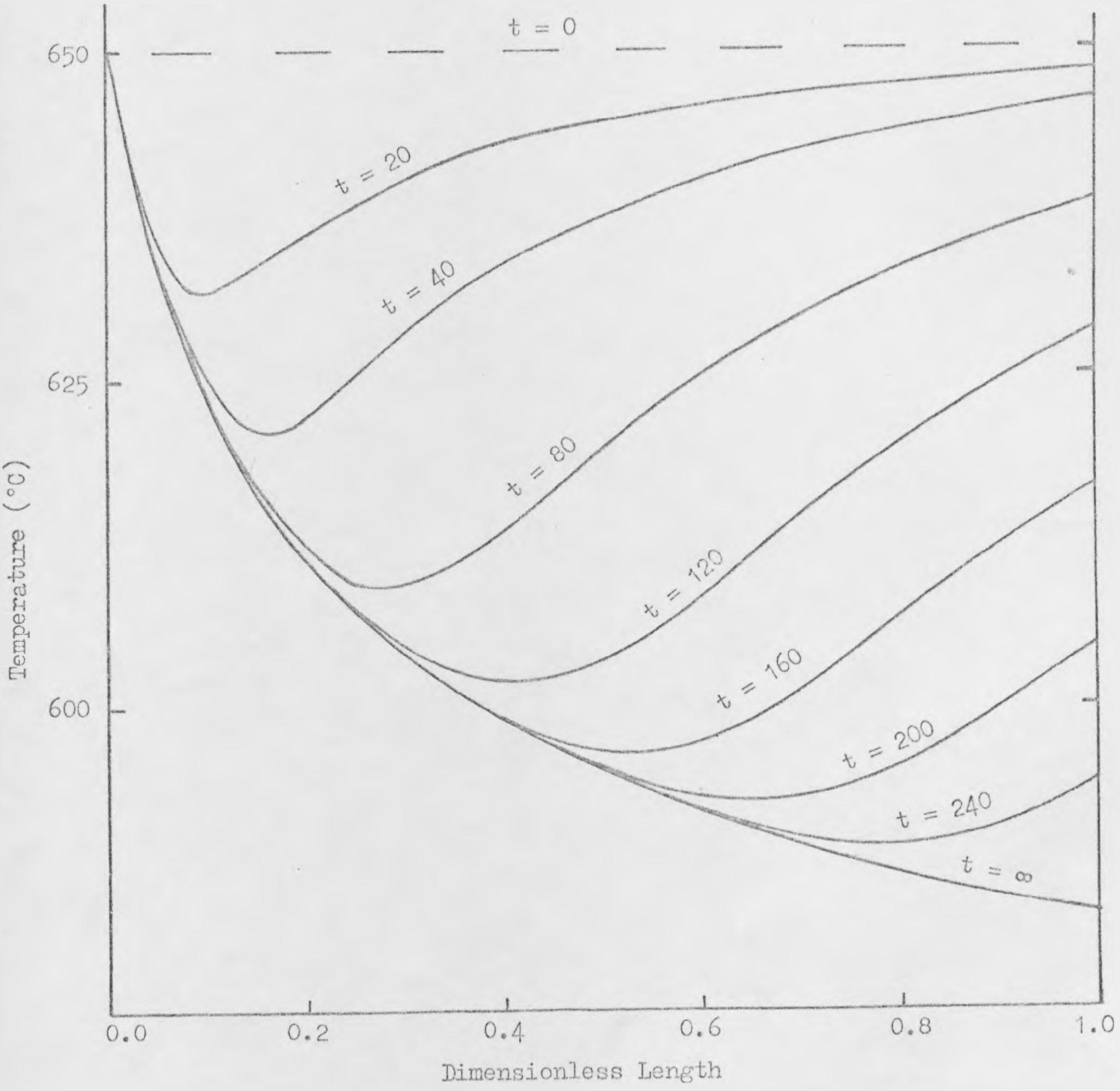

Figure 7.1: Temperature Profiles in a Transient Reactor.

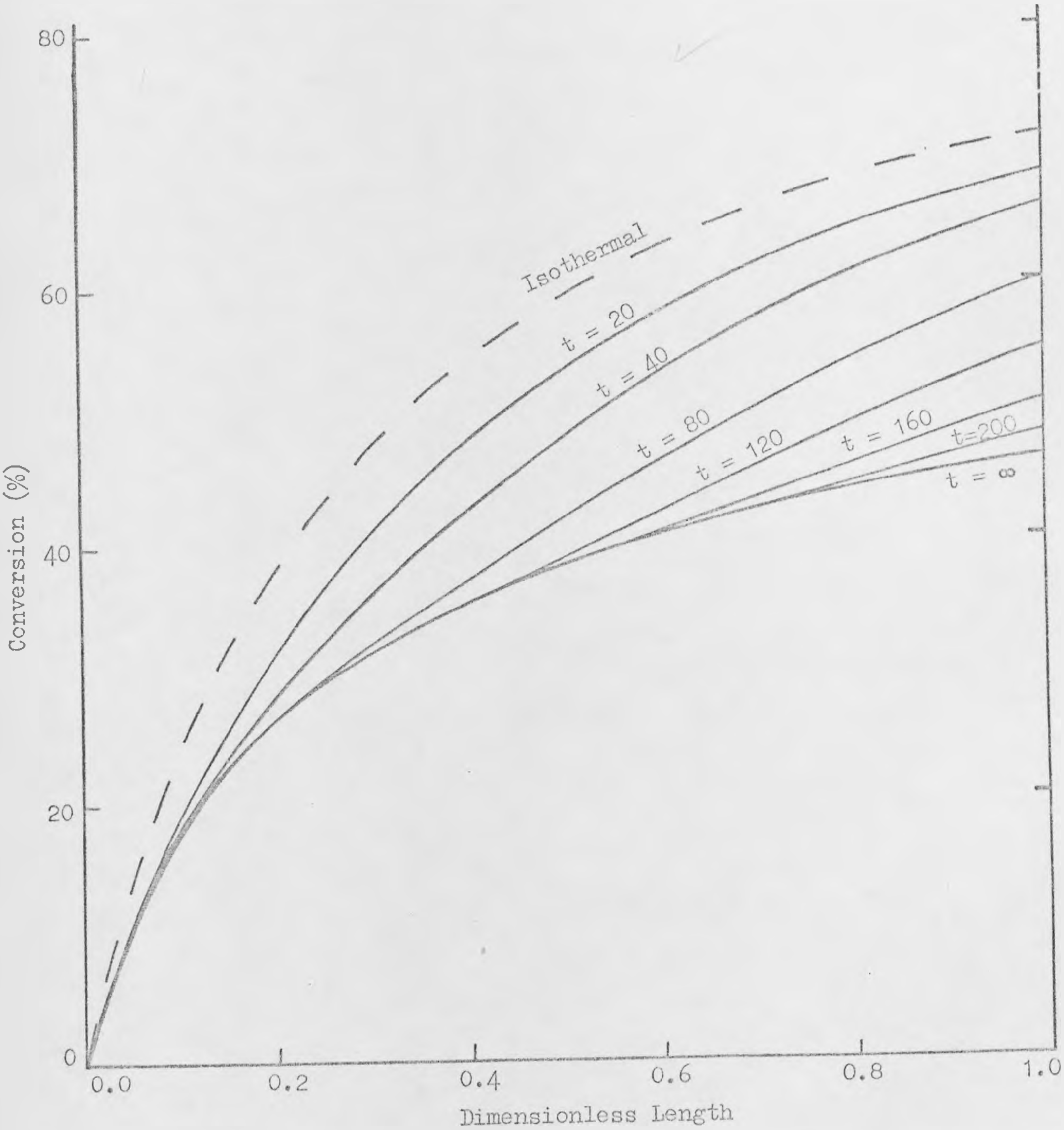

Figure 7.2: Conversion Profiles in a Transient Reactor.

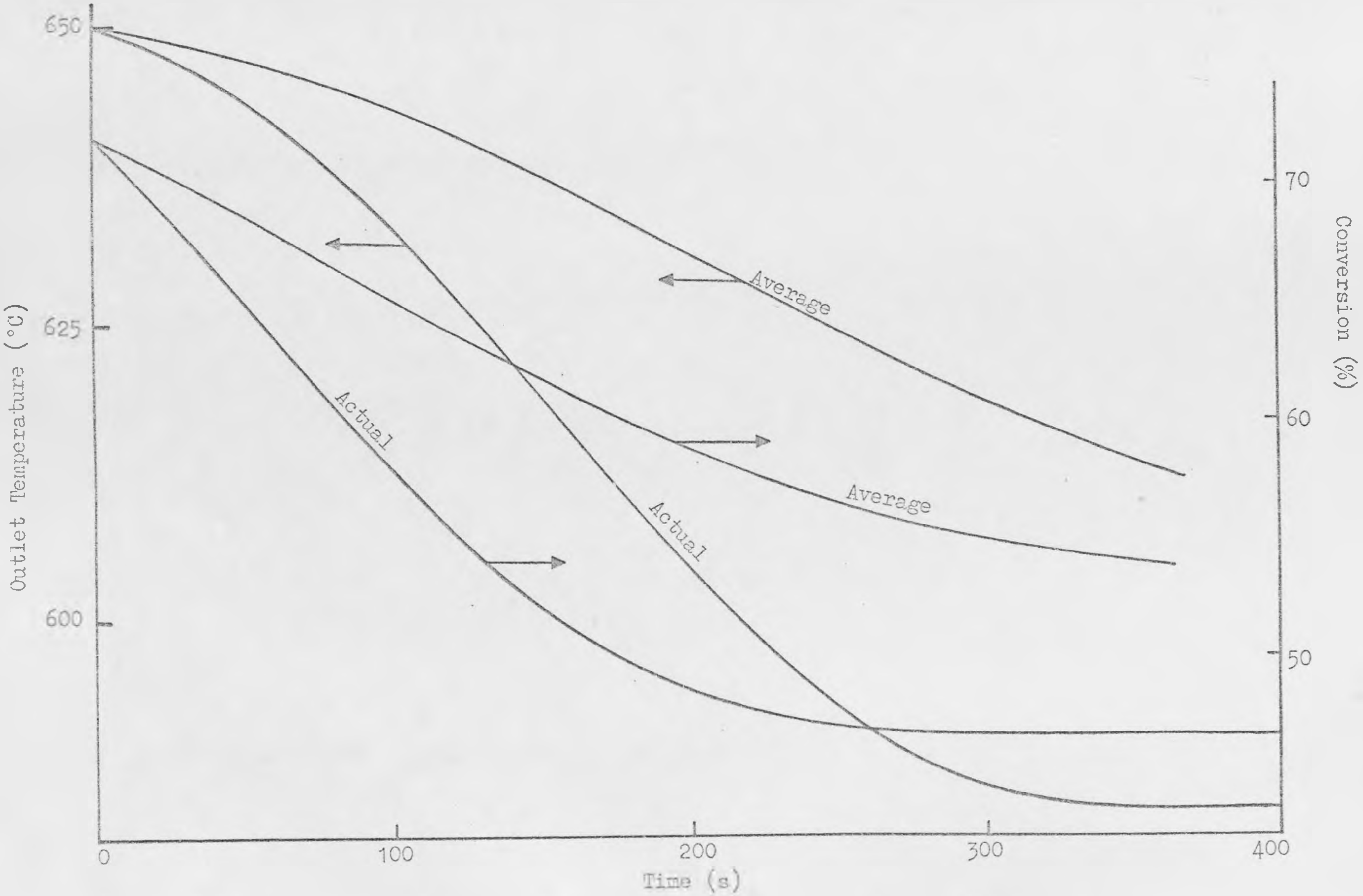

Figure 7.3: Variation of Reactor Outlet Temperature and Conversion with Time.

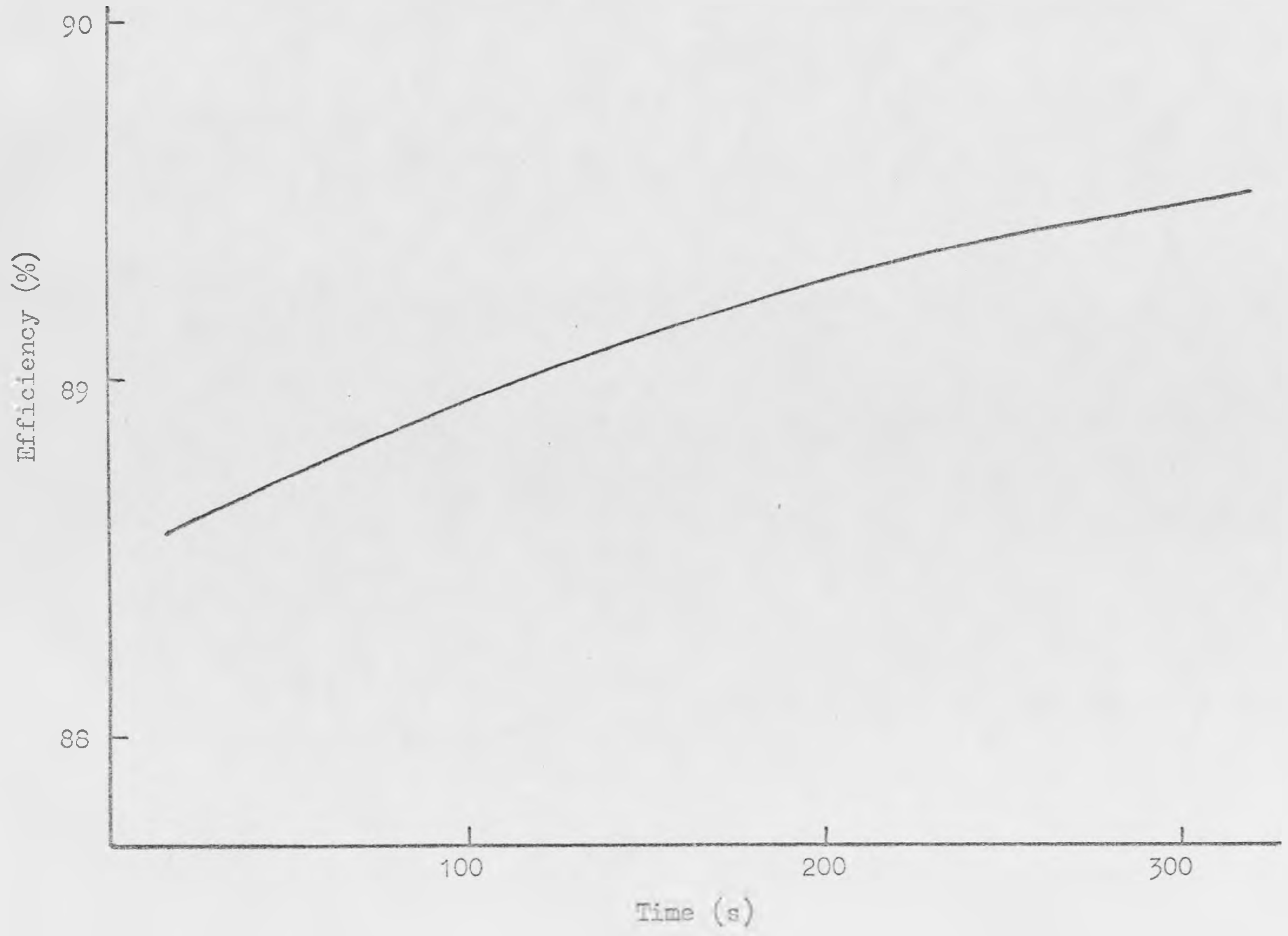

Figure 7.4: Variation of Efficiency with Time from a Transient Reactor.

will be concerned with average values.

Figure 7.4 shows that the efficiency of the average conversion increases with time. The increase is due to the falling conversion and the change is only a single per cent over the time required to achieve steady state.

7.1.1 Cyclic Reactor Period Time

The average conversion shown in Figure 7.3 can be used to check the period times predicted from the steady state results in Section 6.5. These are 90 and 58 seconds for arithmetic mean conversions of 65% and 68% respectively. The times elapsed when the average conversion falls to these values are obtained from Figure 7.3 as approximately 100 and 60 seconds. The steady state calculations, therefore, appear to predict conservative periods, especially at the higher value. This is probably due to the greater deviation of the temperature profile from the isothermal one assumed. The higher outlet temperature in the transient reactor produces a higher conversion than the assumption of a uniform average profile. However, the steady state predictions are simple to obtain and thus are a useful means of obtaining a first approximation for the period time.

In both the steady state and transient studies it is assumed that the initial profile is isothermal at the maximum temperature. The conversion of the cyclic system will be reduced if this is not the case and these predicted periods are therefore the maximum values for the specified conversions.

7.1.2 Effect of Initial Temperature Profile

The reactor conversion depends on the initial bed temperature profile which, in the cyclic system, is determined by the regenerator operation. The effect of various initial isothermal bed temperatures on the average conversion is shown in Table 7.1. The feed temperature in each case is 650°C and so the reactor is tending towards the same steady state. The difference in conversion for the various initial temperatures is, therefore, less as steady state is approached. A reduction in initial bed temperature causes a significant lowering of conversion and hence it is clearly desirable to operate the regenerator at the maximum allowable temperature.

7.1.3 Effect of Feed Temperature

The effect of varying the feed temperature on the average conversion is shown in Table 7.2 for an initial bed temperature of 650°C. The reactor is now tending towards different steady states in each case and so the differences increase with time. A comparison of Tables 7.1 and 7.2 shows that, at the period times of less than 100 seconds predicted above, the effect of a change in feed temperature is considerably less than that of a similar change in the initial temperature. The variation of the cyclic reactor feed temperature caused by the varying regenerator outlet temperature is therefore unlikely to seriously affect the performance. The effect of the variation produced in the regenerator inlet temperature will be greater as this determines the final regenerator (initial reactor) profile.

7.1.4 Effect of Diluent Steam Flow

It was suggested in Chapter 5 that it may be possible to operate the cyclic reactor with a low steam/ethylbenzene ratio as the reaction heat is largely supplied by the heat stored during the regenerator period. Figure 7.5 shows that the actual (not average) conversion is not greatly affected by the steam/ethylbenzene ratio until steady state is approached unless it is very low. Steady state is achieved more quickly with a high steam/ethylbenzene ratio. The corresponding average

Initial Temperature (°C)	Elapsed Time (s)			
	50	100	200	300
650	68.71	65.16	58.85	55.03
640	64.56	61.38	56.19	53.19
630	60.12	57.49	53.51	51.34
620	55.50	53.56	50.86	49.49

Table 7.1: Average Conversion (%) at Various Initial Isothermal Bed Temperatures with the Inlet Temperature at 650°C.

Inlet Temperature (°C)	Elapsed Time (s)			
	50	100	200	500
650	68.71	65.16	58.85	55.03
640	68.45	64.52	57.38	52.99
630	68.21	63.90	55.94	50.96
620	67.98	63.32	54.54	48.98
610	67.77	62.77	53.19	47.04

Table 7.2: Average Conversion (%) at Various Reactor Inlet Temperatures with the Initial Isothermal Bed Temperature at 650°C.

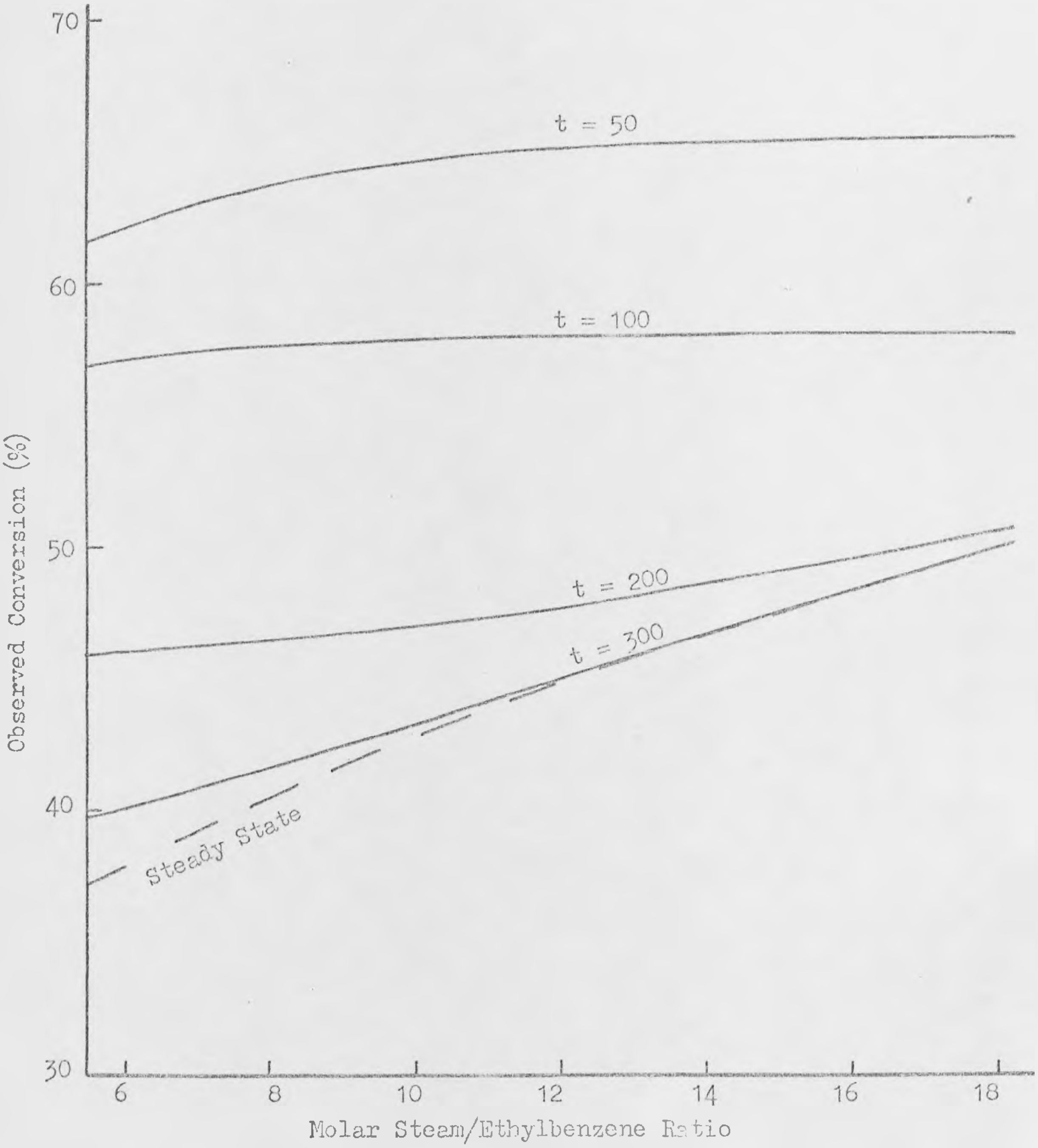

Figure 7.5: Effect of Diluent Steam Flow on the Observed Conversion of a Transient Reactor.

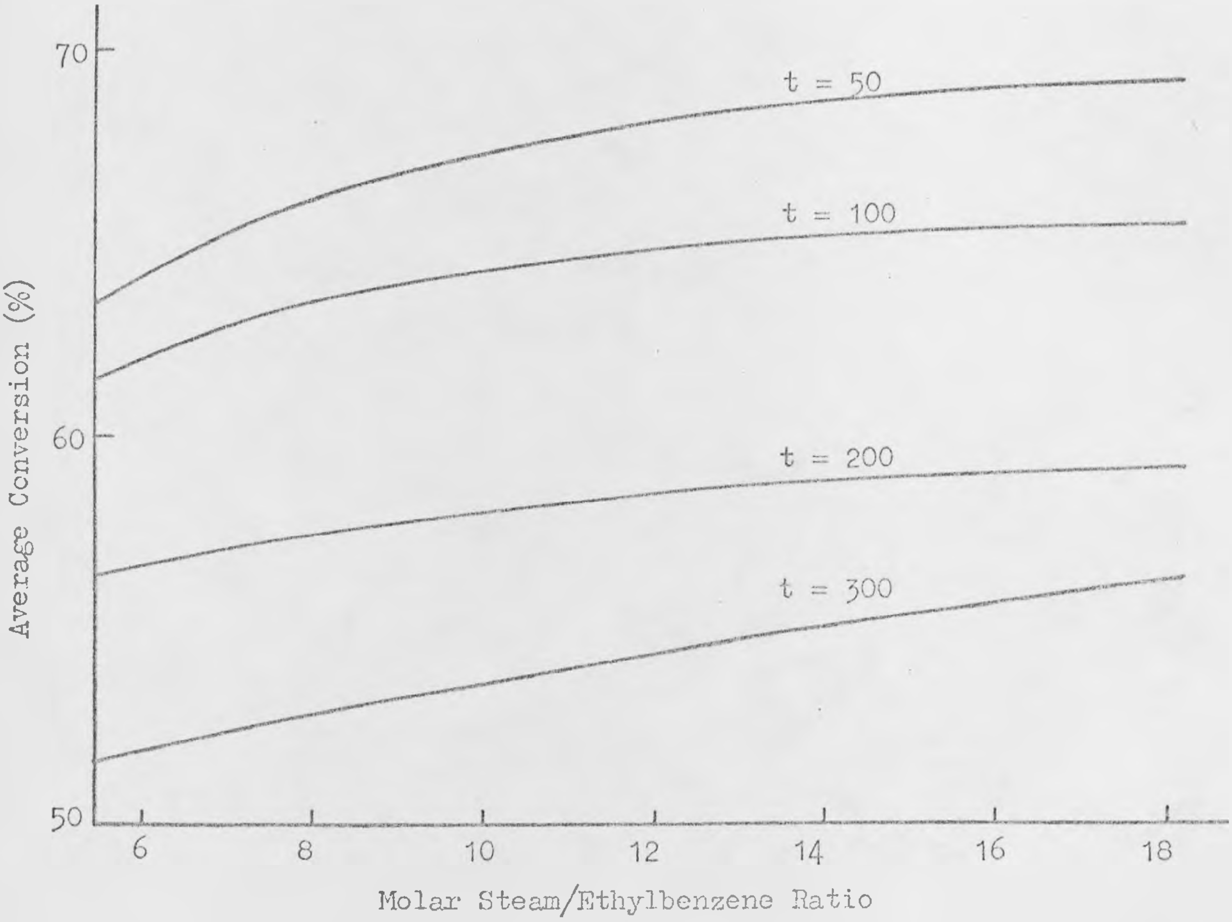

Figure 7.6: Effect of Diluent Steam Flow on the Average Conversion of a Transient Reactor.

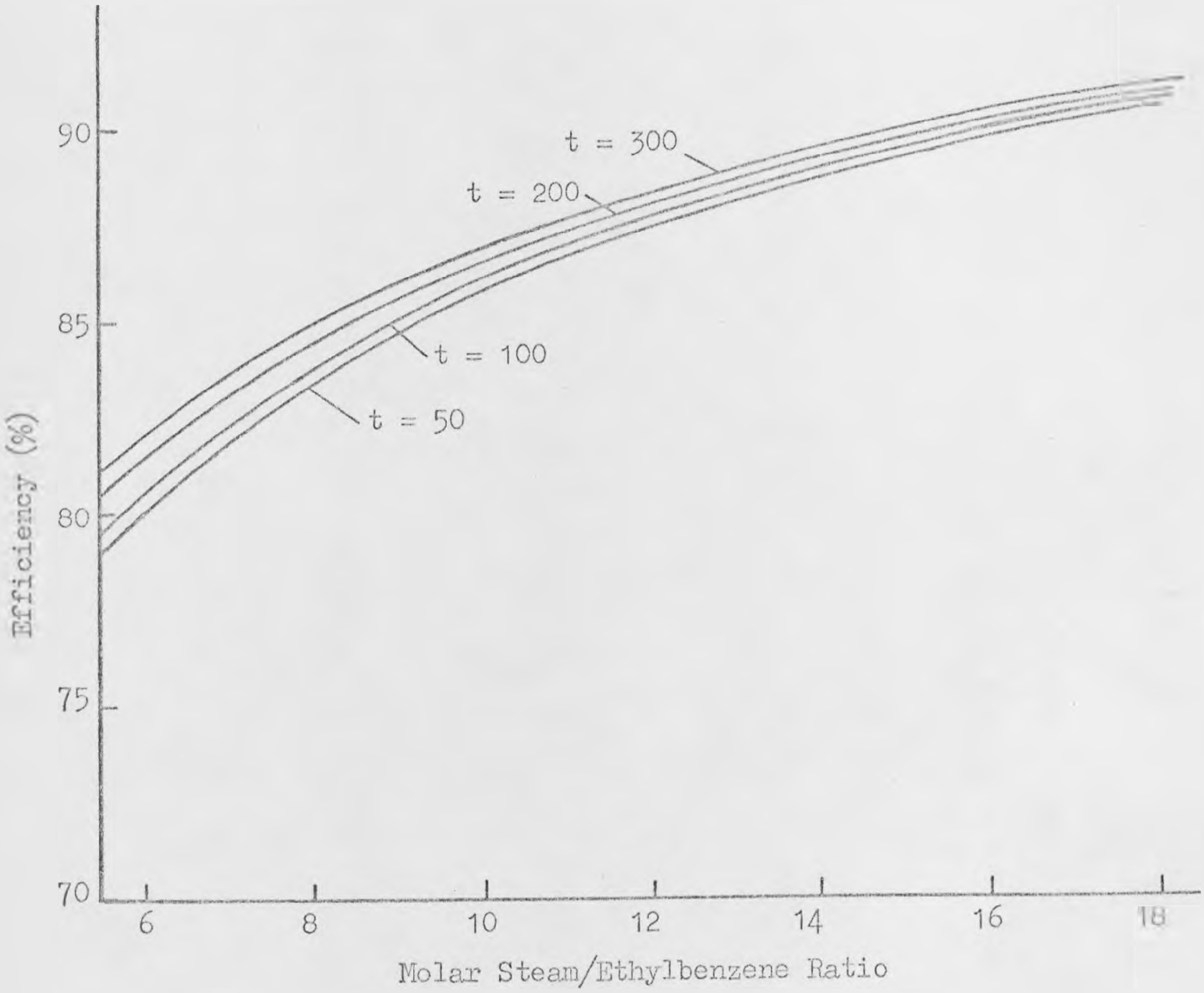

Figure 7.7: Effect of Diluent Steam Flow on the Efficiency of the Average Conversion of a Transient Reactor.

conversions are shown in Figure 7.6. These show that the effect of reducing the diluent steam flow on the performance of the cyclic reactor system will be less than on that of the steady state reactor shown in Figure 7.5. However, reducing the steam flow has an adverse effect on the efficiency, as shown in Figure 7.7. Clearly, a very low value is unacceptable but, if the molar steam/ethylbenzene ratio is not less than 10, the efficiency is still greater than the value of 85.7% determined for a two-bed steady state reactor in Chapter 6. The efficiency is always less than for a single bed steady state reactor as the conversion is much greater. It may therefore be more economic to accept a lower conversion from the cyclic reactor in order to save on the steam cost.

7.1.5 Effect of Bed Heat Capacity

In Chapter 6, it was observed that the heat capacity of the bed has a significant effect on the allowable period time of the cyclic reactor system. If necessary, the heat capacity can be increased by mixing the catalyst with an inert material which is assumed to be particles of catalyst support so that the physical properties are the same. Additional heat capacity also occurs in the reactor wall and the effect of this, in a pilot scale reactor, is considered in Appendix 5.

Table 7.3 compares outlet temperatures and observed conversions after various time intervals for an undiluted bed and one in which various amounts of inert material are added. The parameter y is the amount of inert material added, expressed as a fraction of the catalyst volume. As suggested by equation 5.5,

$$T_{fall} = \frac{F_{EB}\ \Sigma_j\ (x_j\ R_j)}{AZ\ (1-e)\,\rho_s\ C_{ps}} \qquad (5.5)$$

the speed of response of the bed is, to all intents and purposes,

Undiluted Bed (y = 0)					
t (s)	25	50	100	200	300
x (%)	68.83	65.28	58.00	48.67	46.81
T_{OUT} (°C)	647.8	644.4	633.6	604.6	585.9
y = 0.5					
t (s)	37.5	75	150	300	450
x (%)	68.69	65.14	57.86	48.54	46.78
T_{OUT} (°C)	647.8	644.4	633.7	604.8	585.3
y = 1.0					
t (s)	50	100	200	400	600
x (%)	68.62	65.06	57.80	48.47	46.76
T_{OUT} (°C)	647.8	644.4	633.8	604.9	584.9
y = 1.5					
t (s)	75	150	300	600	900
x (%)	68.54	64.99	57.73	48.40	46.75
T_{OUT} (°C)	647.8	644.4	633.8	605.1	584.5

Table 7.3: Effect of Uniformly Mixed Inert Material on the Response of a Transient Reactor.

inversely proportional to the bed heat capacity. The possibility of ignoring the temperature difference between the fluid and inert material by using equations 3.41 - 3.44 was discussed in Chapter 3. This avoids the use of an additional heat balance on the inert material. The results obtained in this case do not differ significantly from those in Table 7.3, and hence the extra heat balance is not necessary.

In practice it will be difficult to produce a uniform mixture of catalyst and inert material and it would therefore be simpler to introduce the inert material in a single region as shown in Figure 7.8. This approximates two catalyst beds with interstage heating as the inert material acts as a heat source and increases the temperature in the second catalyst region before steady state is approached. This effect is shown by the temperature profiles within the bed in Figure 7.9 for equal volumes of catalyst and inert material. In the cyclic reactor system, this inert region would operate as a regenerative heat exchanger between the two catalyst regions. Clearly, the reactor will operate as an undiluted bed if the inert region is at either end. Thus there is an optimum position which gives the maximum conversion during transient operation. This is found by trial and error to be when the inert region starts at about 0.15 of the distance along the bed. This is the case shown in Figure 7.9 and clearly gives more favourable temperature conditions than the undiluted bed shown in Figure 7.1.

The effect of the inert region on the outlet temperature and the observed conversion is shown in Figure 7.10 and compared with a uniformly diluted bed containing the same amount of inert material. When the heat stored in the inert region reaches the reactor exit it causes a considerable reduction in the rates of fall of temperature

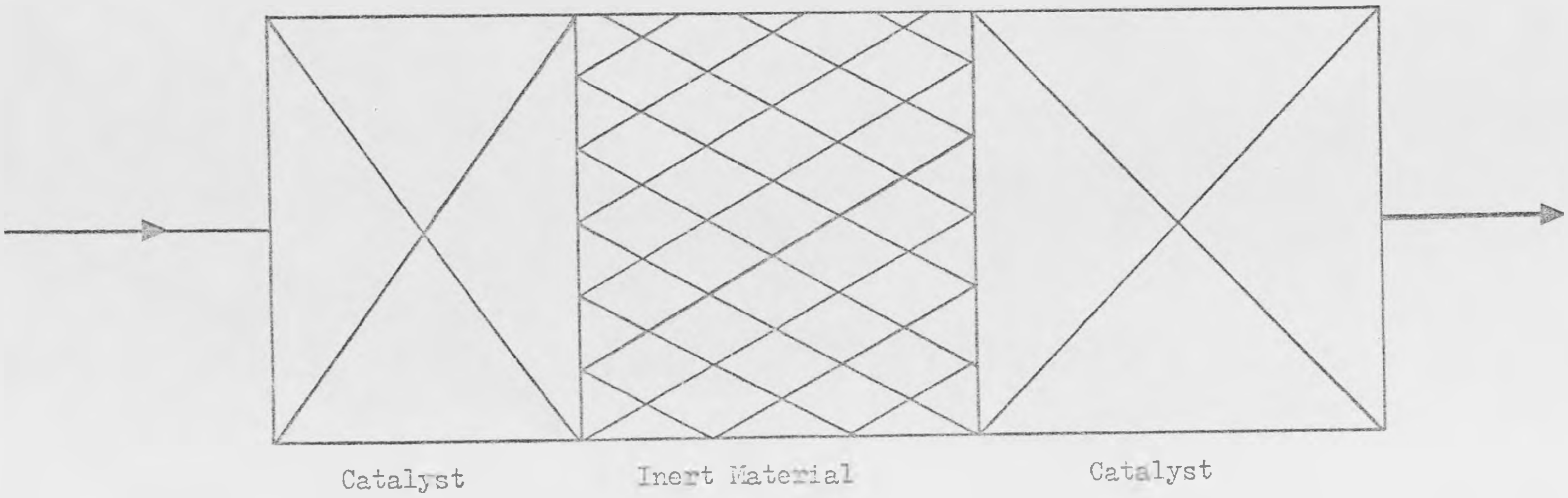
Catalyst
Inert Material
Catalyst

Figure 7.8: Reactor with a Region of Inert Material within the Catalyst Bed.

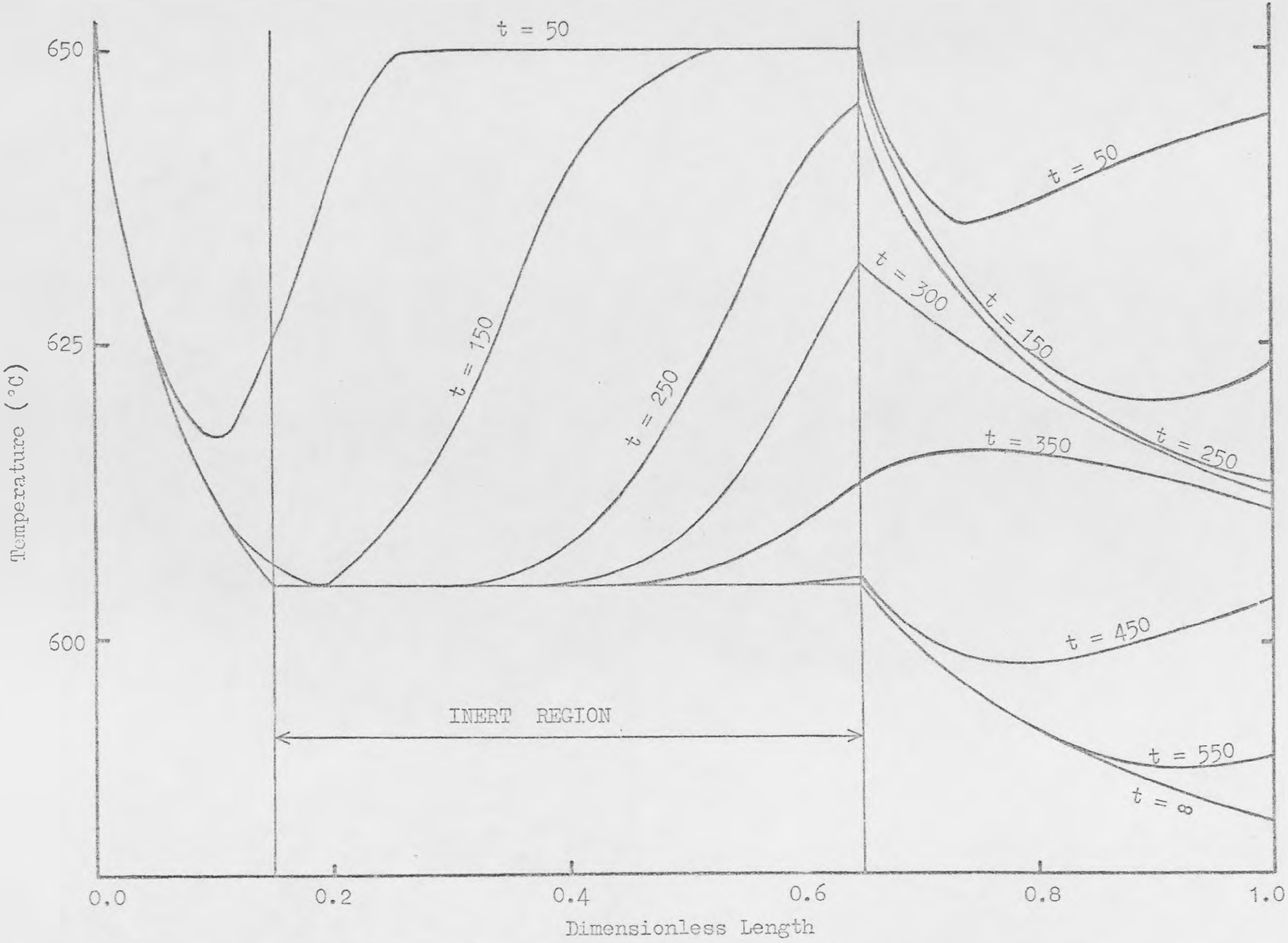

Figure 7.9: Temperature Profiles in a Transient Reactor with Region of Inert.

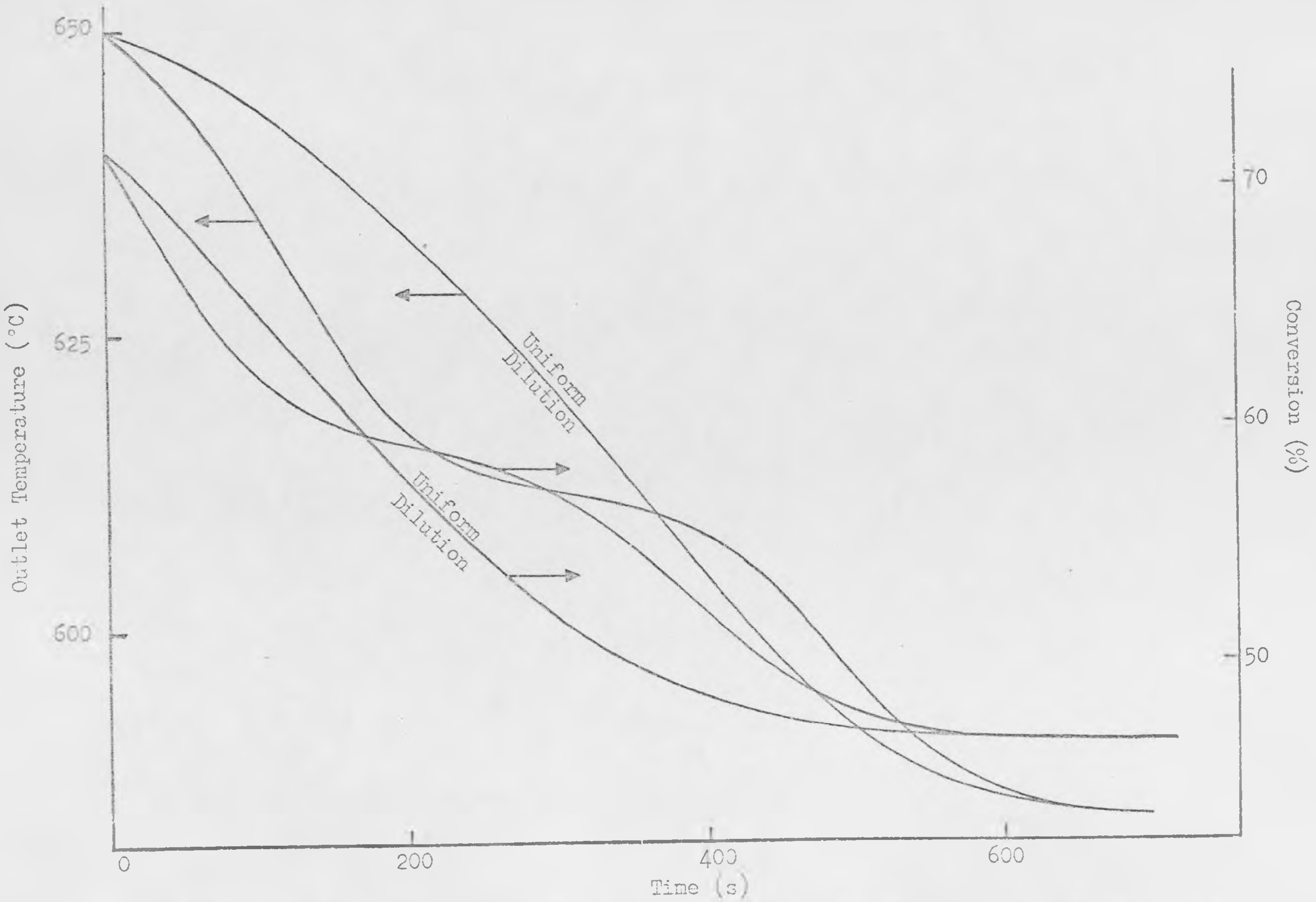

Figure 7.10: Outlet Temperature and Conversion with Time for a Uniformly Diluted Bed and One Containing a Region of Inert.

and conversion, which then exceed those for the uniform mixture until steady state is approached. Although the conversion exceeds that from the uniform mixture after 180 seconds, the average conversion does not do so until after 300 seconds because of the initially higher conversion from the uniformly mixed bed. Thus, unless the period is greater than 300 seconds, a uniform mixture is preferable for the cyclic reactor. However, it appears that a degree of longitudinal non-uniformity in mixing will not seriously affect the conversion unless the period is very short.

A region of inert material at the front of the catalyst bed could be used to reduce the effect of any feed temperature variation in the cyclic reactor and would lessen the effects of thermal shock.

7.2 Regenerator Studies

7.2.1 Steam Flow

It was suggested in Chapter 5 that the analytical solution of the pseudo-homogeneous regenerator model can be used as a simple means of determining the steam flow necessary to just saturate the bed. The saturation time is

$$t_{sat} = \frac{(1-e)\,\rho_s\, C_{ps}}{\bar{u}\,\bar{\rho}_g\,\bar{C}_{pg}}\, Z \qquad (5.7)$$

and the corresponding steam flow is

$$\bar{F}_{STM} = \frac{(1-e)\,\rho_s\, C_{ps}\, AZ}{t_f\,\bar{C}_{pg}\, MW_{STM}} \qquad (5.9)$$

The steady state results predicted steam flows of 46.73 and 30.11 kg h^{-1} for periods of 58 and 90 seconds. Using the more correct value for $\bar{C}_{pg}$ in Table 7.4, equation 5.9 gives flows of 48.86 and 29.35 kg h^{-1} respectively for the periods of 60 and 100 seconds predicted from the transient reactor results in Section 7.1.1.

The solution of equation 5.7 is compared with the film resistance model breakthrough curves in Figure 7.11 where it is shown as the broken vertical lines. The breakthrough curves are obtained for the same step change in inlet temperature with an initially isothermal bed, and using the additional data in Table 7.4 for the norm conditions. The dimensionless temperature (F) in Figure 7.11 is defined by:

$$F = \frac{\overline{T}_{outlet} - \overline{T}_{s,initial}}{\overline{T}_{inlet} - \overline{T}_{s,initial}} \qquad (4.35)$$

Equation 5.7 predicts the positions of the breakthrough curves fairly well as it intersects them close to the midpoint in each case. However, it gives no indication of the spread of the curves and, in this case, the approach to saturation is not close.

$\overline{C}_{pg}$ — 2.232 kJ kg^{-1}°C^{-1}

$\overline{\rho}_g$ — 4.040×10^{-4} kg l^{-1}

$\overline{h}$ — 615.57 W m^{-2}°C^{-1}

Table 7.4: Regenerator Data for the Norm Conditions

The breakthrough curves obtained from the regenerator in the cyclic reactor system will be affected by the initial temperature profile within the bed. This will be the final reactor profile and will not be isothermal. The initial profile is not considered in the pseudo-homogeneous model analytical solution. Figure 7.12 compares the breakthrough curve from an initially isothermal bed with ones from a bed in which the initial profile was that in a steady state reactor; i.e. the $t = \infty$ curve in Figure 7.1. The dimensionless temperature defined by equation 4.35 is again used, where $T_{s,initial}$ is the minimum initial solid temperature. The breakthrough curves are shown for co-current flows of reaction and regenerating gases and also for counter-

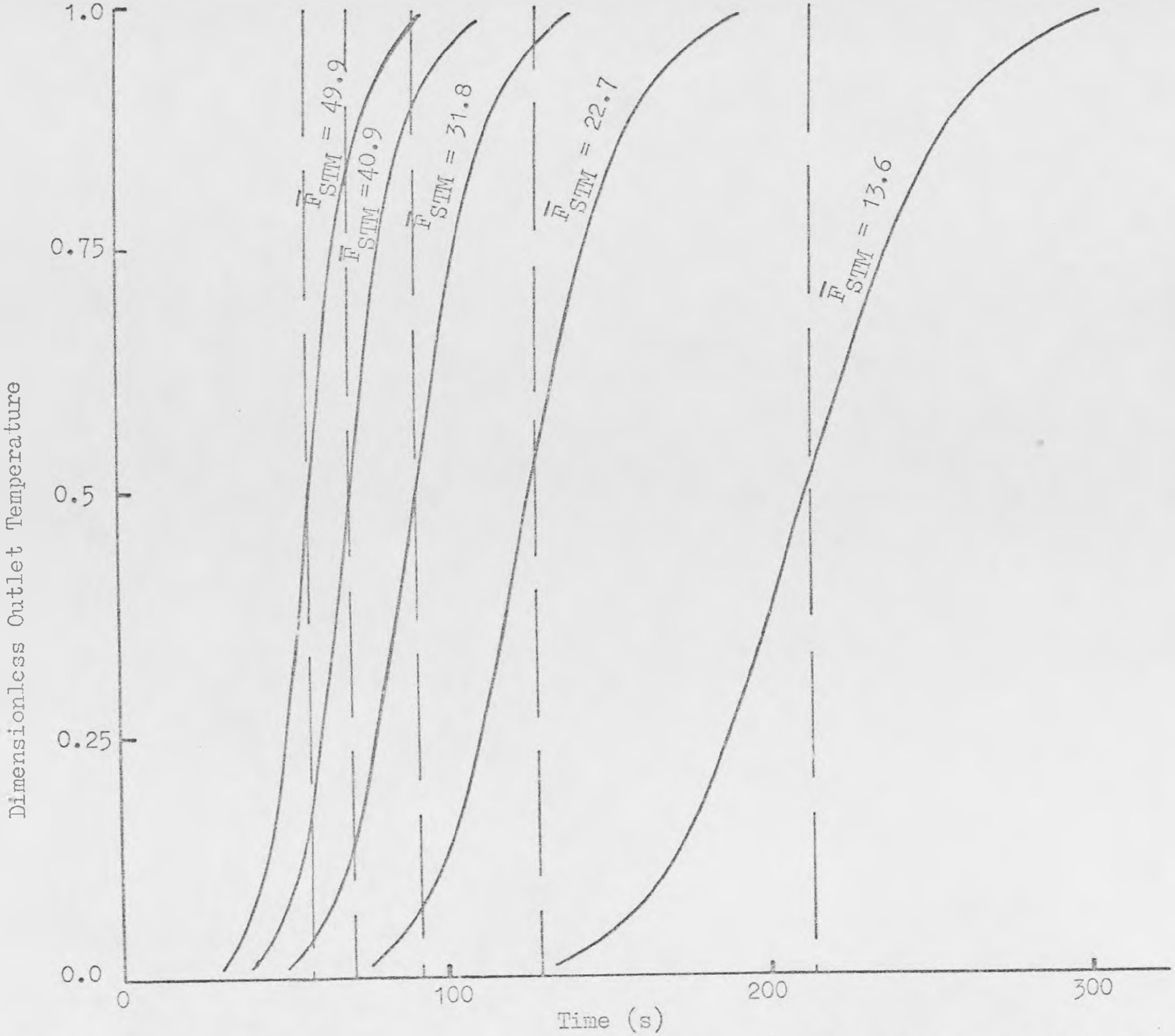

Figure 7.11: Comparison of the Pseudo-Homogeneous Analytical Solution with the Film Resistance Model Breakthrough Curves.

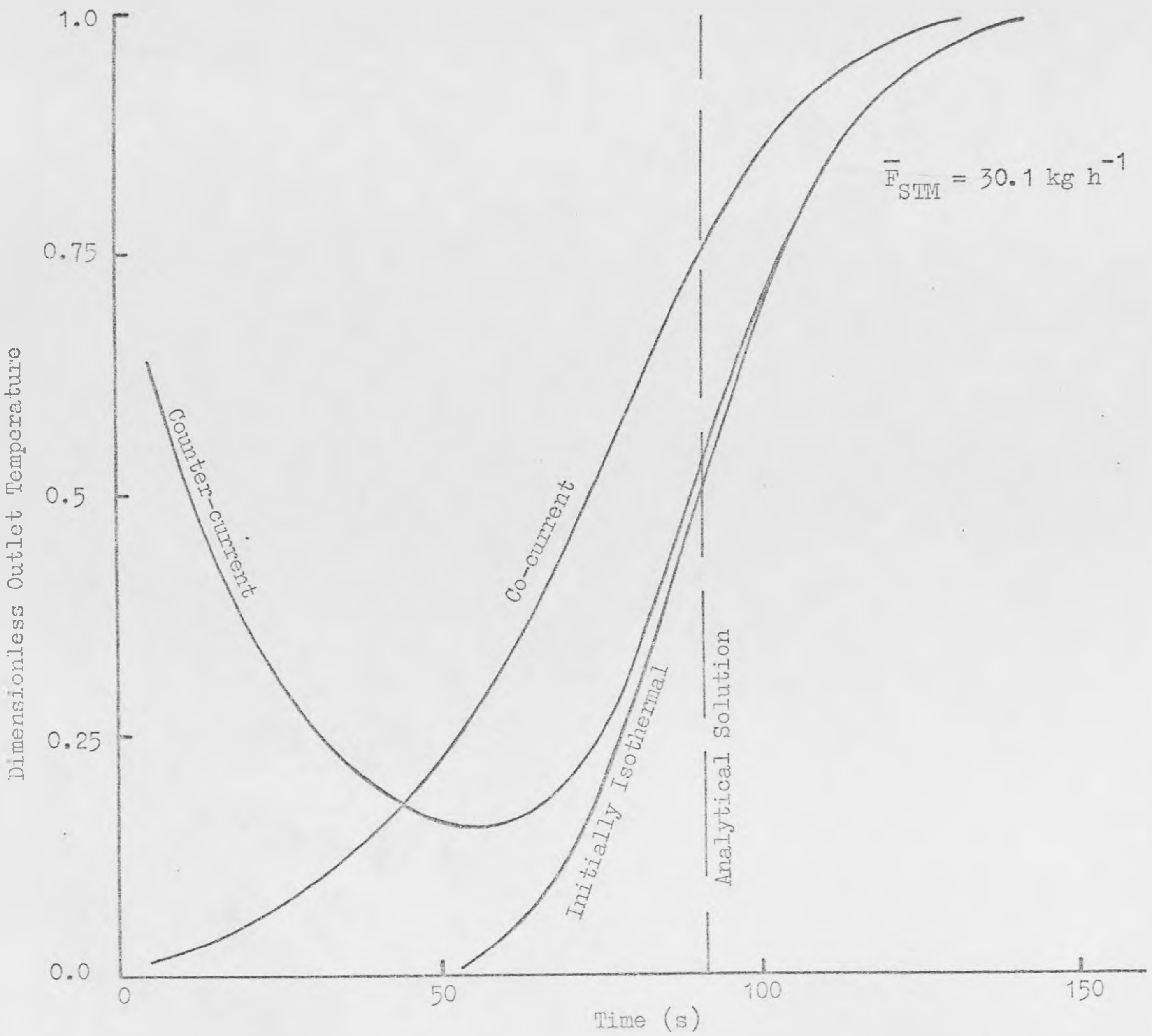

Figure 7.12: Comparison of Breakthrough Curves for an Initially Isothermal Bed and One with a Steady State Reactor Profile.

current flow, when the initial reactor profile was reversed at $t = 0$. The counter-current case shows a minimum as the reactor profile moves out of the bed and then tends towards the initially isothermal curve. The co-current case shows higher temperatures along the breakthrough curve and the dimensionless temperature at $t = t_{sat}$ is 0.76 compared with 0.52 for the initially isothermal bed.

The reactor in the cyclic system will not reach steady state and the final temperature profile will be similar to that for t = 80s in Figure 7.1. This will clearly give a closer approach to saturation at $t = t_{sat}$ than an initially isothermal regenerator profile and it may also be closer than that given by the steady state reactor profile considered above.

7.2.2 Effect of Bed Heat Capacity

The addition of inert material to increase the bed heat capacity is seen by the regenerator simply as an increase in bed size. As shown by equations 5.7 and 5.9, the speed of response is again inversely proportional to the bed size and, to achieve the same performance, a corresponding increase in steam flow or period time is required.

7.3 Cyclic Reactor System Heat Inputs

The superheater heat load and make-up steam temperature were calculated in Section 6.5.3 using equation 5.14 which considers regenerator steam flows calculated from equation 5.9. These were only approximate values as fairly gross assumptions were made regarding the average inlet temperatures to each bed. It is therefore not worthwhile re-evaluating these as the only parameter in equation 5.14 which has been re-assessed is $\bar{C}_{ps}$, and the change in this is only 7.5%.

7.4 Summary of Predicted Parameters for the Cyclic Reactor System

The period times allowed to achieve 65% and 68% average conversions and the corresponding saturation steam flows calculated from equation 5.9 are shown in Table 7.5. The assumptions in the estimates for superheater heat load and make-up steam temperature make it not worthwhile to re-estimate them at this point.

Average Conversion	t_f(s)	$\bar{F}_{STM}$ (kg h^{-1})
68%	60	48.86
65%	100	29.35

Table 7.5: Parameters for cyclic reactor system predicted from transient studies.

CHAPTER 8

CYCLIC REACTOR SYSTEM STUDIES

8.1 Introduction

It was shown in Chapter 5 that the inlet temperatures to both beds in the cyclic reactor system will vary with time due to the changing regenerator outlet temperature. This variation will be damped to some extent by the additional heat capacity of the system other than the two beds, but the model cannot allow for this effect. However, the two extreme situations will be studied. Firstly, it will be assumed that the temperature variation is completely damped out by the system, so that the inlet temperatures to the beds are constant during each period. Secondly, the inlet temperatures to the beds will be assumed to vary directly with the regenerator outlet temperature and the damping of the system will be ignored. A delay of 1 second is then introduced between the regenerator outlet and the bed inlets to allow for the residence time in the pipework.

Although the effect on the reactor performance of the additional system heat capacity cannot be assessed accurately, an indication of its effect may be obtained by introducing a layer of inert material at the front of the reacting bed. This will also indicate which of the two extreme situations gives the better representation of a physical system.

8.2 Preliminary Studies

The system is first studied with constant inlet temperatures to the two beds during each period. This minimizes the interactions within the system which gives a quicker solution and an easier understanding of the system behaviour. The system operates counter-currently using the parameters in Figure 8.1, which were shown in the previous chapter to predict an average conversion of 68%.

Cyclic steady state operation is assumed when the reactor conversion and the normalised outlet temperatures from both beds vary by less than 0.5×10^{-4} at the ends of successive cycles. This is achieved after 3 cycles starting from isothermal beds at 650°C and the conversion and temperature profiles at the end of each cycle are shown in Figure 8.2. Few cycles are required because saturation is closely approached in the regenerator. Figure 8.2 shows that the parameters chosen to check for cyclic steady state are suitable because they show significant changes at successive cycles before the cyclic steady state is achieved. The outlet parameters are also convenient parameters to measure in a physical system.

The reactor temperature and conversion profiles during the period at cyclic steady state are shown in Figures 8.3 and 8.4, and the variation of the outlet temperature and conversion is shown in Figure 8.5. The behaviour of these is as expected from the transient reactor studies in Chapter 7 because of the close approach to saturation in the regenerator for these conditions.

The regenerator temperature profiles during the period at cyclic steady state (Figure 8.6) show this close approach to saturation. The final reactor profile is almost entirely moved out of the regenerator and most of the bed reaches the inlet temperature by the end of the period. The final outlet temperature is 644.7°C. Figure 8.7 shows the variation of the regenerator outlet temperature during the period and this reflects the shape of the initial bed temperature profile. The rising outlet temperature for most of the period might suggest an inefficient use of the heat in the steam flow. However, the steam leaving the regenerator is either passed to the reactor or recycled

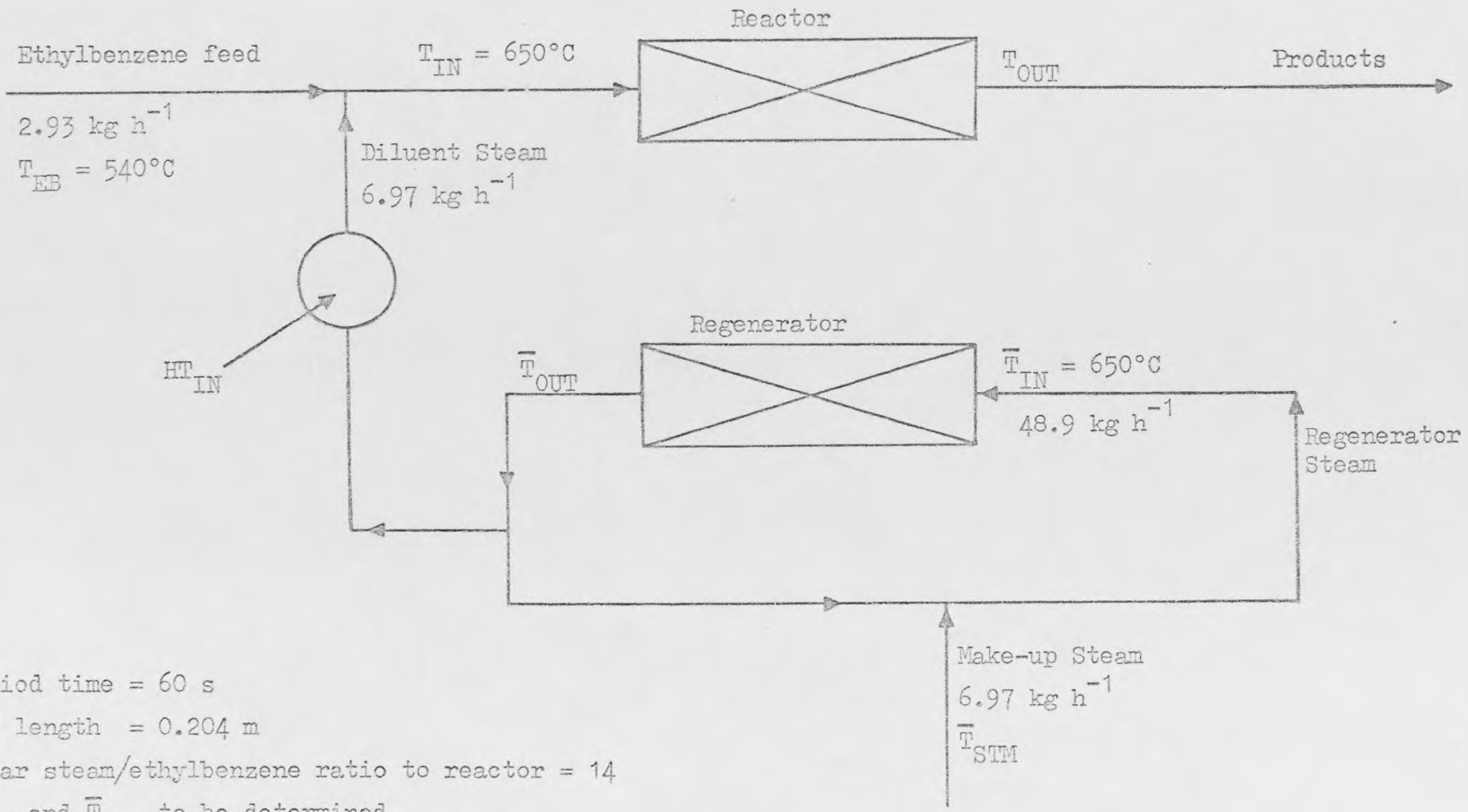
Ethylbenzene feed
2.93 kg h^{-1}
T_{EB} = 540°C
T_{IN} = 650°C
Reactor
T_{OUT}
Products
Diluent Steam
6.97 kg h^{-1}
HT_{IN}
Regenerator
$\overline{T}_{OUT}$
$\overline{T}_{IN}$ = 650°C
48.9 kg h^{-1}
Regenerator Steam
Make-up Steam
6.97 kg h^{-1}
$\overline{T}_{STM}$

Period time = 60 s
Bed length = 0.204 m
Molar steam/ethylbenzene ratio to reactor = 14
HT_{IN} and $\overline{T}_{STM}$ to be determined.

Figure 8.1: Standard Conditions for Cyclic Reactor Studies in Chapter 8.

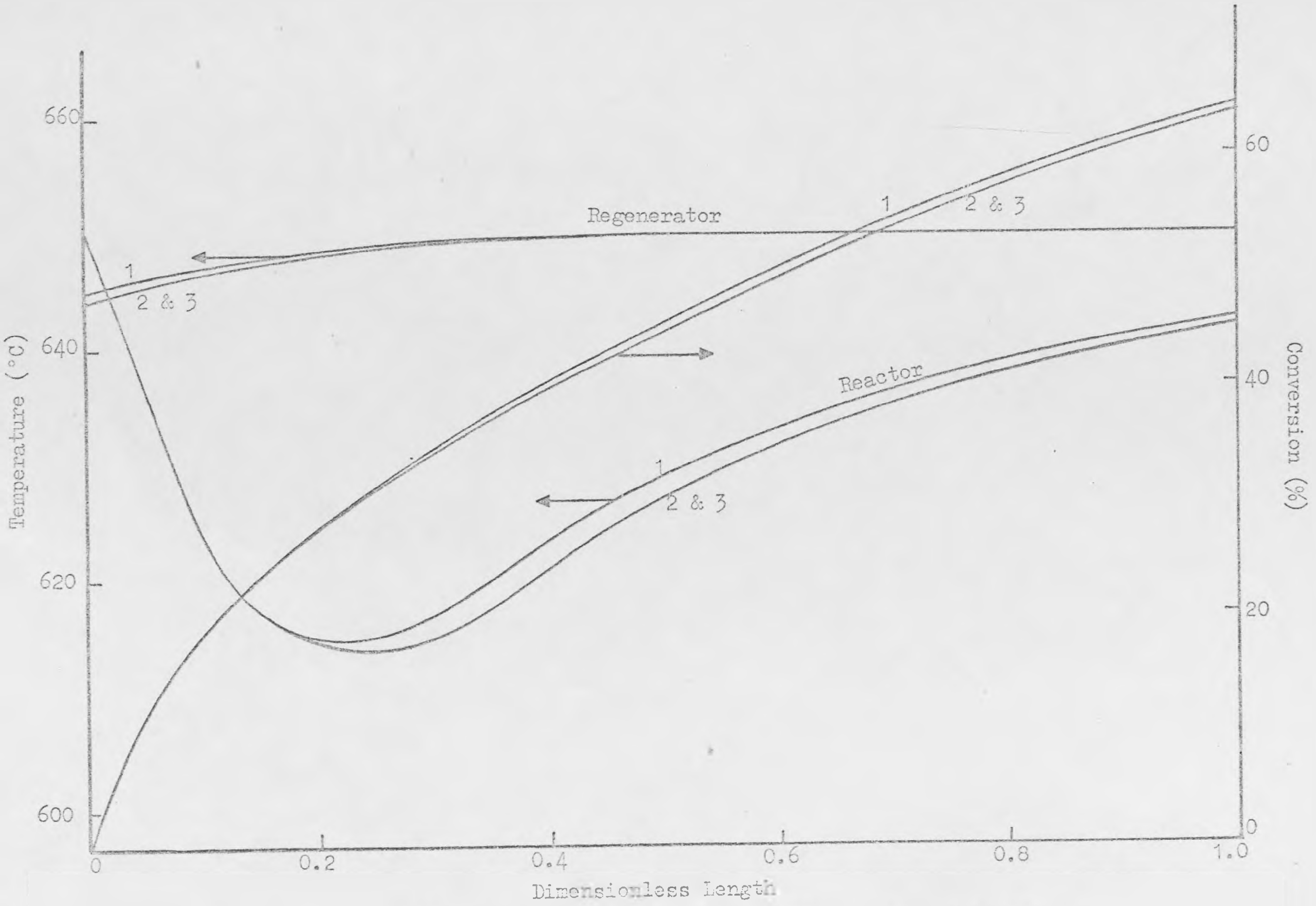

Figure 8.2: Temperature and Conversion Profiles at the Ends of Successive Cycles.

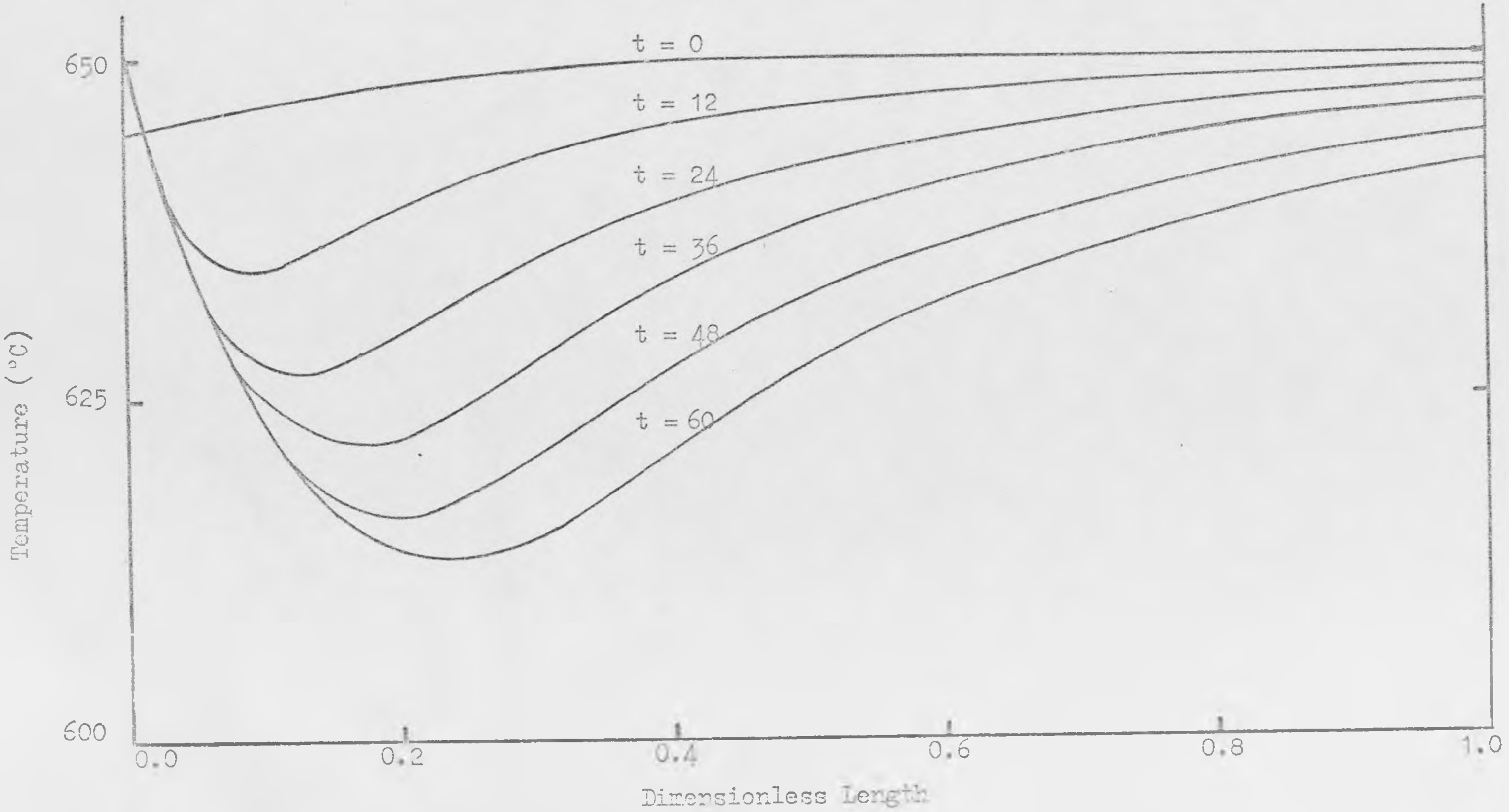

Figure 8.3: Reactor Temperature Profiles during Period at Cyclic Steady State.

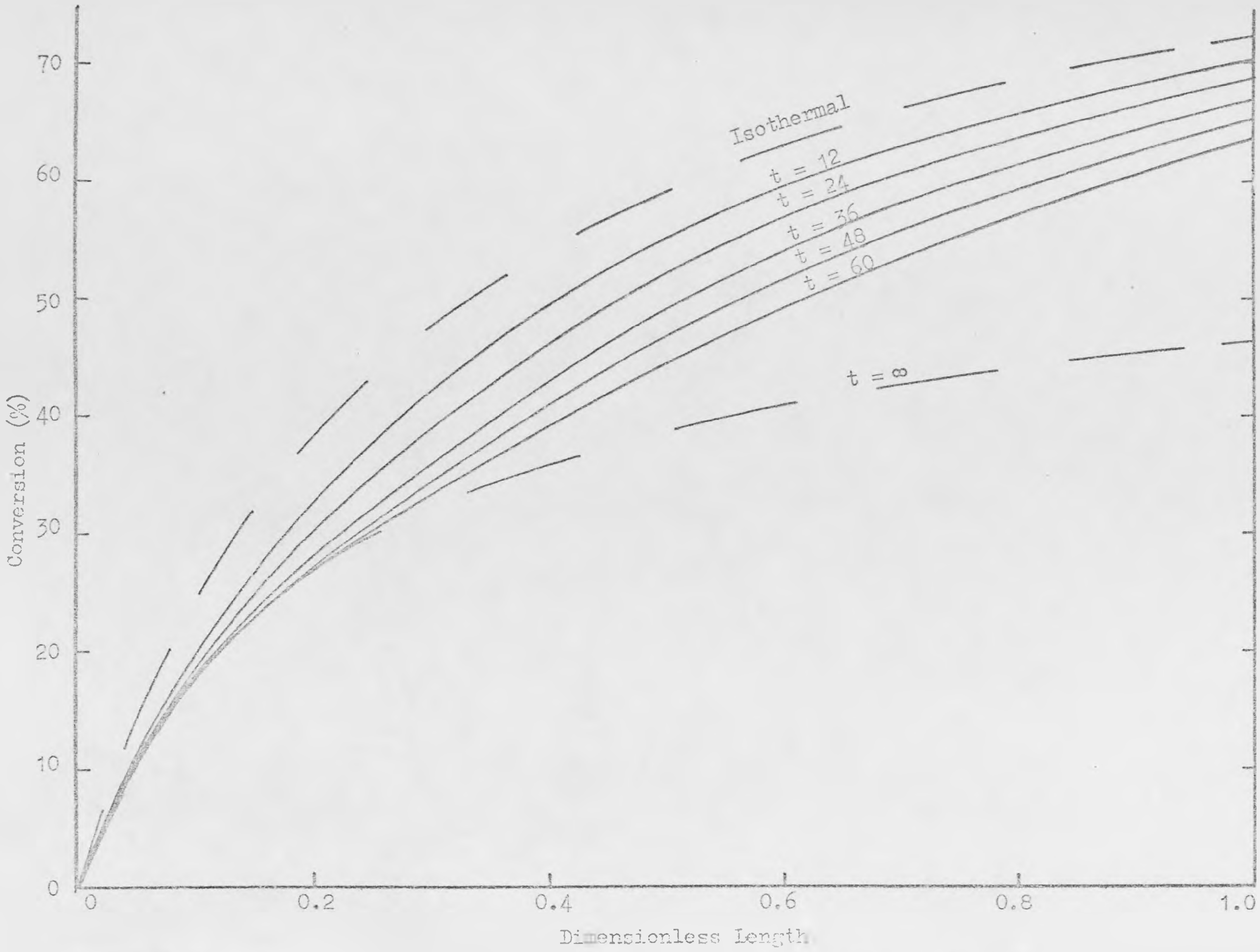

Figure 8.4: Reactor Conversion Profiles during Period at Cyclic Steady State.

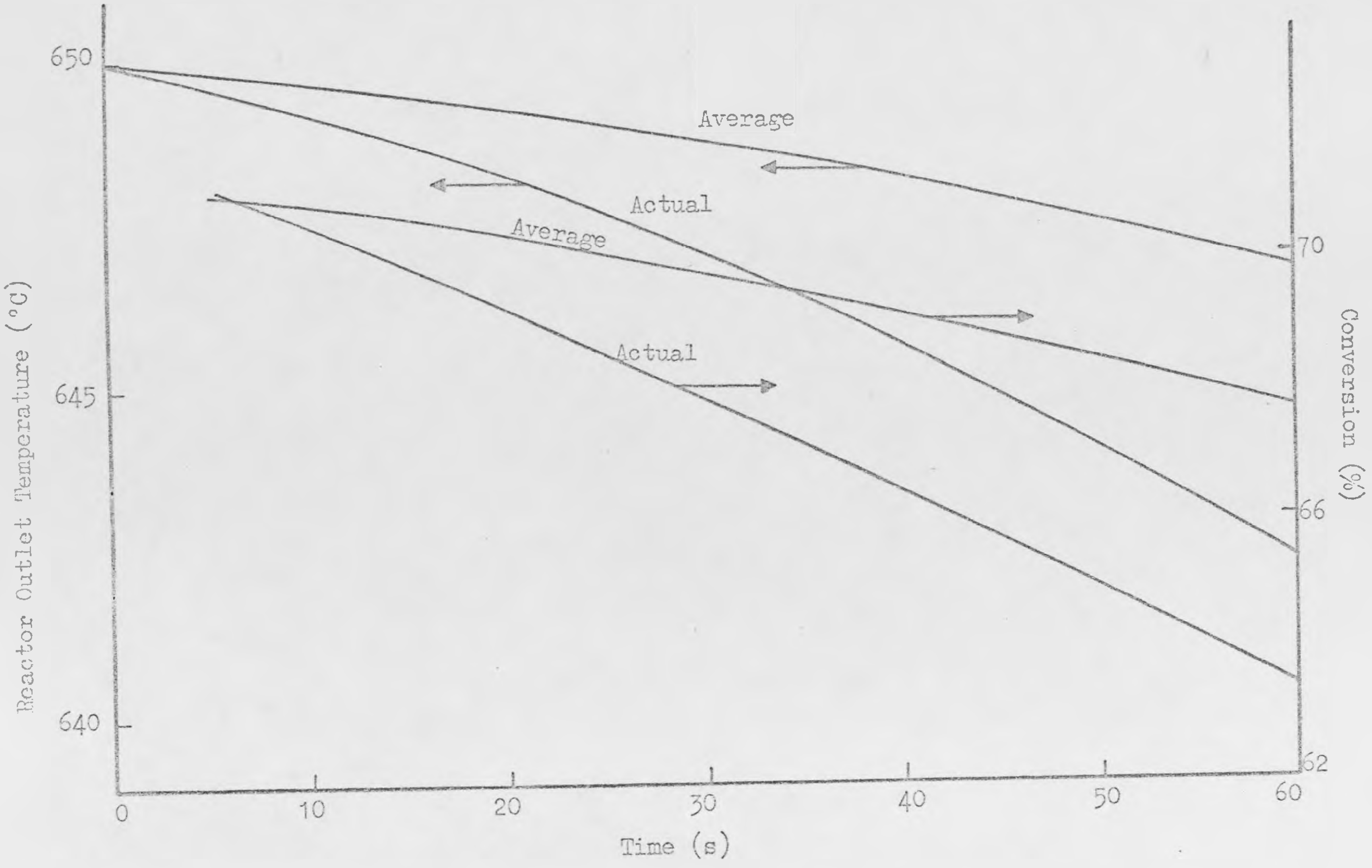

Figure 8.5: Reactor Outlet Temperature and Conversion during a Period at Cyclic Steady State.

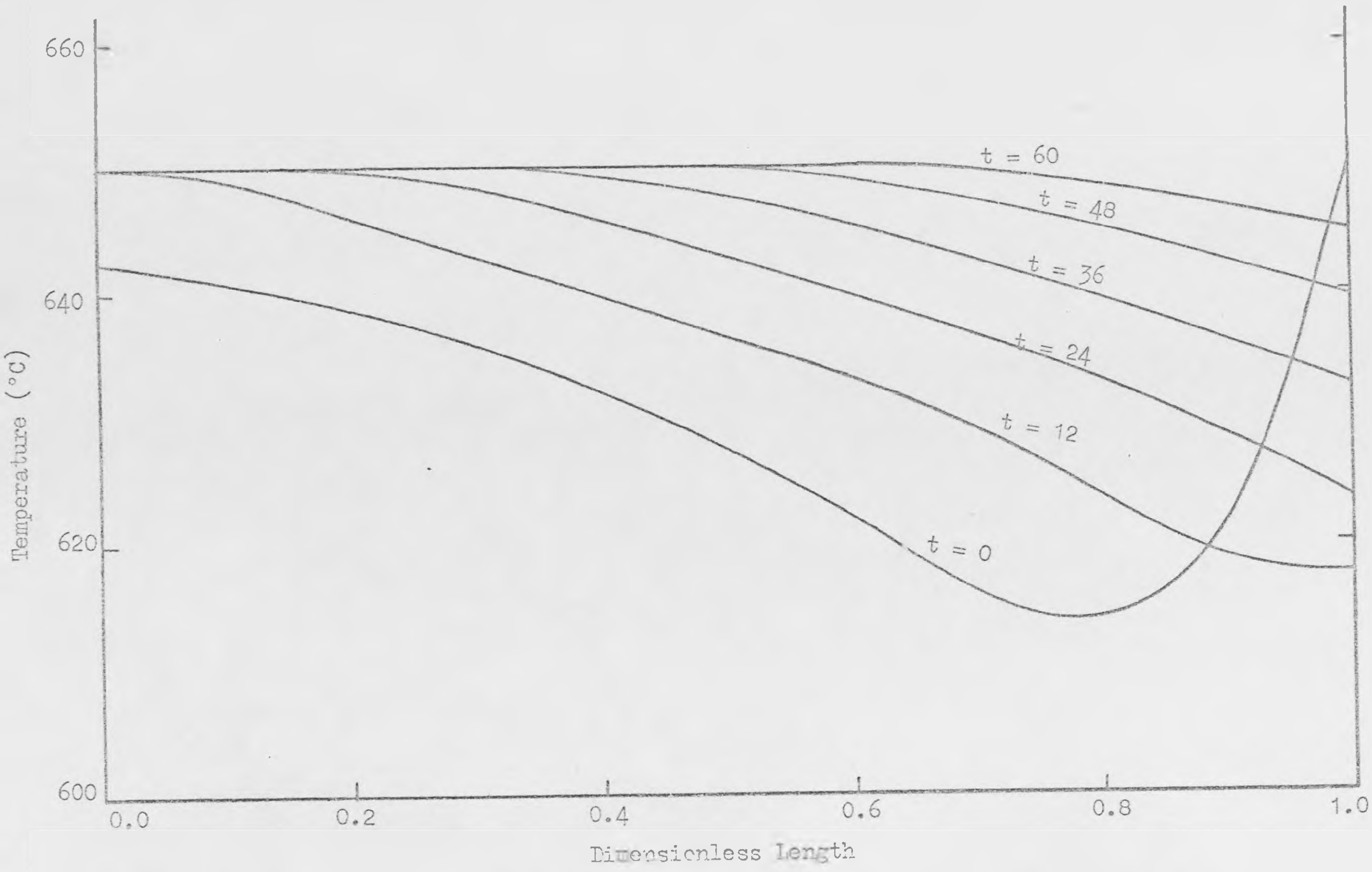

Figure 8.6: Regenerator Temperature Profiles during a Period at Cyclic Steady State.

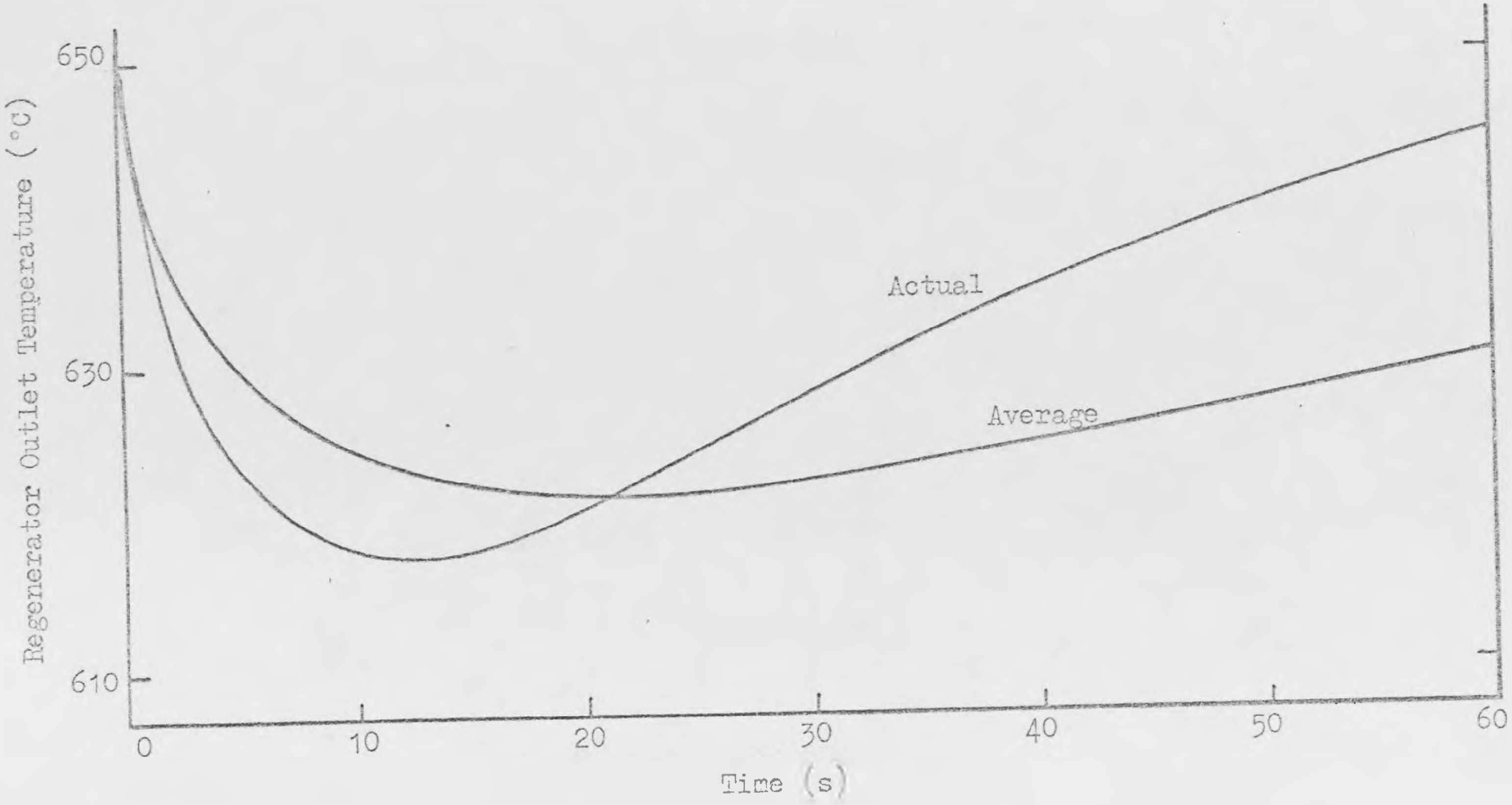

Figure 8.7: Regenerator Outlet Temperature during a Cycle at Cyclic Steady State.

around the regenerator and so the heat is not lost from the system.

8.2.1 Assessment of Predicted Parameters

The parameters of the system were predicted in Chapters 6 and 7 for average conversions of 68% and 65% and the values are given in Tables 6.6 and 7.5. The parameters used in the above study, and shown in Figure 8.1, are those predicted for an average conversion of 68% from the transient reactor studies. The steady state study predictions for this conversion are not appreciably different. The average conversion at cyclic steady state using these predicted values is 67.7% and the efficiency is 88.8%.

The period times predicted by the transient and steady state studies for an average conversion of 65% are 100 s and 90 s respectively. Using the corresponding regenerator steam flows, the cyclic reactor system gives cyclic steady state conversions of 64.5% with a 100 s period and 65.5% with a 90 s period. In each case, saturation of the bed is again closely approached during the regenerator period.

Thus, the simple method of predicting the cyclic system period time using only steady state reactor results, which was described in Chapter 5, gives a good approximation of the system performance when saturation is closely approached in the regenerator.

A close approach to saturation in the regenerator is observed with each of the above period times using the predicted steam flows from the analytical solution of the pseudo-homogeneous regenerator model. For the 60 s period, the dimensionless outlet temperature, as defined by

$$F = \frac{\bar{T}_{outlet} - \bar{T}_{s,initial}}{\bar{T}_{inlet} - \bar{T}_{s,initial}} \qquad (4.35)$$

is 0.85 at the end of the period. For the 90 s and 100 s periods, the values are 0.79 and 0.77 respectively. In Chapter 7, the value was only 0.52 for an initially isothermal bed, or a maximum of 0.76 if the reactor reached the steady state, when the steam flow was calculated for a 90 s period. Thus, as suggested in Chapter 7, the initial regenerator temperature profile in the cyclic reactor system causes a much closer approach to saturation than expected from the breakthrough curve from an initially isothermal bed. The actual approach is well predicted by the assumption of an initial temperature profile from a steady state reactor with co-current flows (Figure 7.12). However, to minimise compression costs in the recycle, it may be desirable to reduce the steam flow. Hence, the effect of varying the flow, and the approach to saturation, on the system performance will be studied further.

With constant bed inlet temperatures, the superheater heat load and the make-up steam temperature can be accurately evaluated from equation 5.13 or 5.14 and equation 5.16 because all the terms are known and the use of the average bed temperature drop has been shown to give good estimates of the period time. For the 60 s period above, these are 0.31 kW and 764°C. The value of the estimates when the inlet temperatures vary with the regenerator outlet temperature will be assessed in Section 8.4.

8.2.2 Co-current Operation

Clearly, if saturation is closely approached in the regenerator, there will be little difference between the performance obtained using co-current or counter-current operation. For the 60 s period considered above, co-current operation gives 67.3% at cyclic steady state, which is achieved after only two cycles. This is slightly below the value of 67.7% given by counter-current operation because the lower final regenerator outlet temperature becomes the reactor outlet temperature, which is then less favourable for the equilibrium.

Figure 8.8 shows the bed temperature profiles during the regenerator period. The outlet temperature at the end of the period is lower than with counter-current operation because it is affected by the trough in the final reactor temperature profile.

Greater differences in the performance from the two modes of operation can be expected when saturation is not approached and this will be studied later.

8.2.3 Efficiency

The efficiency of the average conversion varied little in all the above studies and it was always within the range 88.6 - 89.0%.

8.2.4 Comparison with Steady State Conversion

It was shown in Chapter 6 that the maximum conversion which might be reasonably expected from a two-bed steady state reactor, using the same total catalyst volume as the cyclic system, is about 64% with an efficiency of 85.7%. The above values for the cyclic system of 67.7% conversion and 88.8% efficiency are clearly a significant improvement. It may, therefore, be possible to operate the cyclic system with more economic conditions (e.g. lower steam flows) and still obtain better performance than from a steady state adiabatic reactor.

8.3 Effect of Parameter Variation

The standard conditions for these studies are those in Figure 8.1 which give an average conversion of 67.7%. When a particular parameter is varied, the others are kept constant at these conditions unless otherwise stated. The cyclic steady state performance is considered in each case.

8.3.1 Variation of Regenerator Steam Flow

Figure 8.9 shows the effect of different regenerator steam flows on the average conversion, and on the final regenerator outlet temperature

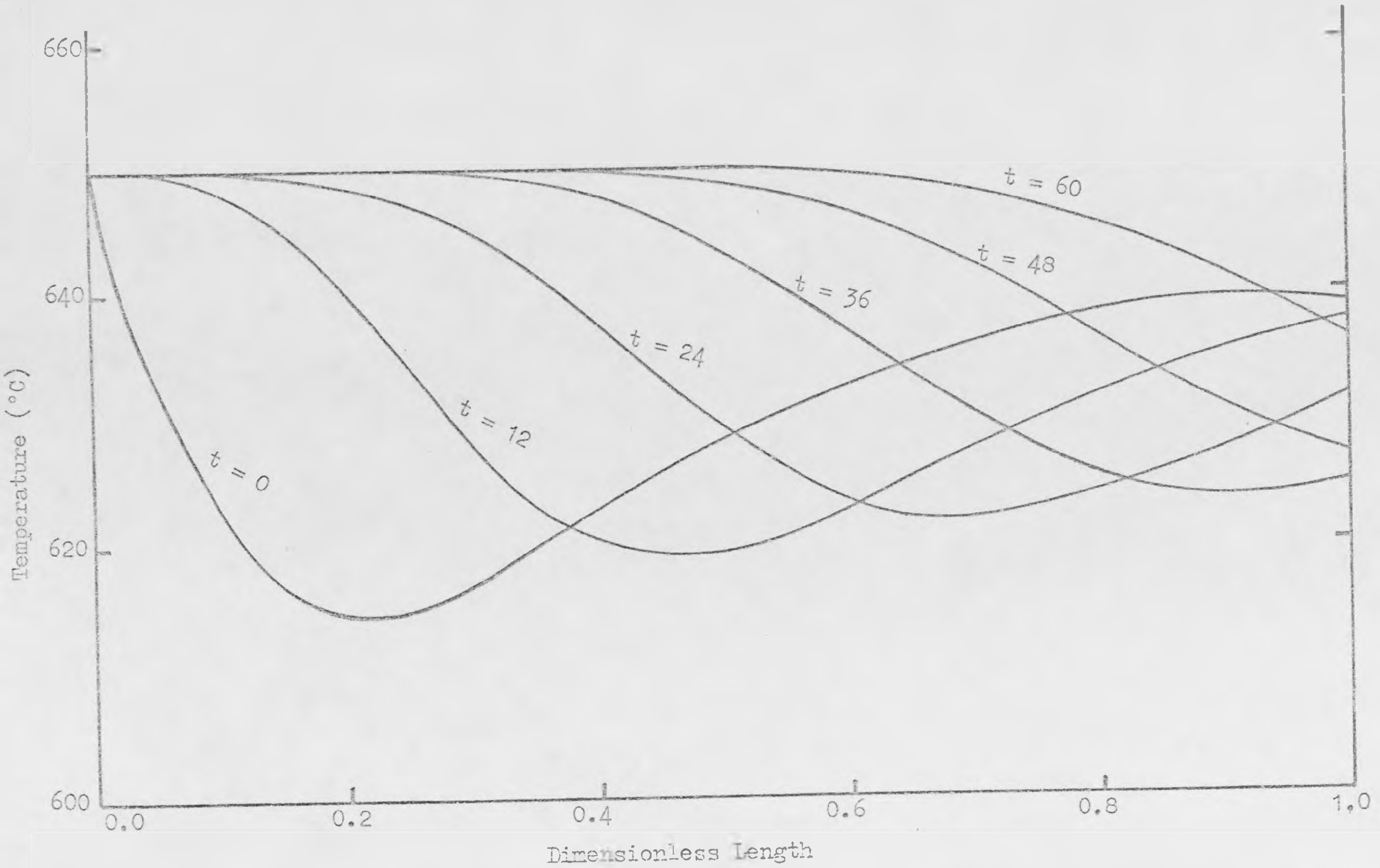

Figure 8.8: Co-Current Regenerator Temperature Profiles during a Period at Cyclic Steady State.

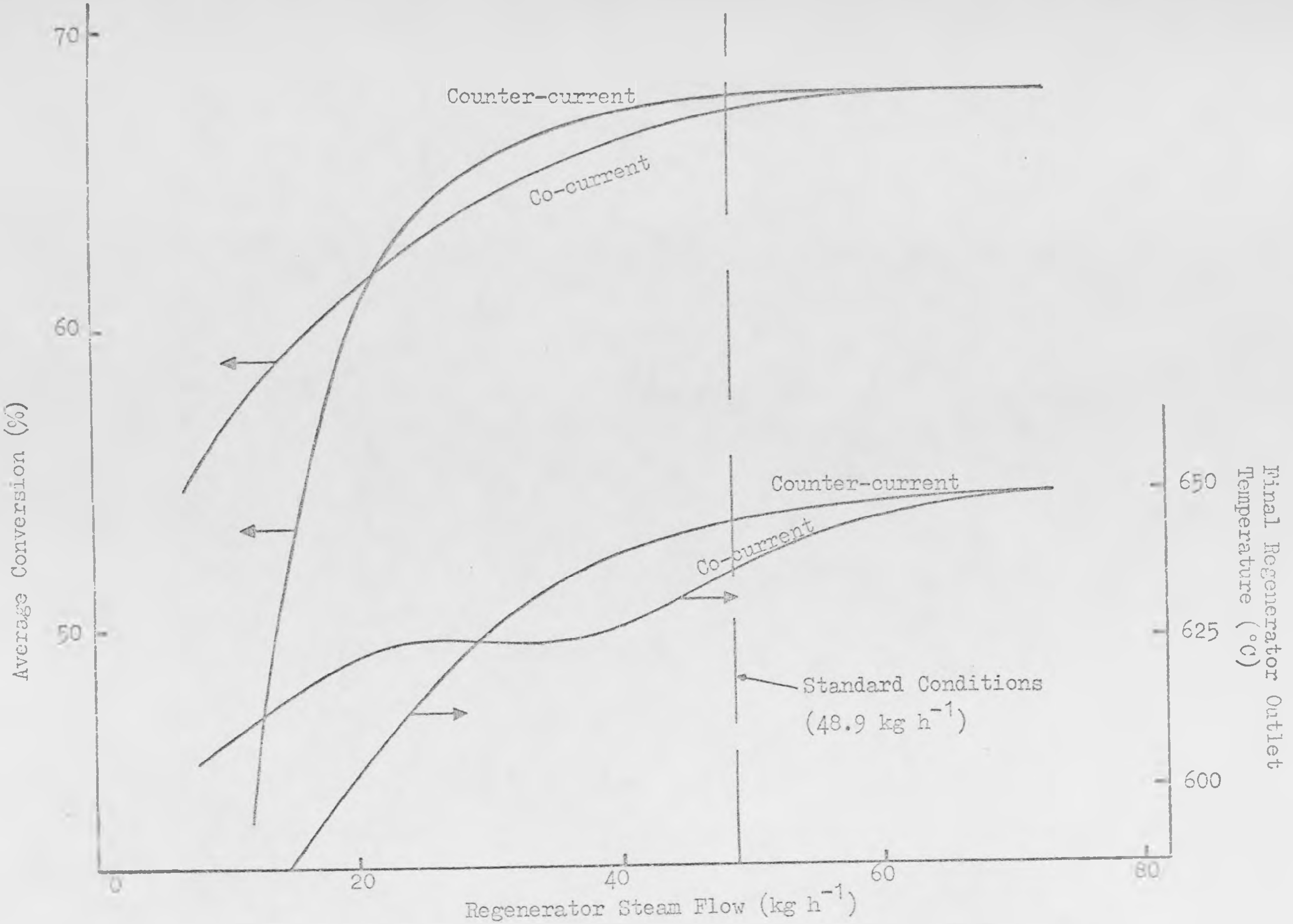

Figure 8.9: Effect of Regenerator Steam Flow on Average Conversion and Final Regenerator Outlet Temperature.

at the end of the period, for both counter-current and co-current operation. The final regenerator outlet temperature indicates the closeness of the approach to saturation. With both modes of operation, the conversion increases with the steam flow, but the rate of increase falls off as saturation is approached. Complete saturation is achieved when the flow is approximately 1.5 times the standard value. As expected from Figures 8.6 and 8.8, a small reduction in steam flow from the standard value has a greater effect on the conversion with co-current operation than with counter-current operation as the final outlet temperature is lower. For example, a 20% reduction in steam flow would give final regenerator profiles similar to the t = 48 s curves in Figures 8.6 and 8.8.

The counter-current conversion falls drastically when the regenerator steam flow is less than half the standard value, which was calculated to saturate the bed, because the temperature trough at the end of the reactor period is not removed from the bed. This causes a lower catalyst temperature at the reactor inlet, which cools the feed and prevents a significant amount of reaction occurring in this region. The effective catalyst bed size is thus reduced. With co-current operation, the initial catalyst temperature near the inlet is always at 650°C.

However, these low steam flows are not of interest because a close approach to saturation in the regenerator is desired. It therefore appears that counter-current operation is preferable. The standard regenerator steam flow gives a suitably close approach to saturation, but reductions of 10% and 20% only reduce the average conversion from 67.7% to 67.4% and 67.0% respectively. Thus, although the standard value is used in these studies, a lower value may be acceptable in practice.

8.3.2 Variation of Period Time

The effect on the average conversion of varying the period time is shown in Figure 8.10. This shows the curve for a constant regenerator steam flow at the standard value and also that obtained when the steam flow is recalculated from equation 5.9 at each period time:

$$\bar{F}_{STM} = \frac{(1 - e)\rho_s \, C_{ps} \, AZ}{tf \, \bar{C}_{pg} \, MW_{STM}} \qquad (5.9)$$

In both cases, the expected fall in conversion with increasing period time is observed because of the increasing fall in reactor temperature. At periods longer than the standard (60 s), the constant steam flow gives higher conversions because complete saturation of the regenerator occurs. However, equation 5.9 shows that this flow is twice the recalculated value for a 120 s period, and three times that for a 180 s period. Thus, above the calculated period it is necessary to relate the regenerator steam flow to the period time in order to avoid an uneconomically high value. A reduction in period cannot be considered with the norm bed size as it is already the minimum value chosen in Chapter 5. However, this is considered in the next section for a larger bed.

8.3.3 Effect of Bed Heat Capacity

It was shown in Chapters 6 and 7 that longer period times, or higher average conversions, may be obtained by increasing the heat capacity of the bed. This may be done by the addition of inert material but, as the kinetics used in this work predict a very small bed size, it is likely in practice that the catalyst bed may be larger than the norm with a correspondingly lower activity per unit volume. It was shown in Chapter 6 that the performance of the commercial reactor studied by Sheel and Crowe[17] could only be reproduced by these kinetics

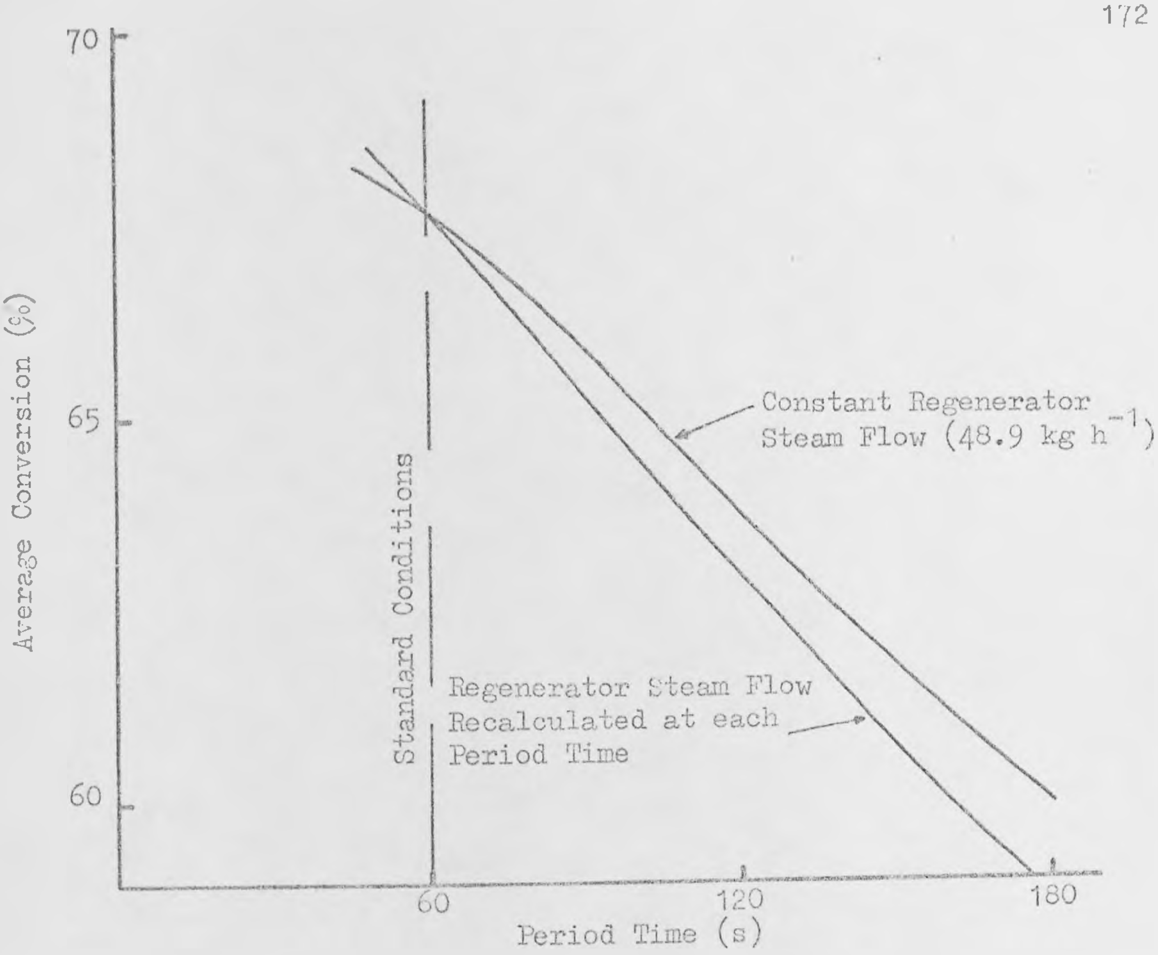

Figure 8.10: Effect of Period Time on Average Conversion with the Norm Bed Size.

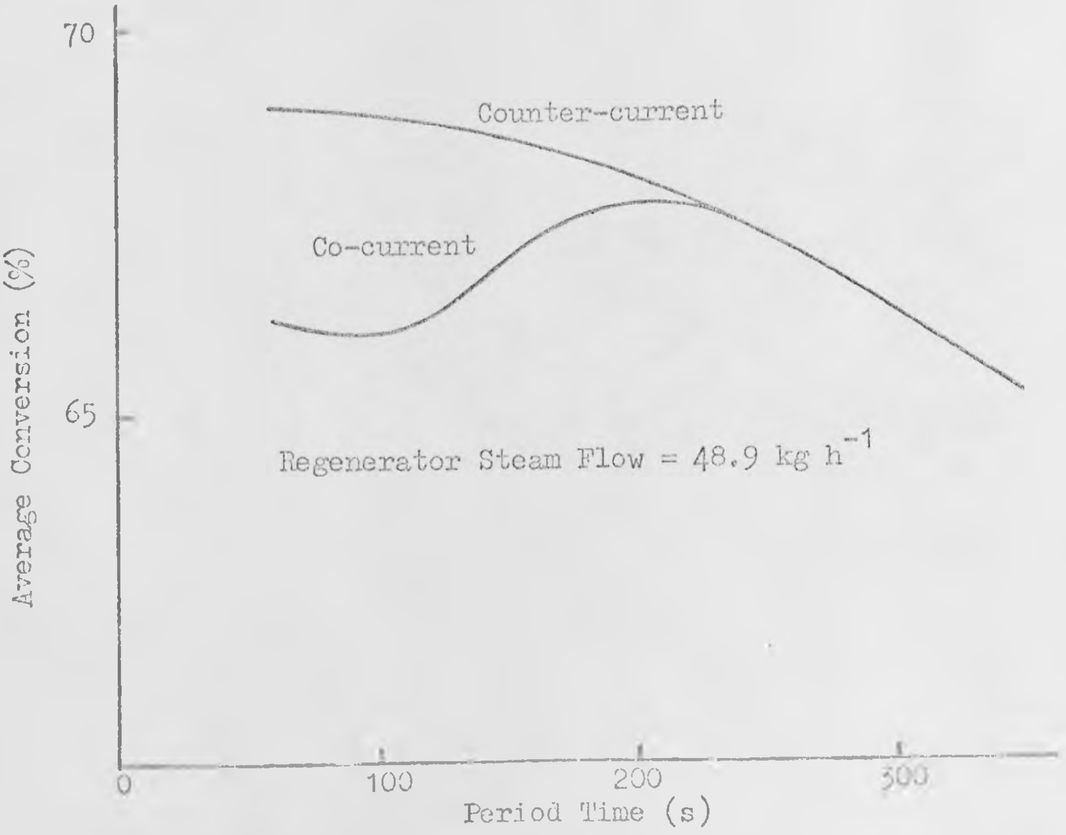

Figure 8.11: Effect of Period Time on Average Conversion with the 0.726 m Bed.

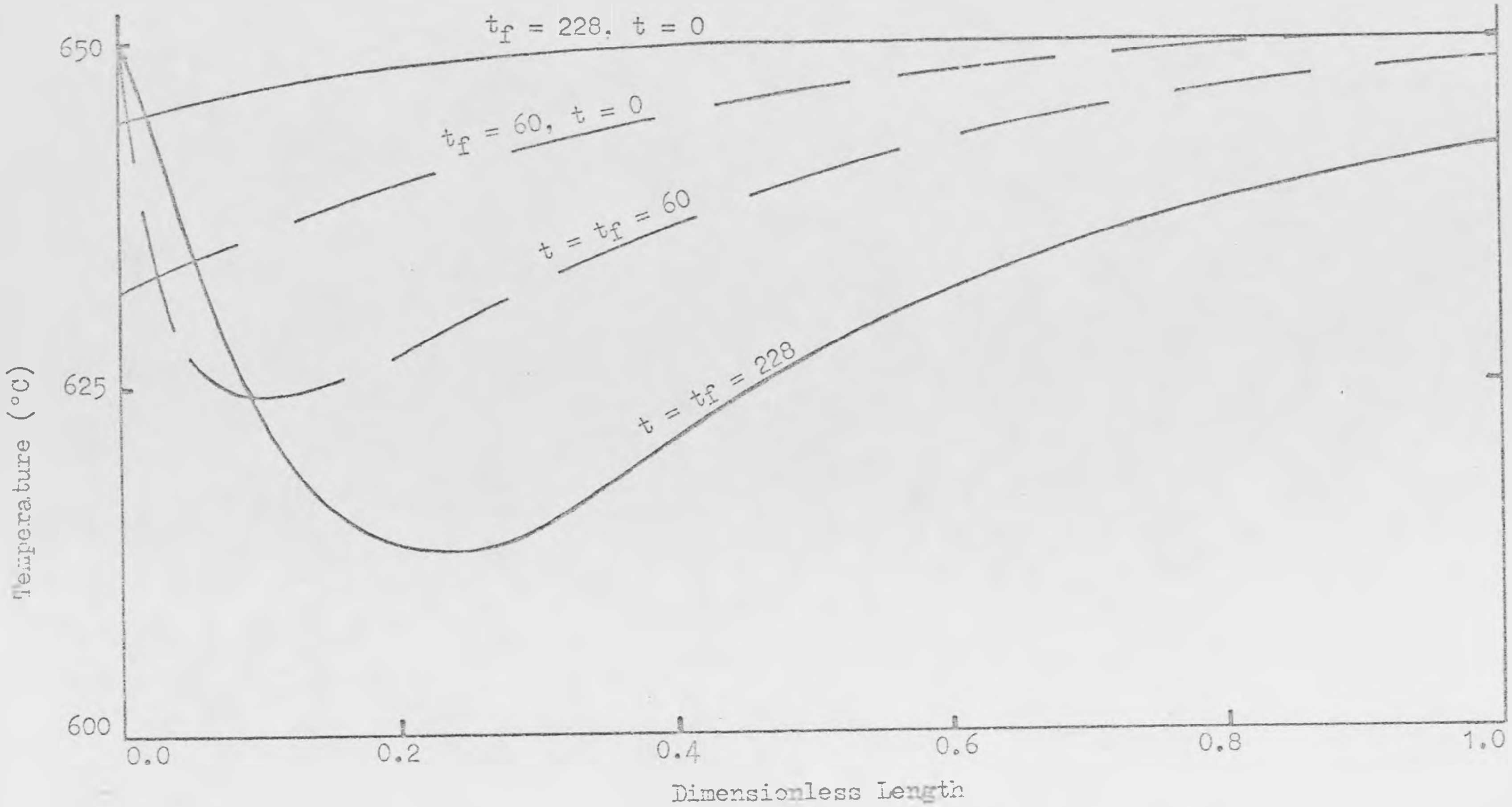

Figure 8.12: Comparison of Reactor Temperature Profiles for the 0.726 m Bed.

if the rate constants were reduced by a factor of 0.28. Using the norm reactor data in Table 6.4, these reduced rate constants predict a bed length of 0.726 m for a 40% steady state conversion, compared with the norm length of 0.204 m, using the same reactor diameter.

Figure 8.11 shows the variation of cyclic reactor average conversion with period time for 0.726 m beds using the standard regenerator steam flow. A period of 228 s gives the same 67.7% conversion as the standard conditions using counter-current operation and a 69.0% conversion is obtained with a 60 s period. If the regenerator steam flow is increased to the saturation flow for this bed size, the conversion is 70.8% for the 60 s period but it is unlikely that the almost fourfold increase in flow will make this economically worthwhile. This period time infringes the constraint that the period should not be less than 100 reactor residence times (i.e. 114 s) which was set in Chapter 5. However, it is used in order to allow a direct comparison with the norm bed size.

Figure 8.11 shows again the superiority of counter-current over co-current operation. The co-current conversion falls as the period is reduced because the temperature trough in the final reactor profile is not then moved out of the bed during the regenerator period. A fall in conversion at low period times might also be expected with counter-current operation as saturation of the regenerator is no longer closely approached. For example, with a 60 s period, the standard regenerator steam flow is just over $\frac{1}{4}$ of the saturation flow given by equation 5.9 for this bed size. However, the temperature drop in the reactor is reduced as the reaction heat is now supplied by a greater heat capacity than in the standard case and this produces higher conversions. This effect is shown in Figure 8.12, which compares the initial and final reactor temperature profiles for a 60 s and 228 s period time, the latter corresponding to the standard case. The smaller temperature drop maintains high reactor outlet temperatures, which favour the equilibrium, and the average reactor temperature over the period is also higher.

The use of a shorter period is, therefore, desirable with counter-current operation, even if the regenerator steam flow is not correspondingly increased. Thus the procedure for estimating the period time, described in Chapter 5, gives a maximum value which can be used to determine a minimum regenerator steam flow.

8.3.4 Variation of Constant Reactor and Regenerator Inlet Temperatures

The variation of the inlet temperatures caused by the varying regenerator outlet temperature will be considered later. This study is concerned with the effect of different constant values. The effect on the average conversion of varying the inlet temperature to each bed, whilst that to the other bed is constant at 650°C, is shown in Figure 8.13. As expected from the transient reactor studies in Chapter 7, the inlet temperature to the regenerator has a far greater effect as it determines the initial reactor temperature profile and should therefore be at the maximum value. Figure 8.12 also suggests that, when considering the effect of the varying regenerator outlet temperature, the temperature variation produced at the reactor inlet is likely to be insignificant compared to that at the regenerator inlet.

8.3.5 Variation of Diluent Steam Flow

The diluent steam flow to the reactor represents a major operating cost as this is the steam consumption of the system. It was suggested in Chapter 5 that this may be reduced because the reaction heat is largely supplied by the heat stored in the bed during the regenerator

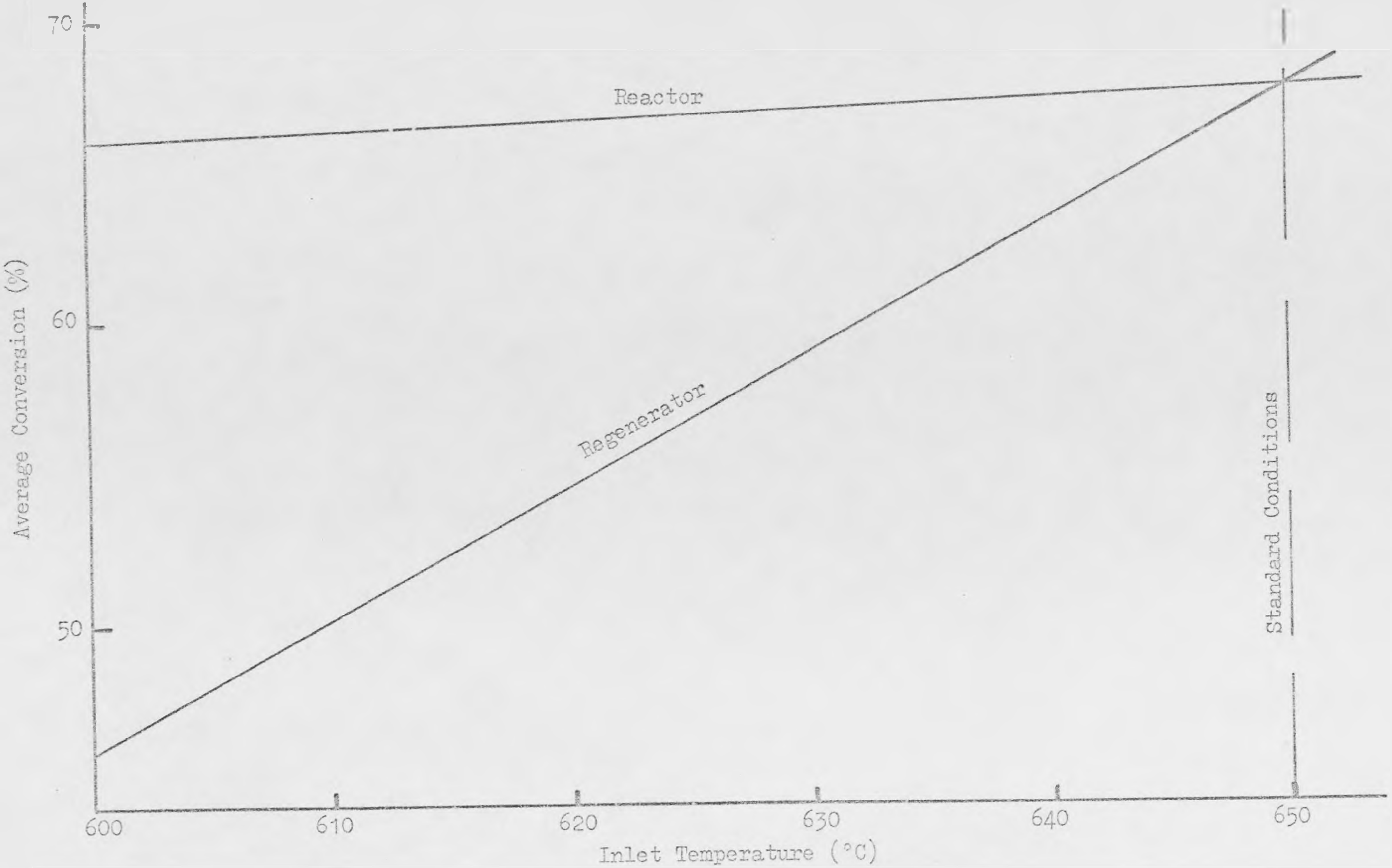

Figure 8.15: Effect of Different Constant Reactor and Regenerator Inlet Temperatures on the Average Conversion.

Figure 8.14: Effect of Reactor Steam Flow on Average Conversion, Efficiency and Steam Consumption.

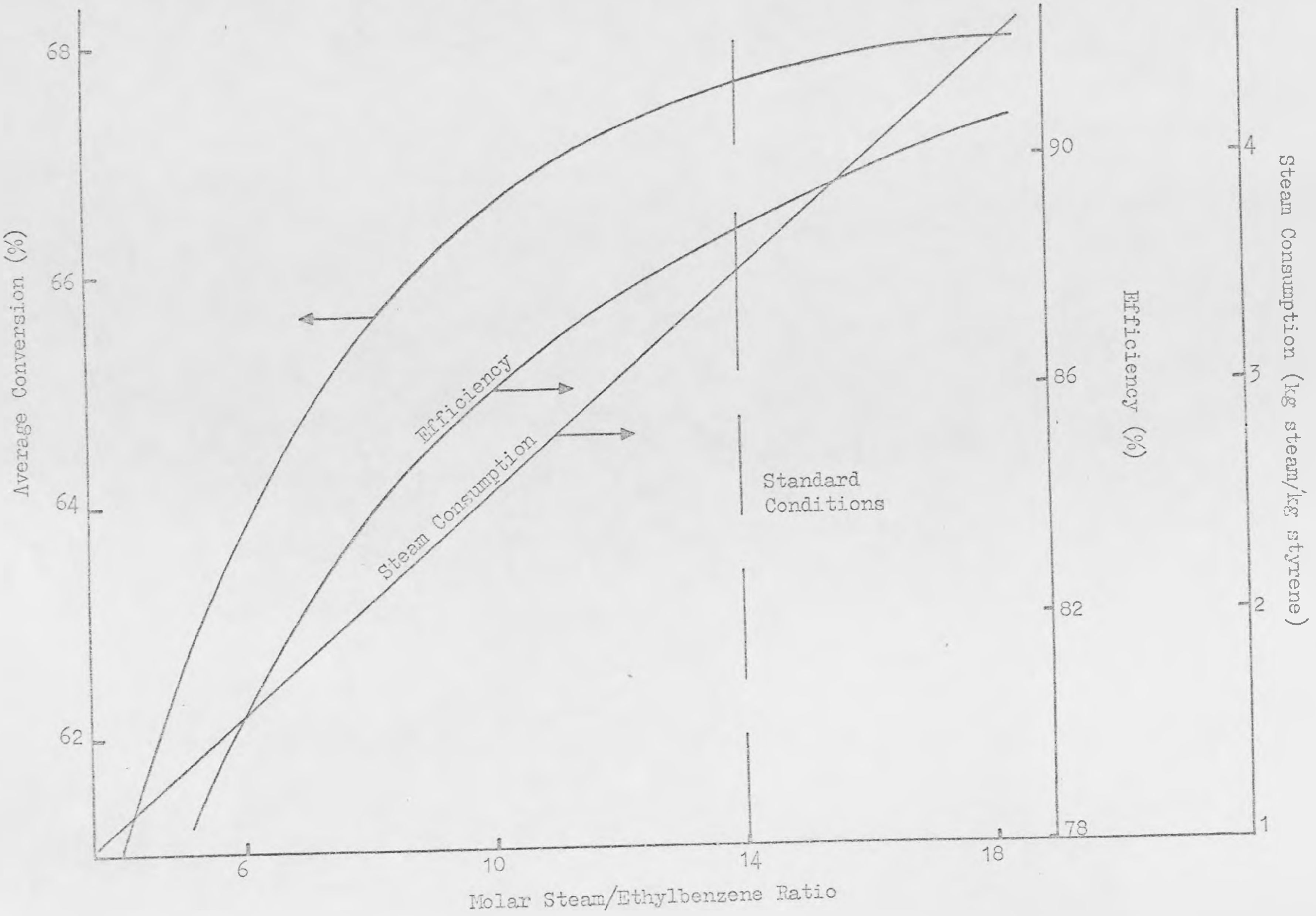

period and this is clearly desirable from an economic point of view. Figure 8.14 shows the fall in conversion and efficiency with steam/ethylbenzene ratio, which is to be expected from the transient reactor studies in Chapter 7. It also shows the steam required per kg of styrene produced, which varies linearly over the range. A considerable saving in steam consumption could be achieved with only a comparatively small reduction in the average conversion, but the drop in efficiency is more important as it represents a loss of ethylbenzene from the system. For example, a 50% reduction in the steam requirement from the standard value produces a 5% drop in average conversion to 64.4%, but an 8% drop in efficiency to less than 82%. Thus, the diluent steam flow must be considered as a major variable in any economic analysis or optimisation of the system.

8.4 Varying Reactor and Regenerator Inlet Temperatures

The inlet temperatures to both the reactor and regenerator will vary during the period due to the changing regenerator outlet temperature. In the previous studies, it was assumed that the additional heat capacity of the system damps out the temperature variation before it affects the inlet temperatures and constant values were assumed. The effect of assuming no additional heat capacity in the system is now studied and the inlet temperatures are allowed to vary directly with the regenerator outlet temperature.

Estimates for the superheater heat load and the make-up steam temperature were obtained in Chapter 6. These are 0.31 kW and 764°C, for the minimum period of 60 s and, due to the assumptions made concerning the average bed inlet temperatures over the period, they are only approximate. It was suggested in Chapter 5 that the maximum regenerator outlet temperature is likely to be observed at the end of the period because of the rising temperature of the bed. The maximum bed inlet temperatures are thus also likely to be observed at the end of the period and, to obtain a high conversion, they should be the maximum allowed value of 650°C at this time. If these values are more than 0.2°C different from 650°C at the end of the period, new estimates for the superheater heat load and the make-up steam temperature are evaluated in order to force them to 650°C. The procedure for accomplishing this is outlined in Chapter 5 and described for the program CH3SC in Appendix 6. The inlet temperatures to the beds will then be below 650°C except at the end of the periods and, hence, the conversion will be less than in the previous studies, when they were constant at 650°C.

The standard conditions for this study are those used in the previous sections and shown in Figure 8.1, except that the inlet temperatures now vary, so that direct comparisons of performance may be made. The performance of the system is again studied when it operates at cyclic steady state.

8.4.1 Counter-current Operation

The system was run to cyclic steady state from initially isothermal beds using the values of superheater heat load and make-up steam temperature predicted in Chapter 6. At cyclic steady state, the inlet temperatures to the reactor and regenerator at the ends of the periods were 643°C and 641°C respectively, which are below the desired value of 650°C. Two re-evaluations of the superheater heat load and make-up steam temperature were required to satisfy this temperature constraint and the final values were 0.325 kW and 754°C. Cyclic steady state operation was achieved after 19 cycles.

As expected, the average conversion at cyclic steady state (62.9%)

is less than the constant inlet temperature value of 67.7% and the efficiency is therefore slightly higher at 89.1% compared with 88.8%. This lower conversion is caused by the lower initial reactor (final regenerator) temperature profile. Figure 8.15 shows the development of this profile during the regenerator period. The falling temperature along the bed is inevitable because the inlet temperature increases with the outlet temperature, but it is always higher as the heat added in the make-up steam is constant.

The temperature and conversion profiles in the reactor during the period are shown in Figures 8.16 and 8.17 and the variation of outlet temperature and conversion with time is shown in Figure 8.18. The shape of the curves in these figures are not greatly different from those in Figures 8.3 - 8.5 for constant inlet temperatures although the actual values are lower.

The variation of the inlet temperatures to the beds during each period is determined by that of the regenerator outlet temperature and these are shown in Figure 8.19. These reflect the shape of the final reactor temperature profile and hence the initial reactor profile is similar to the final one although it is damped by the heat input and passage through the bed. The inlet temperature to the reactor varies less than that to the regenerator because of the damping produced by the greater heat input required to heat the ethylbenzene feed.

The superheater heat load and the make-up steam temperature were calculated to produce inlet temperatures of 650°C at the end of the period. However, the regenerator outlet temperature at the start of the period is higher than at the end and hence the inlet temperatures are initially greater than 650°C. Nevertheless, the inlet temperatures quickly fall, and are only above 650°C for about the first 2 seconds of the period. In a practical system, this extreme variation at the start of the period would certainly be damped out and it will therefore

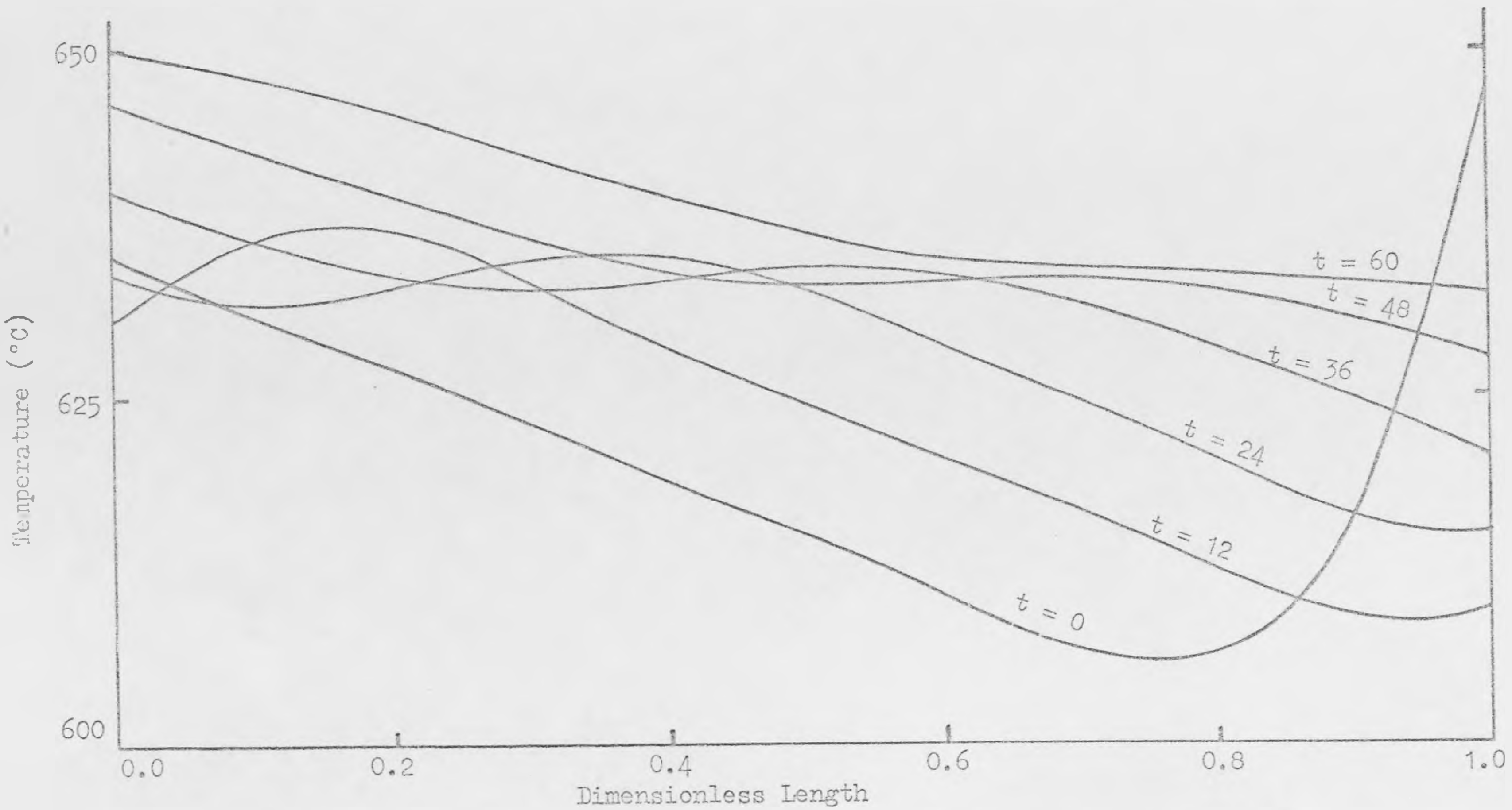

Figure 8.15: Counter-current Regenerator Temperature Profiles during a Period with Varying Inlet Temperatures.

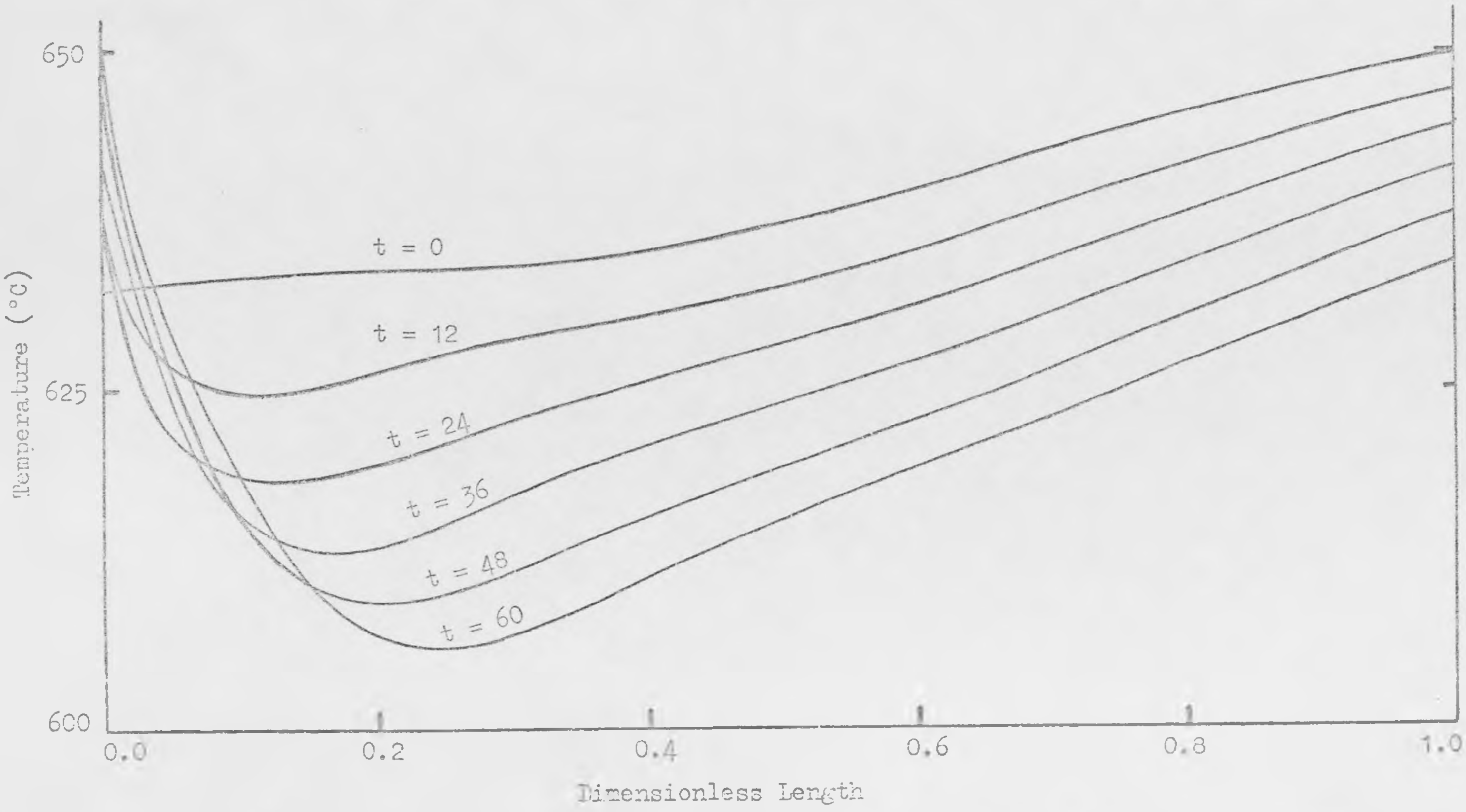

Figure 8.16: Reactor Temperature Profiles during a Period with Varying Inlet Temperatures.

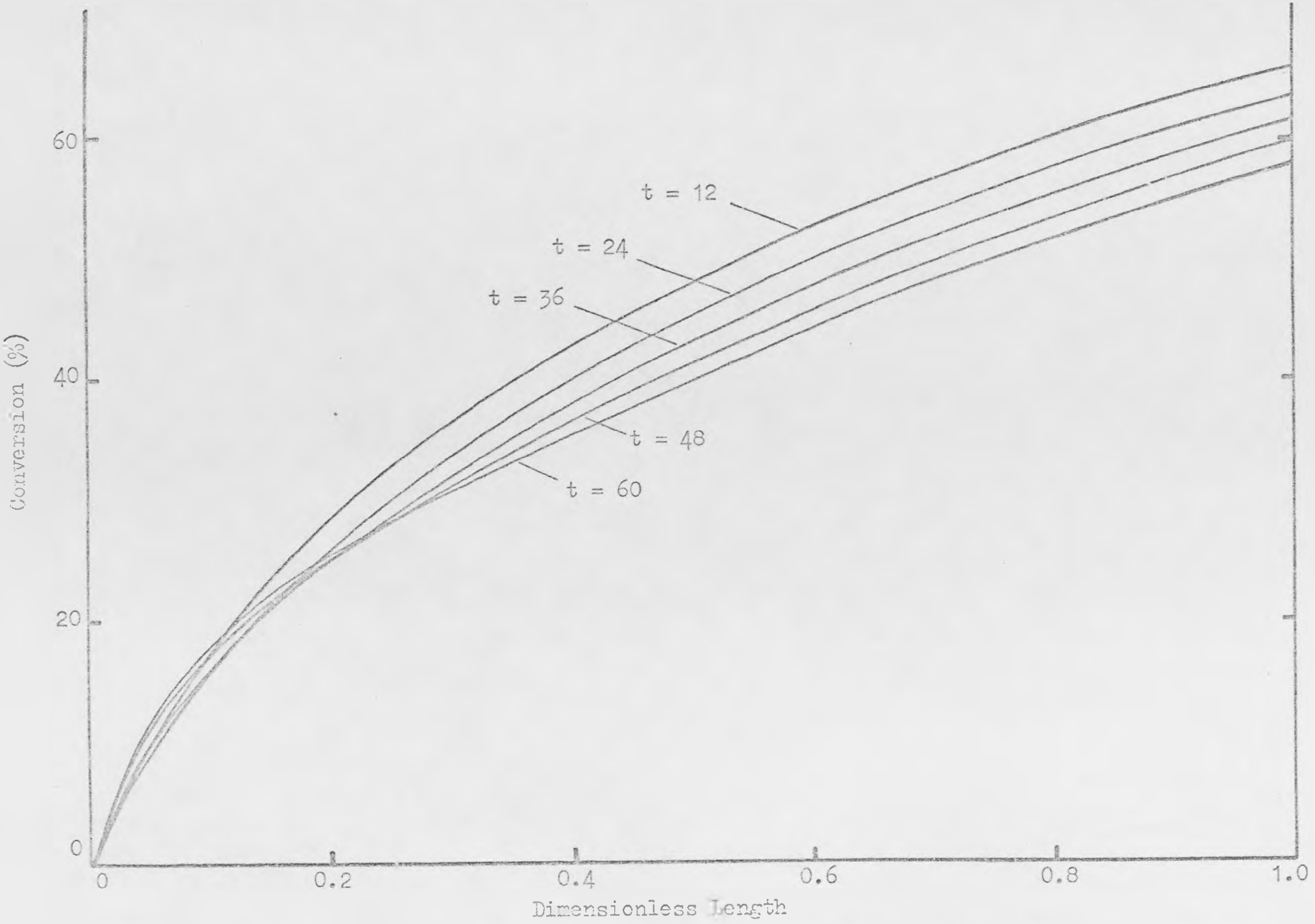

Figure 8.37: Reactor Conversion Profiles during a Period with Varying Inlet Temperatures.

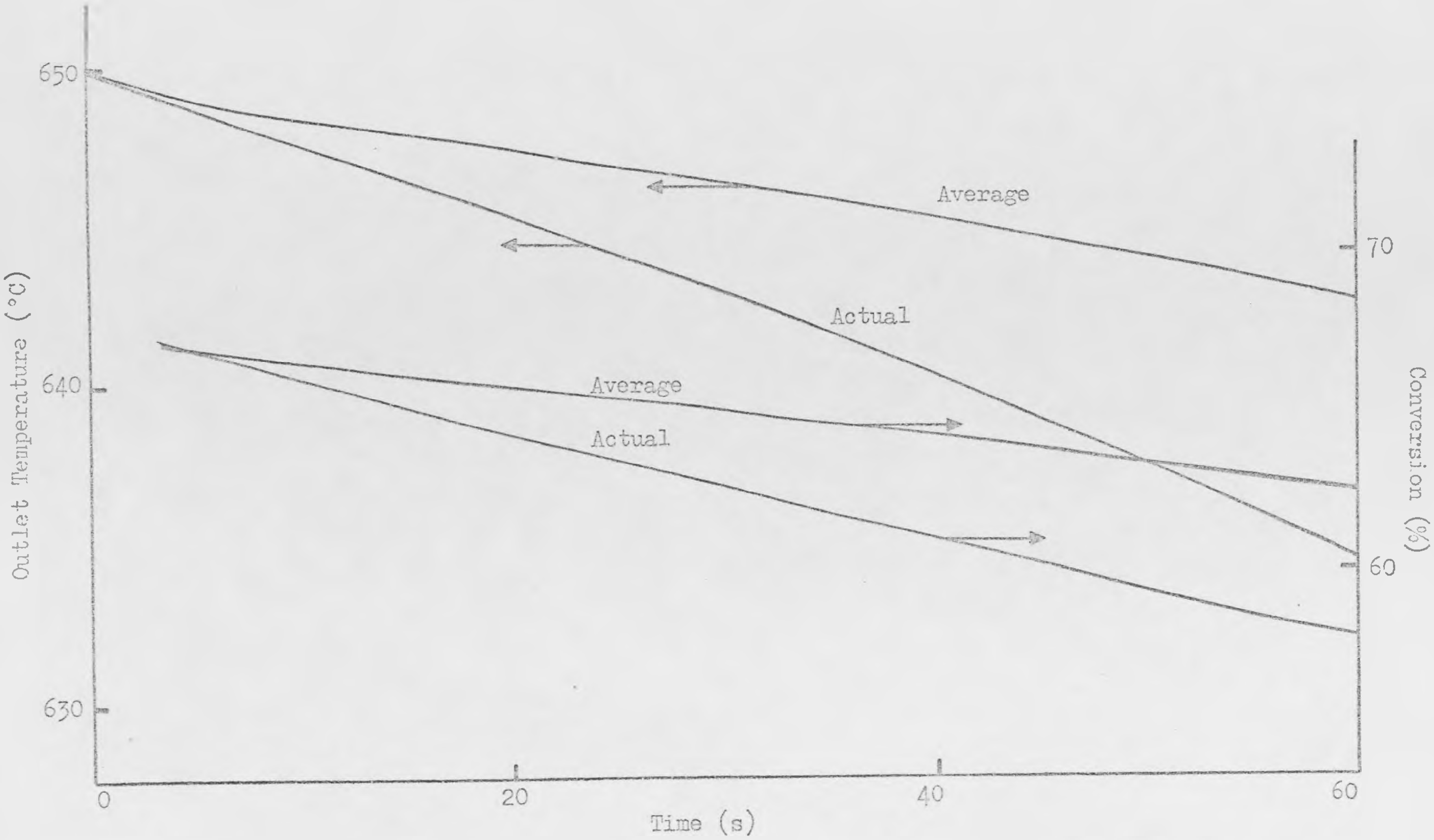

Figure 8.18: Reactor Outlet Temperature and Conversion during a Period with Varying Inlet Temperatures.

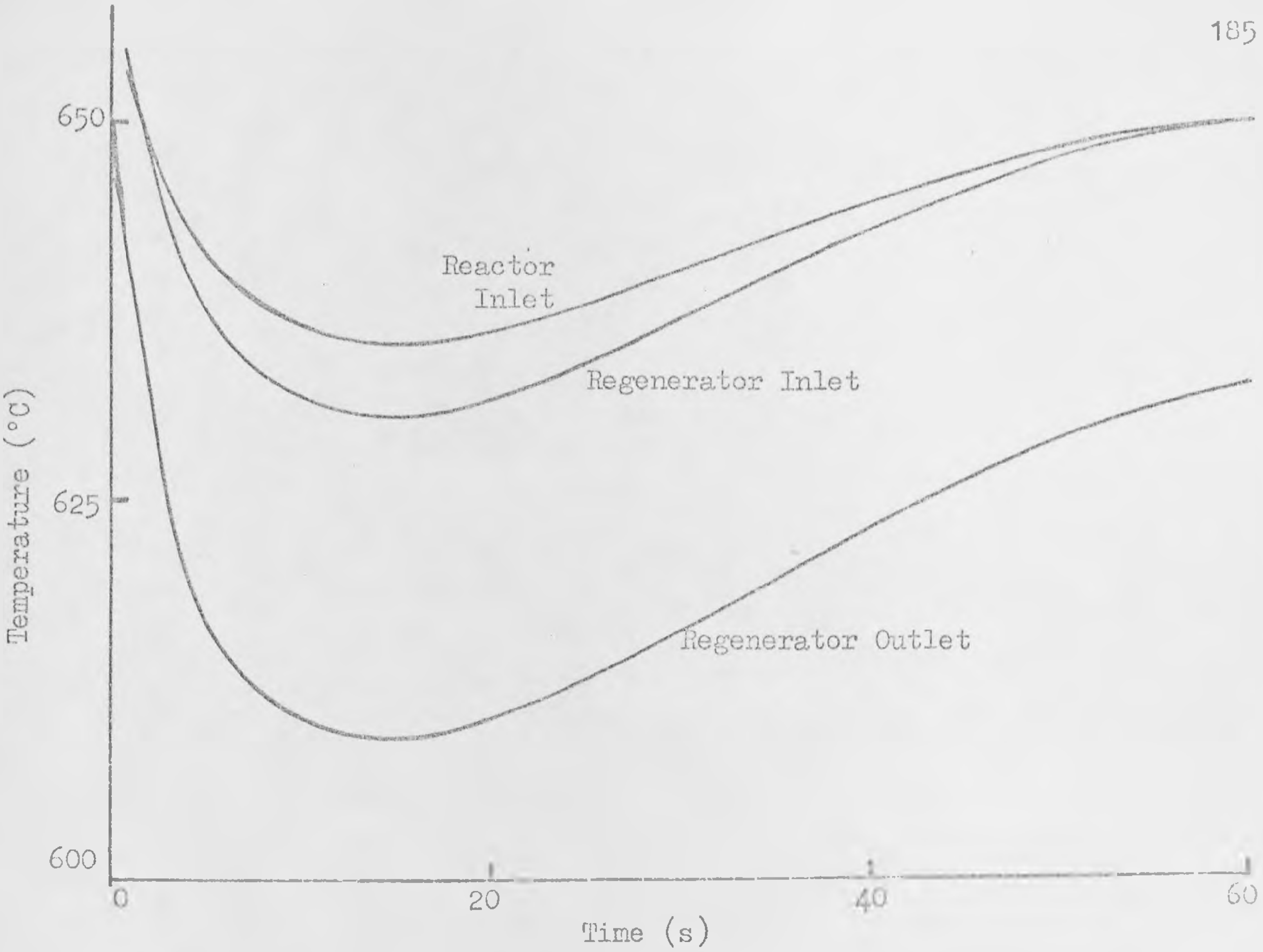

Figure 8.19: Counter-current Bed Inlet and Regenerator Outlet Temperatures during a Period.

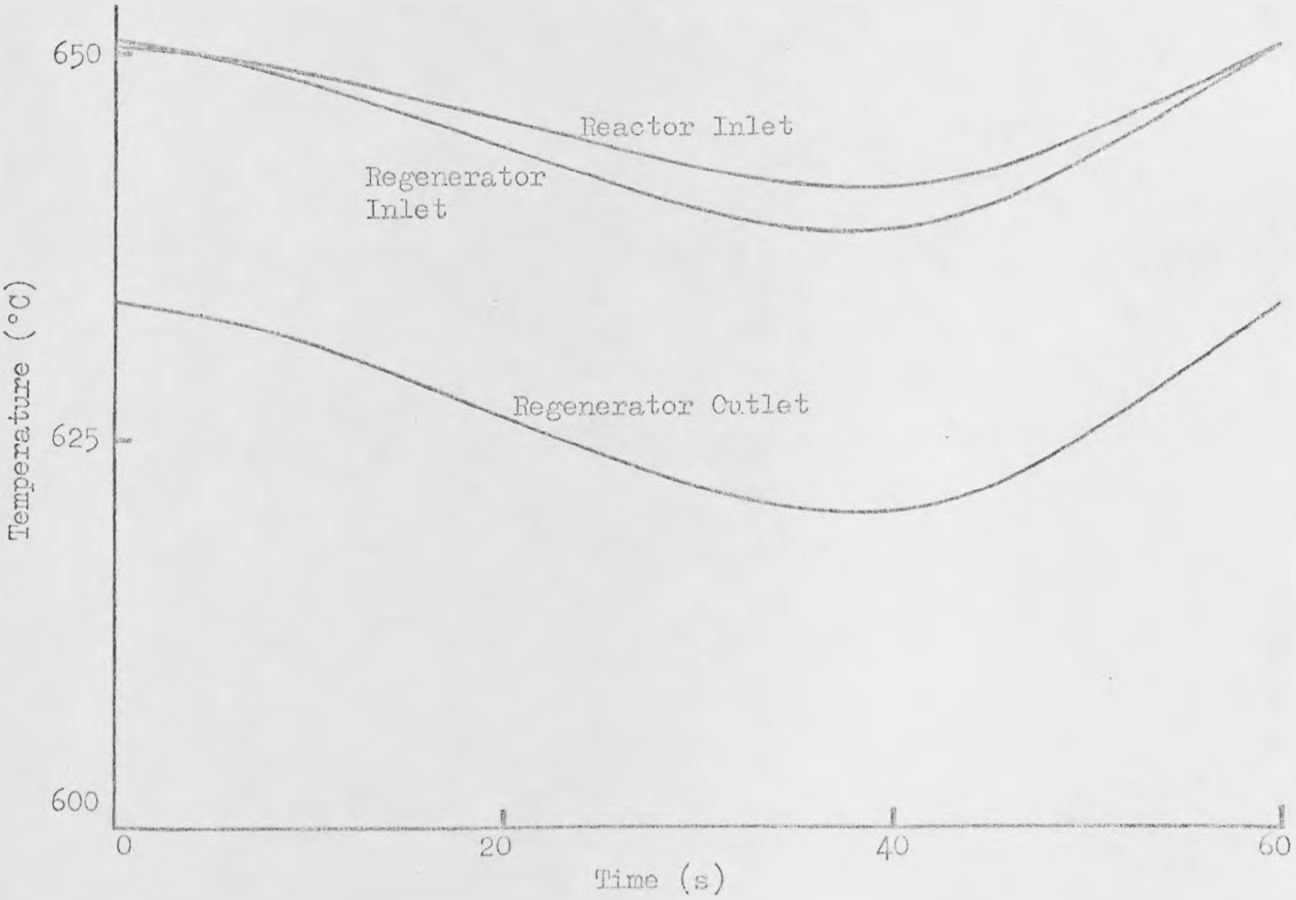

Figure 8.20: Co-current Bed Inlet and Regenerator Outlet Temperatures during a Period.

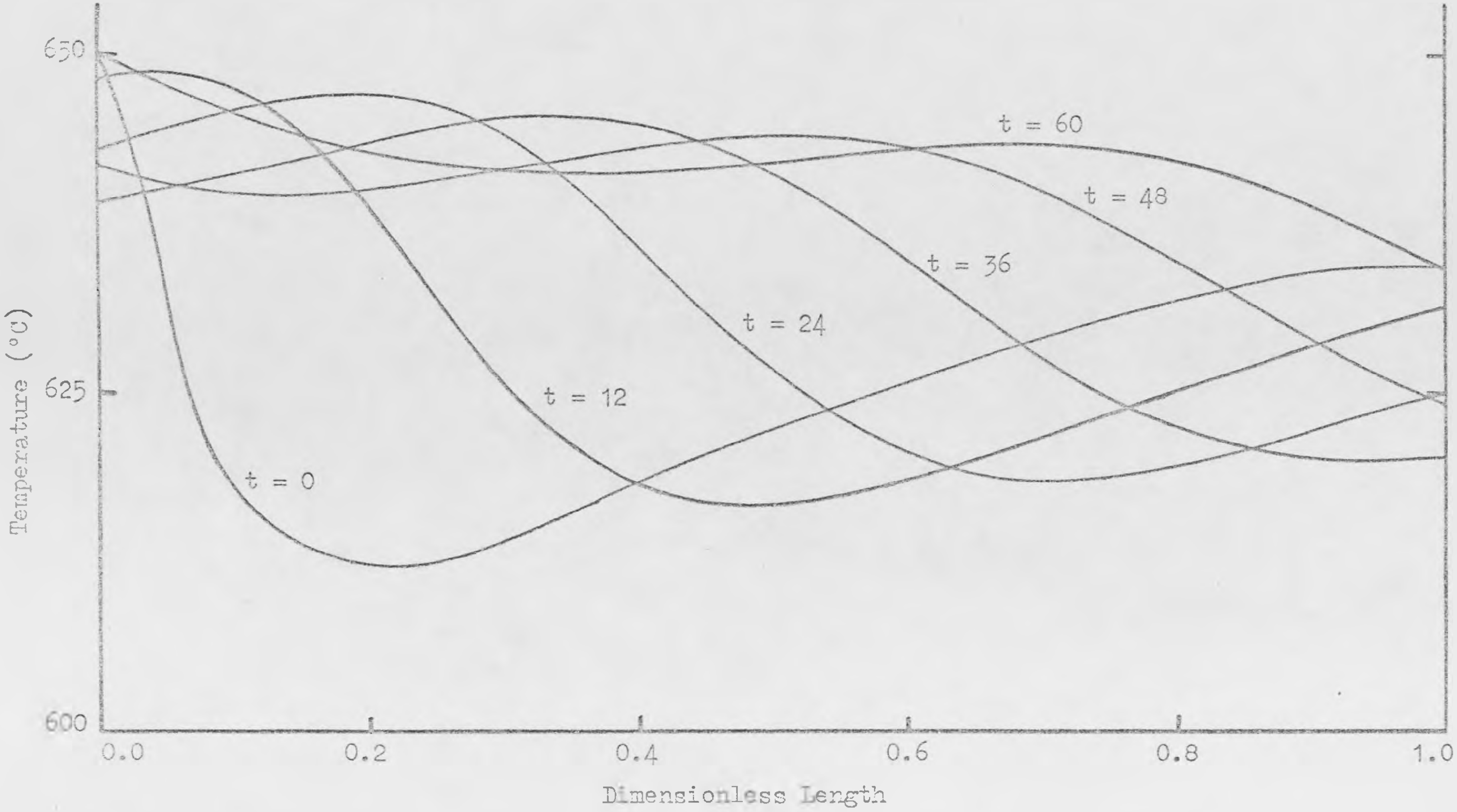

Figure 8.21: Co-current Regenerator Temperature Profiles during a Period with Varying Inlet Temperatures.

be ignored. Figure 8.19 also shows that the procedure for evaluating the make-up steam temperature (equation 5.16) described in Chapter 5 is correct, as both inlet temperatures reach 650°C at the end of the period when the superheater heat load is the correct value to give 650°C at the reactor inlet.

Temperatures above 650°C were observed in earlier cycles before the cyclic steady state was achieved because of the initial assumption of isothermal beds at 650°C. This was overcome by starting with the beds at 630°C and this gave a more rapid attainment of cyclic steady state, which was then achieved after 15 cycles.

8.4.2 Co-current Operation

Using the same initial parameters as in the previous section, co-current operation gave a higher cyclic steady state conversion of 64.7% when the inlet temperatures to the beds at the end of the period were both 650°C. The superheater heat load and the make-up steam temperature were both slightly lower at 0.320 kW and 747°C because less heat was removed from the reactor in the product gases. 16 cycles were required to achieve cyclic steady state operation.

The regenerator outlet temperature, and hence the inlet temperatures to the beds, varies much less over the period than in the counter-current case and these are shown in Figure 8.20. These then produce a higher initial reactor temperature profile and an increased conversion. Figure 8.21 shows the regenerator temperature profiles during the period. The regenerator outlet temperature is not affected by the trough until near the end of the period and the minimum temperature is increased by its passage through the bed. The outlet temperature does not, therefore, show the extreme fluctuation observed with counter-current operation (Figure 8.19). The average regenerator outlet temperature is 626.4°C compared with 620.0°C for counter-current operation.

Thus the increased conversion with co-current operation is due to damping of the temperature fluctuations within the bed. This suggests that the effect of the additional heat capacity of the system, which is ignored in this study, will also cause an increase in conversion by reducing the variation of the inlet temperatures to the beds.

8.4.3 Variation of Regenerator Steam Flow

The effect on the average conversion of varying the regenerator steam flow is shown in Figure 8.22 for counter-current and co-current operation, with a period time of 60 s in each case. As in the study with constant bed inlet temperatures (Figure 8.9) the conversion falls with steam flow below the standard value. The difference in behaviour above the standard steam flow is due to the differing extents to which the final reactor profile is moved back into the regenerator by the variation in the inlet temperature. The final regenerator (initial reactor) temperature profiles at various regenerator steam flows are shown in Figures 8.23 and 8.24 for counter-current and co-current operation.

At low flows, the maximum inlet temperatures to the beds may not be observed at the ends of the periods. Thus the reactor inlet temperature is checked through the period and the maximum value is forced to 650°C whenever it occurs.

8.5 Assessment of the Effect of the System Heat Capacity

It was noted in Section 8.4.2 that co-current operation gives higher conversions than counter-current operation, when the additional heat capacity of the system is ignored, because the bed damps the variation in the regenerator outlet temperature. This effect causes a higher initial reactor temperature profile and the conversion is 64.7%

Figure 8.22: Effect of Regenerator Steam Flow with Varying Inlet Temperatures.

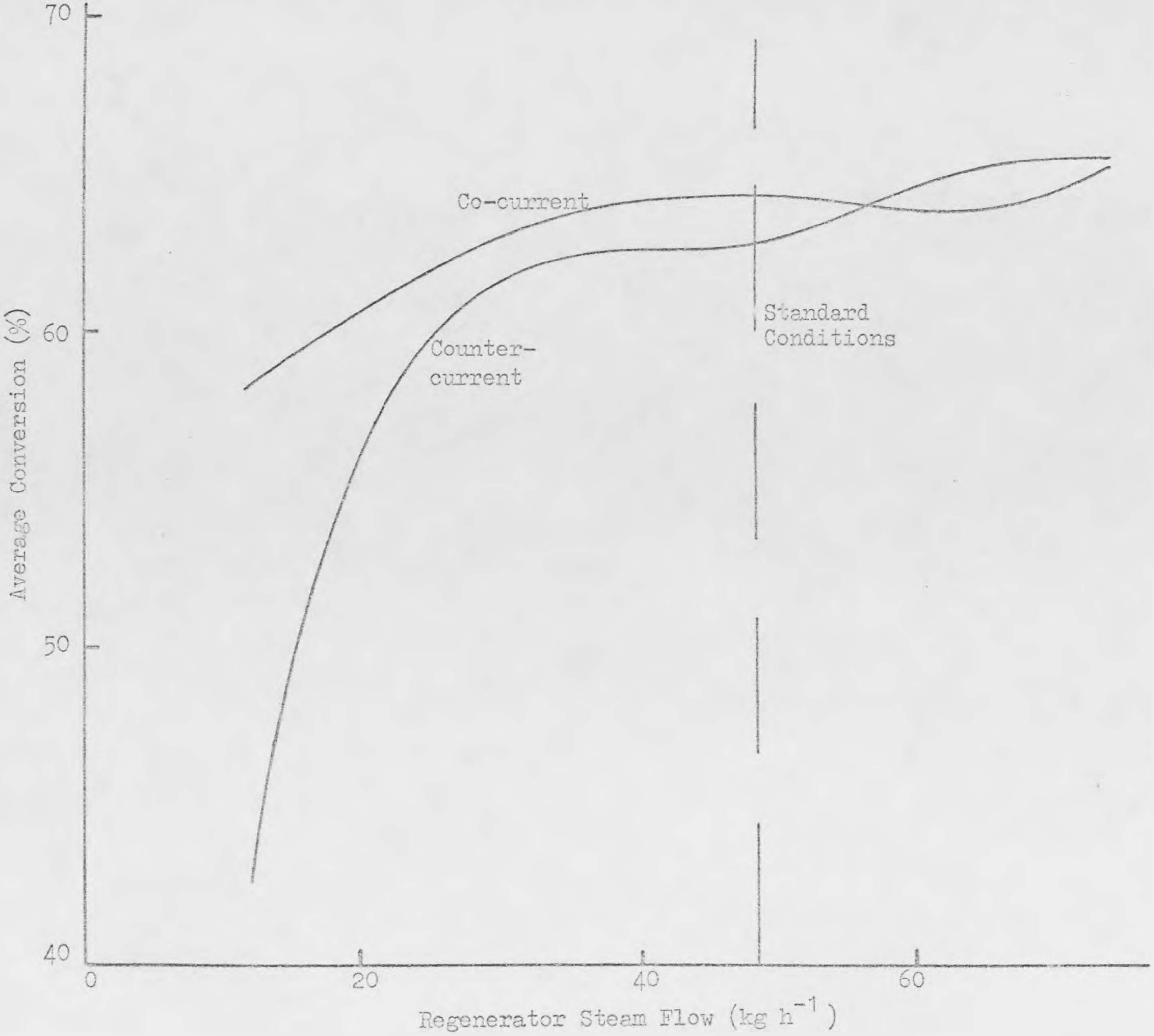

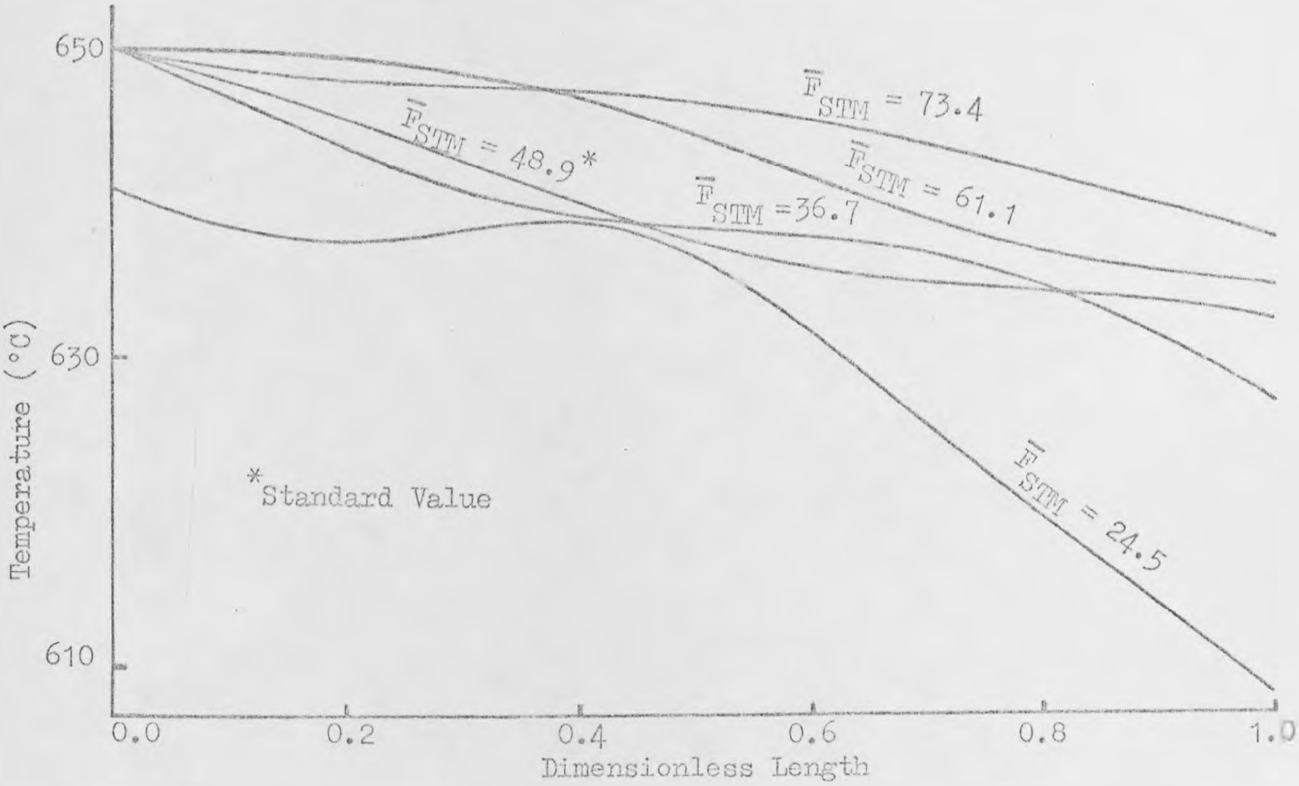

Figure 8.23: Counter-current Final Regenerator Temperature Profiles with Varying Inlet Temperatures.

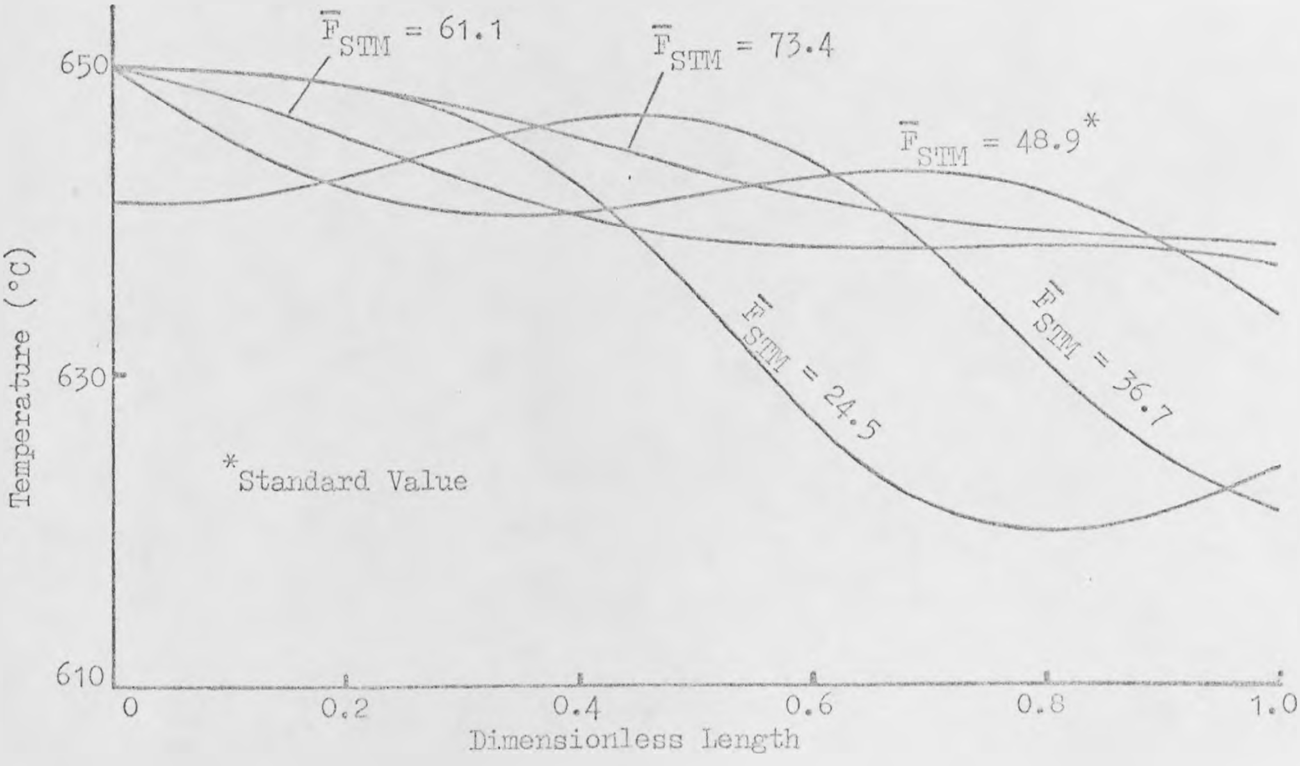

Figure 8.24: Co-current Final Regenerator Temperature Profiles with Varying Inlet Temperatures.

compared with the counter-current value of 62.9%. In practice, the heat capacity of the system as a whole is likely to be considerably larger than that of the beds and hence the damping effect will be correspondingly greater.

The addition of a layer of inert material at the front of the reactor can give some indication of the magnitude of the system damping. Temperatures above 650°C are allowed in the inert material, but not at the inlet to the catalyst region during the reactor period or within the catalyst at the end of the regenerator period.

Using the standard steam flow and norm catalyst bed size, the addition of 25% of the catalyst volume of inert material at the front of the reactor gives average conversions of 64.5% and 65.6% respectively for counter-current and co-current operation. If the volume of the inert material is increased to be equal to the catalyst volume, these conversions become 66.5% and 66.2%, which are approaching the values of 67.7% and 67.3% given with constant bed inlet temperatures at 650°C.

Figure 8.25 shows the counter-current regenerator temperature profiles for equal volumes of catalyst and inert. The temperature trough in the catalyst at the end of the reactor period is moved into the inert material during the regenerator period and the temperature at the end of the period is above 645°C throughout the catalyst. The temperature profiles during the reactor period, in Figure 8.26, show that the variation of the inlet temperature is reduced by the presence of the inert material. The temperature profile in the inert material is not moved far along the bed because the flow of the reactor feed is considerably less than the regenerator steam flow. The corresponding temperature profiles for co-current operation are shown in Figures 8.27 and 8.28. These again show less variation of the inlet temperatures to the catalyst beds but the initial reactor temperature profile in the

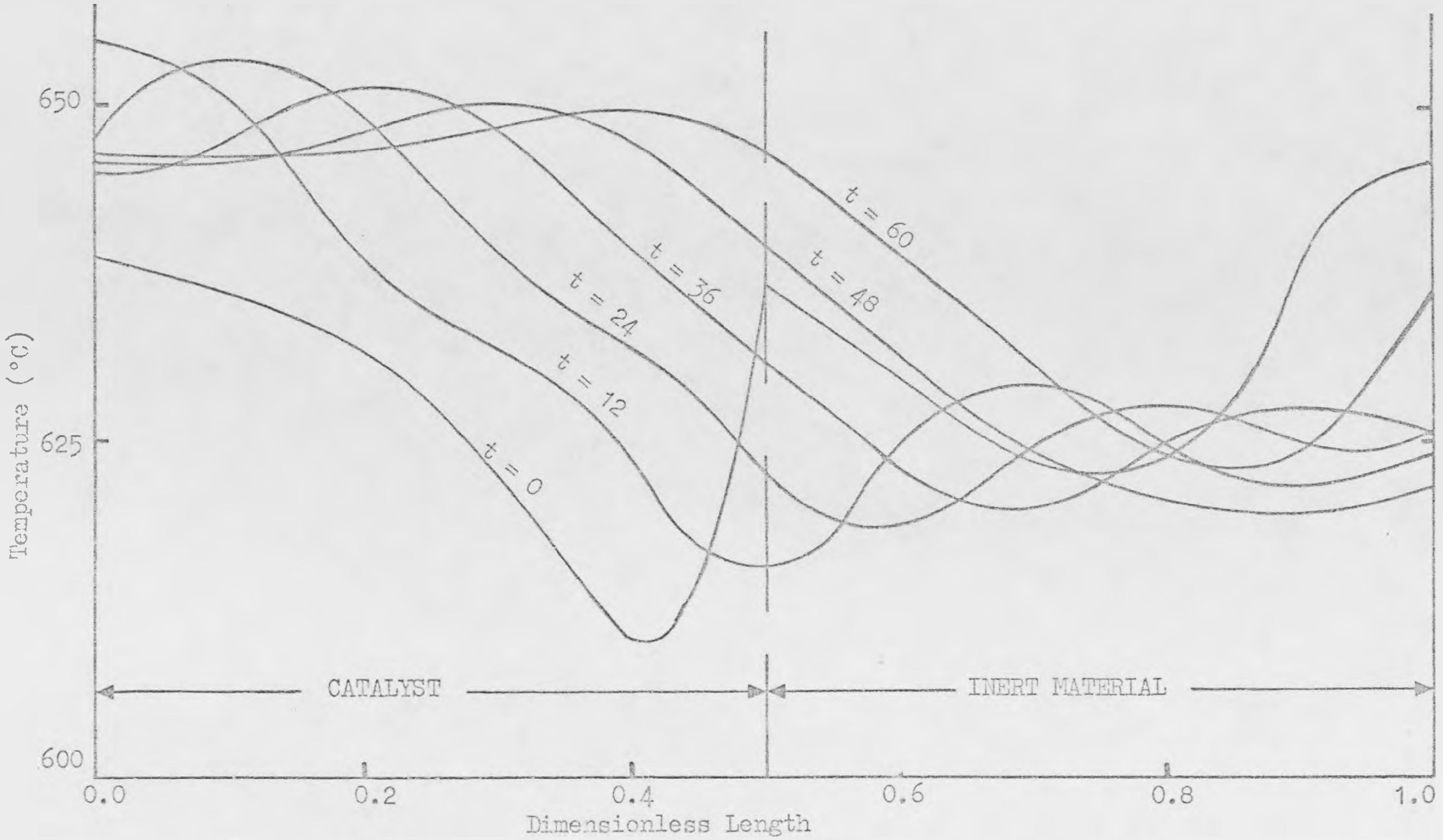

Figure 8.25: Counter-current Regenerator Temperature Profiles with Varying Inlet Temperatures and Inert Material at Reactor Entrance.

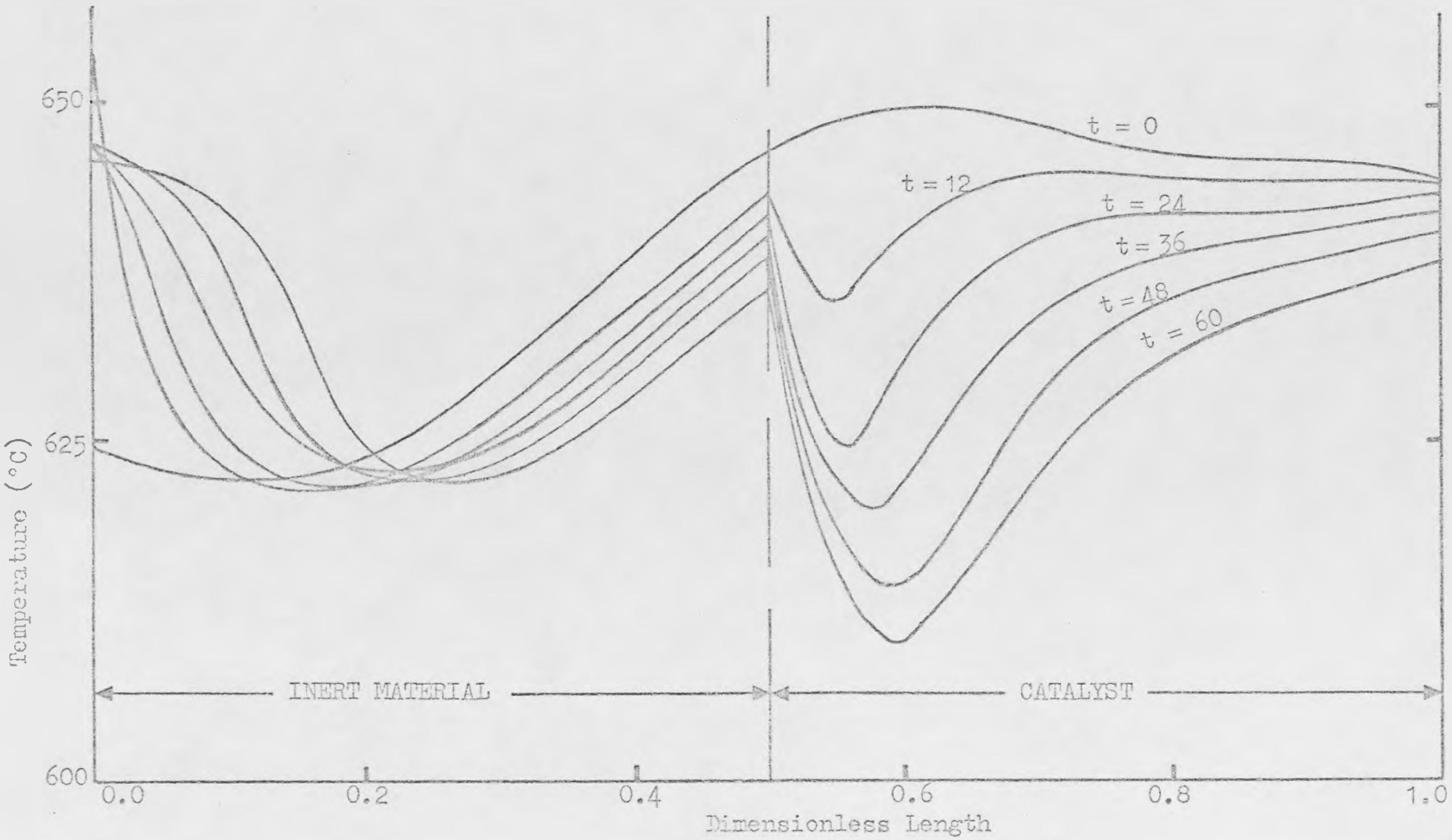

Figure 8.26: Counter-current Reactor Temperature Profiles with Varying Inlet Temperatures and Inert Material at Reactor Entrance.

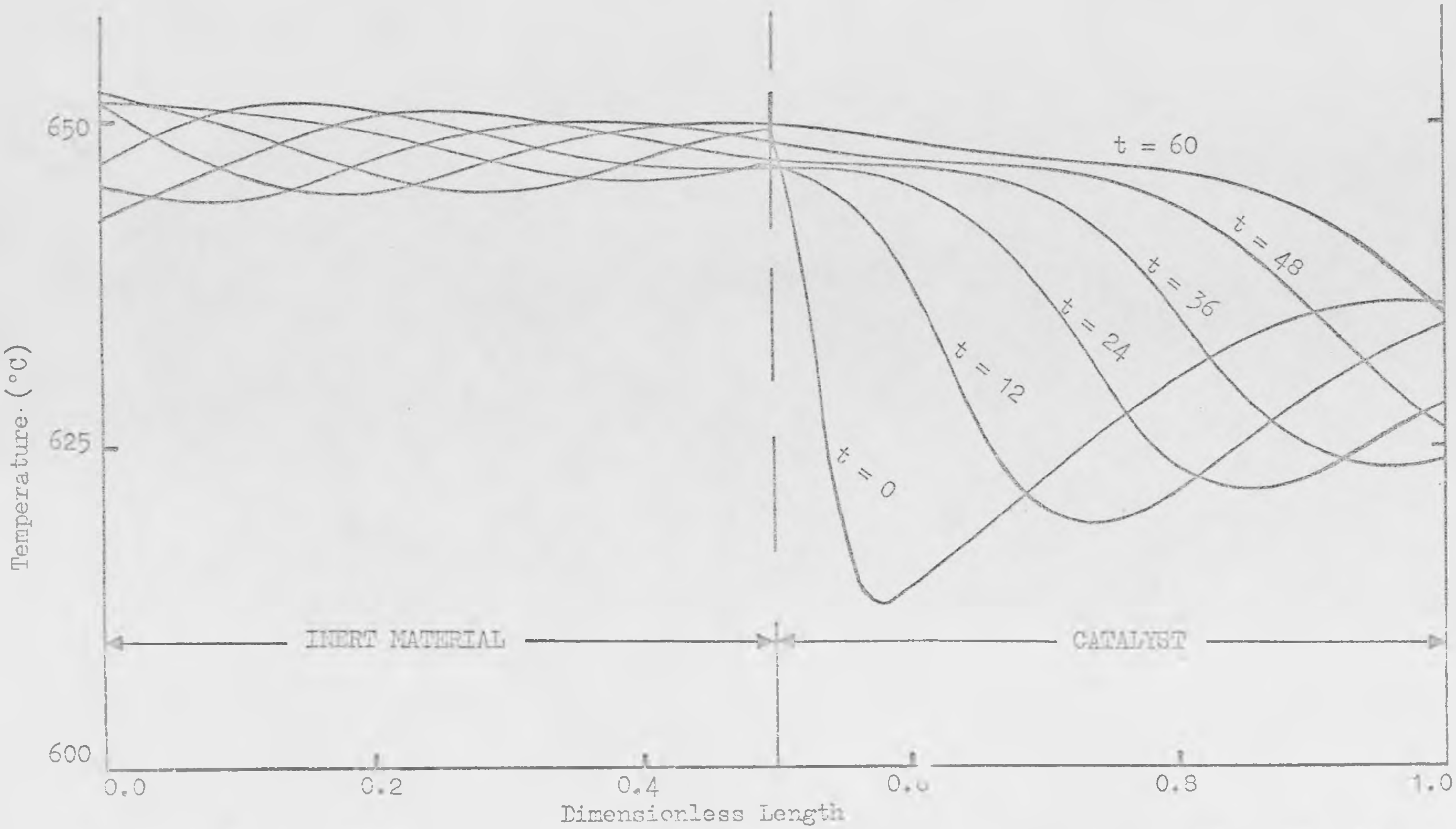

Figure 8.27: Co-current Regenerator Temperature Profiles with Varying Inlet Temperatures and Inert Material at Reactor Entrance.

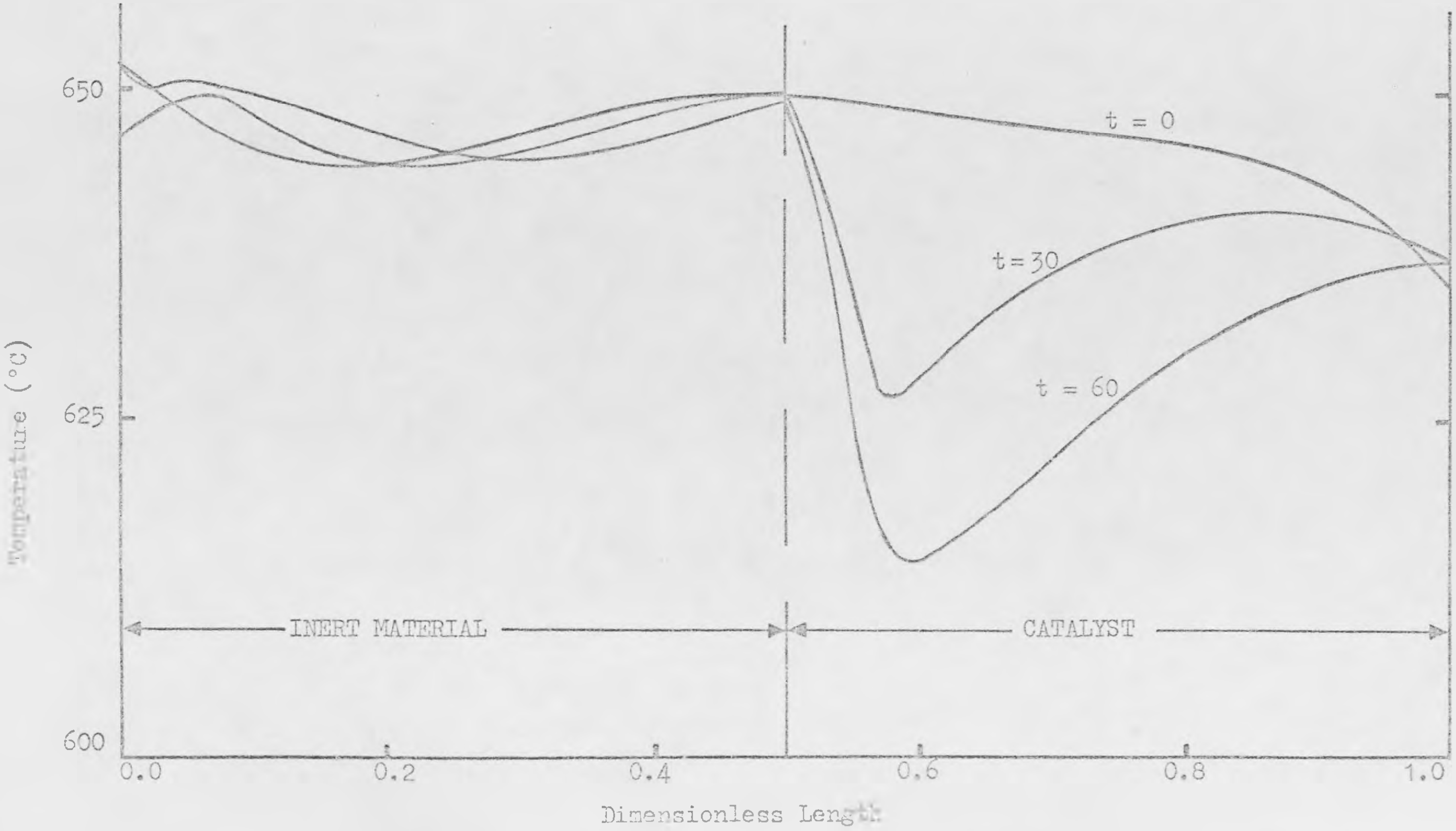

Figure 6.28: Co-current Reactor Temperature Profiles with Varying Inlet Temperatures and Inert Material at Reactor Entrance.

catalyst is less favourable than with counter-current operation.

If the equal volumes of catalyst and inert material are uniformly mixed, the conversions for counter-current and co-current operation are 65.9% and 65.3% respectively. These are lower than when the inert is at the front of the bed, but are better than when no inert is present, especially for counter-current operation. This is caused by the reduced temperature fall during the reactor period which was observed for a larger bed in Section 8.3.3. The variation of the regenerator outlet temperature, and hence the bed inlet temperatures, is therefore reduced. This suggests that the use of high activity catalyst is undesirable in the cyclic reactor system because it gives a small bed size.

These studies show that even the addition of a comparatively small amount of heat capacity within the system has a considerable effect on the system performance. Hence, the additional heat capacity of a physical system cannot be ignored. This will be much greater than that considered above, and so the approach to the conversion given by the assumption of constant bed inlet temperatures will be even closer. Thus this simpler model will give better predictions of the performance of a physical system than one which ignores the damping effect of the system.

8.6 Discussion

It has been shown that the additional heat capacity of the cyclic reactor system, other than that of the two beds, cannot be ignored. Thus, the assumption of constant inlet temperatures to the reactor and the regenerator gives a better representation of a physical system than if they are assumed to vary directly with the regenerator outlet temperature. This is fortunate as the former assumption allows quicker solutions because cyclic steady state operation is achieved in fewer cycles. However, the heat capacity of the reactor walls is shown in Appendix 5 to have little effect on the system performance.

Counter-current, rather than co-current, operation is preferred as it gives higher conversions over the range of practical operating conditions.

The average conversion given by the cyclic system may be significantly higher than the conversion from a steady state reactor using the same total catalyst volume. A 67.7% average conversion is obtained using the data in Figure 8.1 compared with a maximum conversion of 64% from a two bed steady state adiabatic reactor. In all the studies on the cyclic system, except when the diluent steam flow is reduced, the efficiency is greater than 88.6% which is a significant improvement on the steady state reactor value of 85.7%.

The period time calculated from the steady state studies provides a good prediction of the cyclic steady state conversion of the system when saturation is closely approached in the regenerator. The simple method of estimating the regenerator steam flow to give this approach during the calculated period time is also found to be reliable. These calculated periods represent the maximum values, as the conversion falls significantly if the period is lengthened and only a small increase in conversion is gained if the regenerator steam flow is increased. A small reduction in the regenerator steam flow may be worthwhile as this only produces a slight drop in the conversion. A reduction in the period time increases the loss of reactor products at flow reversals, but the reduced reactor temperature drop allows higher conversions. A similar effect is achieved by increasing the heat capacity of the bed by the addition of inert material. The diluent steam superheater heat load and the make-up steam temperature may also be estimated with some confidence as only constant, rather than time-varying, bed inlet temperatures need be considered.

The regenerator inlet temperature is shown to be an important parameter as this determines the catalyst temperature at the start of the reactor period. It should be as high as possible and a relatively small change significantly affects the system performance. On the other hand, the reactor inlet temperature has little effect on the conversion and it may therefore be worth using a lower temperature in order to reduce the heat load on the diluent steam superheater.

The diluent steam flow to the reactor is a major economic variable. Steam savings can only be made at the expense of a lower conversion and efficiency, but the size of the savings are potentially large. These savings cannot be made with steady state adiabatic reactors as the diluent steam provides the heat of reaction and thus a much greater reduction in conversion would occur.

CHAPTER 9

GUIDELINES FOR OPTIMISATION

9.1 Introduction

The aim of optimising the cyclic reactor system studied in this work is to produce styrene at the lowest possible cost. Figure 9.1 shows a system based on the reactor section of the Dow process (Figure 2.3) which will be employed as the example for discussing the guidelines for optimisation. The reactor products are used to vapourise and preheat the ethylbenzene feed and also to preheat the steam feed before it enters the make-up steam superheater. The reactor outlet temperature, therefore, affects the heat loads on both the superheaters, and these cannot be accurately assessed if the heat exchangers are omitted from the system. Thus, although the model of the cyclic reactor system derived in this work is, in itself, not sufficient, it forms the basis of any model for optimisation calculations.

The criterion for an optimisation is necessarily economic and cost factors must be derived for the relevant parameters. The separation costs in the distillation train are affected by the composition of the reactor products, but these would be determined separately by a study similar to that in Chapter 2. It was shown there that the separation costs per kg styrene produced are reduced by a higher reactor conversion, but are increased by a lower efficiency.

9.2 Optimisation Parameters

Values for all the parameters of the system must clearly be defined, but many of them are fixed by the constraints of the system and are not therefore variables for optimisation purposes. In order to simplify an optimisation, it is desirable that values for as many parameters as possible are fixed.

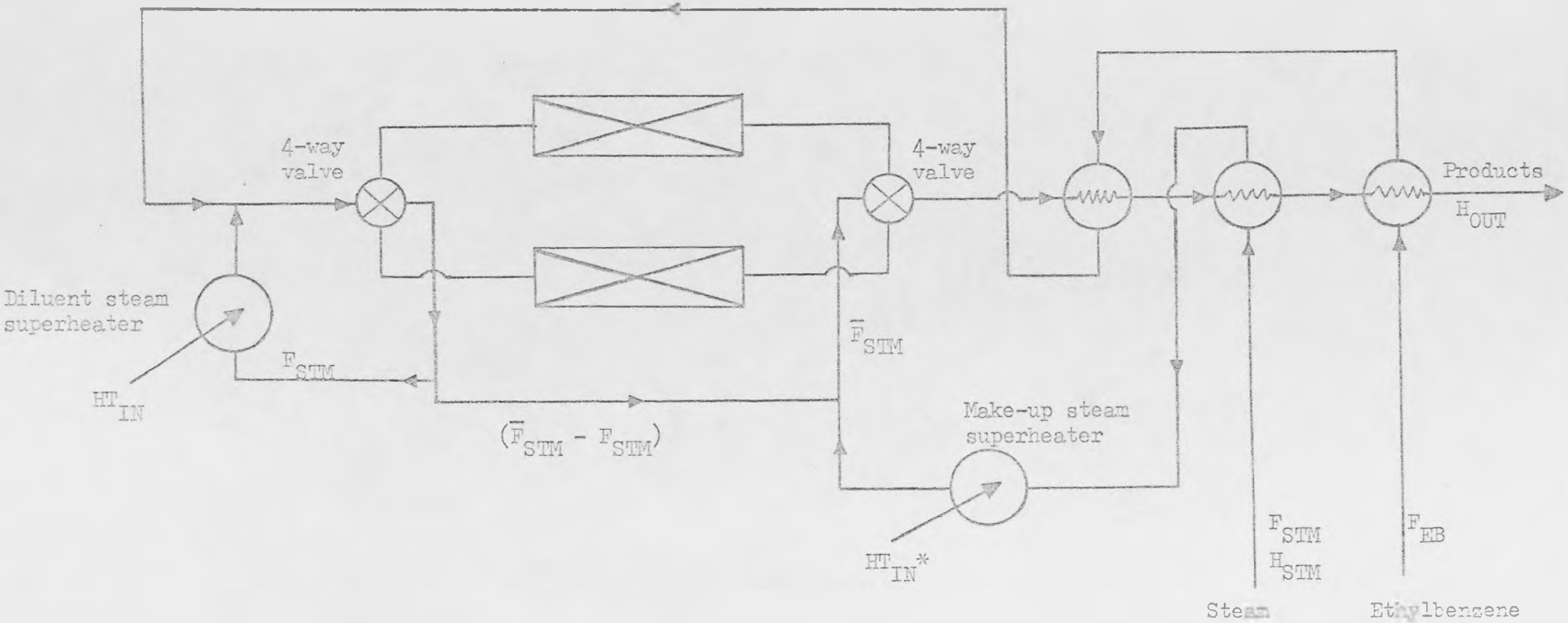
4-way valve
4-way valve
Products
H_{OUT}
Diluent steam superheater
HT_{IN}
F_{STM}
$\overline{F}_{STM}$
$(\overline{F}_{STM} - F_{STM})$
Make-up steam superheater
HT_{IN}^{*}
F_{STM}
H_{STM}
F_{EB}
Steam
Ethylbenzene

Figure 9.1: Reactor System for Use in an Optimisation.

9.2.1 Fixed Parameters

The cost of the styrene production would be related to a given ethylbenzene feed and thus this feed must be fixed at a constant value. The enthalpy of the ethylbenzene feed is also fixed and these are not affected by any of the other parameters. The optimum ethylbenzene flow per unit catalyst volume will normally be specified by the catalyst manufacturers. Thus, the volume of catalyst is fixed by the specified ethylbenzene feed.

It was shown in Chapter 8 that the regenerator inlet temperature should be constant at the maximum value of 650°C. This, therefore, fixes the heat load on the make-up steam superheater for particular values of the diluent and make-up steam flow rates and the reactor and regenerator outlet temperatures. If an existing system is being optimised, the bed size, and hence its heat capacity, is fixed. However, for design purposes, the bed size must be included in the optimisation.

The reactor inlet pressure should be as low as possible and just sufficient to overcome the pressure losses of the system. The difference in pressure drop caused by changing the bed size will be small and the inlet pressure can be fixed at a suitable value.

The reactor outlet temperature depends on the other system parameters but, as it cannot be independently varied, it is a fixed parameter for optimisation purposes. The damping effect of the system on temperature variations was shown, in Chapter 8, to be large and hence the reactor outlet temperature can be assumed constant at the average value, for a particular set of operating conditions.

The operation of the preheat heat exchangers can also be considered fixed, subject to the constraint that the ethylbenzene temperature must not exceed 540°C, or pyrolysis will occur.

9.2.2 Variable Parameters

The steam feed to the system is determined by the diluent steam flow to the reactor. This is a major economic variable as the steam raising cost and the superheater heat loads are approximately proportional to this flow. However, a reduction in this flow causes significant reductions in conversion and efficiency. The maximum flow is that which gives a molar steam/ethylbenzene ratio of about 20 at the reactor entrance. The minimum value is zero.

The regenerator steam flow must be sufficient to produce an acceptable approach to saturation during the period. A lower flow than that required for complete saturation produces only a small reduction in conversion, unless it is below about $\frac{1}{3}$ of the saturation flow. These are therefore suitable constraints on this flow, but their actual values depend on the period time and the bed heat capacity. A reduction in the flow reduces the capital cost for the pipework and also the recycle compression costs. If the compression is by means of an ejector, this allows a lower pressure, and hence enthalpy, steam feed to the system.

The heat load on the diluent steam superheater determines the reactor inlet temperature, which was shown in Chapter 8 to have little effect on the reactor performance. Thus, this temperature may be below the maximum value in order to reduce the superheat cost. The maximum temperature is 650°C and, from the studies in Chapter 8, a reasonable minimum value would be 620°C.

The period time has a considerable effect on the conversion of the reactor, which increases as the period is shortened. However, a shorter period requires a greater regenerator steam flow to achieve saturation and increases the ethylbenzene losses due to the flow reversals. The minimum period was set in Chapter 5 as 60 s or 100 reactor residence times, whichever is the longer. There is no constraint on the maximum period time, but there is little point in continuing if the reactor reaches the steady state.

An increase in bed heat capacity, for a constant overall catalyst activity, has the same effect as a corresponding decrease in period time. This would be achieved by the addition of inert material to the bed. The minimum bed heat capacity is when no inert material is present and the maximum is constrained by the increasing capital cost.

Thus, values for only five parameters have to be determined in order to predict the optimum system performance. These are the diluent and recycle steam flows, the reactor inlet temperature, the period time and the fraction of inert material in the bed.

9.3 The Objective Function

The objective function is an expression which relates the performance and costs of the system and is either maximised or minimised at the optimum conditions. An optimisation of the cyclic reactor system aims to minimise the styrene cost or to maximise the profit from the sale of the product. A suitable objective function is therefore

$$OF = PI - PC \qquad (9.1)$$

where PI is the income from the sale of the product and PC is the product cost. This must be maximised to obtain the optimum performance.

The income for the system per unit time can be expressed as

$$PI = \left(\sum_{j=1}^{3} g_j x_j + g_4 \sum_{j=1}^{3} x_j + g_5 H_{OUT} \right) F_{EB} \qquad (9.2)$$

where g_i are cost factors. The first term represents the income from the sale of styrene, toluene and benzene; the second is the value of the off-gas as a fuel; and the third is the value of the useful enthalpy in the product gases, which may be used for the reboiler heat in the distillation train[110].

The costs involved in the process were discussed in the previous section and the product cost per unit time can be expressed as

$$\begin{aligned} PC = {} & g_6 F_{EB} + g_7 F_{STM} H_{STM} + g_8 HT_{IN} + g_9 HT_{IN}^{*} \\ & + g_{10} \frac{AZ}{t_f} F_{EB} + g_{11}/_{x_{EB}} + g_{12}(x_{BZ} + x_{TOL}) \\ & + g_{13}\, AZ + g_{14} \frac{\bar{F}_{STM} - F_{STM}}{F_{STM}} \end{aligned} \tag{9.3}$$

where g_6 represents the fixed ethylbenzene cost; g_7, the steam raising cost; g_8 and g_9, the superheat costs; g_{10}, the ethylbenzene losses, due to flow reversals and leakage; g_{11} and g_{12}, the separation costs in the distillation train; and g_{13} and g_{14} are the capital costs associated with the bed size and recycle steam flow.

Clearly, a major snag in estimating the product cost lies in the difficulty of obtaining reliable and up to date economic data. This is not available in the literature and operating costs will also vary from plant to plant.

9.4 Optimisation Procedure

It was shown in Chapter 5 that the best operating policy for the cyclic reactor is the use of constant heat inputs to the system. Thus, the heat exchangers and superheaters in Figure 9.1 all operate in the steady state and their performance need only be considered when the reactor system has achieved cyclic steady state operation.

Initial values for the system parameters can be obtained by the methods described in Chapter 5 and the reactor system is run to cyclic steady state. Heat balances will give the superheater heat loads, and the objective function can be evaluated. An optimisation procedure must now estimate new values for [illegible] or all of the variable parameters of the system in order to recalculate the system performance and the objective function.

The technique used to re-estimate the variable parameters determines the efficiency of an optimisation as it is clearly desirable to minimise the required number of evaluations of the system performance. A detailed discussion of techniques for process optimisation is given by Whitehead[111]. Gradient methods, which search for the direction which gives the greatest change in the objective function. are normally efficient. However, they usually require the evaluation of the partial derivatives in terms of the independent variables and analytical expressions do not exist for these. Direct search techniques, which do not require these derivatives, are likely to be more efficient for this system. The procedure is:

(1) Estimate initial parameters.

(2) Calculate system performance.

(3) Calculate objective function.

(4) Check constraints. If violated, select new independent variable(s) and repeat (2) and (3) until satisfied.

(5) Change independent variables by given amounts and repeat steps (2) - (5) until the objective function is a maximum. If the value of the objective function decreases at any step, new estimates for the variables are obtained from values at the previous step and the procedure continued.

9.5 Conclusions

Optimisation of the cyclic reactor system is not possible at this time as the model derived in this work is not sufficiently comprehensive and there is a lack of reliable data. If these were available, the system could be optimised by maximising the difference between the income from product sales and the cost of its manufacture.

Only five variables are considered as variables for an optimisation. These are the diluent and regenerator steam flows, the reactor inlet temperature, the period time and the inert fraction of the bed.

CHAPTER 10

SUMMARY OF CONCLUSIONS

Adiabatic or multitubular steady state reactors do not give the optimum temperature profiles for heterogeneous, catalytic, gas phase reactions, especially if the reaction is equilibrium controlled. A novel reactor system is proposed, which utilises the inherent characteristics of the thermal regenerator to control the longitudinal reactor temperature profile. Adiabatic beds are employed and hence undesirable radial temperature gradients are avoided. One of the thermal periods in the thermal regenerator is replaced by a chemical reaction and each of the two beds in the system operates alternately as reactor and regenerator in successive periods of operation. The inherent control of the reactor temperature profile should enable higher conversions to be obtained than those from steady state reactors.

This cyclic reactor system is investigated using the endothermic, reversible dehydrogenation of ethylbenzene to styrene in the presence of steam as an example. The reaction is commercially important and the steam is a suitable heat transfer fluid for use in the regenerator. The styrene manufacturing process often operates with low (c. 40%) conversion reactors and, hence, a large ethylbenzene recycle to the reactor is required. If the reactor conversion is increased to 60%, a 20% reduction in reactor steam consumption is obtained and the reboiler and condenser requirements in the distillation train may be reduced by as much as 35%. The use of the proposed cyclic reactor system in this process should, therefore, produce considerable utility cost savings. The time-varying reactor product composition can be easily damped by the use of a suitable holding vessel before the distillation train. The variation of the reactor outlet temperature with time will be damped by the thermal inertia of the system.

Kinetic rate expressions presented in the literature for the dehydrogenation of ethylbenzene and the associated side-reactions are compared. None of these can be considered entirely satisfactory as they do not show the expected response to variation of reactor parameters. The rate expression for the dehydrogenation reaction given by Carra and Forni[39], and used by Modell[32], appears to be the most theoretically sound and gives the best predictions of the conversion. However, it predicts very small reactor sizes compared with all other kinetics. None of the proposed rate expressions adequately describe the side-reactions, and more representative expressions are therefore derived from the experimental data of Bogdanova et al[29] for the two main side-reactions.

Models for the reactor and regenerator are presented. Pseudo-homogeneous models do not represent the physical situation in transient operation, although they may be satisfactory in the steady state. A film-resistance model, which includes the interphase diffusion effects, accurately represents the regenerator and should be adequate for the reactor. Intraparticle diffusion is unlikely to be important for the dehydrogenation reaction.

Approximate numerical solutions are required for the reactor model because of the non-linear reaction terms and various solution methods are compared. The most suitable method, which gives an accurate solution and minimises computing requirements, is to solve the Lagrangian equations by the use of backward and central difference approximations for the time and length derivatives respectively. Both the model and the solution method used by Cavalas[11,12], who presents the only published work on a cyclic reactor system, are shown to be unsatisfactory, but the errors caused by the use of large integration step sizes hide some of the faults of the model.

A practical cyclic reactor system for the dehydrogenation of ethylbenzene is described. In order to satisfy the temperature constraints of the reaction, a diluent steam superheater is required between the regenerator and the reactor inlet. The regenerator steam flow must be greater than that to the reactor to achieve a close approach to saturation during the regenerator period. For economic reasons, the excess steam is recycled around the regenerator. This approach to saturation is desired in order to approximate the optimum reactor temperature profile for the endothermic reaction considered.

The most suitable operating policy is shown to be the use of constant heat inputs and flows during each period and to allow the temperatures within the system to vary. Cavalas[11,12] proposes controlling the flows in his regeneratively cooled reactor system in order to produce the desired, time-varying, temperatures at the entrance to each bed. However, he ignores the damping effect of the system on temperature variations and it is shown that, in a practical system, this will be large. In the system proposed for the dehydrogenation of ethylbenzene, this effect seems likely to damp out the variation of the regenerator outlet temperature so that the bed inlet temperatures can be assumed constant during each period.

Counter-current, rather than co-current, operation is preferred as this gives higher conversions over the range of practical operating conditions.

The effect of the system parameters on the performance is studied and is summarised below:

(a) The average conversion increases as the period time is reduced and approaches the isothermal steady state value as the period tends to zero. The adiabatic steady state conversion will be obtained if the period becomes very long.

(b) An increase in bed heat capacity has the same effect as a reduction in period time. The heat capacity of a commercial reactor is likely to be greater than that of the norm size used in this work. Thus this norm represents the 'worst case'.

(c) The average conversion increases with the regenerator steam flow, but the rate of increase falls off as saturation of the bed during the regenerator period is approached. Below approximately $\frac{1}{3}$ of the flow required to produce complete saturation, the conversion falls rapidly with counter-current operation.

(d) Both bed inlet temperatures must be as high as possible to obtain the maximum conversion, but the effect of a reduction in the reactor inlet temperature is negligible compared with a corresponding reduction in that to the regenerator.

(e) The conversion and efficiency both fall as the diluent steam flow to the reactor is reduced and the effect becomes greater at low flows. However, the effect is less than in a steady state adiabatic reactor as the steam does not provide the reaction heat.

In the design of a cyclic reactor system, the parameters for the reacting bed (e.g. temperature, pressure, flowrates) can be determined from studies of existing reactors. The regenerating steam temperature is also fixed by the required reaction temperature. A simple procedure for estimating the remaining parameters of the system is described. These parameters are the period time, the regenerator steam flow, the heat load on the diluent steam superheater and the temperature of the make-up steam. The proposed procedure makes use of steady state reactor results and the analytical solution of the pseudo-homogeneous regenerator model together with heat balances within the system. Thus, the parameters can be estimated without solving the cyclic model and they are found to give good predictions of the cyclic system performance for a given bed size.

The predicted parameters may not give the optimum performance of the system and guidelines for an optimisation are presented. The period time for a given bed size, the regenerator steam flow, and the reactor inlet temperature must be considered in an optimisation, but the major variable is likely to be the diluent steam flow as this determines the steam requirement of the system. However, in the absence of suitable costing data, the proposed design procedure seems to predict reasonable operating conditions.

10.1 Suggestions for Further Work

Shortcomings have been shown to exist in all the published kinetics for the dehydrogenation of ethylbenzene and there is, therefore, a need for more reliable kinetic data. It is desirable that this data should be obtained for a commercially available catalyst which could then be used in experimental work.

An economic optimisation of the cyclic reactor system for the dehydrogenation of ethylbenzene would be valuable as this would determine the main cost variables and enable a further assessment of the proposed design procedure to be made. However, it is necessary for up to date costing data to be made available for this to be more than an academic study.

In order to assess the conclusions of this work, an experimental study of the system is clearly required. This would indicate the validity of the assumptions made and show if a more detailed model of the system heat capacity is necessary.

Only an endothermic reaction has been considered in this work, but the proposed cyclic system could also be used for an exothermic reaction. A separate study is required as the constraints on such a system, e.g. control of the hot-spot temperature, are different. The conclusions of Gavalas[11,12], who considered such a system, must be in some doubt owing to the shortcomings in his model and solution method and his assumption of no additional heat capacity in the system.

APPENDIX 1 Summary of Kinetic Models for the Dehydrogenation of Ethylbenzene

The various reactions which are proposed in the dehydrogenation of ethylbenzene are given in Table A1.1. As well as the dehydrogenation reaction (reaction 1), all authors consider the benzene and toluene producing reactions (reactions 2 and 3). However, there are differences in the choices of further side-reactions considered by different authors.

Table A1.2 shows the rate expressions quoted for the various reactions. The subscript on the rate refers to the reaction number in Table A1.1. The rate constants proposed by various authors are given in Table A1.3 which also shows which reactions are considered by each author. The subscript on the rate constant refers to the reaction number in Table A1.1, and the number of the rate expression in Table A1.2 with which it is used is also given.

Reaction No.			
1	$C_6H_5C_2H_5$	$\rightleftharpoons$	$C_6H_5C_2H_3 + H_2$
2	$C_6H_5C_2H_5$	$\longrightarrow$	$C_6H_6 + C_2H_4$
3	$C_6H_5C_2H_5 + H_2$	$\longrightarrow$	$C_6H_5CH_3 + CH_4$
4	$\frac{1}{2}C_2H_4 + H_2O$	$\longrightarrow$	$CO + 2H_2$
5	$CH_4 + H_2O$	$\longrightarrow$	$CO + 3H_2$
6	$CO + H_2O$	$\longrightarrow$	$CO_2 + H_2$
7	C_2H_4	$\longrightarrow$	$C_2H_2 + H_2$
8	C_2H_2	$\longrightarrow$	$2C + H_2$
9	$C + 2H_2O$	$\longrightarrow$	$CO_2 + 2H_2$
10	CH_4	$\longrightarrow$	$C + 2H_2$
11	$C_6H_5C_2H_5 + 16H_2O$	$\longrightarrow$	$8CO_2 + 21H_2$

Table A1.1: Reactions Proposed in the Dehydrogenation of Ethylbenzene.

Rate Expression No.	
1a	$r_1 = k_1(p_{EB} - p_H p_{ST}/K_p)$
2a	$r_2 = k_2\ p_{EB}$
3a	$r_3 = k_3\ p_{EB} p_H$
1b	$r_1 = k_1 \dfrac{(p_{EB} - p_H p_{ST}/K_p)}{\alpha + p_{EB} + \beta p_{ST}}$
2b	$r_2 = k_2 \dfrac{p_{EB}}{\alpha + p_{EB} + \beta p_{ST}}$
3b	$r_3 = k_3 \dfrac{p_{EB}}{\alpha + p_{EB} + \beta p_{ST}}$
3c	$r_3 = k_3 \dfrac{p_{EB}\ p_H}{\alpha + p_{EB} + \beta p_{ST}}$
4	$r_4 = k_4\ p_{STM}\ (p_{C_2H_4})^{\frac{1}{2}}$
5a	$r_5 = k_5\ p_{STM}\ p_{CH_4}$
6	$r_6 = k_6 \dfrac{P}{T^3}\ p_{STM}\ p_{CO}$
5b	$r_5 = k_5\ p_{CH_4}$
7	$r_7 = k_7\ p_{C_2H_4}$
8	$r_8 = k_8\ p_{C_2H_2}$
9	$r_9 = k_9(p_{STM})^2$
10	$r_{10} = k_{10}\ p_{CH_4}$
11	$r_{11} = k_{11}\ p_{EB}$

Table A1.2: Rate Expressions for Reactions in the Dehydrogenation of Ethylbenzene.

Rate Expression No.	
	Wenner and Dybdal[19]
1a	$\log_{10} k_1 = - \frac{4770}{T} + 4.10$
	Modell[32]
1b	$k_1 = 3.032 \times 10^6 \exp(-23050/T)$
2b	$k_2 = 2.484 \times 10^6 \exp(-25566/T)$
3b	$k_3 = 0.1796 \exp(-10971/T)$
	Sheel and Crowe[17]
1a	$k_1 = \exp(8.1033 - 10925/T)/3600$
2a	$k_2 = \exp(13.2392 - 25000/T)$
3a	$k_3 = \exp(0.2961 - 11000/T)$
4	$k_4 = \exp(-0.0724 - 12500/T)$
5a	$k_5 = \exp(-2.9344 - 7900/T)$
6	$k_6 = \exp(21.2402 - 8850/T)$
	Davidson and Shah[18]
1a	$k_1 = \exp(-6.16 - 5717/T)$
2a	$k_2 = \exp(12.8 - 25600/T)$
3a	$k_3 = \exp(-1.8 - 11000/T)$
5b	$k_5 = \exp(-3.36 - 7900/T)$
6	$k_6 = \exp(3.80 - 8850/T)$
7	$k_7 = 2.15 \times 10^{11} \exp(-38000/T)/T$
8	$k_8 = 1.18 \times 10^9 \exp(-30950/T)/T$
9	$k_9 = 1.11 \times 10^5 \exp(-34000/T)$
	Abet et al[31]
1a	$k_1 = 5.33 \times 10^7 \exp(-9402/T)$
2a	$k_2 = 1.425 \times 10^7 \exp(-10287/T)$

Rate Expression No.	
3a	$k_3 = 2.30 \times 10^7 \exp(-8613/T)$
10	$k_{10} = 3.97 \times 10^{11} \exp(-12724/T)$
	Eckert et al[33]
1a	$k_1 = \exp(-3.6118 - 15128.9/T - 0.0345 \times SR_W - 8.7126/SR_W) \times 101325$
2a	$k_2 = \exp(-3.2823 - 18722.5/T - 0.0323 \times SR_W - 9.220/SR_W) \times 101325$
3a	$k_3 = \exp(-9.3195 - 20090.4/T + 0.0325 \times SR_W - 11.6172/SR_W) \times 101325^2$
11	$k_{11} = \exp(-3.8475 - 19111.7/T - 0.0076 \times SR_W \quad 7.5281/SR_W) \times 101325$
	Derived Kinetics (Chapter 6)
1b	$k_1 = 3.032 \times 10^6 \exp(-23050/T)$
2b	$k_2 = \exp(8.132 - 20336/T)$
3c	$k_3 = \exp(11.109 - 18820/T)$

Table A1.3: Rate Constants for the Reactions in Table A1.1 and the Rate Expressions in Table A1.2.

APPENDIX 2: Method of Characteristics for the Transient Film Resistance Reactor Model

The method of characteristics[94,96] is suitable for hyperbolic partial differential equations such as the Eulerian form of the model given in equations 3.15 - 3.18. The characteristic directions $(\frac{dz}{dt})$, along which the partial differential equations become ordinary differential ones, are first determined. The equations to be solved along these characteristics are then derived.

The heat balances for the model are

$$\frac{\partial T}{\partial t} = -\frac{u}{e}\frac{\partial T}{\partial z} - \frac{S_v h}{e\rho_g C_{pg}}(T - T_s) \qquad (3.16)$$

$$\frac{\partial T_s}{\partial t} = \frac{S_v h}{(1-e)\rho_s C_{ps}}(T - T_s) - \frac{1}{C_{ps}}\sum_j \Delta H_j r_j \qquad (3.18)$$

The differentials can also be expressed as

$$dT = \frac{\partial T}{\partial t}dt + \frac{\partial T}{\partial z}dz \qquad (A2.1)$$

$$dT_s = \frac{\partial T_s}{\partial t}dt + \frac{\partial T_s}{\partial z}dz \qquad (A2.2)$$

and these four equations, in matrix form, are

$$\begin{bmatrix} 1 & \frac{u}{e} & 0 & 0 \\ 0 & 0 & 1 & 0 \\ dt & dz & 0 & 0 \\ 0 & 0 & dt & dz \end{bmatrix} \begin{bmatrix} \frac{\partial T}{\partial t} \\ \frac{\partial T}{\partial z} \\ \frac{\partial T_s}{\partial t} \\ \frac{\partial T_s}{\partial z} \end{bmatrix} = \begin{bmatrix} -\frac{S_v h}{e\rho_g C_{pg}}(T - T_s) \\ \frac{S_v h}{(1-e)\rho_s C_{ps}}(T - T_s) - \frac{1}{C_{ps}}\sum_j \Delta H_j r_j \\ dT \\ dT_s \end{bmatrix} \qquad (A2.3)$$

The characteristic equation is obtained by setting to zero the determinant of the 4 x 4 matrix. This gives

$$dz^2 - dt\, dz \frac{u}{e} = 0 \qquad (A2.4)$$

and hence

$$\left(\frac{dz}{dt}\right)^2 - \frac{u}{e}\frac{dz}{dt} = 0 \qquad (A2.5)$$

The characteristic directions are the solutions of this equation, which are

$$\left.\frac{dz}{dt}\right|_{I} = \frac{u}{e} \qquad (4.18)$$

and

$$\left.\frac{dz}{dt}\right|_{II} = 0 \qquad (4.19)$$

Ames[94] shows that the equations to be solved along the characteristics are obtained by replacing columns in the 4 x 4 matrix by the right hand column vector in equation A2.3 and equating the determinant of the matrix to zero. Replacing the first column gives

$$\begin{vmatrix} -\frac{S_v h}{e\rho_g C_{pg}}(T - T_s) & \frac{u}{e} & 0 & 0 \\ \frac{S_v h}{(1-e)\rho_s C_{ps}}(T - T_s) - \frac{1}{C_{ps}}\sum_j \Delta H_j r_j & 0 & 1 & 0 \\ dT & dz & 0 & 0 \\ dT_s & 0 & dt & dz \end{vmatrix} = 0 \qquad (A2.6)$$

and hence

$$dz^2 \frac{S_v h}{e\rho_g C_{pg}}(T - T_s) + dT\, dz \frac{u}{e} = 0 \qquad (A2.7)$$

Along the characteristic $\left.\frac{dz}{dt}\right|_{II}$, dz is zero and, hence, equation A2.7 only has meaning along $\left.\frac{dz}{dt}\right|_{I}$. Rearranging this gives:

$$\frac{dT}{dz} = -\frac{S_v h}{u\rho_g C_{pg}}(T - T_s) \qquad (A2.8)$$

Replacing the last column in the matrix by the column vector gives:

$$\begin{vmatrix} 1 & \frac{u}{e} & 0 & -\frac{S_v h}{e \rho_g C_{pg}} \\ 0 & 0 & 1 & \frac{S_v h}{(1-e)\rho_s C_{ps}} (T - T_s) - \frac{1}{C_{ps}} \sum_j \Delta H_j r_j \\ dt & dz & 0 & dT \\ 0 & 0 & dt & dT_s \end{vmatrix} = 0 \tag{A2.9}$$

which becomes

$$\left[\frac{S_v h}{(1-e)\rho_s C_{ps}} (T - T_s) - \frac{1}{C_{ps}} \sum_j \Delta H_j r_j\right] (\frac{dz}{dt} - \frac{u}{e}) - \frac{\partial T_s}{dt} (\frac{dz}{dt} - \frac{u}{e}) = 0 \tag{A2.10}$$

This is meaningless along $\left.\frac{dz}{dt}\right|_I$ as all terms are zero and only applies along $\left.\frac{dz}{dt}\right|_{II}$. Substituting for $\frac{dz}{dt}$ by equation 4.19,

$$\frac{\partial T_s}{dt} = \frac{S_v h}{(1-e)\rho_s C_{ps}} (T - T_s) - \frac{1}{C_{pg}} \sum_j \Delta H_j r_j \tag{A2.11}$$

A similar procedure is carried out for the mass balances and, as the coefficients with the derivatives are identical to those in the heat balances, the characteristic directions are the same. It is clear that the mass balances along the characteristics are

$$\frac{dc_i}{dt} = -\frac{S_v k_g}{u} (c_i - c_{si}) \tag{A2.12}$$

along $\left.\frac{dz}{dt}\right|_I$, and

$$\frac{dc_{si}}{dt} = \frac{S_v k_g}{(1-e)e_p} (c_i - c_{si}) + \frac{\rho_s}{e_p} \sum_j a_{i,j} r_j \tag{A2.13}$$

along the characteristic $\left.\frac{dz}{dt}\right|_{II}$.

APPENDIX 3: Fourier Series Method for the Stability of the Regenerator Equations

This method of investigating the stability of finite difference approximations for linear partial differential equations is described by Fox[95] and Smith[97]. The stability criterion is established by examining the propagation of a line of errors which are represented by a finite Fourier series. Using the finite difference nomenclature of Chapter 4, the error (E) at the point (m,n) is

$$E(m,n) = e^{ibz} e^{at} = e^{ibm\Delta z} \xi^{n} \tag{A3.1}$$

where $i = \sqrt{-1}$ and a and b are constants. Then, to avoid an increasing error with time, it is necessary that

$$\left| \xi \right| \leqslant 1 \tag{A3.2}$$

for all real values of b.

A3.1 Pseudo-homogeneous Model

The pseudo-homogeneous regenerator model is

$$\frac{\partial \overline{T}}{\partial t} = - \frac{\overline{u}\, \overline{\rho}_{g}\, \overline{C}_{pg}}{(1-e)\rho_{s} C_{ps}} \frac{\partial \overline{T}}{\partial z} \tag{3.29}$$

Forward difference approximations for both derivatives give

$$\overline{T}(m,n+1) - \overline{T}(m,n) = -Q(\overline{T}(m+1,n) - \overline{T}(m,n)) \tag{A3.3}$$

$$\text{where } Q = \frac{\Delta t\, \overline{u}\, \overline{\rho}_{g}\, \overline{C}_{pg}}{\Delta z\,(1-e)\rho_{s}\, C_{ps}} \tag{A3.4}$$

Replacing the temperatures by the errors at each point gives

$$e^{ibm\Delta z} \xi^{(n+1)} - e^{ibm\Delta z} \xi^{n} = -Q(e^{ib(m+1)\Delta z} \xi^{n} - e^{ibm\Delta z} \xi^{n}) \tag{A3.5}$$

Dividing through by $e^{ibm\Delta z} \xi^{n}$,

$$\xi - 1 = -Q(e^{ib\Delta z} - 1) \qquad (A3.6)$$

and hence

$$\xi = 1 - Q(e^{ib\Delta z} - 1) \qquad (A3.7)$$

This finite difference scheme will therefore be stable if

$$0 \leqslant Q(e^{ib\Delta z} - 1) \leqslant 2 \qquad (A3.8)$$

The left hand inequality is always satisfied as Q is positive and $e^{ib\Delta z}$ is greater than 1. However, the right hand inequality satisfies equation A3.2 only if

$$(e^{ib\Delta z} - 1) \leqslant \frac{2}{Q} \qquad (A3.9)$$

and hence the scheme may be unstable if the error is large. If the size of the error is fixed, the stability depends on Q and therefore on the step sizes. This scheme is therefore conditionally stable as it is not stable for all values.

Using a backward difference for both derivatives, the scheme is

$$\overline{T}(m,n) - \overline{T}(m,n-1) = -Q(\overline{T}(m,n) - \overline{T}(m-1,n)) \qquad (A3.10)$$

and hence

$$e^{ibm\Delta z}\,\xi^{n} - e^{ibm\Delta z}\,\xi^{(n-1)} = -Q(e^{ibm\Delta z}\,\xi^{n} - e^{ib(m-1)\Delta z}\,\xi^{n}) \qquad (A3.11)$$

This gives $$\xi = \frac{1}{1 + Q(1 - e^{-ib\Delta z})} \qquad (A3.12)$$

This satisfies equation A3.2 as Q and $(1 - e^{-ib\Delta z})$ are always positive and this scheme is therefore stable for all values.

A3.2 Film Resistance Model

This model contains two variables, $\overline{T}$ and $\overline{T}_s$, and there will be errors associated with each. These errors will be of the same form and hence the error associated with $\overline{T}$ is

$$E(m,n) = A\,e^{ibm\Delta z}\,\xi^{n} \qquad (A3.13)$$

and that associated with $\overline{T}_s$ is

$$E_s(m,n) = Be^{ibm\Delta z}\,\xi^n \qquad (A3.14)$$

A3.2.1 Lagrangian Equations

The Lagrangian regenerator representation is

$$\frac{\partial \overline{T}}{\partial z} = -\frac{S_v\,\overline{h}}{\overline{u}\,\overline{\rho}_g\,\overline{C}_{pg}}(\overline{T} - \overline{T}_s) \qquad (4.9)$$

$$\frac{\partial \overline{T}_s}{\partial \theta} = \frac{S_v\,\overline{h}}{(1-e)\rho_s C_{ps}}(\overline{T} - \overline{T}_s) \qquad (4.10)$$

The forward difference approximation for equation 4.9 is

$$\overline{T}(m+1,n) - \overline{T}(m,n) = -Q1(\overline{T}(m,n) - \overline{T}_s(m,n)) \qquad (A3.15)$$

$$\text{where } Q1 = \frac{\Delta z\,S_v\,\overline{h}}{\overline{u}\,\overline{\rho}_g\,\overline{C}_{pg}} \qquad (A3.16)$$

Replacing the temperatures by the errors gives

$$Ae^{ib(m+1)\Delta z}\,\xi^n - Ae^{ibm\Delta z}\,\xi^n = -Q1(Ae^{ibm\Delta z}\,\xi^n - Be^{ibm\Delta z}\,\xi^n) \qquad (A3.17)$$

$$\text{and hence } \frac{A}{B} = \frac{Q1}{e^{ib\Delta z} - 1 + Q1} \qquad (A3.18)$$

The forward difference approximation for equation 4.10 gives

$$\overline{T}_s(m,n+1) - \overline{T}_s(m,n) = Q2(\overline{T}(m,n) - \overline{T}_s(m,n)) \qquad (A3.19)$$

$$\text{where } Q2 = \frac{\Delta\theta S_v\,\overline{h}}{(1-e)\rho_s C_{ps}} \qquad (A3.20)$$

Hence

$$Be^{ibm\Delta z}\,\xi^{(n+1)} - Be^{ibm\Delta z}\,\xi^n = Q2(Ae^{ibm\Delta z}\,\xi^n - Be^{ibm\Delta z}\,\xi^n) \qquad (A3.21)$$

$$\text{and } \frac{A}{B} = \frac{\xi - 1 + Q2}{Q2} \qquad (A3.22)$$

Equating 3.18 and 3.22,

$$\xi = 1 - \frac{Q2(e^{ib\Delta z} - 1)}{Q1 + (e^{ib\Delta z} - 1)} \qquad (A3.23)$$

and this scheme is stable if

$$0 \leqslant \frac{Q2(e^{ib\Delta z} - 1)}{Q1 + (e^{ib\Delta z} - 1)} \leqslant 2 \qquad (A3.24)$$

All the terms are positive and hence the left hand inequality is satisfied. The right hand inequality may, or may not, be satisfied depending on the size of the error and the values of Q1 and Q2. This is therefore conditionally stable.

If backward difference approximations are used for both derivatives, then

$$\xi = \frac{1}{1 + \frac{Q2(1-e^{-ib\Delta z})}{Q1 + (1-e^{-ib\Delta z})}} \qquad (A3.25)$$

which is always stable as all the terms are positive.

A3.2.2 Eulerian Equations

The analysis of the stability of the finite difference forms of the Eulerian equations is more complex as the equation for ξ is quadratic. Using forward difference approximations,

$$\xi = 1 - \frac{Q \pm \sqrt{Q^2 + 4Q1\ Q3(e^{ib\Delta z} - 1)}}{2} \qquad (A3.26)$$

where $Q = Q2 + Q3 + Q1(e^{ib\Delta z} - 1)$ (A3.27)

$$Q1 = \frac{\Delta t\ \bar{u}}{\Delta z e} \qquad (A3.28)$$

$$Q2 = \frac{\Delta t\ S_v\ \bar{h}}{e\ \bar{\rho}_g\ \bar{C}_{pg}} \qquad (A3.29)$$

$$Q3 = \frac{\Delta t\ S_v\ \bar{h}}{(1-e)\rho_s C_{ps}} \qquad (A3.30)$$

Hence for stability,

$$0 \leqslant Q \pm \sqrt{Q^2 + 4Q1\,Q3(e^{ib\Delta z} - 1)} \leqslant 2 \qquad (A3.31)$$

The square root term must be greater than Q, and hence the left hand inequality will be violated if it is subtracted from Q as all terms are positive. The right hand inequality could be satisfied with suitable coefficient and step size values and a small error. This scheme is therefore conditionally stable, but it is found to be always unstable with typical coefficient values.

The use of backward difference approximations gives

$$\xi = \frac{2}{2 + Q \pm \sqrt{Q^2 - 4Q3Q1(1-e^{-ib\Delta z})}} \qquad (A3.32)$$

where $Q = Q2 + Q3 + Q1(1-e^{-ib\Delta z})$ (A3.33)

This is always stable if the square root term is positive. This can be shown to be the case if Q2 is greater than Q3, which equations A3.29 and A3.30 show is always true.

APPENDIX 4: Solution of the Transient Film Resistance Model

It was concluded in Chapter 4 that the Lagrangian form of the model should be employed and solved by the use of backward and central difference approximations for the time and length derivatives respectively.

A4.1 Reactor Equations

Consider first the fluid phase mass balance

$$\frac{\partial c_i}{\partial z} = -\frac{S_v k_g}{u}(c_i - c_{si}) \tag{4.3}$$

The finite difference representation is

$$\frac{c_i(m,n) - c_i(m-1,n)}{\Delta z} = -\frac{S_v k_g}{2u}\Big[c_i(m,n) + c_i(m-1,n) - c_{si}(m.n) - c_{si}(m-1,n)\Big] \tag{A4.1}$$

which can be rearranged as

$$c_i(m,n) = A1\ c_i(m-1,n) + A2\Big[c_{si}(m,n) + c_{si}(m-1,n)\Big] \tag{A4.2}$$

where
$$A1 = \frac{1 - \dfrac{\Delta z\ S_v\ k_g}{2u}}{1 + \dfrac{\Delta z\ S_v\ k_g}{2u}} \tag{A4.3}$$

and
$$A2 = \frac{\dfrac{\Delta z\ S_v\ k_g}{2u}}{1 + \dfrac{\Delta z\ S_v\ k_g}{2u}} \tag{A4.4}$$

Similarly, the fluid phase heat balance,

$$\frac{dT}{dz} = -\frac{S_v\ h}{u\rho_g\ C_{pg}}(T - T_s) \tag{4.4}$$

becomes

$$T(m,n) = B1\ T(m-1,n) + B2\Big[T_s(m,n) + T_s(m-1,n)\Big] \tag{A4.5}$$

where
$$B1 = \frac{1 - \dfrac{\Delta z\ S_v\ h}{2u\rho_g\ C_{pg}}}{1 + \dfrac{\Delta z\ S_v\ h}{2u\rho_g\ C_{pg}}} \tag{A4.6}$$

$$\text{and } B2 = \frac{\dfrac{\Delta z\, S_v\, h}{2u\rho_g\, C_{pg}}}{1 + \dfrac{\Delta z\, S_v\, h}{2u\rho_g C_{pg}}} \qquad (A4.7)$$

The solid phase mass balance is

$$\frac{\partial c_{si}}{\partial \theta} = \frac{S_v\, k_g}{(1-e)e_p}(c_i - c_{si}) + \frac{\rho_s}{e_p}\sum_j a_{i,j}\, r_j \qquad (4.5)$$

and the finite difference representation is

$$\frac{c_{si}(m,n) - c_{si}(m,n-1)}{\Delta\theta} = \frac{S_v\, k_g}{(1-e)e_p}\left[c_i(m,n) - c_{si}(m,n)\right] + \frac{\rho_s}{e_p}\sum_j a_{i,j} r_j(m,n) \qquad (A4.8)$$

Substituting for $c_i(m,n)$ from A4.2 and rearranging gives

$$c_{si}(m,n) = C1\; c_{si}(m,n-1) + C2\; c_{si}(m-1,n) + C3\; c_i(m-1,n) + C4\, \Sigma_j\; a_{i,j}\; r_j(m,n) \qquad (A4.9)$$

$$\text{where } C1 = \frac{1}{1 + \dfrac{\Delta\theta\, S_v\, k_g}{(1-e)e_p}(1 - A2)} \qquad (A4.10)$$

$$C2 = A2\; C1\; \frac{\Delta\theta\, S_v\, k_g}{(1-e)e_p} \qquad (A4.11)$$

$$C3 = A1\; C1\; \frac{\Delta\theta\, S_v\, k_g}{(1-e)e_p} \qquad (A4.12)$$

$$\text{and} \quad C4 = C1\, \frac{\Delta\theta\, \rho_s}{e_p} \qquad (A4.13)$$

Similarly the solid phase heat balance

$$\frac{\partial T_s}{\partial \theta} = \frac{S_v\, h}{(1-e)\rho_s C_{ps}}(T - T_s) - \frac{1}{C_{ps}}\sum_j \Delta H_j\, r_j \qquad (4.6)$$

becomes

$$T_s(m,n) = D1\; T_s(m,n-1) + D2\; T_s(m-1,n) + D3\; T(m-1,n) - D4\sum_j \Delta H_j\; r_j(m,n) \qquad (A4.14)$$

where $$D1 = \frac{1}{1 + \frac{\Delta\theta S_v h}{(1-e)\rho_s C_{ps}}(1-B2)} \qquad (A4.15)$$

$$D2 = B2\ D1 \frac{\Delta\theta\ S_v\ h}{(1-e)\rho_s C_{ps}} \qquad (A4.16)$$

$$D3 = B1\ D1 \frac{\Delta\theta\ S_v\ h}{(1-e)\rho_s\ C_{ps}} \qquad (A4.17)$$

$$D4 = D1 \frac{\Delta\theta}{C_{ps}} \qquad (A4.18)$$

The solid phase equations must be solved simultaneously by an iterative procedure as the rate term is a non-linear function of both temperature and concentration. In order to reduce the amount of computation at each iteration, equations A4.9 and A4.14 are written as

$$c_{si}(m,n) = C5 + C4 \sum_j a_{i,j}\ r_j(m,n) \qquad (A4.19)$$

$$T_s(m,n) = D5 - D4 \sum_j \Delta H_j\ r_j(m,n) \qquad (A4.20)$$

where C5 and D5 contain the terms from previous integration steps and are evaluated before the equations are iterated. Equations A4.19 and A4.20 are solved by repeated substitution as this method was found to give the quickest solution. It is convenient to normalise the temperature and concentration as this gives residuals of comparable magnitude when the convergence of the iteration is tested. The temperature is divided by a reference value, which may be the inlet temperature, and the concentration by the inlet ethylbenzene concentration. The normalised styrene concentration then represents the conversion.

The coefficients C4 and D4 now become

$$C4 = C1 \frac{\Delta\theta\ \rho_s}{e_p\ C_{EBo}} \qquad (A4.21)$$

$$D4 = D1 \frac{\Delta \theta}{C_{ps} T_{IN}} \qquad (A4.22)$$

When the solid phase temperature and concentration have been evaluated, these can be substituted into equations A4.2 and A4.5 to give the fluid values.

A4.2 Regenerator Equations

Following the above procedure, the regenerator equations

$$\frac{\partial \bar{T}}{\partial z} = - \frac{S_v \bar{h}}{\bar{u} \bar{\rho}_g \bar{C}_{pg}} (\bar{T} - \bar{T}_s) \qquad (4.9)$$

$$\frac{\partial \bar{T}_s}{\partial \theta} = \frac{S_v \bar{h}}{(1-e) \rho_s C_{ps}} (\bar{T} - \bar{T}_s) \qquad (4.10)$$

become

$$\bar{T}(m,n) = E1 \; \bar{T}(m-1,n) + E2 \; (\bar{T}_s(m.n) + \bar{T}_s(m-1,n)) \qquad (A4.23)$$

$$\bar{T}_s(m,n) = F1 \; \bar{T}_s(m,n-1) + F2 \; \bar{T}_s(m-1,n) + F3 \; \bar{T}(m-1,n) \qquad (A4.24)$$

where the coefficients are identical to those given above for the corresponding reactor heat balances except that the barred parameters are used. These equations are explicit if equation A4.24 is solved before A4.23. In order to be consistent with the reactor equations, the temperatures are again normalised.

A4.3 Subroutine TM1SC

The above equations are solved for the cyclic reactor system model program in the subroutine TM1SC which is listed in Appendix 7. The subroutine is first called with the argument IENT set to 1 in order to calculate the coefficients A1 - F3. During the reactor period, it is called with IENT = 2 and the reactor equations are solved for each point along the bed. Similarly, with IENT = 3, the regenerator equations are solved along the bed.

APPENDIX 5

EFFECT OF WALL HEAT CAPACITY IN A PILOT SCALE REACTOR

Experimental reactors are necessarily smaller than those used in commercial processes. The heat capacity of the reactor wall will therefore have a much greater effect on the transient response. The norm bed size and conditions defined in Chapter 6 are those for a pilot scale reactor to be used in experimental work which will complement this research. The actual size is not important in a computer model as the wall effects are ignored and the small catalyst bed may be considered as part of a larger one.

The heat losses from such a reactor are minimised by the use of a layer of insulating material around the outside of the wall, but this does not remove the effect of the wall heat capacity. However, it is proposed to reduce this effect by a layer of ceramic paper between the catalyst and the inside reactor wall, which reduces the heat transfer between them. A section of the wall and insulation is shown in Figure A5.1.

The heat capacity of the insulation is ignored as it is only about $^1/2000$ of that of the wall, and the radial thermal conductivity of the wall is assumed to be infinite. The heat balance on the wall is then

$$\frac{\partial T_W}{\partial t} = \frac{2U_I\,(R - z_I)\,(T - T_W) - 2U_o(R + z_W + z_o)\,\Delta T_o}{\rho_W\, C_{pw}\,(2Rz_W + z_W^2)} + \frac{k_W}{\rho_W C_{pw}}\,\frac{\partial^2 T_W}{\partial z^2} \qquad (A5.1)$$

where T_W is the wall temperature and ΔT_o is the temperature difference between the wall and the surroundings. U_I and U_o are the overall heat transfer coefficients on the inside and outside of the wall respectively and U_I is given by

$$U_I = \frac{1}{\frac{1}{h} + \frac{z_I}{k_I}} \qquad (A5.2)$$

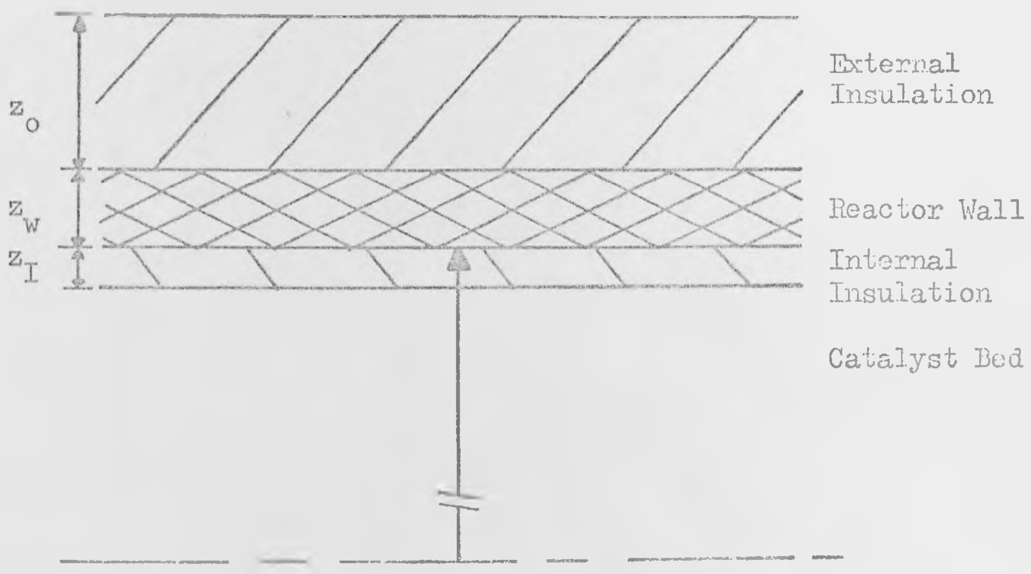
z_o
z_w
z_I
External Insulation
Reactor Wall
Internal Insulation
Catalyst Bed

Figure A5.1: Section of Reactor Wall Showing External and Internal Insulation.

$z_w = 3.2$ mm

$\rho_w = 7.817$ kg l^{-1}

$C_{pw} = 0.4605$ kJ kg^{-1} °C^{-1}

$k_w = 20.77$ W m^{-1} °C^{-1}

$z_I = 2.0$ mm

$k_I = 0.0685$ W m^{-1} °C^{-1}

$z_o = 0.089$ m

$U_o = 0.685$ W m^{-2} °C^{-1}

$\Delta T_o = 600$°C.

Table A5.1: Parameters Used in Study of Wall Effect.

To simplify the solution, adiabatic boundary conditions, where no heat flows past the end of the wall, are assumed. These are

$$\frac{\partial T_w}{\partial z} = 0 \quad \text{at } z = 0 \text{ and } z = Z \text{ for } t \geqslant 0 \tag{A5.3}$$

and the initial condition is

$$T_w = f(z) \quad \text{at } z \geqslant 0 \text{ for } t = 0 \tag{A5.4}$$

Ignoring the thickness of the internal insulation and any radial temperature gradient, the fluid phase heat balance is

$$\frac{\partial T}{\partial t} = -\frac{u}{e}\frac{\partial T}{\partial z} - \frac{S_v h}{e \rho_g C_{pg}}(T - T_s) - \frac{2U_I}{Re \rho_g C_{pg}}(T - T_w) \tag{A5.5}$$

and the solid phase heat balance is equation 3.18 as before.

In order to use a similar solution procedure as described in Appendix 4 for the fluid and solid phase equations, an explicit finite difference formula is used for equation A5.1. A forward difference approximation (equation 4.25) is used for the time derivative and the second order length derivative is approximated by

$$\frac{\partial^2 T_w}{\partial z^2} = \frac{T_w(m+1,n) - 2T_w(m,n) + T_w(m-1,n)}{\Delta z^2} \tag{A5.6}$$

In order to obtain a stable solution, the time step size must not be greater than 0.25 s.

A5.1 Wall Effect in a Transient Regenerator

Using the data in Table A5.1, with the norm bed size and data in Tables 6.4 and 7.4, the effect of the wall heat capacity on the regenerator breakthrough curve is shown in Figure A5.2. This shows the response to a step change in the inlet temperature at t = 0, with an initially isothermal bed and wall. With no internal insulation, the response is slower than when the wall effect is ignored because of the additional heat capacity in the wall. However, when a 2 mm layer of

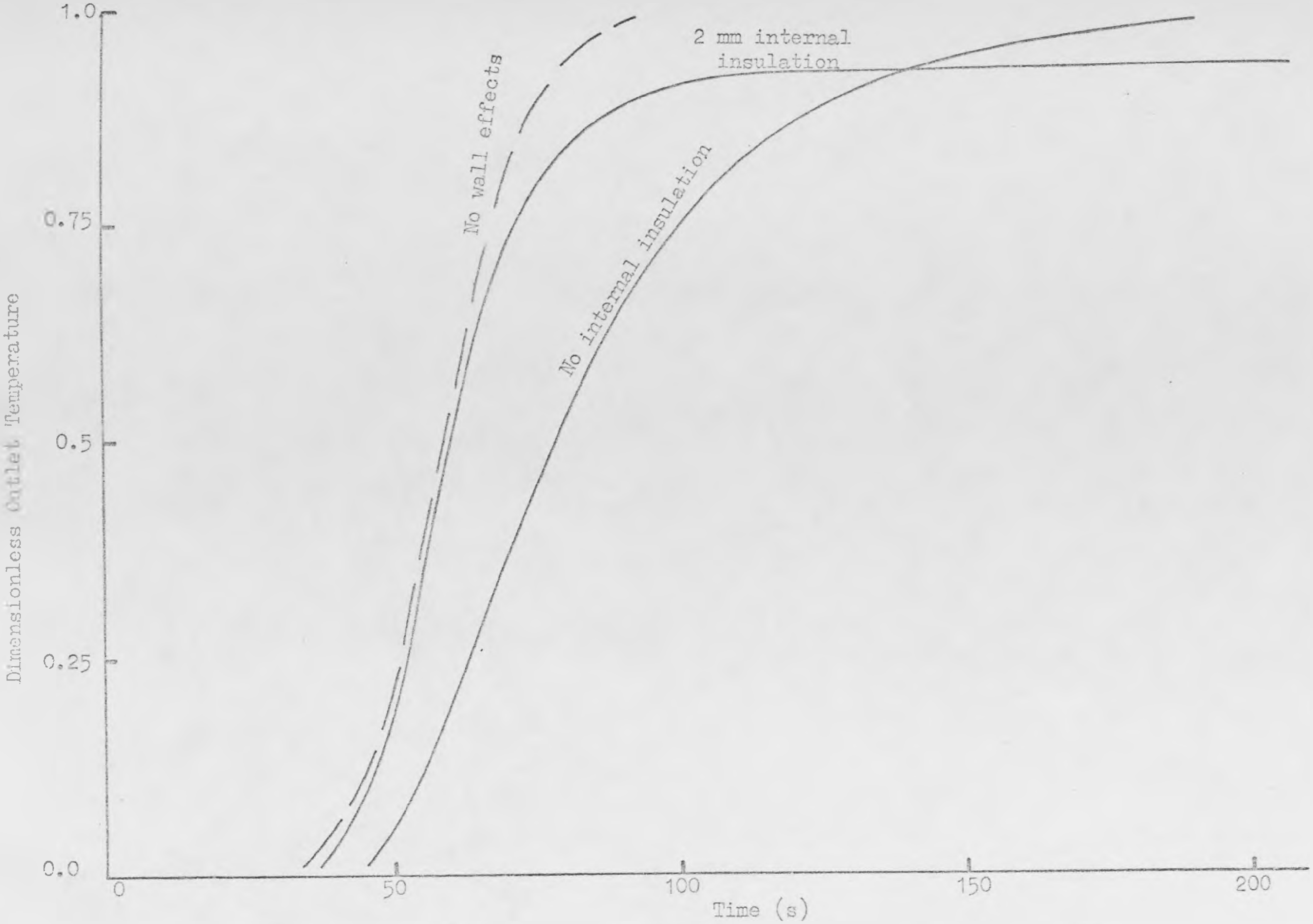

Figure A5.2: Effect of Wall Heat Capacity on Regenerator Breakthrough Curve.

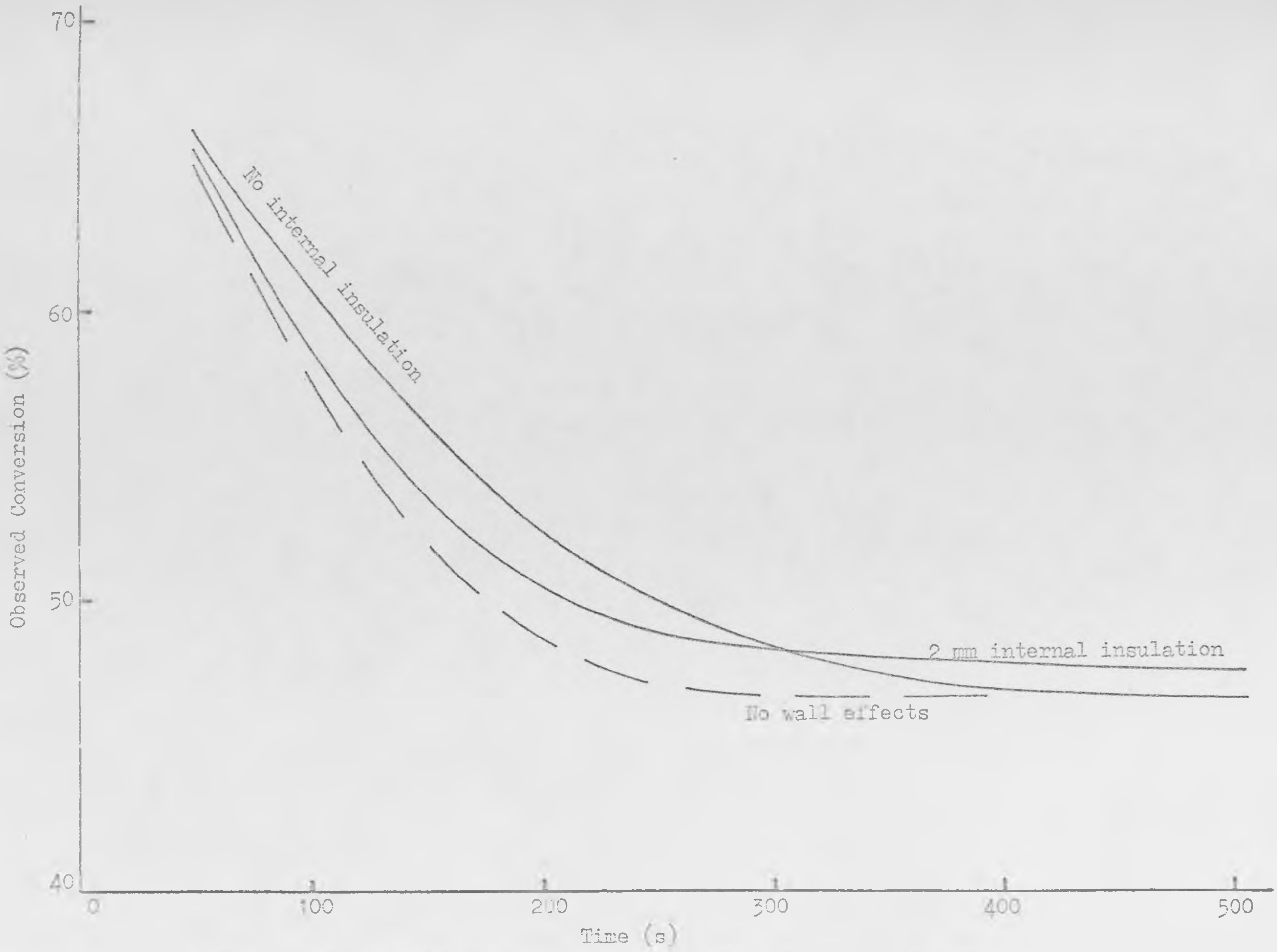

Figure A5.3: Effect of the Reactor Wall on a Transient Reactor.

internal insulation is used, the breakthrough curve follows that for no wall effects until saturation is approached. This is due to the low rate of heat transfer to the wall until the temperature difference between them is large. The actual approach to saturation is very slow because of the resistance to the heat transfer and the decreasing temperature difference.

The conduction of heat along the wall is found to have little effect on the breakthrough curves. If the conduction is ignored, the difference in the time required to reach any point on the curve is changed by less than 1%. A larger time step can then be used and quicker solutions obtained. The effect of the heat loss through the wall is also found to be negligible, except when saturation is very closely approached.

A5.2 Wall Effect in a Transient Reactor

The effect of the wall on the reactor conversion is shown in Figure A5.3 and is as expected from the regenerator study. The response is slower with no internal insulation but a 2 mm layer of internal insulation brings the response close to that with no wall effects after short time intervals. The approach to the steady state is again very slow with the internal insulation and the effect of conduction in the wall is negligible.

A5.3 Wall Effect in a Cyclic Reactor System

The wall heat capacity has little effect on the average conversion from a cyclic reactor system. The regenerator study shows that a less close approach to saturation is achieved during the regenerator period which gives a lower initial reactor temperature profile and has an adverse effect on the conversion. However, this is partially offset by the reduced rate of temperature fall during the reactor period. The average conversion, therefore, only falls from the value of 67.7%, obtained when the wall effects were neglected, to 67.4% with no internal insulation or 67.5% with a 2 mm insulating layer.

The wall has a significant effect on the number of cycles required to reach cyclic steady state operation. This increases from 3 to 5, with no internal insulation, and to 11 with a 2 mm layer.

A5.4 Conclusions

The heat capacity of the wall for a single transient bed, whether a reactor or a heat exchanger, may have a significent effect on performance as the response of the bed is slower. The introduction of a layer of insulation on the inside of the wall reduces this effect considerably as long as the steady state is not approached. Near the steady state, this insulation will cause greater differences in performance. In the cases studied, the conduction along the wall, and the heat loss, are negligible.

However, in a cyclic reactor system, the wall effect is negligible as the effects in alternate periods oppose each other. This need not, therefore, be considered when interpreting experimental results, although the heat capacity of the rest of the system cannot be ignored.

APPENDIX 6: Description of the Cyclic Reactor Model Program - CH3SC

The cyclic reactor system described in Chapter 5 is modelled by the computer program CH3SC, which is written in FORTRAN IV and requires 16 K of core storage. A listing of the program is given in Appendix 7 and this contains a large number of comments to describe its operation. A simple flowsheet, showing the main structure of the program, is given in Figure A6.1 and the more detailed structure of the reactor period calculations is shown in Figure A6.2. The structure of the regenerator period is similar to that of the reactor period except that it may not be interrupted as its calculation is relatively quick.

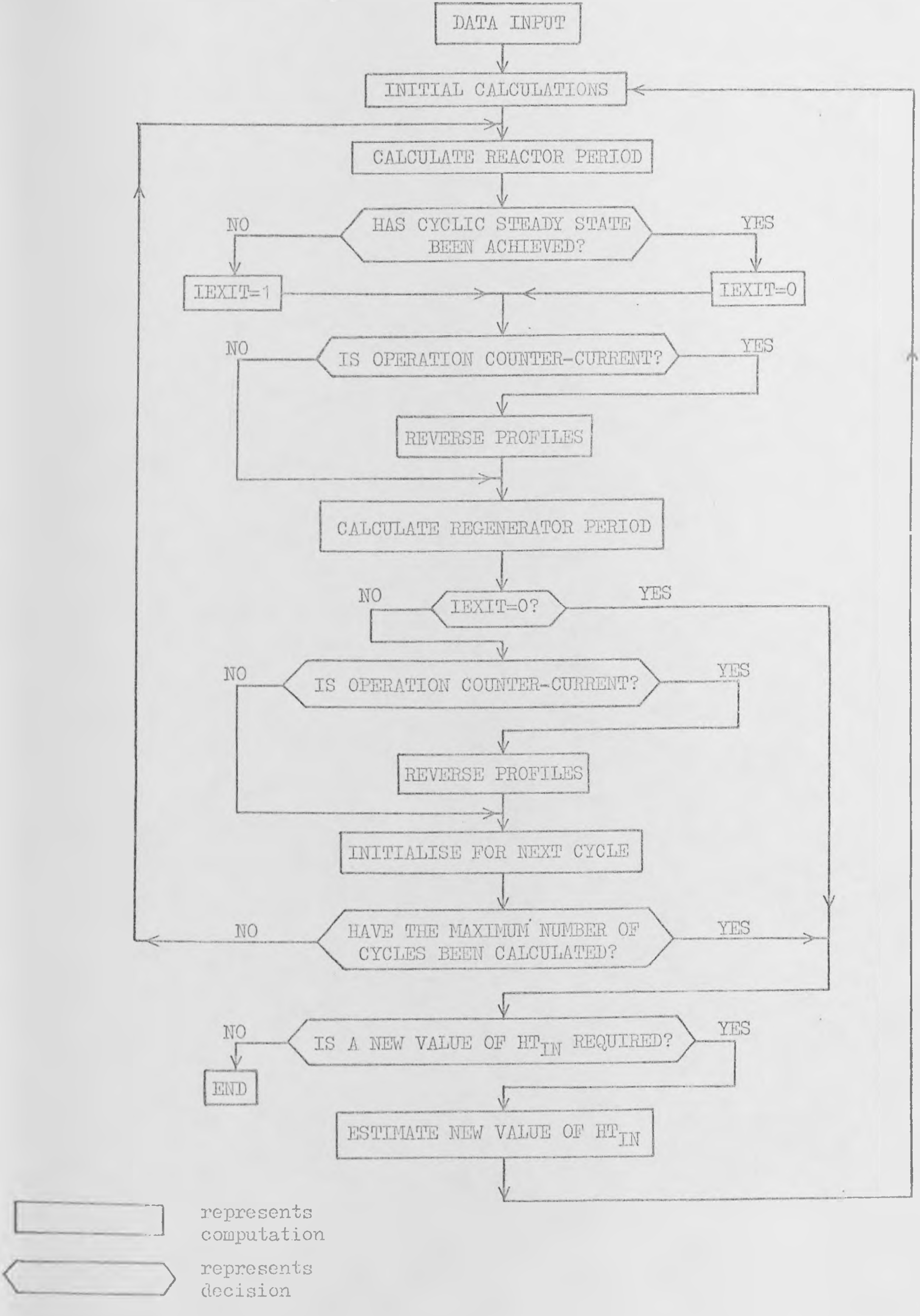
DATA INPUT
INITIAL CALCULATIONS
CALCULATE REACTOR PERIOD
HAS CYCLIC STEADY STATE BEEN ACHIEVED?
NO
YES
IEXIT=1
IEXIT=0
IS OPERATION COUNTER-CURRENT?
NO
YES
REVERSE PROFILES
CALCULATE REGENERATOR PERIOD
IEXIT=0?
NO
YES
IS OPERATION COUNTER-CURRENT?
NO
YES
REVERSE PROFILES
INITIALISE FOR NEXT CYCLE
HAVE THE MAXIMUM NUMBER OF CYCLES BEEN CALCULATED?
NO
YES
IS A NEW VALUE OF HT_{IN} REQUIRED?
NO
YES
END
ESTIMATE NEW VALUE OF HT_{IN}
represents computation
represents decision

Figure A6.1: Flowsheet for the Program CH3SC.

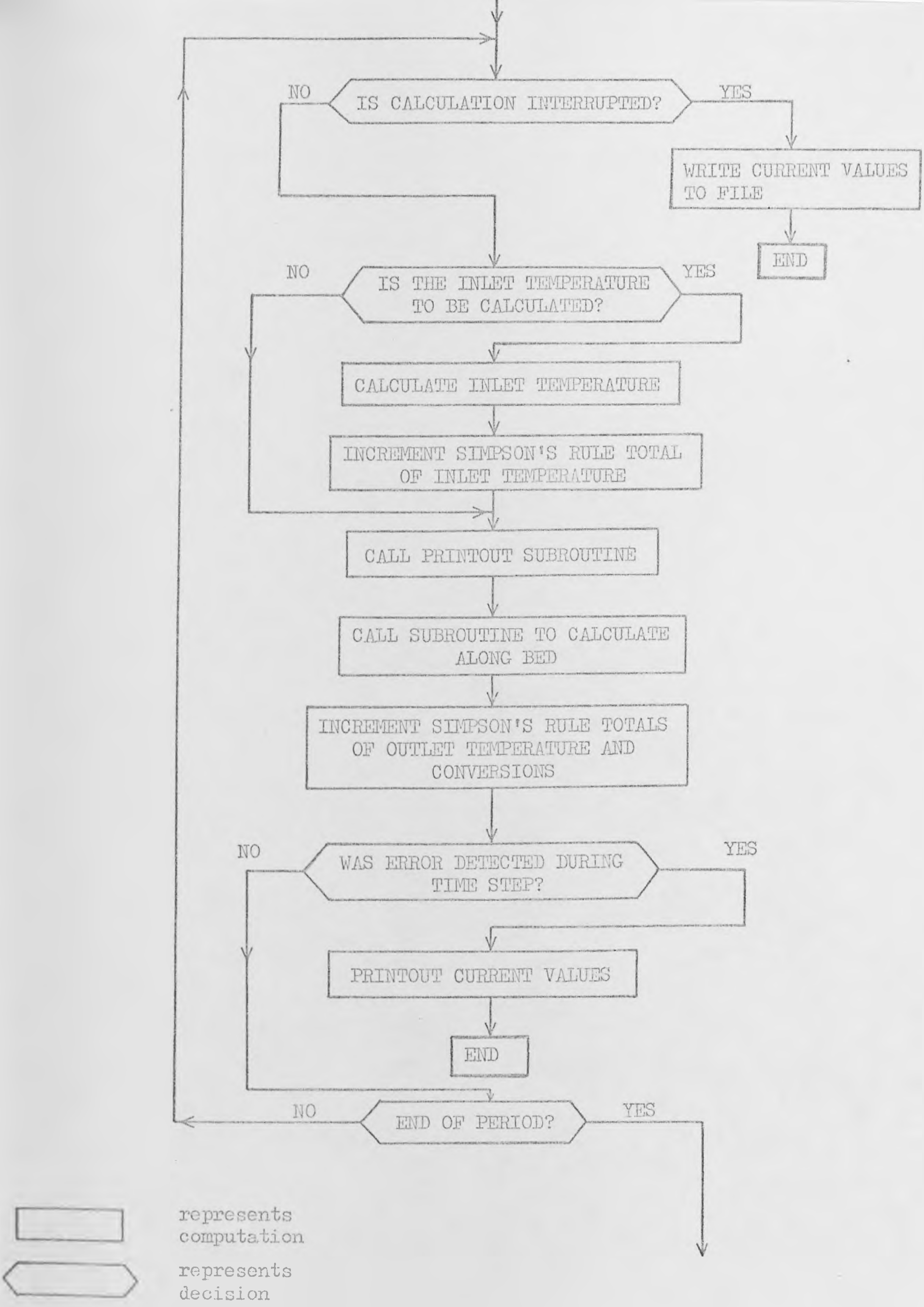
IS CALCULATION INTERRUPTED?
NO
YES
WRITE CURRENT VALUES TO FILE
END
IS THE INLET TEMPERATURE TO BE CALCULATED?
NO
YES
CALCULATE INLET TEMPERATURE
INCREMENT SIMPSON'S RULE TOTAL OF INLET TEMPERATURE
CALL PRINTOUT SUBROUTINE
CALL SUBROUTINE TO CALCULATE ALONG BED
INCREMENT SIMPSON'S RULE TOTALS OF OUTLET TEMPERATURE AND CONVERSIONS
WAS ERROR DETECTED DURING TIME STEP?
NO
YES
PRINTOUT CURRENT VALUES
END
END OF PERIOD?
NO
YES
represents computation
represents decision

Figure A6.2: Flowsheet for Reactor Period of Program CH3SC.

A6.1 Data Input

The data set for the program is as follows, assuming card input, and the format is F10.0 or I10.

Card 1 - Title Card - reproduced on printout.

Card 2

DIAM - Reactor internal diameter (m)

Z - Reactor length (m)

CPS - Bed specific heat (J kg^{-1} °K^{-1})

RS - Particle density (kg m^{-3})

E - Void fraction

PDIAM - Particle diameter (m)

SV - Surface area of catalyst per unit bed volume (m^{2}m^{-3})

Card 3

FEB - Ethylbenzene feed (kg h^{-1})

FSTM - Diluent steam flow (kg h^{-1})

YIN - Reference temperature (°K)

P - Reactor pressure (bar)

RK - Inert fraction of bed

HTIN - Superheater heat load (W)

Card 4

TF - Period time (s)

DT - Time step (s)

NSTEP - Number of length steps

TOL - Tolerance on errors for repeated substitution routine

LIMIT - Maximum number of iterations allowed for repeated substitution and Newton-Raphson calculations.

KSW -)
) Print parameters - defined on program listing
ISW -)

Card 5

RIT - Regenerator inlet temperature if constant
Otherwise maximum value (°K)

RFSTM - Regenerator steam flow (kg h^{-1})

NOC - Maximum number of cycles permitted

STRT - Position of inert region for subroutine TM4SC

A6.2 Output

The input data is reproduced on the printout together with the following variables.

A - Reactor cross-sectional area (m^2)

AKG - Mass transfer coefficient (m s^{-1})

CEB - Ethylbenzene concentration in reactor feed (k mol m^{-3})

CSTM - Steam concentration in reactor feed (k mol m^{-3})

SR - Molar steam/ethylbenzene ratio in reactor feed

AVMW - Average molecular weight of reactor feed (kg $kmol^{-1}$)

VISC - Viscosity (N s m^{-2})

DZ - Length step size (m).

The following variables are printed for the reactor and the regenerator.

Reactor	Regenerator	
CPG	RCPG	- Gas specific heat (J kg^{-1} °K^{-1})
RG	RRG	- Gas density (kg m^{-3})
U	RU	- Superficial velocity (m s^{-1})
G	REGG	- Mass velocity (kg $m^{-2}s^{-1}$)
RE	RRE	- Reynold's number based on particle diameter
H	RH	- Interphase heat transfer coefficient (Wm^{-2} °K^{-1})
RTM	RRTM	- Residence time (s)
DP	RDP	- Pressure drop across the bed (bar).

The output during and/or at the end of each cycle may give the average temperatures, conversions and efficiencies, together with temperature and concentration profiles for both phases, depending on the print parameter values. Several print options are available in order to give only the desired amount of output. Final values for the last two cycles are always printed if the maximum number of cycles is exceeded and a warning that cyclic steady state has not been achieved is also printed.

A sample output is given in Table A6.1.

A6.3 Use of the Program

The reactor and regenerator equations are solved in the subroutine TM1SC for each time step. The solution of these equations is described in Appendix 4. The reactor and regenerator periods are calculated alternately, until cyclic steady state is achieved or until the maximum number of cycles specified is exceeded depending on which occurs sooner.

The program assumes constant heat inputs to the system and either constant or varying inlet temperatures to each bed may be considered. Constant inlet temperatures are assumed if the superheater heat load is specified as zero in the input data. The inlet temperature of the reactor is then YIN and for the regenerator, RIT. In this case, when cyclic steady state is reached, or the maximum number of cyclies is exceeded, the execution finishes and the next data set is read. If the superheater heat load (HTIN) is specified, the inlet temperatures are calculated at each time step. The maximum temperature of the system is then checked and, if it is more than 0.2°C from the maximum specified value (YIN), a new value of HTIN is evaluated at the end of the execution and the whole calculation is

```
                                   ...  C H 3 S C  ...
                                        ---------
                     *****     SAMPLE OUTPUT FROM PROGRAM CH3SC  -  STANDARD DATA     *****
   DIAM               Z                CPS               RS               E                PDIAM              SV
0.101600E 00     0.204000E 00     0.104670E 04     0.175007E 04     0.400000E 00     0.316990E-02     0.123999E 04

   FEB              FSTM               YIN                P               RK                HTIN
0.293672E 01     0.696714E 01     0.923000E 03     0.170000E 01     0.000000E 00     0.000000E 00

   TF                DT         NSTEP        TOL         LIMIT     KSW     ISW        FIT              RFSTM           NOC
0.670000E 02     0.100000E 01    100    0.100000E-02    200        5       1     0.923000E 03     0.000000E 00       15

   A              AKG              CEB             CSTM              SR              AVMW             VISC             DZ
0.910731E-02   0.118150E 00   0.149843E-02   0.209487E-01    0.139804E 02   0.238743E 02   0.214859E-04   0.204000E-02

   CPG              RG               U                G               RE                H               RTM              DP
0.241692E 04   0.535911E 00   0.633059E 00   0.339263E 00    0.500527E 02   0.265401E 03   0.322244E 00   0.459762E-02

   RCPG             RRG              RU              REGG             RPE               RH              RRTM             RDP
0.232215E 04   0.494049E 00   0.414334E 01   0.167411E 01    0.246988E 03   0.747137E 03   0.492355E-01   0.884865E-01
   RFSTM  =    49.8613
   STEAM TEMPERATURE  -   900.042
                                   ...  SUBROUTINE  TM1SC  ...
                                        -------------------
   CYCLE NO.  4
   ------------         MEAN OUTLET TEMPERATURE ..   913.794          MEAN CONVERSION  ...   0.67753   0.01564   0.06891
                        EQUILIBRIUM CONVERSION  ..   [illegible]      EFFICIENCY       ...   0.88758   0.02191   0.09025
 923.00000  895.36156  885.63173  888.13432  [illegible]  900.39927  905.07582  908.66201  911.43360  913.61921  915.37655
 923.00000  894.79292  886.22397  [illegible]  [illegible]  901.00042  [illegible]  909.08486  911.73240  913.85745  915.56974
   0.00000    0.12407    0.27198  [illegible]  [illegible]  [illegible]  [illegible]    0.53560    0.57335    0.60708  [illegible]
   0.00000  [illegible]    0.28051  [illegible]  [illegible]  [illegible]  [illegible]    0.54436    0.55148    0.61343  [illegible]
   0.00000    0.00417  [illegible]  [illegible]  [illegible]  [illegible]  [illegible]    0.01105    0.01409  [illegible]  [illegible]
   0.00000  [illegible]    0.00566  [illegible]  [illegible]  [illegible]    0.01216    0.01328    0.01430    0.01521  [illegible]
   0.00000    0.00671    0.01287  [illegible]  [illegible]  [illegible]  [illegible]    0.04442    0.05070    0.05654    0.06218
   0.00000    0.00813    0.01410    0.01902    0.02603    0.03244  [illegible]    0.04578    0.05200    0.05785    0.06331
REGENERATOR             MEAN OUTLET TEMPERATURE ..   [illegible]
 923.00000  922.99998  922.99995  [illegible]  [illegible]  922.95454  922.78905  922.33011  921.38533  919.84789  917.73784
 923.00000  922.99998  922.99934  [illegible]  [illegible]  922.93078  922.73474  922.19582  921.14133  919.48481  917.26936
                     ----------------------------------------------------------------------------------------
   KG STEAM / KG STYRENE  =   3.5709                          HEAT INPUT / KG STYRENE  =  0.345246E 07
   EXECUTION TIME  -   18.78 MINS.
```

Table A6.1: Sample Output from CH3SC using Standard Data in Figure 8.1.

repeated. This process is repeated if the maximum observed temperature is still not satisfactory.

For varying inlet temperatures, the make-up steam temperature is calculated assuming that the desired regenerator inlet temperature is RIT when the reactor inlet temperature is YIN. In order to estimate an initial value of HTIN using the average bed temperature drop (ΔT) as described in Chapter 5, the value of HTIN in the input data is set at - ΔT.

The saturation steam flow is calculated from equation 5.9 if the value of RFSTM is specified as zero. If some multiple or fraction of this value is desired, this is obtained by setting RFSTM to the negative value of the appropriate factor. Operation of the system is normally counter-current. Co-current operation is obtained by specifying NOC as negative.

If an inert fraction of the bed is specified when using the subroutine TM1SC, it is assumed to be uniformly mixed and the temperature and concentrations in the inert material are the same as the fluid phase values. This is the model described by equations 3.41 - 3.44 with equations 3.19 and 3.20. In order to consider a separate, uniformly mixed, inert phase heat balance or an inert region in the bed, the subroutine TM1SC must be replaced by TM3SC or TM4SC respectively. The wall heat capacity, described in Appendix 5, is modelled in subroutine TM5SC, which replaces TM1SC.

The program may be controlled, to some extent, during execution by the use of console switches. A particular switch is checked by calling the subroutine DATSW(M,N), where M is the number of the switch (0-15) and N is returned as 1 if the switch is on (raised) or 2 if it is off. The switches used, and their action on the programme, is given in Table A6.2. The other system routine called is SECON(T) which returns T as the time of day and is used to calculate the execution time.

The error messages printed by the program are self-explanatory except for error 100. This error arises when a satisfactory value of HTIN has not been estimated by the third (and final) evaluation.

Switch No.	Action
0	When raised, the program is interrupted and the current values are written to a file.
1	When raised, it causes the current execution to be abandoned and the next data set read.
3	When raised, it causes the temperatures and concentrations to be printed at each time step.
9	When raised, it prevents subsequent re-evaluations of the superheater heat load.
10	If switch is off at the start of the execution, it proceeds using the values stored in the file when switch 0 was raised. If raised, execution starts from initial conditions.

Table A6.2: Effect of Console Switches on the Program CH3SC.

A6.4 Details of Ancillary Calculations

A6.4.1 Average temperatures and conversions

The average conversions and inlet and outlet temperatures are integrated over the elapsed time interval by Simpson's Rule[109]. If T_{OUT} is the outlet temperature and N is the number of time steps, then

$$T_{AVE} = \frac{\Delta T}{3t_f}\left[T_o + 4T_1 + 2T_2 + 4T_3 + \ldots\ldots + 2T_{N-2} + 4T_{N-1} + T_N \right] \tag{A6.1}$$

where t_f is the elapsed time. N must be an even integer and this is checked by the program. A running total of the appropriate multiples of the outlet temperature is incremented at each time step and is finally divided by $\frac{\Delta t}{3t_f}$ which is $\frac{1}{3N}$. A similar procedure is used to average the conversions and varying inlet temperatures.

A6.4.2 Heat balance equations

The enthalpies of the various streams for which the temperatures are required are quartic functions of temperature. The temperature is therefore obtained from the enthalpy by a Newton-Raphson technique[109].

A6.4.3 Estimation of HTIN

An initial estimate of HT_{IN} is obtained from equation 5.13 as described in Chapter 5. If this value is not satisfactory, as discussed in A6.3, a new estimate is calculated from equation 5.12. The regenerator outlet temperature for equation 5.12 is the observed average value in the last cycle calculated, less the difference between the observed and specified (YIN) maximum temperatures. The average reactor inlet temperature used is YIN less half the difference between YIN and the calculated value from the last cycle. A third estimate, if required, is obtained by linear interpolation between the previous values using the maximum temperatures observed with each. The interpolation produces the value which will give a maximum temperature of YIN.

This interpolation was found to give a good estimate for HT_{IN} unless one of the previous estimates was very poor.

A6.5 Flags used in CH3SC

A number of flags are set by the program to indicate internally the action to be taken at various points. These are as follows:

IERR - Error flag. This is set to the error number if an error is detected. If no error, IERR = 1.

JERR - Normally 1. Set to 2 if intermediate printout required after an odd number of steps and causes a warning to be printed that the averaged values (evaluated by Simpson's Rule) are incorrect.

ICURR - Set to 1 for counter-current operation, or 2 for co-current operation.

IEXIT - Initially 1. Set to zero when cyclic steady state achieved.

IREG - Set to 1 for constant inlet temperatures, or 2 for varying inlet temperatures.

ICALC - HT_{IN} only re-evaluated if ICALC = 2.

NENT - Number of evaluations of HT_{IN}.

NSTRT - Indicates the start of the catalyst region if a layer of inert material is at the entrance of the reactor.

NEND - Indicates the end of the catalyst region if a layer of inert material is at the exit of the reactor.

APPENDIX 7: Listing of the Program CH3SC

A7.1 CH3SC

```
C**************************************************************************************
C
C                         CYCLIC REACTOR-REGENERATOR MODEL    -   CH3SC.
C                         -------------------------------------------------
C
C        THE REACTION EB = STY + H2 IS CONSIDERED WITH THE TOLUENE AND BENZENE
C        PRODUCING SIDE REACTIONS.
C
C           CONCENTRATIONS    ...     X(1,I)   -   STYRENE
C                                     X(2,I)   -   BENZENE
C                                     X(3,I)   -   TOLUENE
C
C        INLET TEMPERATURES ARE CONSTANT AT YIN AND RIT IF HTIN (SUPERHEATER
C        HEAT LOAD) IS ZERO.
C
C        IF HTIN IS SPECIFIED, REACTOR AND REGENERATOR INLET TEMPERATURES
C        ARE CALCULATED.
C        RIT IS THE TEMPERATURE OF THE REGENERATOR INLET WHEN THE REACTOR
C        INLET TEMPERATURE IS YIN.
C        IF HTIN IS SPECIFIED NEGATIVE, THE INITIAL VALUE IS ESTIMATED USING
C        THE SPECIFIED VALUE AS THE STEADY STATE TEMPERATURE DROP.
C
C        SUBSEQUENT VALUES OF HTIN ARE CALCULATED AFTER CYCLIC STEADY STATE
C        IS ACHIEVED.
C
C        IF RESTM IS SPECIFIED AS ZERO, IT IS CALCULATED FROM THE PSEUDO -
C        HOMOGENEOUS ANALYTICAL SOLUTION.
C        IF IT IS NEGATIVE, THE CALCULATED VALUE IS MULTIPLIED BY (-RESTM)
C
C        FOR CO-CURRENT OPERATION SPECIFY NOC AS NEGATIVE.
C
C        THE EQUATIONS ARE SOLVED IN THE SUBROUTINE TM1SC OR A SUBROUTINE
C        EQUATED TO IT.
C        IF IENT = 1   ..   EVALUATE CONSTANTS          (IENT = FIFTH ARGUMENT)
C                  2   ..   REACTOR CALCULATIONS
C                  3   ..   REGENERATOR CALCULATIONS
C                  4   ..   EVALUATE CONSTANTS AFTER INTERRUPTION
C                  5   ..   CALL FOR ACTION ON INTERRUPTION
C        ON A SUCCESSFUL RETURN FROM TM1SC THE ERROR FLAG (IERR) IS 1.
C
C        THE AVERAGE CONVERSIONS AND INLET AND OUTLET TEMPERATURE  ARE
C        EVALUATED USING SIMPSON'S RULE.
C
C        PRINT PARAMETERS
C              KSW   =   1   ..   ALL INTERMEDIATE AND FINAL PRINTOUT
C                        2   ..   FINAL PRINTOUT EACH CYCLE AND INTERMEDIATE
C                                 ON FINAL CYCLE
C                        3   ..   FINAL PRINTOUT EACH CYCLE
C                        4   ..   INTERMEDIATE PRINTOUT IN FINAL CYCLE
C                        5   ..   FINAL OUTPUT ONLY
C
C              ISW   =   1   ..   PROFILES PRINTED WITH ALL VALUES
C                        2   ..   NO PROFILES FOR SIDE REACTIONS
C                        3   ..   TEMPERATURE PROFILES ONLY
C                        4   ..   PROFILES PRINTED WITH FINAL VALUES ONLY
C**************************************************************************************
      REAL MTCSC
      DIMENSION X(3,102),XS(3,102),Y(102),YS(102),RY(50),ENTH(4),
     *          CPEB(4),CPSTM(4),HTN(2),Y1(2)
      DEFINE FILE 1(1200,3,U,NREC)
      DEFINE FILE 2(1000,3,U,NREC1)
      COMMON RK,P,[illegible],CSN,[illegible]IN,[illegible],PDIAM,CSTM,TF,CPSST,DIAM,STRT,
     *[illegible],N1,[illegible],E,SV,DT,TOL,LINIT,AKG,DC,U,H,CPG,RG,RU,RH,RCPG,
     *[illegible],[illegible]B,[illegible]IN,RESTM,G,NTIME,ITIME,KOUNT,ISW,KSW,NREC,I[illegible],M,SR,
     *TOUT,CONV(3),[illegible],RSTRT,NDAT
      DATA IE/50/
      DATA TCH/813.0/
      DATA CPEB /[illegible],100.563, 0.667167E3, -0.418806, 0.100274E-3/
      DATA CPSTM/[illegible], 1.9234, 0.10555E-1, -0.359521E-5/
C
 1001 FORMAT(20A4)
 1002 FORMAT(F10.0)
 1003 FORMAT(3F10.3,I10,F10.8,4I10)
 2000 FORMAT([illegible]... C H 3 S C ...'/50X,9(1H-))
 2001 FORMAT([illegible]20A4)
 2002 FORMAT(//[illegible]'[illegible]',10X,'Z',16X,'CPS',16X,'RS',16X,'[illegible]',15X,'PDIAM',
     *[illegible]10.5)
 2003 FORMAT(/[illegible]',14X,'RESTM',1[illegible]'YIN',16X,'P',17X,'RK',14X,'HTIN'
     *[illegible],5E19.6)
 2004 FORMAT([illegible]16X,'DT',8X,'NSTEP',[illegible]'TOL',8X,'LINIT',[illegible]'KSW',
     *[illegible]',15X,'RESTM',[illegible]'NOC'/[illegible]E1[illegible].6,E1[illegible].6,I[illegible]16.6,
     *[illegible]17.3E17.6,I8)
 2005 FORMAT([illegible],13X,'CPG',13X,'CCB',11X,'[illegible]TM',14X,'SR',11X,
     *[illegible],12[illegible]'VIN[illegible]',13X,'DC'[illegible]E1[illegible](E1[illegible].6,F1[illegible].6))
 2006 FORMAT([illegible],14X,'RG',14X,'U',1[illegible],15X,'RE',13X,'R',14X,
     *[illegible],12X,'D[illegible]'[illegible]E15.6,E15.6))
 2007 FORMAT(/[illegible]'RCPG',12X,'RPG',14X,'RU',11X,'RECC',13X,'RRE',13X,
     *'[illegible]',1[illegible]'RPIM',12X,'RDP'[illegible]F15.6[illegible]E1[illegible].6,E15.6))
 2008 FORMAT(/ 5X,'[illegible] CO-CURRENT OPERATION ****')
 3000 FORMAT('1')
 3001 FORMAT(/ 5X,'STEAM TEMPERATURE   =',F9.3)
 3002 FORMAT(/ 5X,'[illegible]   =',F10.4)
 3003 FORMAT(  5X,'[illegible]CUTION TIME   =',F[illegible].2,' MINS.')
 3004 FORMAT(/ 5X,'KG STEAM / KG STYRENE   =',F8.4,20X,'HEAT INPUT / KG S
     *TYRENE   =',E14.[illegible])
 3005 FORMAT(/ 20X,[illegible](1H-))
 3006 FORMAT(//  35X,'RUN',I2,'.   -   HTIN RECALCULATED AS',E15.6/34X,
     *[illegible](1H[illegible]))
 4001 FORMAT(-15X,10(1H*),'   CALCULATION FAILS WITH ERROR CODE',I4,2X,
     *10(1H*))
 4002 FORMAT(//20X,10(1H*),'   TF/DT IS NOT AN EVEN INTEGER   -',E14.6,2X,
     *10(1H*))
 4003 FORMAT([illegible]10X,10(1H*),'   WARNING   -   INTERMEDIATE MEAN VALUES INCOR
     *RECT DUE TO ODD NUMBER OF STEPS   ',10(1H*))
 4004 FORMAT([illegible]X,10(1H*)'   CYCLIC STEADY STATE NOT ACHIEVED   -
     *10(1H*)/4[illegible]3[illegible](1H[illegible]))
 4005 FORMAT([illegible]10X,10(1H*),'   NUMBER OF TIME STEPS REQUESTED EXCEEDS MAX
     *IMUM   ',10(1H*))
 4006 FORMAT(/ 10X,10(1H*),'   WARNING   -   REACTOR RESIDENCE TIME EXCEEDS
     * 1 P.C. OF THE PERIOD   ',10(1H*))
C
      NDATA = 0
C
C                CHECK FOR INITIALISATION
C                ************************
C
C           IF SW 10 RAISED   -   INITIALISE
C           IF SW 10 DOWN     -   READ FROM FILE
C
      CALL DATSW(10,KOUNT)
      GO TO (21,22),KOUNT
   21 NDAT = 1
      GO TO 23
   22 READ(1'1)NDAT
   23 CONTINUE
```

```
C
C                        READ AND WRITE INPUT DATA
C                        *************************
C
   30 NDATA = NDATA + 1
      WRITE(1'1)NDATA
      READ(2,1001)(WKS(I),I=1,20)
      READ(2,1002)DIAM,Z,EPS,RS,E,PDIAM,SV
      READ(2,1003)FEB,FSTM,YIN,P,RK,ATIN
      READ(2,1004)TF,DT,NSTEP,TOL,LIMIT,KSW,ISW
      READ(2,1005)RIT,RFSTM,NOC,STRT
C
C     CHECK REQUIRED NUMBER OF DATA SETS READ IF PROGRAM WAS INTERRUPTED
C
      IF(NDAT - NDATA) 34,35,30
   34 WRITE(3,3000)
   35 CONTINUE
C
C     CHECK VALUES OF 'ISW', 'KSW', 'NSTEP' AND NUMBER OF TIME STEPS
C     IF OUT OF RANGE  -  DEFAULT VALUES SELECTED
C
      IF (ISW) 42,42,41
   41 IF (ISW - 4) 45,45,42
   42 ISW    = 2
C
   45 IF (KSW) 48,48,47
   47 IF (KSW - 5) 50,50,48
   48 KSW    = 5
C
   50 IF (NSTEP) 55,55,54
   54 IF (NSTEP - 100) 56,56,55
   55 NSTEP  = 100
   56 CONTINUE
C
      IF(IFIX(TF/DT) - (1000/IRY)*IRY) 59,59,58
   58 WRITE(3,4005)
      GO TO 800
   59 CONTINUE
C
      WRITE(3,2000)
      WRITE(3,2001)(WKS(I),I=1,20)
      WRITE(3,2002)DIAM,Z,EPS,RS,E,PDIAM,SV
      WRITE(3,2003)FEB,FSTM,YIN,P,RK,ATIN
      WRITE(3,2004)TF,DT,NSTEP,TOL,LIMIT,KSW,ISW,RIT,RFSTM,NOC
C
C
C                        PRELIMINARY CALCULATIONS
C                        ************************
C
      IERR   = 1
      NENT   = 1
      N1     = NSTEP + 1
      DZ     = Z/NSTEP
      A      = DIAM * DIAM * ATAN(1.0)
      B      = TF/DT
      LSW    = KSW
      JSW    = ISW
      NTIME  = B + 0.5
      ITIME  = NTIME / 10
      TOLN   = 0.5E-04 * DT
      NITRT  = 1
      NDAT   = N1
C
C     CHECK TF/DT IS AN EVEN INTEGER (FOR SIMPSON'S RULE CALCULATION)
C
      IF(ABS(B-FLOAT(NTIME))-1.0E-09)70,70,71
   70 IF (MOD(NTIME,2))71,72,71
   71 WRITE(3,4002)B
      GO TO 800
   72 IF(MOD(ITIME,2)) 73,74,73
   73 JERR   = 2
      GO TO 75
   74 JERR   = 1
   75 CONTINUE
C
C     REACTOR PARAMETERS
C
      DH(1)  = (28343.0 - 1.09*YIN) * 4186.8
      DH(2)  = ([illegible].0 - 1.90*YIN) * 4186.8
      DH(3)  = (-13702. - 3.15*YIN) * 4186.8
      FEB    = FEB/3600./106.
      FSTM   = FSTM/3600./18.
      B      = FEB + FSTM
      RGM    = P*273.0/22.4/YIN
      U      = B/RGM/A
      CEB    = FEB * RGM / B
      CSTM   = FSTM * RGM / B
      SR     = FSTM/FEB
      AVMW   = (FEB*106. + FSTM*18.) / B
      CPGEB  = CPEB(1)  + YIN*(CPEB(2)  + YIN*(CPEB(3)  + YIN*CPEB(4)))
      CPGS   = CPSTM(1) + YIN*(CPSTM(2) + YIN*(CPSTM(3) + YIN*CPSTM(4)))
      CPG    = (FEB*CPGEB + FSTM*CPGST)/B/AVMW
      RG     = RGM * AVMW
      G      = RG * U
      VISC   = FVISC(YIN)
      RE     = G * PDIAM / VISC
      RTM    = Z/U
      H      = HTCSC(G,RE,CPG,VISC,YIN,E)
      AKG    = MTCSC(U,RE,RG,VISC,CSTM,RGM,YIN,E)
      DP     = PRDSC(Z,U,E,PDIAM,VISC,RG)
C
      WRITE(3,2005)A,AKG,CEB,CSTM,SR,AVMW,VISC,DZ
      WRITE(3,2006)CPG,RG,U,G,RE,H,RTM,DP
C
      IF (RTM - TF/100.) 78,78,77
   77 WRITE(3,4006)
   78 CONTINUE
C
C     REGENERATOR PARAMETERS
C
      RCPG   = CPCST / 18.
      RRG    = RGM * 18.
      IF (RFSTM) 81,80,82
   80 RFSTM  = 1.0
   81 RFSTM  = (1.0-E)*RS*CPS*RGM*A*Z/TF/RRG/RCPG * 3600.*18. * (-RFSTM)
      IERR   = 2
   82 RFSTM  = RFSTM/3600./18.
      RU     = RFSTM/RGM/A
      G      = RRG * RU
      RE     = G * PDIAM / VISC
      RTM    = Z/RU
      RH     = HTCSC(G,RE,RCPG,VISC,YIN,E)
      DP     = PRDSC(Z,RU,E,PDIAM,VISC,RRG)
      WRITE(3,2007)RCPG,RRG,RU,G,RE,RH,RTM,DP
C
      GO TO (86,85),IERR
   85 B      = RFSTM * 3600. * 18.
      WRITE(3,2008) B
      IERR   = 1
   86 CONTINUE
C
C
C               CK FOR CO- OR COUNTER-CURRENT OPERATION
C               ***************************************
C
      IF [illegible] 90,91,92
   90 IF [illegible]
      [illegible]
      [illegible]
      [illegible]
   91 [illegible]  2
   92 [illegible]  1
   95 CONTINUE
```

```
C
C          INLET TEMPERATURE CALCULATIONS
C          ******************************
C
      DO 110 I=1,4
  110 CMTH(I) = FEB*CPEB(I) + FSTM*CPSTM(I)
      CSTM    = ENTSC(CTIN,CPEB) * FEB
      T       = ENTSC(YIN,CMTH)
C
C     CHECK FOR MODE OF OPERATION
C
      IF (HTIN) 120,115,125
C
C          CONSTANT INLET TEMPERATURES - CALCULATE DILUENT STEAM TEMPERATURE
C
  115 IREG    = 1
      ICALC   = 1
      B       = 1.0
      ENTY    = (T - CSTM)/FSTM
      T       = YIN
      CALL NRTSC(T,ENTY,0.0,CPSTM.CPSTM,LIMIT.IERR)
      WRITE(3,3001)  T
      HT      = FEB * (ENTSC(YIN, CPEB)   - ENTSC(409.,CPEB)   + 151.7)
     *        + FSTM * (ENTSC(YIN, CPSTM) - ENTSC(407.,CPSTM)  + 631.0)
      GO TO 155
C
C          VARYING INLET TEMPERATURES
C
C     ESTIMATE INITIAL VALUE OF HTIN IF REQUIRED
C
  120 HTIN    = FEB*ENTSC(YIN+HTIN/2.,CPEB)-CSTM- FSTM*A*Z*(1.0-E)*RS*CPS*
     * HTIN/RESTM-TF
      WRITE(3,3000) NENT,HTIN
C
C
  125 IREG    = 2
      CALL DATSW(9,ICALC)
      GO TO (145,130),ICALC
  130 KSW     = 5
C
C     CALCULATE TEMPERATURE OF STEAM ENTERING SYSTEM
C
  145 RE      = (RFSTM - FSTM) /RFSTM
      RENTY   = ENTSC(RIT,CPSTM)*RFSTM/FSTM - (T - CSTM - HTIN)*RE
      B       = RIT
      CALL NRTSC( B, RENTY,0.0,CPSTM,CPSTM,LIMIT,IERR)
      WRITE(3,3001)B
C
C
      RE      = (RFSTM - FSTM)/RFSTM
      RENTY   = ENTSC( B, CPSTM) * FSTM/RFSTM
      HT      = CSTM - FEB * (ENTSC(409.,CPEB) + 151.7)  +
     *          FSTM * (ENTSC( B, CPSTM) - ENTSC(407.,CPSTM)+631.) + HTIN
      ENTY    = CSTM + HTIN
      B       = 0.975
  155 CONTINUE
C
C
C          INITIALISE IF SWITCH 10 RAISED OR FOR NEW DATA
C          **********************************************
C
      GO TO (160,180,160,185),KOUNT
  160 EXTM    = 0.0
      YN1     = 1.0
      TOUT    = B
      IEXIT   = 1
      LSTRT   = 1
      NCYCL   = 1
      NREC1   = 1
      K       = 0
      DO 161 J=1,3
  161 CONV(J) = 0.0
      DO 165 I=1,IRY
  165 RY(I)   = B
      J       = 1000/IRY
      DO 166 I=1,J
      WRITE(2'NREC1) RY
  166 CONTINUE
      READ (2'1) RY
      DO 168 I=1,101
      Y(I)    = B
      YS(I)   = B
      DO 168 J=1,3
      X(J,I)   = 0.0
  168 XS(J,I)  = 0.0
      IF (KOUNT - 1) 170,170,185
C
C          CALL TMISC TO EVALUATE COEFFICIENTS
C
  170 CALL TMISC(X,Y,XS,YS,1,IERR)
      NEND    = NDAT
      GO TO 185
C
C     IF PROGRAM WAS INTERRUPTED, READ FROM FILE
C
  180 READ (1'1) [illegible](X(J,I),XS(J,I),J=1,3),Y(I),YS(I),I=1,101),
     *(CONV(I),I=1,3),EXTM,TOUT,YN1,LSTRT,NCYCL,KSW,RTM,IEP,IEXIT,
     *ISW,YN1,G,NREC1,[illegible]NENT,ICALC,(CMTH(I),Y1(I),I=1,20),HTIN,YIN,T
      CALL TMISC(X,Y,XS,YS,4,IERR)
      NEND    = NDAT
      READ(2'NREC1) RY
      IF (NENT - 1) 185,185,182
  182 KOUNT = 4
      WRITE(3,5006) NENT,HTIN
      GO TO (185,145),IREG
  185 CONTINUE
C
C
C     CHECK FOR ERROR
C
      IF(IERR - 1) 195,195,190
  190 WRITE(3,3001)IERR
      GO TO 800
  195 CONTINUE
C
C        CALL TIME OF DAY
C
      CALL SECON(TIM1)
C
C
C
C                         START OF CYCLE
C                         **************
C
      DO 500 M = NCYCL,NOC
C
       IF(M-NOC+1) 210,201,205
  201 IF (KSW - 2) 210,203,203
  203 KSW = KSW - 2
      GO TO 220
C
  205 IF (ISW - 2) 207,207,206
  206 ISW = 2
  207 IF (KSW - 2) 212,208,220
  208 KSW   1
      GO TO 212
C
  210 IF (KSW - 1) 220,212,220
  212 GO TO (220,214),[illegible]
  214 WRITE(3,3024)
  220 CONTINUE
      NDAT    = NEND
```

```
C
C                    REACTOR   CALCULATIONS
C                    ****************************
C
      DO 300 KOUNT = LSTRT,NTIME
      KNT1   = KOUNT - 1
C
C     PROGRAM INTERRUPTED BY RAISING SWITCH ZERO
C     IF SW 1 ALSO RAISED  -  NEXT DATA SET READ
C
      CALL DATSW(0,I)
      GO TO (230,235),I
  230 CALL SECOND(T)
      EXTM   = EXTM + T - TIM1
      B      = EXTM / 60.
      WRITE(3,3008) B
      NREC1  = NREC1 - IRY
      WRITE(1'1)NDATA,((X(J,I),XS(J,I),J=1,3),Y(I),YS(I),I=1,101),
     *(CONV(I),I=1,3),EXTM,TOUT,YIR,KOUNT,M,KSW,RTM,DP,IEXIT,
     *ISW,YN1,G,NREC1,K,NENT,ICALC,(ATN(I),Y1(I),I=1,2),ATIN,Y1(3)
      CALL TMISC(X,Y,XS,YS,5,IERR)
      CALL DATSW(1,I)
      GO TO (232,235),I
  232 CALL EXIT
  235 CONTINUE
C
C     ALLOW 10*LIMIT ITERATIONS AT FIRST TIME STEP
C
      IF (KOUNT - 2) 240,242,244
  240 LIMIT = LIMIT * 10
      GO TO 244
  242 LIMIT = LIMIT / 10
  244 CONTINUE
C
C     CALCULATE REACTOR INLET TEMPERATURE IF NOT FIXED
C
      GO TO (270,245),IREG
C
C     READ FROM FILE IF ARRAY EXHAUSTED
C
  245 IF (MOD(KNT1,IRY)) 250,246,250
  246 IF (KNT1) 250,250,247
  247 K      = K + 1
      READ(2'NREC1) RY
  250 CONTINUE
C
      J         = KOUNT - K*IRY
      B         = RY(J) * YIN
      CALL HPTSC(B,ENTY,FSTM,CPSTM,ENTH,LIMIT,IERR)
      Y(1)      = B/YIN
      YS(1)     = B/YIN
C
C     AVERAGE INLET TEMPERATURE BY MEANS OF SIMPSON'S RULE
C
      IF (KNT1) 262,262,263
  262 YIR = Y(NSTRT)
      GO TO [illegible]
  263 J      = (KNT1 - (KNT1/2)*2 + 1) * 2
      YIR = YIR + J*Y(NSTRT)
C
C     CHECK MAXIMUM INLET TEMPERATURE
C
      J         = 6.0/DT
      IF (KOUNT - J) 270,268,266
  266 IF (Y1(NENT) - Y(NSTRT)) 268,270,270
  268 Y1(NENT) = Y(NSTRT)
  270 CONTINUE
C
C     INTERMEDIATE PRINTOUT
C
      CALL OUTSC(X,Y,XS,YS,2)
C
C     CALCULATE ALONG BED
C
      CALL TMISC(X,Y,XS,YS,2,IERR)
C
C     AVERAGE CONVERSION AND OUTLET TEMPERATURE CALCULATED USING
C     SIMPSON'S RULE
C
      IF (KNT1) 280,280,285
  280 DO 282 I=1,3
  282 CONV(I) = X(I,N1)
  285 J         = (KOUNT - (KOUNT/2)*2 + 1) * 2
      DO 286 I=1,3
  286 CONV(I) = CONV(I) + J*X(I,N1)
      TOUT      = TOUT + J*Y(NEND)
C
C
C     CHECK FOR ERROR RETURN FROM TMISC
C
      IF(IERR-1) 300,300,290
  290 WRITE(3,3001) IERR
      CALL OUTSC(X,Y,XS,YS,1)
      GO TO 800
  300 CONTINUE
C
C                  CHECK FOR CYCLIC STEADY STATE
C                  *****************************
C
      IF (M - 1) 316,312,312
  312 IF (ABS(DP   -   YN1 ) - TOLN )  313,313,316
  313 IF (ABS(RTM-Y(NEND)) - TOLN )  315,315,316
  315 IF (ABS(G  - X(1,N1)) - TOLN )  320,320,316
  316 DP   = YN1
      RTM  = Y(NEND)
      G    = X(1,N1)
      GO TO 330
  320 IEXIT = 0
      IF (ISW - 2) 325,325,322
  322 ISW    = 2
  325 IF (KSW - 4) 332,335,332
C
C                   REACTOR   PRINTOUT
C                   ****************
C
  330 IF(KSW-4)332,[illegible]
  332 CALL OUTSC(X,Y,XS,YS,1)
      T         = TOUT
      TF        = YIR
  335 CONTINUE
C
C
C                   FLOW   REVERSAL
C                   ***************
C
C     REVERSE PROFILES FOR COUNTER CURRENT OPERATION
C
      GO TO (360,365),ICURR
  360 KOUNT = N[illegible]
      DO 362 I=2,KOUNT
      J = N1 + 2 - I
      B         = Y(I)
      Y(I)      = Y(J)
      Y(J)      = B
      B         = YS(I)
      YS(I)     = YS(J)
  362 YS(J)     = B
      RY(1)     = Y(2)
      GO TO 36[illegible]
C
C
C                  REGENERATOR   CALCULATIONS
C                  ****************************
C
  365 RY(1)     = Y(N1)
  366 Y(1)      = [illegible]
      YS(1)     = Y(1)
      NDAT      = N1
      TOUT      = Y(N1)
      NREC1     = 1
      K         = 0
```

```
C
      IF (KSW - 1) 375,371,375
  371 GO TO ([illegible]),JERR
  373 WRITE(3,4003)
  375 CONTINUE
C
      DO 400 KOUNT = 1,NTIME
C
C     CALCULATE INLET TEMPERATURE IF REQUIRED
C
      GO TO (300,[illegible]),IREG
  300 IF (KOUNT - 1) 302,301,302
  301 B      = RY(1) * YIN
      GO TO 303
  302 B      = Y(N1) * YIN
  303 CALL NRTSC(B,PENTY,RE,CPSTM,CPSTN,LIMIT,IEXIT)
      Y(1)   = [illegible]
      YS(1)  = B/YIN
C
C     AVERAGE INLET TEMPERATURE
C
      J      = KOUNT - 1
      IF (J) 384,384,386
  384 YIR    = Y(1)
      GO TO 388
  386 J      = (J - (J/2)*2 + 1) * 2
      YIR    = YIR + J*Y(1)
  388 CONTINUE
C
C     INTERMEDIATE PRINTOUT
C
      CALL OUTSC(X,Y,XS,YS,3)
C
C     CALCULATE ALONG BED
C
      CALL TM1SC(X,Y,XS,YS,3,IERR)
C
C     STORE OUTLET TEMPERATURES -  WRITE TO FILE IF ARRAY FULL
C
      IF(MOD(KOUNT,IRY))395,390,395
  390 K      = K + 1
      WRITE(2'NREC1) RY
  395 J      = KOUNT + 1 - K*IRY
      RY(J)  = Y(N1)
C
C     AVERAGE OUTLET TEMPERATURE USING SIMPSON'S RULE
C
      J      = (KOUNT - (KOUNT/2)*2 + 1) * 2
      TOUT = TOUT + J*Y(N1)
C
  400 CONTINUE
C
      WRITE(2'NREC1) RY
      YN1    = Y(N1)
C
C                       REGENERATOR  PRINTOUT
C                       *********************
C
      IF (KSW - 4) 405,406,404
  404 IF (IEXIT - 1) 405,406,190
  405 CALL OUTSC(X,Y,XS,YS,4)
      WRITE(3,[illegible])
  406 CONTINUE
C
C                   REVERSE REGENERATED PROFILES (COUNTER CURRENT OPERATION)
C                   ********************************************************
C
      GO TO (410,420),ICURR
  410 KOUNT = NSTEP/2
      DO 415 I=2,KOUNT
      J      = N1 + 2 - I
      B      = Y(I)
      Y(I)   = Y(J)
      Y(J)   = B
      B      = YS(I)
      YS(I)  = YS(J)
  415 YS(J)  = B
  420 CONTINUE
C
C                        CHECK FOR EXIT
C                        **************
C
      IF (IEXIT - 1) 422,426,190
  422 GO TO (520,424,520,424,520),KSW
  424 KSW    = 1
  426 CONTINUE
C
C
C                      INITIALISE FOR NEXT CYCLE
C                      *************************
C
      IF (M - MOC) 430,500,500
  430 LSTRT  = 1
      TOUT   = Y(NEND)
      READ (2'1) RY
      K      = 0
      Y(1)   = 1.0
      YS(1)  = 1.0
      DO 440 J=1,3
      CONV(J) = 0.0
      DO 440 I=2,N1
      X(J,I)  = 0.0
  440 XS(J,I) = 0.0
C
  500 CONTINUE
C
      WRITE(3,4004)
C
C          CALCULATE LB STEAM AND HEAT INPUT /LB STYRENE
C          *********************************************
C
  520 B      =   FEB  * (1.0 + CONV(1) + CONV(2))
      HT     =   HT + [illegible]
     *           - FSTM*(ENTSC(T,CPSTM) - ENTSC(273.0,CPSTM))
      T      =   CONV(1) * FEB * 104.
      HT     =   HT / T
      SR     =   FSTM * 18. / T
      WRITE(3,[illegible]) SR,HT
C
C                       EXECUTION TIME
C                       **************
C
      CALL SECOND(T)
      EXTM   = ([illegible] + T - TIM1) / 60.
      IF (EXTM) 552,554,554
  552 EXTM   = 1440.0 + EXTM
  554 WRITE(3,3003)EXTM
C
C                     HEAT LOAD CALCULATIONS
C                     **********************
C
      GO TO (800,600),ICALC
C
C     CHECK FOR MAXIMUM TEMPERATURE
C
  600 DO 620 I=LSTRT,NEND
      IF (Y(NEND) - Y(I)) 610,620,620
  610 Y(NEND) = Y(I)
  620 CONTINUE
C
C     CHECK IF VALUE OF RMIN WAS SATISFACTORY
C
      IF ([illegible]) 800,800,630
  630 LSTM   = [illegible]
      T      = [illegible]
      WRITE(3,[illegible])
```

```
C
      GO TO (660,670,650),NENT
  650 IERR   = 100
      GO TO 190
C
C     ESTIMATE 2ND VALUE OF HTIN
C
  660 HTN(1)  = HTIN
      B       = (Y1(1)   1.0) * YIN
      TE      = YIN - ABS(YIN-TE) /2.0
      HTIN    = ENTSC(TE,ENIN)  -   CSTM - ESTM*ENTSC(TOUT-B,CPSTM)
      IF (B*(HTN(1)-HTIN)) 665,668,668
  665 HTIN    = HTN(1) + (HTN(1) - HTIN)/2.0
  668 HTN(2)  = HTIN
      KSW     = 5
      GO TO 680
C
C     INTERPOLATE FOR 3RD VALUE OF HTIN
C
  670 HTIN    = HTN(1) + (HTN(2)-HTN(1))*(1.0-Y1(1))/(Y1(2)-Y1(1))
      KSW     = LSW
      ISW     = JSW
      IF (KSW - 5) 680,700,700
C
  680 WRITE(3,2000)
  700 NENT    = NENT + 1
      WRITE(3,190) NENT,HTIN
      KOUNT = 3
      GO TO (800,145),IREG
C
  800 KOUNT = 1
      NBAR  = 1
      GO TO 30
      END
```

```
      FUNCTION HTCSC(G,RE,CPG,VISC,T,E)
C
C     HEAT TRANSFER COEFFICIENT FOR STYRENE REACTION BY J-FACTOR
C     CORRELATION  -  HANDLEY AND HEGGS.
C
      THCON=(-.8109644460E-5+T*(0.7696878840E-7+T*(-0.1500688716E-9+T*
     *0.1106182630E-12))) *  6230.52
      HTCSC = 0.255*CPG*G/E/(CPG*VISC/THCON)**(2.0/3.0)/RE**0.335
      RETURN
      END
```

```
      REAL FUNCTION MTCSC(U,RE,RG,VISC,CSTM,CT,T,E)
C
C     MASS TRANSFER COEFFICIENT FOR STYRENE REACTION BY J-FACTOR
C     CORRELATION  -  HANDLEY AND HEGGS.
C
      D = 0.3048*0.3048*7.0827E-5 * (T/273.)**1.5
      MTCSC = 0.255*U*CT/E/CSTM/(VISC/RG/D)**(2.0/3.0)/RE**0.335
      RETURN
      END
```

```
      FUNCTION PRDSC(DZ,U,E,PDIAM,VISC,RG)
C
C     PRESSURE DROP ALONG ELEMENT DZ OF LENGTH CALCULATED BY THE ERGUN
C     EQUATION.
C
      C1 = 1.E-5 * DZ*(1.0-E)/PDIAM/E/E/E
      C2=150.0*(1.0-E)/PDIAM
      PRDSC=C1*U*(C2*VISC+1.75*U*RG)
      RETURN
      END
```

```
      FUNCTION FVISC(T)
C
C     VISCOSITY OF STEAM AS A FUNCTION OF TEMPERATURE.
C
      FVISC=(.1765800190E-05+T*(0.1309706430E-7+T*0.6845110420E-12))*1.4882
      RETURN
      END
```

```
      FUNCTION EQXSC(T,P,SR,YIN)
C
C     EQUILIBRIUM CONVERSION OF ETHYLBENZENE TO STYRENE AT A GIVEN
C     TEMPERATURE PRESSURE AND STEAM/EB RATIO.
C
      PK=1.0+P/EXP(16.12-15350.0/YIN/T)
      EQXSC=(-SR+SQRT(SR*SR+4.0*PK*(1.0+SR)))/2.0/PK
      RETURN
      END
```

```
      SUBROUTINE NRTSC(T,ENTY,FLOW,CP1,CP2,LIMIT,IERR)
C
C     NEWTON-RAPHSON SOLUTION FOR HEAT BALANCES
C
      DIMENSION CP1(4),CP2(4)
      F1(A,B,C,D) = A + T*(B + T*(C + T*D))
 1001 FORMAT(//10X,10(1H*)'  ERROR  -  FAILURE IN TEMPERATURE CALCULATIO
     *N  ',10(1H*)/22X,'TEMPERATURE   =',E14.6)
C
      ENTHY = ENTY + FLOW * ENTSC(T,CP1)
C
      DO 50 I=1,LIMIT
      D   = ( ENTHY + ENTSC(T,CP2))/F1(CP2(1),CP2(2),CP2(3),CP2(4))
      IF (ABS(D) - 0.001) 100,100,25
   25 T   = T - D
   50 CONTINUE
C
      WRITE(3,1001) T
      IERR   = 9
  100 RETURN
      END
      FUNCTION ENTSC(T,A)
C
C     FUNCTION TO CALCULATE ENTHALPY FOR CH3SC
C
      DIMENSION A(4)
C
      ENTSC  = T *  (A(1) + T*(A(2)/2. + T*(A(3)/3. + T*A(4)/4.)))
      RETURN
      END
```

```
      SUBROUTINE OUTSC(X,Y,XS,YS,IENT)
C
C     PRINTOUT SUBROUTINE FOR CH3SC
C        IENT  =  1  ..  REACTOR FINAL OUTPUT (CH3SC)
C                 2  ..  REACTOR INTERMEDIATE OUTPUT
C                 3  ..  REGENERATOR INTERMEDIATE OUTPUT
C                 4  ..  REGENERATOR FINAL OUTPUT
C
      DIMENSION X(3,102),XS(3,102),Y(102 ,YS(102),CON(3),EFF(3)
      COMMON PC,P,[illegible],YIN,[illegible](9),[illegible],N1,DUM(4),DT,TOL,LIMIT
     *DMM(14),ITIME,JTIME,KOUNT,ISW,KSW,NREC,IREG,N,SR,IOUT,CONV(3),YIR
     *,NSTRT,NEND
C
 3001 FORMAT(/ 5X,'TIME =',F6.1,6X,'MEAN OUTLET TEMPERATURE ..',  F9.3)
 3002 FORMAT(/ ' REGENERATOR',11X,'MEAN OUTLET TEMPERATURE ..',  F9.3)
 3003 FORMAT(23X,'MEAN INLET TEMPERATURE   ..',F9.5)
 3004 FORMAT(1X,F10.5,10F11.5)
 3005 FORMAT(/ 5X,'TIME =',F6.1,6X, 'MEAN OUTLET TEMPERATURE ..',F9.5,
     * 8X,'MEAN CONVERSION   ...',3F9.5)
 3006 FORMAT(  5X,'CYCLE NO.',I3,  X,12(1H-),  X'MEAN OUTLET TEMPERATURE .
     *.',  F9.3,8X, 'MEAN CONVERSION   ...',3F9.5)
 3007 FORMAT(   2 X,           'EQUILIBRIUM CONVERSION   ..',F9.5,8X
     *'EFFICIENCY          ...',3F9.5)
C
C
C        CHECK IF PRINTOUT REQUIRED
C        **************************
C
      KNT1   = KOUNT - 1
      GO TO (10,1,1,10),IENT
    1 IF(MOD(KNT1,ITIME)) 3,2,3
    2 IF(KSW-1)3,5,3
    3 CALL DATSW(5,I)
      GO TO (5,200),I
    5 IF (ISW - 2) 10,12,6
    6 JSW    = 2
      GO TO 14
   10 YIR    = YIR + 2.0*Y(1)
   12 JSW    = ISW
   14 L1     = (N1 - 1)/10
      TIME   = KNT1 * DT + 0.000005
      IF (JSW - 2) 18,16,18
   16 NRC    = 1
      GO TO 19
   18 NRC    = 3
   19 CONTINUE
C
C        TEMPERATURE PROFILES
C        ********************
C
      DO 20 I=1,11
      J      = (I-1)*L1 + 1
      WKS(I)       = Y(J) *YIN
   20 WKS(I+11)  = YS(J)*YIN
      B      = (TOUT - Y(NEND))*YIN / 3.0 / KNT1
C
C        CHECK 'IENT' FOR MODE OF OPERATION
C        **********************************
C
      GO TO (100,100,30,40),IENT
C
C        REGENERATOR PRINTOUT
C        ********************
C
   30 WRITE(3,3001)TIME,B
      GO TO 45
   40 WRITE(3,3002)B
   45 J      = 1
      IF (JSW - 3) 50,155,155
   50 JSW    = 3
      GO TO 155
C
C        CONVERSION AND EFFICIENCIES
C        ***************************
C
  100 A = 0.0
      DO 110 I=1,3
      CON(I)  = (CONV(I)-X(I,N1))/3.0/KNT1
  110 A = A + CON(I)
      DO 120 I=1,3
  120 EFF(I) = CON(I)/A
      A = COREC(Y(NEND),P,SR,YIN)
C
C        REACTOR PRINTOUT
C        ****************
C
      IF(IENT-2) 140,130,130
  130 WRITE(3,3005)TIME,B,(CON(I),I=1,3)
      GO TO 150
  140 WRITE(3,3006)N,B,(CON(I),I=1,3)
      DO 145 I=1,3
  145 CONV(I) = CON(I)
  150 WRITE(3,3007)A,(EFF(I),I=1,3)
      J      = NSTRT
  155 GO TO (170,160),IREG
  160 A      = (YIR - Y(J)) * YIN / 3.0/ KNT1
      WRITE(3,3003)A
  170 GO TO (190,190,190,200),JSW
  190 WRITE(3,3004)WKS
      GO TO (195,195,200,200),JSW
  195 WRITE(3,3004)((X(J,I),I=1,N1,L1),(XS(J,I),I=1,N1,L1),J=1,NRC)
  200 GO TO (210,220,220,210),IENT
  210 YIR    = B
      TOUT   = B
  220 RETURN
      END
      SUBROUTINE TM1SC(X,Y,XS,YS,IENT,IERR)
C
C     TRANSIENT FILM RESISTANCE MODEL
C     LAGRANGIAN             ..     TIME    -   BACKWARD DIFFERENCE
C     ----------                    LENGTH  -   CENTRAL DIFFERENCE
C     EQUATIONS SOLVED BY REPEATED SUBSTITUTION IN RSNSC
C
      EXTERNAL FX1SC,ER1SC
      DIMENSION X(3,102),XS(3,102),Y(102),YS(102)
      COMMON RK,P,EPU,L,T,YIN,DHC(3),B(3),C4,D,D4,WKS(22),N1,CPS,RS,E,SV,
     *DT,TOL,LIMIT,AKG,DZ,U,H,CPG,RG,RU,RH,RCPG,RRG
 1001 FORMAT(/ 42X,' ...  SUBROUTINE  TM1SC  ...'/42X,17(1H-))
C
      GO TO (10,20,30,10,26),IENT
C
C     EVALUATE CONSTANTS
C
   10 WRITE(3,1001)
      D =1.0-RK
      A2=DZ*SV*AKG/2.0/U*D
      A1=(1.0-A2)/(1.0+A2)
      A2=A2/(1.0+A2)
      B2=DZ*SV*H/2.0/U/RG/CPG*D
      B1=(1.0-B2)/(1.0+B2)
      B2=B2/(1.0+B2)
      C3=DT*SV*AKG/(1.0-E)/E*D
      C1=1.0/(1.0+C3*(1.0-A2))
      C2=C1*C3*A2
      C3=C1*C3*A1
      C4=C1*DT*RS/E/DEN*D
      D3=DT*SV*H/(1.0-E)/RS/CPS*D
      D1=1.0/(1.0+D3*(1.0-B2))
      D2=D1*D3*B2
      D3=D1*D3*B1
      D4 = D1*DT/CPS/YIN*D
C
      E2=DZ*SV*RH/2.0/RU/RRG/RCPG
      E1=(1.0-E2)/(1.0+E2)
      E2=E2/(1.0+E2)
      F3=DT*SV*RH/(1.0-E)/RS/CPS
      F1=1.0/(1.0+F3*(1.0-E2))
      F2=F1*F3*E2
      F3=F1*F3*E1
      RETURN
C
C         REACTOR CALCULATIONS
C
   20 DO 25 I=2,N1
      J=I-1
      D=D1*YS(I)+D2*YS(J)+D3*Y(J)
      WKS(1) = YS(J)
      DO 22 K=1,3
      B(K) = C1*XS(K,I) + C2*XS(K,J) + C3*X(K,J)
   22 WKS(K+1) = XS(K,J)
      CALL RSNSC(WKS(1),WKS(5),4,LIMIT,TOL,IERR,FX1SC,ER1SC)
      YS(I) = WKS(1)
      Y(I)=B1*Y(J)+B2*(YS(I)+YS(J))
      DO 23 K=1,3
      XS(K,I) = WKS(K+1)
   23 X(K,I) = A1*X(K,J) + A2*(XS(K,I) + XS(K,J))
      IF (IERR-1) 25,25,26
   25 CONTINUE
   26 RETURN
C
C     REGENERATOR CALCULATIONS
C
   30 DO 35 I=2,N1
      J=I-1
      YS(I)=F1*YS(I)+F2*YS(J)+F3*Y(J)
      Y(I)=E1*Y(J)+E2*(YS(I)+YS(J))
   35 CONTINUE
      RETURN
      END


      SUBROUTINE RSNSC(X,Y,N,LIMIT,TOL,IERR,FUNCT,ER1SC)
C
C  REPEATED SUBSTITUTION METHOD OF SOLVING A SET OF NONLINEAR EQUATIONS
C     X      - INITIAL GUESS AND SOLUTION VECTOR
C     Y      - WORKING ARRAY OF SIZE N
C     N      - NUMBER OF EQUATIONS
C     LIMIT  - MAXIMUM NUMBER OF ITERATIONS
C     TOL    - UPPER BOUND ON SUM OF ABSOLUTE VALUES OF RESIDUALS
C     IERR   - RESULTANT ERROR CODE
C         IERR = 1   -   NO ERROR
C                2   -   MAXIMUM NUMBER OF ITERATIONS EXCEEDED
C                3   -   RESIDUAL CONSTANT FOR 5 SUCCESSIVE EVALUATIONS
C
C                4   -   RESIDUAL INCREASES AT 5 SUCCESSIVE EVALUATIONS
C     FUNCT IS THE USER SUPPLIED SUBROUTINE TO CALCULATE THE FUNCTIONS
C     WHICH ARE OF THE FORM X = F(X)
C     ER1SC IS A USER SUPPLIED SUBROUTINE TO DETERMINE ACTION IF AN ERROR
C     IS DETECTED
C
      DIMENSION X(2),Y(2)
      RES1 = 1.0E38
      IERR = 1
      NCON = 0
      NINC = 0
      LOOP = 0
      CALL FUNCT(X,Y,N)
    1 LOOP = LOOP + 1
      IF(LOOP-LIMIT)3,3,2
    2 IERR = 2
      GO TO 10
    3 CALL FUNCT(Y,X,N)
      RES2 = 0.0
      DO 4 I=1,N
    4 RES2 = RES2 + ABS(X(I) - Y(I))
      IF (RES1-RES2)6,5,7
    5 NCON = NCON + 1
      IF(NCON-5)8,8,50
   50 IERR = 3
      GO TO 10
    6 NINC = NINC + 1
      IF(NINC-5)8,8,60
   60 IERR = 4
      GO TO 10
    7 NCON = 0
      NINC = 0
      IF (RES2-TOL)11,11,8
    8 RES1 = RES2
      DO 9 I=1,N
    9 Y(I) = X(I)
      GO TO 1
   10 CALL ER1SC(IERR,LOOP,RES1,RES2,X,Y,N)
   11 RETURN
      END
      SUBROUTINE ER1SC(IERR,LOOP,RES1,RES2,X,Y,N)
C
C     ERROR HANDLING ROUTINE FOR RSNSC.
C
      DIMENSION X(1),Y(1)
  100 FORMAT(  10X,10(1H*),'   ER1SC   -   MAXIMUM NUMBER OF ITERATIONS EXC
     *EEDED  ',10(1H*))
  101 FORMAT(//10X,10(1H*),'   ER1SC   -   RESIDUAL CONSTANT  ',10(1H*))
  102 FORMAT(//10X,10(1H*),'   ER1SC   -   RESIDUAL DIVERGES  ',10(1H*))
  103 FORMAT(//10X,'CURRENT VALUES AT ITERATION NO.',I5//15X,'RES1 =',
     *E18.9,20X,'RES2 =',E18.9//20X,'X',30X,'Y',(/E20.9,E31.9))
C
      GO TO (5,1,2,3),IERR
    1 WRITE(3,100)
      GO TO 4
    2 WRITE(3,101)
      GO TO 4
    3 WRITE(3,102)
    4 WRITE(3,103)LOOP,RES1,RES2,(X(I),Y(I),I=1,N)
    5 RETURN
      END


      SUBROUTINE FX3SC(X,Y,N)
C
C     HEAT AND MASS BALANCE EQUATIONS FOR STYRENE, TOLUENE AND BENZENE
C     REACTIONS FOR THE SUBROUTINE RSNSC.
C     EQUATIONS OF THE FORM X(I+1) = Y(I) = F(X(I))
C
      DIMENSION X(2),Y(2),R(3)
      COMMON RK,P,CEB,CT,YIN,DH(3),A(3),B,C,D
C
      CALL R3BSC(X(1),X(2),R,RK,P,CEB,CT,YIN)
      Y(1) = D
      DO 2 I=1,3
      Y(1) = Y(1) - D*DH(I)*R(I)
    2 Y(I+1) = A(I)  +  B*R(I)
      RETURN
      END


      SUBROUTINE R3BSC(Y,X,R,RK,P,CEB,CT,YIN)
C
C     EVALUATION OF REACTION RATES USING DERIVED KINETICS
C     REACTION   1     ..   EB        = STY + H2
C                2     ..   EB        = BZ  + C2H4
C                3     ..   EB + H2 = TOL + CH4
C
      DIMENSION X(3),R(3)
      DATA IENT/1/
 1000 FORMAT('     (R3BSC)')
C
      GO TO (1,2),IENT

    1 IENT = 2
      WRITE(3,1000)
      F1 = 3.0318[illegible]333E6
    2 CONTINUE
C
      T=Y*YIN
      C=CEB*P/CT
      XEB = 1.0 - X(1) - X(3) - [illegible]
      C1 = 1.0 + [illegible]03.0 * EXP(-(-36819.52 + 54.05*T)/(1.987/T))*C  +
     * CB + 8.0 [illegible](1)
      R(1) = F1*[illegible](-30849.0230 /T) * (XEB - X(1)*(X(1)-X(3))[illegible]
     *EXP(16.1[illegible] 15.[illegible]50.-[illegible])/C1
      R(2) = EXP(-[illegible].9[illegible]0/T + 6.18[illegible]127)*[illegible]/C1 * 7.
      R(3) = EXP(-[illegible]1.0034/T + 9.163[illegible]0.4)*XEB* (X(1)-X(3))*C/C1 * 7.
      RETURN
      END
```

A7.2 Subroutine TM3SC

This subroutine replaces TM1SC in CH3SC if a uniformly mixed inert fraction of the bed is to be represented by a separate heat balance. The temperatures of the inert along the bed are in the array YW(I).

```
      SUBROUTINE TM3SC(X,Y,XS,YS,IENT,IERR)
C
C     TRANSIENT FILM RESISTANCE MODEL
C     LAGRANGIAN          ..     TIME     -  BACKWARD DIFFERENCE
C     -------------              LENGTH   -  CENTRAL DIFFERENCE
C     EQUATIONS SOLVED BY REPEATED SUBSTITUTION IN KBNSC
C
C          ****   UNIFORM DILUTION OF CATALYST   ****
C     THE DILUENT IS CONSIDERED BY A SEPARATE HEAT BALANCE.
C     INERT FRACTION IN BED IS GIVEN BY 'RK'
C
      EXTERNAL FX3SC,ER1SC
      DIMENSION X(3,102),XS(3,102),Y(102),YS(102),YW(102)
      COMMON RK,P,CEB,CT,YIN,DH(3),B(3),C4,D,DG,WKS(20),H1,CPS,RS,E,SV,
     *DT,TOL,LIMIT,AKG,DZ,U,H,CPG,RG,RU,RH,SCPG,RRG,FFR,FSTN,RF,TM,A,
     *NTIME,ITIME,KOUNT,ISW,KSW,NREC
 1001 FORMAT(' ',32X,'...  SUBROUTINE  TM3SC   -    UNIFORM DILUTION  ...
     *'/37X,42(1H-))
 1002 FORMAT(' INERT TEMPERATURES'/(1X,F10.5,10F11.5))
 1003 FORMAT(//10X,'FRACTION OF BED MADE UP OF INERT MATERIAL  ...',F8.4)
C
      GO TO (10,20,30, 1,40),IENT
C
C     READ VALUES OF YW(I) IF PROGRAM HAS BEEN RESTARTED
C
    1 READ(1'NREC)(YW(I),I=1,101)
C
C     EVALUATE CONSTANTS
C
   10 WRITE(3,1001)
      XDIL1  = 1.0-RK
      WRITE(3,1003)RK
      L1  = N1/10
      A   = DT*SV*H/(1.0-E)/RS/CPS
      G1  = 1.0/(1.0+A)
      G2  = A * G1
      A2  = DZ*SV*AKG/2.0/U * XDIL1
      A1  = (1.0-A2)/(1.0+A2)
      A2  = A2/(1.0+A2)
      B4  = DZ*SV*H/2.0/U/RG/CPG
      D   = 1.0/(1.0+B4*(1.0 - RK*G2))
      B1  = D * (1.0-B4)
      B2  = D * B4*RK*G1
      B3  = D * B4*RK
      B4  = D * B4*XDIL1
      C3  = DT*SV*H[illegible](1.0-E)/E*XDIL1
      C1  = 1.0/(1.0+C3*(1.0-A2))
      C3  = C3 * C1
      C2  = C3*A2
      C3  = C3*A1
      C4  = C1*DT*RS/E/CEB * XDIL1
      D1  = 1.0/(1.[illegible](1.0-B4))
      D2  = D1 * A * B4
      D3  = D1 * A * B1
      D4  = D1 * A * B2
      D5  = D1 * A * B3
      D6  = D1 * DT    /CPS/YIN
C
      E2=DZ*SV*RH/2.0/RU/RRG/RCPG
      E1=(1.0-E2)/(1.0+E2)
      E2=[illegible]
      F3=DT*SV*RH/(1.0-E)/RS/CPS
      F1=1.0/(1.0+F3*(1.0-E2))
      F2=F1*F3*E2
      F3=F1*F3*E1
      RETURN
C
C     REACTOR CALCULATIONS
C
   20 IF(KOUNT - 1) 210,201,210
  201 DO 202 I=1,N1
  202 YW(I) = YS(I)
  210 DO 23 I=2,N1
      J = I - 1
      D = D1*YS(I) + D2*YS(J) + D3*Y(J) + D4*YW(I) + D5*YW(J)
      WKS(1) = YS(I)
      DO 21  K=1,3
      P(K) = C1*X(K,I) + C2*XS(K,J) + C3*X(K,J)
   21 WKS(K+1) = XS(K,I)
      CALL KBNSC(YS(I),WKS(5),4,LIMIT,TOL,IERR,FX3SC,ER1SC)
      YS(I) = WKS(1)
      Y(I)   = B1*Y(J) + B2*YW(I) + B3*YW(J) + B4*(YS(I) + YS(J))
      YW(I)  = G1*YW(I) + G2*Y(I)
      DO 22  K=1,3
      XS(K,I) = WKS(K+1)
   22 X(K,I)    = A1*X(K,J) + A2*(XS(K,I) + XS(K,J))
      IF (IERR-1)23,24,24
   23 CONTINUE
      IF(KOUNT - NTIME) 29,24,24
   24 IF (ISW - 4) 25,29,29
   25 DO 26 I=1,11
      J = (I-1)*L1 + 1
   26 WKS(I)     = YW(J) * YIN
      WRITE(3,1002)(WKS(I),I=1,11)
   29 RETURN
C
C     REGENERATOR CALCULATIONS
C
   30 DO 35 I=2,N1
      J = I - 1
      YS(I)=F1*YS(I)+F2*YS(J)+F3*Y(J)
      Y(I)=E1*Y(J)+E2*(YS(I)+YS(J))
   35 CONTINUE
      RETURN
C
C     STORE VALUES IF INTERRUPTED
C
   40 WRITE(1'NREC)(YW(I),I=1,101)
      RETURN
      END
```

A7.3 Subroutine TM4SC

This subroutine represents an inert region within the catalyst bed or at either end of it and replaces TM1SC in CH3SC. The inert region is represented by the reactor equations from which the reaction term is omitted.

```
      SUBROUTINE TM4SC(X,Y,XS,YS,IENT,IERR)
C
C     TRANSIENT FILM RESISTANCE MODEL
C     LAGRANGIAN           ..      TIME     -   BACKWARD DIFFERENCE
C     ----------                   LENGTH   -   CENTRAL DIFFERENCE
C     EQUATIONS SOLVED BY REPEATED SUBSTITUTION IN FSNSC
C
C     REACTOR HAS A REGION OF INERT MATERIAL WITHIN THE BED
C     INERT FRACTION IS GIVEN BY 'RK'
C     POSITION OF START OF INERT REGION IS GIVEN BY 'D4' AT FIRST ENTRY
C
      EXTERNAL FX3SC,ER1SC
      DIMENSION X(3,102),XS(3,102),Y(102),YS(102)
      COMMON RK,R,CEB,CT,YIN,DH(3),B(3),C4,N,D4,WKS(22),N1,CPS,RS,E,SV,
     *DT,TOL,LIMIT,ALG,DZ,U,H,CPG,RG,RU,RH,RCPG,RRG,DUM(4),IDUM(8),
     *DUMM(6),NSTRT,NEND
 1001 FORMAT(' [illegible]     SUBROUTINE  TM4SC    -     INERT REGION IN BED
     *',/,3X,45(1H-)//10X,'FRACTION OF BED MADE UP OF INERT MATERIAL
     *',F8.4/10X,'INERT REGION STARTS AT Z = ',F8.4)
 1002 FORMAT(//10X,10(1H*),'   TM4SC       INERT FRACTION LESS THAN ONE LEN
     *GTH STEP   ',10(1H*))
 1003 FORMAT(//10X,10(1H*),'   TM4SC   -   INERT REGION EXTENDS BEYOND REAC
     *TOR   ',10(1H*))
C
      GO TO (10,20,30,10,20),IENT
C
C     EVALUATE CONSTANTS
C
   10 WRITE(3,1001)RK,D4
      IF(RK - 1.0/FLOAT(N1-1))13,13,14
   13 WRITE(3,1002)
      IERR  =  7
      RETURN
C
   14 NEND1  =  D4*N1  +  1
      NSTR1  =  NEND1  +  1
      NEND2  =  RK*N1  +  NEND1
      NSTR2  =  NEND2  +  1
      IF(NEND1  -   1)  205,140,145
  140 NSTRT  =  NEND2
  145 IF(NEND1  -  N1)  15,16,16
   15 IF(NEND2  -  N1)  17,160,16
   16 WRITE(3,1003)
      IERR   =  8
      RETURN
C
  160 NEND   =  NEND1
   17 A2=DZ*SV*RKG/2.0/U
      A1=(1.0-A2)/(1.0+A2)
      A2=A2/(1.0+A2)
      B2=DZ*SV*H/2.0/U/RG/CPG
      B1=(1.0-B2)/(1.0+B2)
      B2=B2/(1.0+B2)
      C3=DT*[illegible]/(1.0-E)/E
      C1=1.0/(1.0+C3*(1.0-A2))
      C2=C1*C3*A2
      C3=C1*C3*A1
      C4=C1*DT*RS/E/CEB
      D3=DT*SV*H/(1.0-E)/RS/CPS
      D1=1.0/(1.0+D3*(1.0-B2))
      D2=D1*D3*B2
      D3=D1*D3*B1
      D4  =  D1*DT/CPS/YIN
C
      E2=DZ*SV*RH/2.0/RU/RRG/RCPG
      E1=(1.0-E2)/(1.0+E2)
      E2=E2/(1.0+E2)
      F3=DT*SV*RH/(1.0-E)/RS/CPS
      F1=1.0/(1.0+F3*(1.0-E2))
      F2=F1*F3*E2
      F3=F1*F3*E1
      RETURN
C
C         REACTOR CALCULATIONS
C
   20 CONTINUE
      IF(NEND1  -  1)  205,240,210
  205 WRITE(3,1003)
      IERR   =  6
      RETURN
C
C     FIRST CATALYST REGION
C
  210 DO 23  I=2,NEND1
      J=I-1
      D=D1*YS(I)+D2*YS(J)+D3*Y(J)
      WKS(1)  =  YS(I)
      DO 21 K=1,3
      B(K)  =  C1*X(K,I)  +  C2*XS(K,J)  +  C3*X(K,J)
   21 WKS(K+1)  =  XS(K,I)
      CALL FSNSC(WKS(1),WKS(5),4,LIMIT,TOL,IERR,FX3SC,ER1SC)
      YS(I)  =  WKS(1)
      Y(I)  =  B1*Y(J)  +  B2*(YS(I)  +  YS(J))
      DO 22 K=1,3
      XS(K,I)  =  WKS(K+1)
   22 X(K,I)   =  A1*X(K,J)  +  A2*(XS(K,I)  +  XS(K,J))
C
      IF(IERR-1)23,23,28
   23 CONTINUE
C
C     INERT REGION
C
  240 DO 24  I=NSTR1,NEND2
      J=I-1
      YS(I)=F1*YS(I)+F2*YS(J)+F3*Y(J)
      Y(I)  =  E1*Y(J)  +  E2*(YS(I)  +  YS(J))
      DO 24 K=1,3
      XS(K,I)  =  C1*XS(K,I)  +  C2*XS(K,J)  +  C3*X(K,J)
   24 X(K,I)    =  A1*X(K,J)  +  A2*(XS(K,I)  +  XS(K,J))
```

```
C
C      SECOND CATALYST REGION
C
       IF (NSTR2 - N1) 250,250,28
  250  DO 27 I=NSTR2,N1
       J=I-1
       D=D1*YS(I)+D2*YS(J)+D3*Y(J)
       WKS(1) = YS(I)
       DO 25 K=1,3
       D(K) = C1*XS(K,I) + C2*XS(K,J) + C3*X(K,J)
   25  WKS(K+1) = D(K)
       CALL FUNCT (WKS(1),WKS(5),4,LIMIT,TOL,IERR,FX3SC,ERISC)
       YS(I) = WKS(1)
       Y(I) = B1*Y(J) + B2*(YS(I) + YS(J))
       DO 26 K=1,3
       XS(K,I) = WKS(K+1)
   26  X(K,I) = A1*X(K,J) + A2*(XS(K,I) + XS(K,J))
       IF(IERR-1)27,27,28
   27  CONTINUE
   28  RETURN
C
C      REGENERATOR CALCULATIONS
C
   30  DO 35 I=2,N1
       J=I-1
       YS(I)=E1*YS(I)+E2*YS(J)+E3*Y(J)
       Y(I)=F1*Y(J)+F2*(YS(I)+YS(J))
   35  CONTINUE
       RETURN
       END
```

A7.4 Subroutine TM5SC

This subroutine includes the effect of the reactor (or regenerator) wall as described in Appendix 5, and replaces TM1SC in CH3SC. The following additional parameters are specified in DATA statements.

ZW -- Wall thickness (m)
RW - Wall density (kg m^{-3})
CPW - Wall specific heat (J kg^{-1} °K^{-1})
AKW - Wall thermal conductivity (Wm^{-1} °K^{-1})
ZI - Thickness of internal insulation (m)
AKI - Thermal conductivity of internal insulation (Wm^{-1} °K^{-1})
ZO - Thickness of external insulation (m)
AKO - Thermal conductivity of external insulation (Wm^{-1} °K^{-1})
DTO - Temperature drop between external insulation and surroundings (°C)
HO - Convective heat transfer coefficient to surroundings (Wm^{-2} °K^{-1})

The wall temperatures along the length of the bed are in the array YW(I).

This subroutine only operates counter-currently as the wall temperature profile is reversed after each period.

```
      SUBROUTINE TM5SC(X,Y,XS,YS,IENT,IERR)
C
C     TRANSIENT FILM RESISTANCE MODEL
C     LAGRANGIAN        ..       TIME    -   BACKWARD DIFFERENCE
C                                LENGTH  -   CENTRAL DIFFERENCE
C     EQUATIONS SOLVED BY REPEATED SUBSTITUTION IN RSNSC
C
C ****   HEAT CAPACITY OF WALL INCLUDED   *****
C     LAYERS OF INSULATING MATERIAL CAN BE CONSIDERED ON BOTH THE INSIDE
C     AND THE OUTSIDE OF THE WALL
C     THERMAL CONDUCTION ALONG THE WALL IS INCLUDED
C     THERMAL CONDUCTION RADIALLY IN THE WALL IS INFINITE.
C     HEAT CAPACITY OF THE INSULATION IS NEGLECTED
C
      EXTERNAL [illegible]
      DIMENSION [illegible](3,102),Y(102),YS(102),YW(103)
      COMMON FK,P,CFA,CF,YIN,DH(5),B(5),C4,[illegible],WRS(20),N1,CFS,RS,E,SV,
     *DT,THE,LIMIT,[illegible],RG,RO,RH,RCPG,RRG,FFB,FSTM,FFSTM,A,
     *NTIME,JTIME,LOAD,[illegible]
      DATA ZW,RW,CPW,AKW/[illegible]0127, 7817.27, 460.548,  20.7[illegible]/
      DATA ZI,AKI,ZO,AKO,DTO/0.003, 0.06854,0.089, 0.0685[illegible],100.0/
      DATA HO/6.2305/
C
 1001 FORMAT(/ 30X,'...   SUBROUTINE  TM5SC    -     WALL HEAT CAPACITY  ',
     *[illegible])
 1002 FORMAT(/' WALL  TEMPERATURES'/(11X,10F11.5))
 1003 FORMAT(/ 7X,'ZW',11X,'RW',10X,'CPW',10X,'AKW',11X,'ZI',10X,'AKI',
     *11X,'ZO',10X,'AKO',10X,'DTO'/9E13.5)
C
      GO TO (10,20,30,10,40),IENT
C
C     EVALUATE CONSTANTS
C
   10 WRITE(3,1001)
      WRITE (3,1003) ZW,RW,CPW,AKW,ZI,AKI,ZO,AKO,DTO
      L1     = [illegible]
      HW     = 1.0/(1.0/H + ZI/AKI)
      HO     = 1.0/(1.0/HO + ZO/AKO)
      R      = [illegible]
      G3     = [illegible]*ZW + ZW*ZW)/RW/CPW
      G2     = [illegible]
      G4     = [illegible]*R*ZW + ZW*ZW)/RW/CPW/YIN
      G1     = [illegible]
      A2     = [illegible]
      A1     = [illegible]
      H      = [illegible]
      B3       = DZ*HW*R/H*RG/CPG
      B2       = DZ*SV*H/H*RG/CPG/2.0
      D        = 1.0/(1.0+B2+B3)
      B1       = D * (1.0-B2-B3)
      B2       = D * B2
      B3       = D * B3
      C3       = DT*SV*RKG/(1.0-E)*R
      C1       = 1.0/(1.0 + C3*(1.0-A2))
      C3       = C3 * C1
      C2       = C3 * A2
      C3       = C3 * A1
      C4       = C1*DT*RS/E/CEB
      D4       = DT*SV*H*(1.0-E)/RS/CPS
      D1       = 1.0/(1.0 + D4*(1.0-B2))
      D2       = D1 * D4 * B2
      D3       = D1 * D4 * B1
      D4       = D1 * D4 * B3
      D5       = D1 * DT/CPS/YIN
C
      HW       = 1.0/(1.0/RH + ZI/AKI)
      H3       = DT*2.0*(R-ZI)*HW/(2.*R*ZW + ZW*ZW)/RW/CPW
      H2       = DT*AKW/RW/CPW/DZ/DZ
      H4       = 2.*DT*(R+ZW)*HW*H0*DTA/(2.*R*ZW + ZW*ZW)/RW/CPW/YIN
      H1       = 1.0 - H3 - 2.0*H2
      E3       = DZ*HW/R*RW/RG/RCPG
      E2       = DZ*SV*RH/RW/RG/RCPG/2.0
      D        = 1.0/(1.0+E2+E3)
      E1       = D * (1.0-E2-E3)
      E2       = D * E2
      E3       = D * E3
      F4       = DT * SV * RH/(1.0-E)/RS/CPS
      F1       = 1.0/(1.0 + F4*(1.0-E2))
      F2       = F1 * F4 * E2
      F3       = F1 * F4 * E1
      F4       = F1 * F4 * E3
      IF (IENT - 4) 12,14,12
   12 J        = N1 + 2
      DO 13 I=1,J
   13 YW(I)  = YS(I)
      GO TO 16
   14 READ(1'NREC) (YW(I),I=1,100)
   16 RETURN
C
C     REACTOR CALCULATIONS
C
   20 IF (KOUNT - 1) 200,200,205
  200 J        = (N1-1) / 2
      DO 202 I=2,J
      K        = N1 + 2 - I
      D        = YW(I)
      YW(I)  = YW(K)
  202 YW(K)  = D
C
  205 DO 231 J = 2,N1
      K        = N1 + 4 - J
  231 YW(K)  = YW(K-1)
C
      YW(2)  = YW(4)
      YW(N1+2)  = YW(N1)
      DO 23 I=2,N1
      J        = I-1
      J1       = I+1
      D        = D1*YS(I) + D2*YS(J) + D3*Y(J) + D4*(YW(J1)+YW(I))
      WKS(1) = YS(I)
      DO 21 K=1,3
      B(K) = C1*XS(K,I) + C2*XS(K,J) + C3*X(K,J)
   21 WKS(K+1) = XS(K,I)
      CALL RSNSC(WKS(1),WKS(5),4,LIMIT,TOL,IERR,FX3SC,ER1SC)
      YS(I)  = WKS(1)
      Y(I)   = B1*Y(J) + B2*(YS(I)+YS(J)) + B3*(YW(J1)+YW(I))
      YW(I)  = G1*YW(J1) + G2*(YW(I+2) + YW(I)) + G3*Y(I) - G4
      DO 22 K=1,3
      XS(K,I) = WKS(K+1)
   22 X(K,I)  = A1*X(K,J) + A2*(XS(K,I) + XS(K,J))
      IF(IERR-1)23,23,220
  220 ISW = 1
      GO TO 240
   23 CONTINUE
C
  230 CALL DATSW(3,I)
      GO TO (240,235),I
  235 CONTINUE
C
      IF(KOUNT - NTIME) 26,24,24
   24 IF (KSW - 4) 240,29,29
  240 DO 25 I=1,10
      J     = I*L1 + 1
   25 WKS(I)     = YW(J)*YIN
      WRITE(3,1002) (WKS(I),I=1,10)
      RETURN
   26 IF (MOD(KOUNT,ITIME))29,27,29
   27 IF (KSW - 1) 29,240,29
   29 RETURN
C
C     REGENERATOR CALCULATIONS
C
   30 IF (KOUNT - 1) 31,31,33
   31 J        = (N1-1) / 2
      DO 32 I=2,J
      K        = N1 + 2 - I
      D        = YW(I)
      YW(I)  = YW(K)
   32 YW(K)  = D
C
   33 DO 320 J=2,N1
      K        = N1 + 4 - J
  320 YW(K)  = YW(K-1)
C
      DO 35 I=2,N1
      J        = I-1
      YS(I)  = F1*YS(I) + F2*YS(J) + F3*Y(J) + F4*(YW(I+1) + YW(I))
      Y(I)   = E1*Y(J) + E2*(YS(I)+YS(J)) + E3*(YW(I+1) + YW(I))
      YW(I)  = H1*YW(I+1) + H2*(YW(I+2)+YW(I)) + H3*Y(I) - H4
   35 CONTINUE
C
      GO TO 230
C
C     STORE VALUES IF INTERRUPTED
C
   40 WRITE(1'NREC) (YW(I),I=1,100)
      RETURN
      END
```

NOMENCLATURE

a - Constant

$a_{i,j}$ - Stoichiometric coefficient

A - Cross-sectional area of bed (m^2)

- Constant - in Appendix 3

b - Constant

b_i - Adsorption coefficient (bar^{-1})

B - Constant

c_i - Concentration ($kmol\ m^{-3}$)

C_p - Specific heat ($J\ kg^{-1}\,°C^{-1}$)

D_e - Effective diffusivity ($m^2 s^{-1}$)

D_p - Particle diameter (m)

DS - Kinetics of Davidson and Shah[18]

e - Void fraction

E - Kinetics of Eckert et al[33]

$E(m,n)$ - Error at point (m,n)

F - Dimensionless Temperature

F_{EB} - Ethylbenzene feed ($kmol\ s^{-1}$)

F_{STM} - Steam flow ($kmol\ s^{-1}$)

g_i - Cost factors

h - Interphase heat transfer coefficient ($Wm^{-2}\,°C^{-1}$)

H - Enthalpy (J)

HT_{IN} - Diluent steam superheater heat load (W)

HT_{IN}^* - Make-up steam superheater heat load (W)

I_k - Modified Bessel function of the first kind

k_e - Effective catalyst thermal conductivity ($Wm^{-1}\,°K^{-1}$)

k_g - Interphase mass transfer coefficient ($m\ s^{-1}$)

k_I - Thermal conductivity of insulation material ($Wm^{-1}\,°K^{-1}$)

k_j - Rate constant of the j^{th} reaction

k_w – Thermal conductivity of reactor wall ($Wm^{-1}{}^\circ K^{-1}$)

K_p – Equilibrium constant (bar)

m – Number of length steps

M – Kinetics of Modell[32]

M1 – Derived kinetics

MW – Molecular weight (kg $kmol^{-1}$)

n, N – Number of time steps

OF – Objective function

p_i – Partial pressure (bar)

P – Total pressure (bar)

PC – Product cost

PI – Product income

Q, Q1, Q2, Q3 – Constants

r – Reaction rate (kmol s^{-1} kg $catalyst^{-1}$)

R – Radius of the bed (m)

SC – Kinetics of Sheel and Crowe[17]

SR – Molar steam/ethylbenzene ratio

S_v – Catalyst surface area/unit bed volume ($m^2 m^{-3}$)

t – Time (s)

T – Temperature (°K)

t_f – Period time (s)

T_{fall} – Rate of temperature fall ($^\circ C\ s^{-1}$)

t_{sat} – Saturation time of the bed (s)

u – Velocity ($m\ s^{-1}$) superficial

U_I – Overall heat transfer coefficient between fluid and wall ($Wm^{-2}{}^\circ C^{-1}$)

U_o – Overall heat transfer coefficient between wall and surroundings ($Wm^{-2}{}^\circ C^{-1}$)

x – Conversion

X – Dimensionless time

x_e – Equilibrium conversion

Y – Dimensionless length

z – Length (m)

Z – Total bed length (m)

z_I – Thickness of internal insulation (m)

z_o – Thickness of external insulation (m)

Superscript – All parameters with a bar, e.g. $\bar{u}$, refer to the regenerating bed.

Subscripts

Bz – Benzene

EB – Ethylbenzene

g – Gas phase

H – Hydrogen

i – Component number

I – Inert material

IN – Inlet value

j – Reaction number

O – Inlet condition

OUT – Outlet value

p – Pellet

s – Solid (catalyst) phase

ST – Styrene

STM – Steam

TOL – Toluene

w – Wall

Greek Letters

α - Inverse adsorption coefficient of ethylbenzene (bar)

β - Relative adsorption coefficient of styrene/ethylbenzene

γ - Inert fraction of bed

ΔH - Heat of reaction ($J\ kmol^{-1}$)

Δt - Time step size (s)

ΔT - Average steady state reactor bed temperature difference (°C)

ΔT_{max} - Maximum pellet temperature difference (°C)

ΔT_o - Temperature difference between wall and surroundings (°C)

Δz - Length step size (m)

$\Delta \theta$ - Lagrangian time step size (s)

θ - Lagrangian time (s)

μ - Viscosity ($N\,s\,m^{-2}$)

ξ - Stability criterion parameter

ρ - Density ($kg\ m^{-3}$)

Φ - Factor defined by equation 3.5

REFERENCES

1. Levenspiel, O. Chemical Reaction Engineering, 2nd Ed., Wiley, New York, 1972.

2. Smith, J.M. Chemical Engineering Kinetics, 2nd Ed., McGraw Hill, New York, 1970.

3. Aris, R. Elementary Chemical Reactor Analysis, Prentice Hall, New Jersey, 1969.

4. Thomas, J.M. and Thomas, W.J. Introduction to the Principles of Heterogeneous Catalysis, Academic Press, London, 1967.

5. Petersen, E.E. Chemical Reaction Analysis, Prentice Hall, New Jersey, 1965.

6. Hlavacek, V. Ind. Eng. Chem. 62, 7, 8 (1970).

7. Heggs, P.J. and Cockcroft, C.S. Symposium on Computer Application in Process Development, Erlangen, W. Germany, 1974.

8. Jakob, M. Heat Transfer, Vol. 2, Wiley, New York, 1965.

9. Froment, G.F. Proceedings of the 5th European/2nd International Symposium on Chemical Reaction Engineering, Amsterdam, 1972.

10. Ray, W.H., ibid.

11. Gavalas, G.R. Ind. Eng. Chem. Fund. 10, 1, 71 (1971).

12. Gavalas, G.R. A.I.Ch.E.J. 17, 4, 787 (1971).

13. Miller, S.A. and Donaldson, J.W. Chem. Eng. Progr. 48, 12, 37 (1967).

14. Kirk-Othmer (Ed.), Encyclopedia of Chemical Technology, Vol. 19, 55-85, Wiley, New York, 1969.

15. Mitchell, J.E. T.A.I.Ch.E. 42, 2, 293 (1946).

16. Neth. Pat. Appl. 6,500,118 and 6,515,037.
    Belg. Pat. 657,838.

17. Sheel, J.G.P. and Crowe, C.M. Canad. J. Ch. E. 47, 183 (1969).

18. Davidson, B. and Shah, M.J. IBM J. Res. Develop. 9, 389 (1965).

19. Wenner, R.R. and Dybdal, E.C. Chem. Eng. Progr. 44, 4, 275 (1948).

20. Hydrocarbon Processing, 48, 11, 235 (1969).

21. Berdutin, A.Ya., Terekhin, R.M., Yukelson, I.I., Khim. Prom. (Moscow), 45, 9, 662 (1969).

22. Hausmann, E.D. and King, J.D. Ind. Eng. Chem. Fund. 5, 3, 295 (1966).

23. Webb, G.A. and Corson, B.B. Ind. Eng. Chem. 39, 1153 (1947).

24. Badger, G.M. and Spotswood, T.M. J. Chem. Soc. (London), p.4420, 1960.

25. Esteban, G.L., Kerr, J.A. and Trotman-Dickenson, A.F., ibid, p.3873, 1963.

26. U.S. Pat. 3,326,996.

27. U.S. Pat. 3,402,212; 3,515,763; 3,542,889.

28. U.S. Pat. 3,502,737; Br. Pat. 1,176,916.

29. Bogdanova, O.K., Sheheglova, A.P., Balandin, A.A. and Belomestnykh, I.P. Petrol. Chem. USSR, 1, 1, 120 (1962).

30. Data Sheet, Girdler G-64 catalyst, Girdler-Sudchemie, Munich.

31. Abet, F., Mauri, M., Piovan, M., Quad. Ing. Chem. Ital. 3, 9, 154 (1967).

32. Modell, D.J. Chem. Eng. Comput. 1, 100 (1972).

33. Eckert, E., Marek, M. and Spevacek, J. Symposium on Computers in the Design and Erection of Chemical Plants, Karlovy Vary, Czechoslovakia, 1975.

34. Br. Pat. 892,779.

35. Br. Pat. 966,704.

36. Neth. Pat. 6,507,180.

37. Fr. Pat. 1,344,654; Ger. Pat. 1,917,279.

38. Ohlinger, H. and Stadelmann, S. Chem. Ingr. Tech. 37, 4, 361 (1965).

39. Carra, S. and Forni, L. Ind. Eng. Chem. Des. Develop. 4, 3, 281 (1965).

40. Hinshelwood, C.N. The Kinetics of Chemical Change, Clarendon Press, Oxford, England, 1940.

41. Bohm, H.G. and Wenske, R. Kinetic Reaction Investigation of the Dehydrogenation of Ethylbenzene, Research Paper, Inst. of Chemicalogen, Dresden, E. Germany, 1965.

42. Rase, H.F. and Kirk, R.S. Chem. Eng. Progr. 50, 1, 35 (1954).

43. Heyman, H.W.C. and Van Der Baan, H.S. 3rd International Symposium on Chemical Reaction Engineering, Evanston, U.S.A., 1974.

44. Davidson, B. and Shah, M.J. IBM Technical Report, TR 02.340, IBM Systems Develop. Lab., San Jose, California, 1965.

45. Styrene, Hydrocarbon Processing, 52, 11, 179 (1973).

46. U.S. Pat. 3,525,776.

47. Styrene, Hydrocarbon Processing, 52, 11, 180 (1973).

48. Frank, J.C., Geyer, G.R. and Kehde, H. C.E.P. 65, 2, 79 (1969).

49. Flowpack Users' Manual, ICI Ltd., 1972.

50. Fenske, M.R. Ind. Eng. Chem. 24, 482 (1932).

51. Gilliland, E.R., ibid, 32, 1220 (1940).

52. Underwood, A.J.V., J. Inst. Pet. Tech. 32, 614 (1946).

53. McAdams, W.H. Heat Transmission, 3rd Ed., McGraw Hill, London, 1954.

54. Valstar, J.M. A study of the fixed bed reactor with application to the synthesis of vinyl acetate; Delftsche Uitgevers Maatschappy, N.V. Delft, 1969.

55. Beek, J. Advances in Chemical Engineering 3, 203 (1962).

56. Deans, H.A. and Lapidus, L. A.I.Ch.E.J. 6, 4, 656 (1960).

57. Roemer, M.H. and Durbin, L.D. Ind. Eng. Chem. Fund. 6, 1, 120 (1967).

58. Vanderveen, J.W., Luss, D. and Amundson, N.R. A.I.Ch.E.J. 14, 4, 636 (1968).

59. Ferguson, N.B. and Finlayson, B.A. Chem. Eng. Jl. 1, 327 (1970).

60. Berty, J.M., Bicker, J.H., Clark, S.W., Dean, R.D. and McGovern, T.J., 5th European/2nd International Symposium on Chemical Reaction Engineering, Amsterdam, 1972.

61. Levenspiel, O. and Bischoff, K.B. Advances in Chemical Engineering, Vol. 4, Academic Press, 1963.

62. Feick, J. Ph.D. Thesis, University of Alberta, Edmonton, Alberta, 1968.

63. Stanek, V. and Szekely, J. Canad. J. Ch. E. 51, 22 (1973).

64. Carberry, J.J. and Wendel, M.M. A.I.Ch.E.J. 9, 1, 129 (1963).

65. Karenth, N.G. and Hughes, R. Symposium on Heterogeneous Vapour Phase Reactions, University of Salford (1972).

66. Jefferson, C.P. A.I.Ch.E.J. 18, 2, 409 (1972).

67. Bischoff, K.B. Canad. J. Ch. E. 40, 161 (1962).

68. Asbjornsen, O.A. and Wang, B. Chem. Eng. Sci. 26, 585 (1971).

69. Feick, J. and Quon, D. Canad. J. Ch. E. 48, 205 (1970).

70. McGreavy, C. and Cresswell, D.L. ibid, 47, 583 (1969).

71. Satterfield, C.N. Mass Transfer in Heterogeneous Catalysis, MIT Press, 1970.

72. Liu, S.L. and Amundson, N.R. Ind. Eng. Chem. Fund. 1, 3, 200 (1962).

73. Liu, S.L. and Amundson, N.R. ibid, 2, 3, 183 (1963).

74. Thornton, J.M. Ph.D. Thesis, University of Leeds, 1970.

75. Cockcroft, C.S. and Heggs, P.J. Proceedings of Chempor '75, Lisbon, Portugal, 1975.

76. Paris, J.R. and Stevens, W.F. Canad. J. Ch. E. 48, 100 (1970).

77. Hlavacek, V. and Hofmann, H. Chem. Eng. Sci. 25, 1517 (1970).

78. Valstar, J.M., Van Den Berg, P.J. and Oyserman, J. Proceedings of the CHISA Conference, Czechoslovakia, 1972.

79. Venkatachalam, P., Kershenbaum, L., Grossmann, E. and Earp, R. 5th European/2nd International Symposium on Chemical Reaction Engineering, Amsterdam, 1972.

80. Prater, C.D. Chem. Eng. Sci. 8, 284 (1958).

81. Bokhoven, C. and Van Raayen, W. J. Phys. Chem. 58, 471 (1954).

82. Perry, J.H. Chemical Engineers Handbook, 4th Ed., McGraw Hill, New York, 1963.

83. Bolz, R.E. and Tuve, G.L. (Eds.), Handbook of Tables for Applied Engineering Science, 2nd Ed., CRC Press, Cleveland, Ohio, 1973.

84. Weisz, P.B. Z. Phys. Chem. 11, 8 (1957).

85. Chilton, T.H. and Colburn, A.P. Ind. Eng. Chem. 26, 1183 (1934).

86. Handley, D. and Heggs, P.J. T.A.I.Ch.E., 46, 251 (1968).

87. Aris, R. Chem. Eng. Sci. 24, 149 (1969).

88. Mercer, M.C. and Aris, R. Lat. Am. J. Chem. Eng. & Appl. Chem., 2, 149 (1971).

89. Ergun, S. Chem. Eng. Progr. 48, 89 (1952).

90. Seinfeld, J.H. and Lapidus, L. Mathematical Methods in Chemical Engineering, Vol. 3, Prentice Hall, New Jersey, 1974.

91. McGreavy, C., Nussey, C. and Cresswell, D.L. I. Ch. E. Symposium Series No. 23, p.111 (1967).

92. Girdler-Sudchemie, Munich, private communication, 1974.

93. Kobe, K.A. Thermochemistry of Petrochemicals, Reprint No. 44, 2nd printing, University of Texas, Austin, Texas.

94. Ames, W.F. Nonlinear Partial Differential Equations in Engineering, Academic Press, New York, 1965.

95. Fox, L. Numerical Solution of Ordinary and Partial Differential Equations, Addison-Wiley, Reading, Mass., 1962.

96. Crandall, S.H. Engineering Analysis, McGraw Hill, New York, 1956.

97. Smith, G.D. Numerical Solutions of Partial Differential Equations, Oxford University Press, London, 1965.

98. Hyman, M.A. On the Numerical Solution of Partial Differential Equations, Hyman, Baltimore, 1953.

99. Robinson, S.M. Siam. J. Numer. Anal. 3, 650 (1966).

100. Powell, M.J.D. Harwell Report AERE R5947, HMSO, 1968.

101. Lapidus, L. Digital Computation for Chemical Engineers, McGraw Hill, New York, 1962.

102. Lapidus, L. and Seinfeld, J.H. Numerical Solutions of Ordinary Differential Equations, Academic Press, New York, 1971.

103. Forsythe, G.E. and Wasow, W.R. Finite-Difference Methods for Partial Differential Equations, Wiley, New York, 1960.

104. Price, C.B.A. Ph.D. Thesis, University of London, 1964.

105. Schumann, T.E.W. J. Franklin Inst. 208, 405 (1929).

106. Heggs, P.J. Ph.D. Thesis, University of Leeds, 1967.

107. Bogard, M.J.P. and Long, R.H. Chem. Eng. Progr. 58, 7, 90 (1962).

108. Hydrocarbon Processing, 47, 7, 230 (1968).

109. Kreyszig, E., Advanced Engineering Mathematics, Wiley, New York, 1968.

110. U.S. Pat. 3,515,767; 3,256,355.

111. Whitehead, B.D. Ph.D. Thesis, University of Leeds, 1973.